U.S. DEPARTMENT OF COMMERCE
DANIEL C. ROPER, Secretary
BUREAU OF STANDARDS
LYMAN J. BRIGGS, Director

# BUREAU OF STANDARDS JOURNAL OF RESEARCH

September 1933
Vol. 11, No. 3

UNITED STATES
GOVERNMENT PRINTING OFFICE
WASHINGTON : 1933

For sale by the Superintendent of Documents, Washington, D.C. - - Price 25 cents; $2.50 per year on subscription

U.S. Department of Commerce, Bureau of Standards

RESEARCH PAPER RP593

*Part of Bureau of Standards Journal of Research, Vol. 11, September 1933*

# A METHOD OF PROVIDING COURSE AND QUADRANT IDENTIFICATION WITH THE RADIO RANGE-BEACON SYSTEM

By F. W. Dunmore

ABSTRACT

Certain circumstances may arise, especially when near the radiobeacon, when a pilot may pass from one course or quadrant to another without his knowledge of it. When once so lost, he may wander many miles in an attempt to reorient himself, since the 4 courses are all practically identical, and 2 of the 4 quadrants between the courses give identical indications. This paper describes a method of obviating this difficulty by transmitting a directive signal composed of 1 dot in a westerly direction, a similar signal of 2 dots in an easterly direction, 3 dots north, and 4 dots south. Depending upon which set of these signals is the loudest, a pilot may determine his general direction from the beacon. Methods of transmitting these signals with practically no interruption to the visual beacon signals and during the station identification interruption of the aural beacon are described.

The change from the figure-of-eight transmission for the courses to the unidirectional cardioid transmission may be accomplished either by changing the point of coupling into suitable phasing sections in the transmission line feeding the antenna or by superimposing on a figure-of-eight radiation through a suitable hybrid coil circular radiation in phase with the figure-of-eight radiation. Standard relays operated by a motor-driven dot-sending device serve to make these changes. In the latter method a simple reversing relay serves to reverse the direction of transmission of the cardioid signals in a given set of antenna systems.

CONTENTS

| | Page |
|---|---|
| I. Introduction | 310 |
| II. Principle of operation | 310 |
| III. Method of using identification signals | 311 |
| IV. Application to the visual, aural, and combined visual and aural radio range-beacons | 313 |
| 1. Aural system | 313 |
| 2. Visual system | 313 |
| 3. Combined aural and visual system | 314 |
| V. Method of sending the cardioids from the TL antenna system | 314 |
| 1. Method of securing the figure-of-eight course signals | 315 |
| 2. Method of securing the cardioid identification signals | 315 |
| (*a*) Method in which each antenna is supplied with a single current of proper phase | 315 |
| (*b*) Method of sending the cardioid signals by superimposing in-phase nondirectional radiation from both antennas on a figure-of-eight radiation from these antennas | 319 |
| VI. Application of the identification signals to the established airway radio range system | 323 |

## I. INTRODUCTION

In the radio range-beacon system now used on the airways the determination of absolute direction or position is difficult. Certain circumstances may arise, especially when the aircraft is near the radio beacon, when a pilot may pass from one quadrant or course to another without his knowledge of it. When once so lost, it becomes a very difficult matter for him to reorient himself and he may wander many miles from the beacon in the attempt. His course indications may show him to be in either of two quadrants or on any one of four courses; he does not know which. Only by a laborious method involving flying over a considerable distance [1] can he reorient himself. In fact, tests have shown that the average pilot when flying under the hood and purposely lost requires about an hour to get on a known course. A radio range-beacon should not only function to keep a pilot on a definite course, which the present system does admirably, but it should also provide means whereby in case he does become lost be may readily orient himself and get on a known course. This paper outlines a means for doing this without any extra equipment on the airplane and with but slight modification at the radiobeacon. Flight tests at the Bureau's experimental field at College Park, Md., have shown that a pilot may easily reorient himself when lost, by means of this system.

## II. PRINCIPLE OF OPERATION

The system as worked out assumes the range-beacon to be equipped with the new TL antenna now being installed at many radio range-beacon stations.[2] The 4 quadrants and 4 courses are identified by 4 aural signals each transmitted in a different direction.

Referring to figure 1, *B* and *C* represent the usual beacon figure-of-eight directional transmissions; each may be modulated at a different audio frequency, as in the case of the visual beacon system, or coded with "*A*" and "*N*" signals interlocked as with the aural beacon system, and produce courses *D*, *E*, *F*, and *G*. The antennas of the TL antenna system for producing the figure-of-eight radiation characteristics shown at *H*, *I*, *J*, and *K*, are preferably arranged to coincide with the four cardinal points of the compass. *L*, *M*, *P*, and *Q* are the respective transmission lines. By properly phasing the currents in antennas *H* and *J* by means of phasing sections in transmission lines *L* and *P* (to be described later), an aural signal *R*, consisting of a dot, may be transmitted in a westerly direction with a directional transmission characteristic similar to the shape of a cardioid. In a like manner (see fig. 2) a similar signal, *S*, consisting of 2 dots, may be sent in an easterly direction; similarly, a 3-dot signal, *T*, sent north, and then a 4-dot signal, *U*, sent south. Figure 3 shows each identification signal as it is sent separately. From the relative intensities of these different sets of dot signals, which come in the order 1, 2, and 3, 4, a pilot may determine his approximate location with respect to the beacon as illustrated below.

[1] See Air Commerce Bulletin, Sept. 15, 1932, p. 148.

[2] The cause and elimination of night effects in radio range-beacon reception, H. Diamond, B.S.Jour. Research, vol. 10 (RP513), p. 7, January 1933. On the solution of the problem of night effects with the radio range-beacon system, H. Diamond, Proc. I.R.E., vol. 21, p. 808, June 1933.

## III. METHOD OF USING IDENTIFICATION SIGNALS

A pilot may be lost on any one of the four courses of the radiobeacon, in the 65-cycle or *A* quadrant, of which there are 2, or in the 86⅔-cycle or *N* quadrant, of which there are 2. The identification signals tell him which one of the four courses he is on or which one of the four quadrants he is in. For example, referring to figure 2:

(1) Assume the beacon course signals give an on-course indication. This means the pilot may be on any one of the four courses, *OD*, *OE*, *OF*, or *OG*, he does not know which. When the 1-dot, 2-dot identifi-

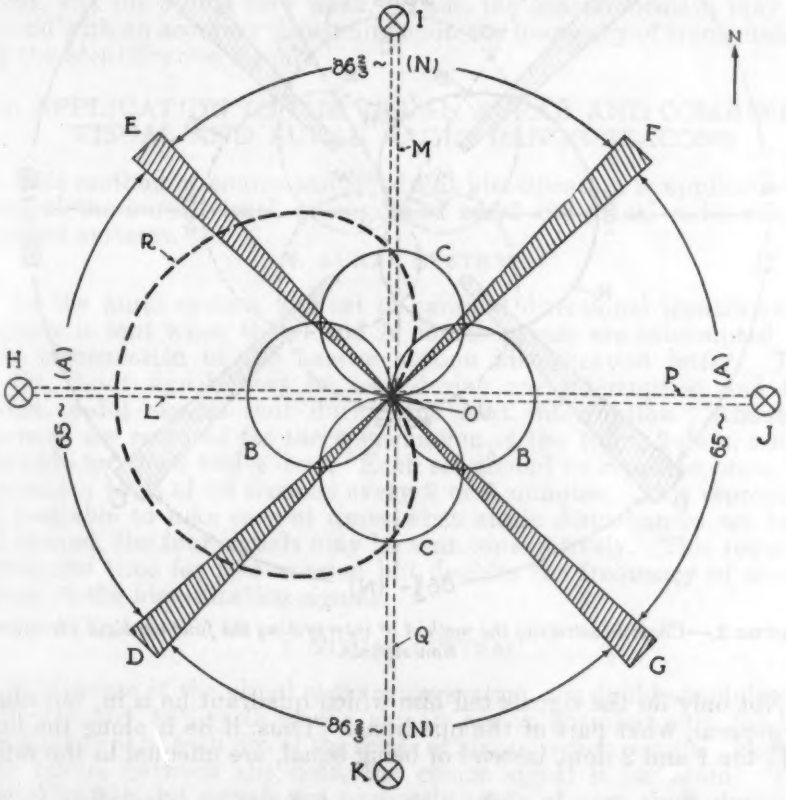


FIGURE 1.—*A single cardioid identification signal showing its relation to the radio beacon courses and quadrants.*

cation signal is heard the 1 dot is loud and the 2 dots weak. This places him on course *OE* or *OD*. When the 3-dot, 4-dot signal is heard, the 3 dots are loud and the 4 dots weak. This places him on course *OE* as distinct from course *OD*.

(2) Suppose the beacon-course signal received by the pilot is a strong 86⅔-cycle or *N* signal. This places him somewhere in the region north of the beacon or south of it, not east or west of it. When the dot identification signal is heard, the 1 and 2 dots are about equal, confirming the beacon-course signal indication that the pilot is north or south of the beacon. When the 3- and 4-dot signals are heard, the 3 dots are loud and the 4 dots missing. This places him definitely

in the north (86⅔-cycle) quadrant and not in the south (86⅔-cycle) quadrant, as in the latter quadrant the 3 dots would have been missing, and the 4 dots loud.

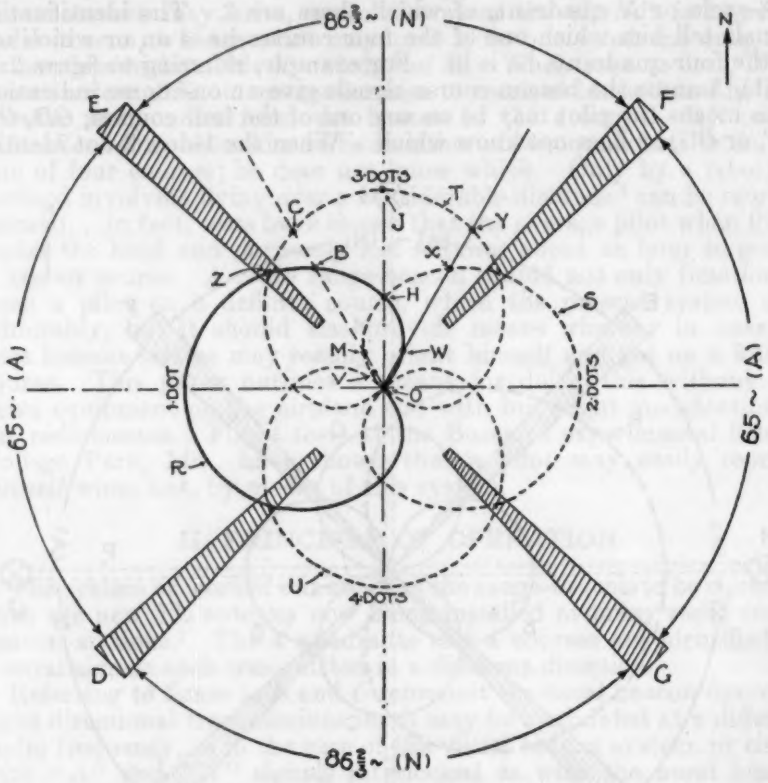


FIGURE 2.—*Chart illustrating the method of interpreting the four cardioid identification signals.*

Not only do the signals tell him which quadrant he is in, but also, in general, what part of the quadrant. Thus, if he is along the line *OY*, the 1 and 2 dots, instead of being equal, are unequal in the ratio

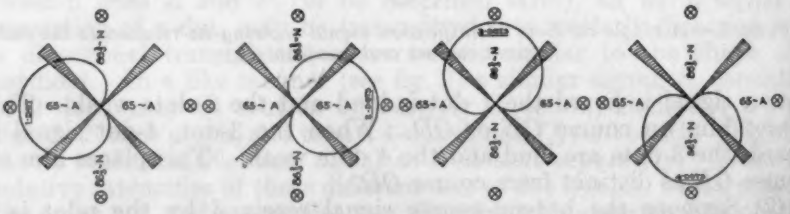

FIGURE 3.—*Chart showing how each cardioid identification signal is sent into a different quadrant.*

of *OW* to *OX*. If he is along the line *OJ*, the 1 and 2 dots are equal in intensity, while along the line *OC*, the 1 dot is louder than the 2 dots in the ratio of *OB* to *OM*.

A further use to which the identification signals may be put is to give the pilot the very necessary information as to whether or not he has passed by the beacon when coming in on a course, in case he should miss the zero-signal zone over the beacon, which indication occurs so quickly that it may easily be missed. Thus, suppose a pilot to be flying in toward the beacon located at O, figure 2 on course *OF*. As long as he remains northeast of the beacon, he hears the 1 dot weak and the 2 dots loud, also the 3 dots loud and the 4 dots weak. The minute he passes over the beacon on to course *OD* southwest of the beacon, the 1 dot becomes loud, the 2 dots very weak, the 4 dots loud, and the 3 dots very weak. Thus, the beacon location may be found with an accuracy depending upon the frequency of transmission of the identification signals.

## IV. APPLICATION TO THE VISUAL, AURAL, AND COMBINED VISUAL AND AURAL RADIO RANGE-BEACONS

This method of course and quadrant identification is applicable to any of the aural, visual, or combined aural and visual radio range-beacon systems.

### 1. AURAL SYSTEM

In the aural system, the set of cardioid directional identification signals is sent when the *A* and *N* course signals are interrupted for the transmission of the beacon station identification letter. The 1-dot, 2-dot signals may be sent during one interruption and the 3-dot, 4-dot signals sent during the next interruption. About 2 seconds are required for the transmission of the 1-dot, 2-dots, and 3 seconds for the 3 and 4 dots. Each set should be repeated once, requiring a total of 10 seconds every 2 or 3 minutes. This repetition is desirable to take care of times when static disturbances are bad. If desired, the four signals may be sent consecutively. This requires twice the time for transmission but doubles the frequency of occurrence of the identification signals.

### 2. VISUAL SYSTEM

In the case of the visual radio range system, the double-modulation 65-cycle and 86⅔-cycle course signals are interrupted only for the time interval of each dot of the series of identification signals. During the spaces between the dots, the course signal is on again. The identification dot signals are purposely made of very short duration so that the course signals are interrupted for such a short interval of time that the reeds in the visual course indicator have time to drop only about one third their amplitude. As the reeds are equally damped, the relative amplitude of the two reeds does not change during this drop, so that the course indications of the reed indicator are not appreciably affected by the identification signals.

The effect of the identification signals is even less noticeable on the converter type of course indication, as the high damping on the microammeter, used as the course indicator, will not allow the needle to move appreciably during the very short interruption of the beacon course signals. Furthermore, when flying on-course, as is usually the case, the needle is at its null position to which it normally returns when the course signal is not present, which is the case at the instant

of sending the dots of the cardioid signal. The 1,000-cycle note comprising the identification signals is kept out of the reed indicator or reed converter circuits, where it might cause interference, by suitable audio filter circuits whereby the 1,000-cycle note is sent to the head phones with very little of the low-frequency course signals and the low-frequency 65-cycle and 86⅔-cycle course signals are sent to the reed indicator or reed converter with very little of the 1,000-cycle identification signals.

### 3. COMBINED AURAL AND VISUAL SYSTEM

The application to this sytem is a combination of the application to the aural and visual systems. The aural course signals are interrupted for the space of time (10 seconds) required to send two sets

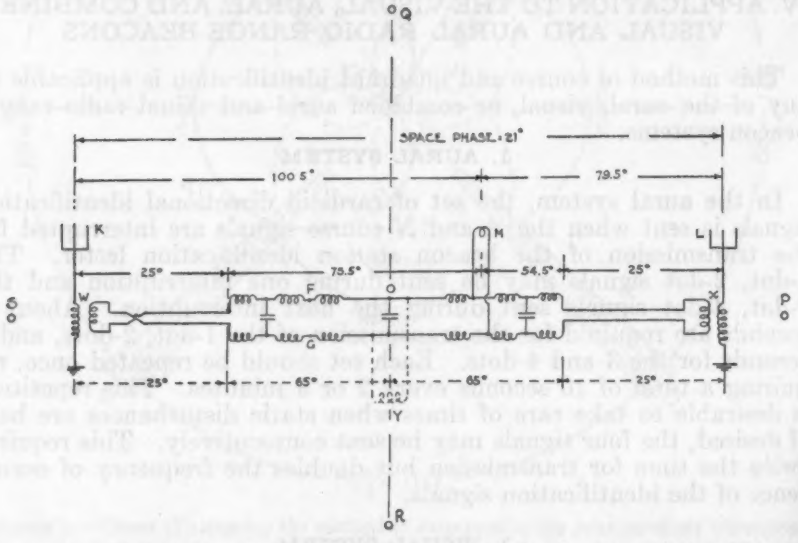


FIGURE 4.—*Method of introducing phasing sections in the transmission lines for obtaining cardioid directional transmission from the* TL *antenna system.*

of identification signals, while visual course signals are interrupted only for the period of each dot.

## V. METHOD OF SENDING THE CARDIOIDS FROM THE TL ANTENNA SYSTEM

The cardioid transmission characteristic may be obtained from the TL antenna system in two ways—by supplying current to the 2 antennas in the proper phase, or by supplying current to the 2 antennas 180° out of phase along with a superimposed current in phase in the 2 antennas and of such amplitude and phase relation as to combine with the first 2 currents to give a cardioid transmission characteristic. Figure 4 shows the arrangement used on the experimental beacon at College Park, Md., in making the test on the first-mentioned method. For simplicity, but one set of TL antennas is shown.

## 1. METHOD OF SECURING THE FIGURE-OF-EIGHT COURSE SIGNALS

For sending the figures-of-eight for the beacon course signals at College Park, the time phase between the point $Y$, figure 4, where the beacon signal power is supplied, and each of the antennas, was made 90° in order to secure phase synchronization of the currents in the 2 antennas.[3] Of this, 25° was in the transmission line and 65° in an artificial line section. As the coupling at $X$ is reversed from that at $W$, the current in antenna $L$ is 180° out of phase with that in antenna $K$. Thus, at points along the line $QOR$, a minimum signal will be received, while along the line $SOP$, a maximum signal will be received, giving the usual figure-of-eight transmission characteristic for producing the course signals.

## 2. METHOD OF SECURING THE CARDIOID IDENTIFICATION SIGNALS

### (a) METHOD IN WHICH EACH ANTENNA IS SUPPLIED WITH A SINGLE CURRENT OF PROPER PHASE

In this method where the cardioid transmission has a maximum signal in the direction $OP$, figure 4, and minimum signal in the direc-

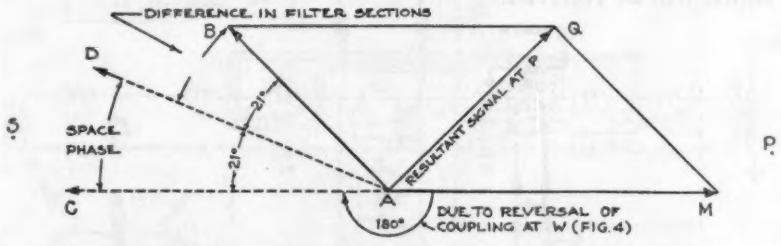


FIGURE 5.—*Phase relation of the signals from the two beacon antennas when sending the cardioid identification signal in the direction of point P.*

tion $OS$, the point of coupling the signal into the artificial transmission line is shifted from $Y$ for the course signal to $M$ for the cardioid signal. The point $M$ is chosen so that a time phase of 100.5° is obtained between $M$ and antenna $K$, and 79.5° time phase between $M$ and antenna $L$. The reason for the choice of these values is shown below. The space phase between the two antennas as used at College Park was 21°. Referring to figure 5, $AM$ represents the signal which would be received at $P$ from antenna $L$ alone. $AC$ represents the signal which would be received at $P$ from antenna $K$, not considering the space or time phase betwen the two antennas, but considering the reversal of coupling at $W$. $AD$ represents the signal from antenna $K$ at $P$ considering, in addition, the 21° space phase between the two antennas. $AB$ represents the signal from antenna $K$ at $P$ considering both the reversal of coupling, the space phase, and the 21° introduced by the difference in the electrical length of the artificial lines in the transmission line to antenna $K$ and to antenna $L$. This 21° is the $100.5° - 79.5° = 21°$ shown in figure 4. In other words, $AB$ is the signal received at $P$ due to antenna $K$. Adding the two vectors, $AM$ and $AB$, we get $AQ$, which is the resultant signal received in the direction $OP$. To obtain the signal received in the opposite

[3] Phase synchronization in directive antenna arrays with particular application to the radio range beacon. By F. G. Kear, B.S.Jour. Research, vol. 11, (RP581), p. 123, July 1933.

direction, i.e., at $S$, let $AM$, figure 6, represent the signal received at $S$ due to antenna $L$, not considering the space and time phase between the two antennas. $AC$ represents the signal which would be received from antenna $K$ alone, considering only the reversal of coupling at $W$. Then $AT$ represents the signal at $S$ from antenna $L$ due to a

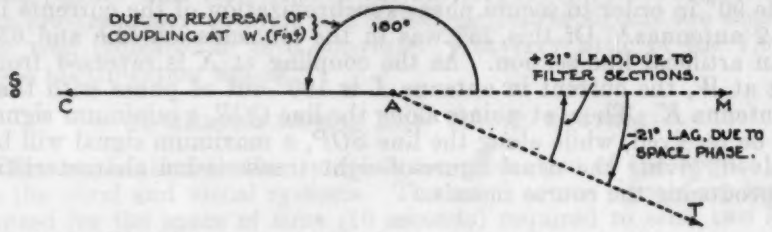


FIGURE 6.—*Phase relation of the signals from the two beacon antennas when sending the cardioid identification signal in a direction opposite from that to point P.*

21° lag caused by the space phase between the two antennas. Due to the difference in the phasing sections, the current in antenna $L$ is given a 21° lead over that in antenna $K$, $+100.5°-79.5°=+21°$. Therefore, at $S$ the currents from $L$ and $K$ are 180° out of phase and no signal will be received.

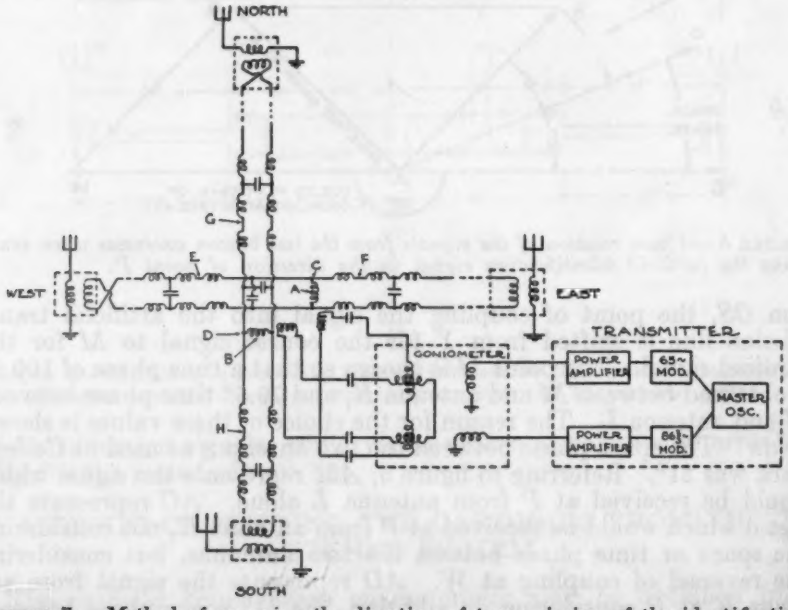


FIGURE 7.—*Method of reversing the direction of transmission of the identification signals, by connecting input coils A and B to different points in the phasing sections in the transmission lines.*

There are several methods of reversing the direction of transmission of the maximum signal from $P$ to $S$. One method adopted is to shift coil $M$ to terminals $FG$ in the artificial line (see fig. 4), a system of relays making the necessary changeovers. The use of relays in this method is described below.

Circuit arrangement for sending the cardioid dot signals.—A simplified circuit arrangement of a double modulation radio range-beacon

with transmission line antenna system is shown in figure 7. The energy from the transmitting set is coupled into the transmission lines through a goniometer and coupling coils *A* and *B*. With the coils *A* and *B* at the points *C* and *D*, respectively, the figure-of-eight course signals are sent. By moving *A* to point *E* and short-circuiting the north-south transmission lines, the phase relations of the currents in the east and west antennas are such that a cardioid directional signal is sent in a westerly direction. By moving coil *A* to point *F*, the phase relations are such that the cardioid signal is sent in an easterly direction. During these cardioid transmissions 1,000 cycles is supplied to the modulator circuits instead of 65 cycles and 86⅔ cycles.

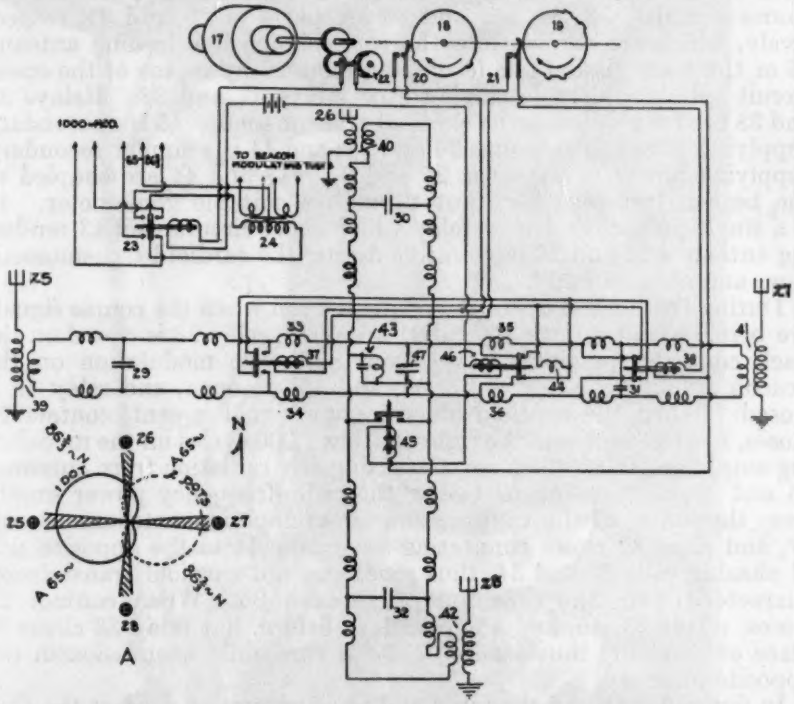


FIGURE 8.—*Circuit arrangement with relays for changing from the figure-of-eight transmission for the courses to the cardioid transmission for quadrant and course identification as applied to one set of antennas.*

In a similar fashion, if coil *B* is moved to point *G* and the east and west transmission line short-circuited, a cardioid signal is sent north, and then south when coil *B* is moved to point *H*.

In order to make the quick changes from the figure-of-eight transmission used for the course signals to the cardioid dot signals and from the 65-cycle and 86⅔-cycle modulation to 1,000-cycle modulation, a system of relays is used to throw the coupling coil *A* from point *C* to *E* or *F* and coupling coil *B* from point *D* to *G* or *H*, and 1,000 cycles on the two modulators in the transmitter.

Figure 8 shows a circuit arrangement with the necessary relays applied to 1 set of antennas for sending 2 of the 4 cardioid signals. This relay system changes to the cardioid transmission only during

the period of each dot of the identification signals. In this circuit, 17 is a motor driving the 1-dot sending disk 18 and 2-dot disk 19. 20 and 21 are contacts for making the dots, 22 is a timing switch for sending the cardioid signals as often as desired, 23 is a double-pole double-throw relay operated by contacts 20 and 21 and serves to disconnect the 65-cycle and 86⅔-cycle modulation from the primary of transformer 24, supplying the beacon amplifiers, and supplies 1,000 cycles to this primary during the time of the cardioid transmissions. 25, 26, 27, and 28 are the vertical antennas. 39, 40, 41, and 42 are the coupling units to antennas 25, 26, 27, and 28, respectively. 29, 30, 31, and 32 are the phasing sections in the transmission lines for producing the figure-of-eight transmission for the beacon course signals. 33, 34, 35, and 36 are parts of 29 and 31, respectively, which are thrown into the transmission line feeding antenna 25 or the transmission line feeding antenna 27 by means of the open-circuit type double-pole single-throw relays 37 and 38. Relays 37 and 38 are for producing the cardioid transmission. 43 is a secondary supplying power to antennas 26 and 28; and 44 is a similar secondary supplying power to antennas 25 and 27. 43 and 44 are coupled to the beacon transmitter output through a suitable goniometer. 45 is a single-pole single-throw relay which short-circuits coil 43 rendering antennas 26 and 28 inoperative during the cardioid transmissions from antennas 25 and 27.

During the normal operation of the beacon when the course signals are being sent, contacts 20 and 21 are open, relay 23 is closed on the back contacts, putting 65-cycle and 86⅔-cycle modulation on the beacon amplifiers. Relays 37, 38, and 45 are open, and relay 46 is closed. When the cardioid identification signal is sent, contact 20 closes, relay 23 closes to the right putting 1,000 cycles on the modulating amplifiers, relay 45 closes preventing any radiation from antennas 26 and 28, relay 46 opens taking the radio-frequency power supply from the center of the transmission lines supplying antennas 25 and 27, and relay 37 closes connecting secondary 44 to the opposite side of phasing coils 33 and 34, thus sending a dot cardioid transmission characteristic in the direction of antenna 25. When contact 21 closes, relays 23, 46, and 45 operate as before, but relay 38 closes in place of relay 37, thus sending a 2-dot cardioid transmission in the opposite direction.

In figure 9 is shown the relay and phasing unit as used at the College Park beacon. It is shown removed from its shielding housing and contains the phasing sections 33, 34, 35, and 36, condenser 47, and relays 37, 38, 46, and 45, shown in figure 8.

For sending the full set of 4 identification signals in the 4 different directions, the circuit arrangement in figure 8 should be modified to that shown in figure 10, where the relays and phasing sections shown in the east and west transmission line have been repeated in the north and south transmission lines. A single code wheel—48—with the set of 1-, 2-, 3-, and 4-dot sectors on it, operates the proper relays at the proper time by means of selector brushes 49, 50, 51, and 52. This code wheel is shown in figure 11. This arrangement sends the 1-dot cardioid directional identification signal west, the 2-dot signal east every other revolution of code wheel 48, the 3-dot signal north, and the 4-dot signal south every intermediate other revolution of code wheel

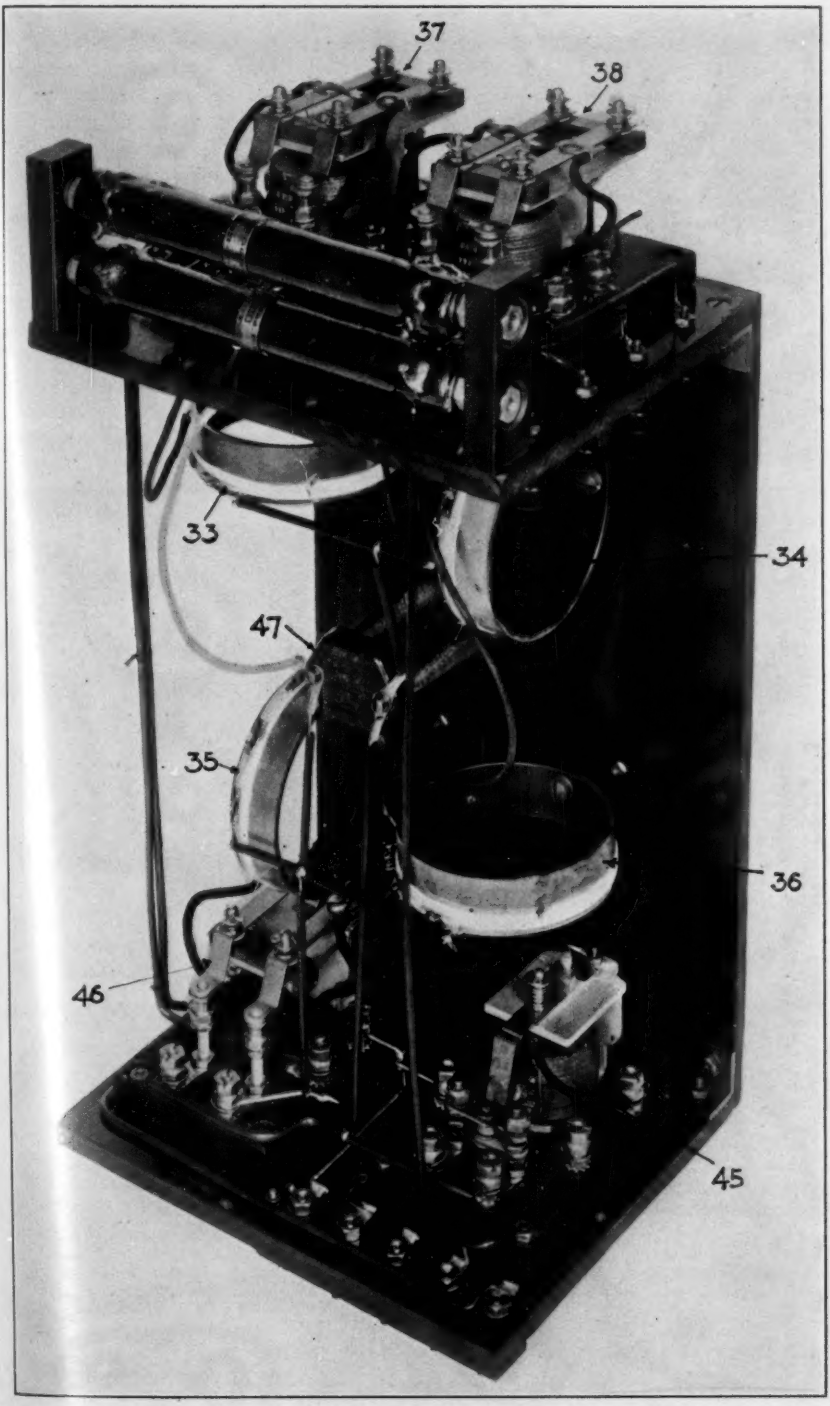


FIGURE 9.—*A "building out" or phasing section showing relays for altering its position in the transmission line when reversing the direction of transmission of the identification signals.*

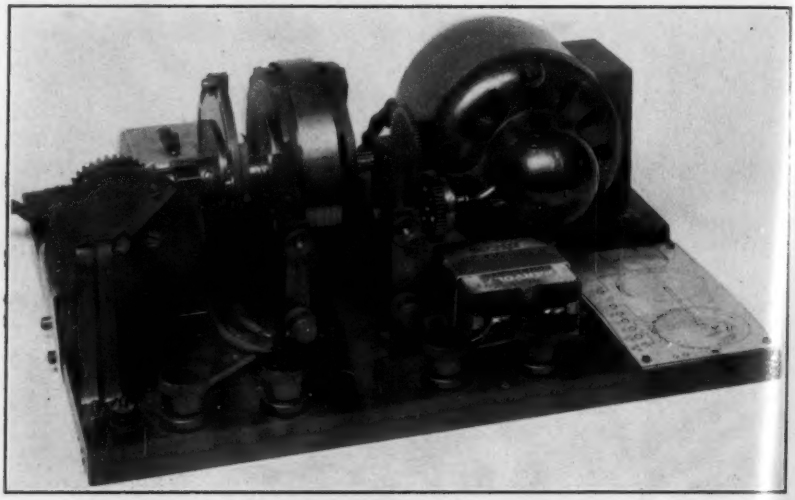

FIGURE 11.—*The coding wheel for making the dot signals in proper sequence.*

48, or, if desired, the full set of signals may be sent each revolution of code wheel 48.

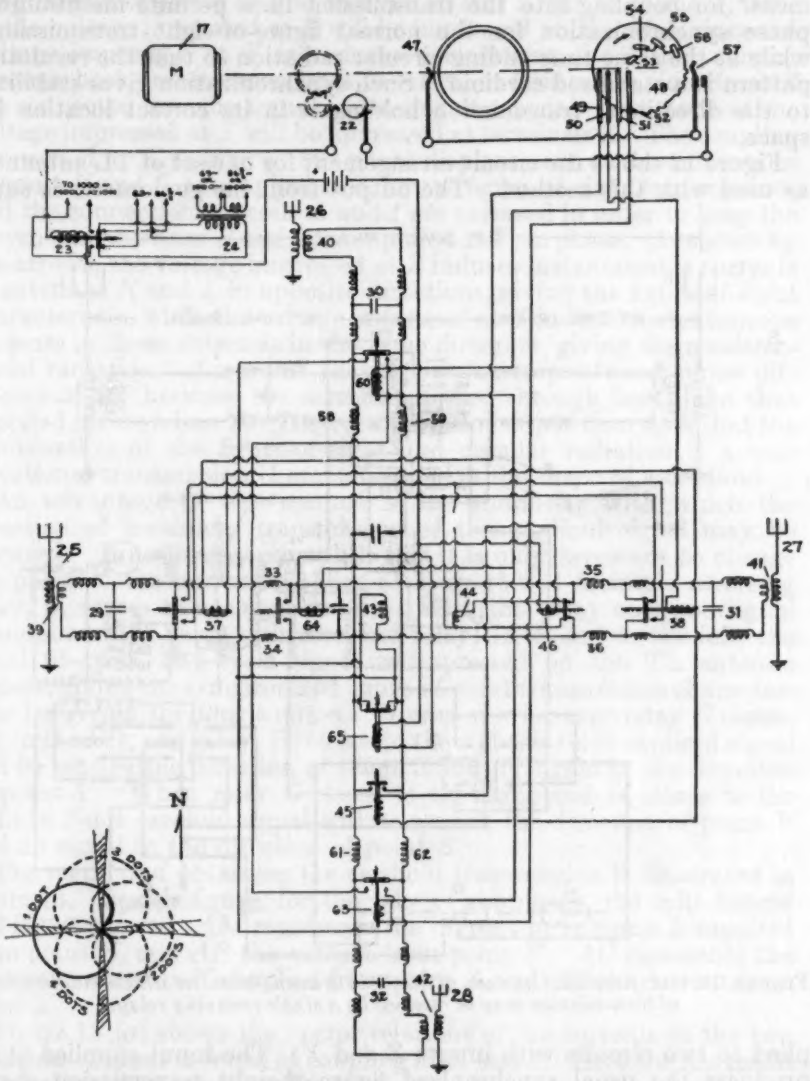


FIGURE 10.—*One of the complete circuit arrangements as used at the experimental beacon station at College Park, Maryland, for sending the course signals and the course and quadrant identification signals.*

### (b) METHOD OF SENDING THE CARDIOID SIGNALS BY SUPERIMPOSING IN-PHASE NONDIRECTIONAL RADIATION FROM BOTH ANTENNAS, ON A FIGURE-OF-EIGHT RADIATION FROM THESE ANTENNAS

This method is better than the one just described, particularly with respect to the stability of the cardioid signal in space and with respect to the ease of adjustment during installation. The cardioid directional characteristic is obtained by combining with the normal figure-of-eight transmission a non-directional transmission in such

phase relation to the figure-of-eight transmission that the resultant is a cardioid directional transmission. A split hybrid coil arrangement[4] for coupling into the transmission lines permits maintaining phase synchronization for the normal figure-of-eight transmission, while at the same time adding circular radiation so that the resultant pattern is a stabilized cardioid. Such synchronization gives stability to the directional transmission holding it in its correct location in space.

Figure 12 shows the circuit arrangement for one set of TL antennas as used with this method. The output from the goniometer is sup-

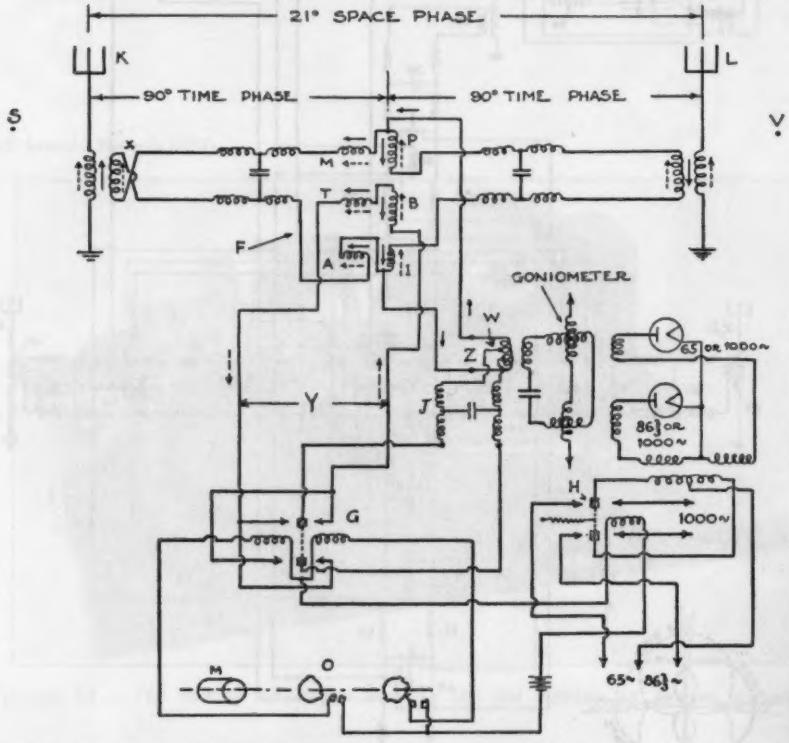


FIGURE 12.—*A simplified system of cardioid transmission in which the direction of transmission may be reversed by a single reversing relay.*

plied to two circuits with inputs $Z$ and $Y$. The input supplied at $Z$ produces the usual synchronized figure-of-eight transmission characteristic for producing the beacon courses. The input supplied at $Y$ produces substantially nondirectional radiation from antennas $K$ and $L$. The voltage supplied at $Z$ and that supplied at $Y$ remains independent due to the use of hybrid coils at $F$. These coils consist of units $M$, $T$, and $A$, all wound in the same direction and closely coupled, and $P$, $B$, and $I$ also wound in the same d rection and closely coupled but not coupled to $M$, $T$, and $A$. The connections to coils $A$ and $I$ are reversed. The full arrows show the circulating currents at a given instant due to the voltage applied at $Z$ and the dotted arrows

[4] Suggested by W. E. Jackson, Airways Division, Dept. of Commerce.

show the circulating currents at a given instant due to the voltage supplied at $Y$. Since the current induced in coil $T$ from $A$ and $M$ is equal and opposite to that induced in coil $B$ due to $P$ and $I$, none of the voltage impressed at $Z$ will be impressed at $Y$. Also, since the voltage impressed at $Y$ introduces a clockwise circulating current through both transmission lines in series, and since the lines from $Z$ are connected into the transmission line at a nodal point, none of the voltage impressed at $Y$ will be impressed at terminals $Z$. The coupling is reversed at $X$ to give a 180° phase displacement of the currents in antenna $K$ and $L$, as supplied at $Z$, for the figure-of-eight transmission; and the connections to coils $A$ and $I$ are reversed in order to keep the currents in antennas $K$ and $L$, as supplied at $Y$, in phase. As shown by the arrows, the voltage impressed at $Z$ induces instantaneous currents in antennas $K$ and $L$ in opposite directions, giving the figure-of-eight characteristic, while the voltage impressed at $Y$ induces instantaneous currents in these antennas in the same direction, giving the nondirectional radiation. $J$ is a 90° phasing section to produce a phase difference of 90° between the current supplied through line $Z$ and that supplied through line $Y$. The vector relationship is then such that the combination of the figure-of-eight and circular radiation is a unidirectional transmission characteristic with the shape of a cardioid.

An advantage of this method is the simplicity with which the direction of maximum transmission of the cardioid signal may be reversed. In order to accomplish this it is only necessary to change the phase of the current supplied at $Y$ by 180°. A simple reversing relay, $G$, serves to accomplish this. With this relay open, no signal is supplied at $Y$, and with a second relay, $H$, closed to the left, the usual 65-cycle, 86⅔-cycle signal is impressed on the TL antenna system, giving the synchronized figure-of-eight transmission characteristic for giving the four courses. However, whenever relay $G$ closes, say to the left, and relay, $H$, closes to the right, a 1-dot cardioid signal will be sent in the direction of point $S$ and no signal in the direction of point $V$. When relay $G$ closes to the right and $H$ closes to the right, a 2-dot cardioid signal will be sent in the direction of point $V$ and no signal in the direction of point $S$.

The method of obtaining the cardioid transmission is illustrated in figure 13. In this figure, for the sake of simplicity, the split hybrid coil is not shown. $AM$ represents the current in antenna $L$ supplied from point $Z$, and $AP$ the current from point $Y$. $AC$ represents the current in antenna $K$ supplied from point $Z$, and $AT$ the current from point $Y$.

Figure 13 ($a$) shows the vector relations of the currents in the two antennas without reversal of coupling at $X$ and $I$. Here the net result of the signal impressed at $Y$ is zero.

Figure 13 ($b$) shows the effect of reversing the coupling at $I$. This 180° change produces a current $AT$ 180° out of phase with $AC$ and a current $AP$ in phase with $AM$, leaving $AC$ and $AM$ unchanged.

Figure 13 ($c$) shows the effect of reversing the coupling at $X$. This rotates $AT$ and $AC$ 180°, leaving $AM$ and $AP$ unchanged.

Figure 13 ($d$) shows the effect of adding the 90° phasing section $J$, causing a 90° lag in both $AT$ and $AP$.

Figure 13 ($e$) shows at $AC'$ and $AT'$ an additional lag of 21° in both $AC$ and $AT$ when considering the signal as received in line with the two antennas at some point $V$. This 21° is the space phase due to the

physical separation of antennas $L$ and $K$. The vector sum of $AM$ and $AC'$ is $AQ$, and the vector sum of $AP$ and $AT'$ is $AR$. As $AR$ can be made equal in intensity to $AQ$ by means of a clip connection on inductance $W$ (fig. 12) and is 180° out of phase with $AQ$, no signal will be received at point $V$.

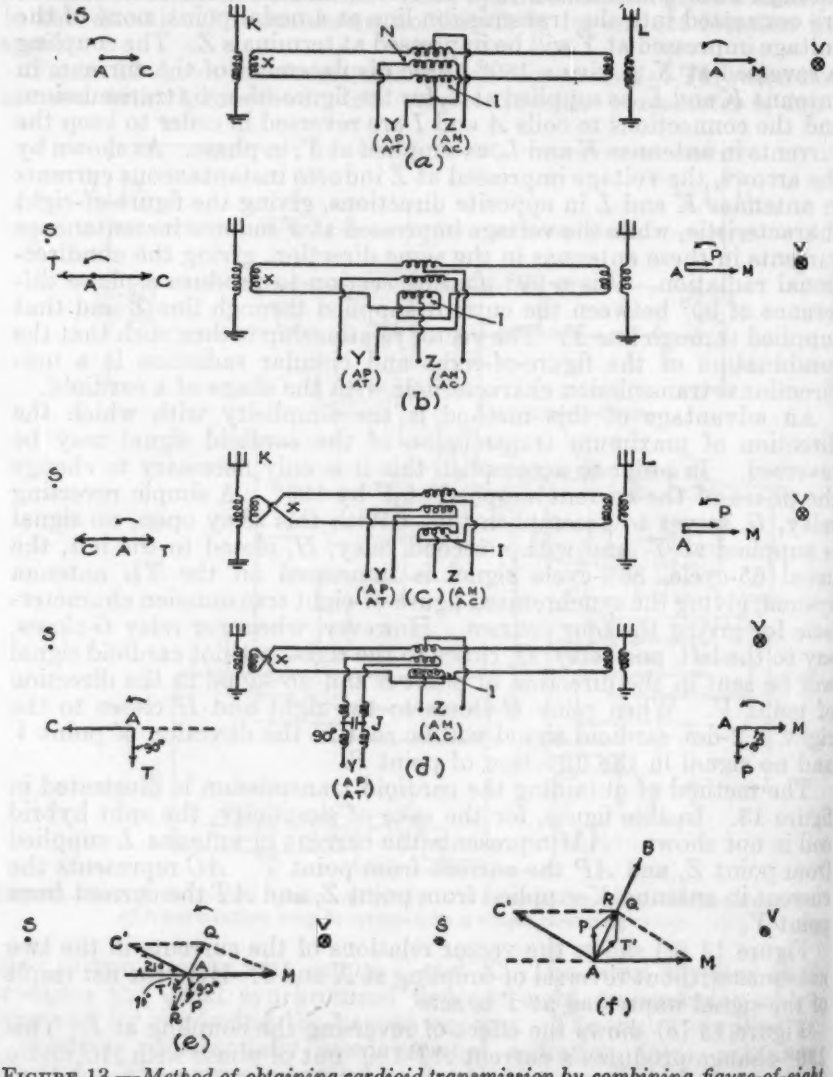


FIGURE 13.—*Method of obtaining cardioid transmission by combining figure-of-eight radiation with two nondirectional in-phase radiations from the two antennas.*

Figure 13 (*f*) shows the effect of reversing the currents supplied at $Y$ by means of reversing relay $G$. The phase of $AP$ and $AT'$ are both changed by 180° and the resultant $AR$ will be in phase with $AQ$ and a signal of double the intensity $AB$ will be received at point $V$. This corresponds to the signal received at $S$ corresponding to the conditions of fig. 13 (*e*).

## VI. APPLICATION OF THE IDENTIFICATION SIGNALS TO THE ESTABLISHED AIRWAY RADIO RANGE SYSTEM

This system of course and quadrant identification is easily applied to existing beacon stations of either the visual or aural types using the TL antenna system, as it requires no alterations to the antenna structure but merely adds relays and phasing sections in the transmission lines inside the beacon station house. A motor-driven code wheel is also required in the case of the visual beacon and a code wheel geared to the motor operating the interlocking A–N switch in the case of the aural beacon.

There are three methods of applying the cardioid transmissions to fit in with the established airways:

(1) The simple cases where the TL antennas are laid out along the four cardinal points of the compass, as has already been described, in which case the 1 dot is always sent west, 2 dots east, 3 dots north, and 4 dots south, as in figures 3 and 10.

(2) Cases where the TL antennas are laid out without any relation to the four cardinal points of the compass. There are two alternative methods under this heading:

(*a*) Either to transmit the cardioid signals from both TL antenna systems simultaneously such that the resultant cardioids will be in directions corresponding to the four cardinal points of the compass, resulting in cardioid signals as in case 1, or:

(*b*) To transmit the cardioid signals in the direction of the TL antennas and to provide the pilot with a set of rules and a map showing the direction of transmission of the cardioid signals for each beacon.

Of the two cases, (*a*) and (*b*), the latter seems somewhat preferable, as the simultaneous transmission of two cardioids required in case (*a*) complicates the radio-transmitting equipment somewhat.

Considering case (*b*), therefore, where the cardioid signals are sent in 4 different directions not coinciding with the 4 cardinal points of the compass, it is only necessary to illustrate the direction of transmission of the coded identification signal on the pilot's chart of each beacon, which he always has at hand, to give him all the necessary information. Such a chart illustrating the application to three radio beacons designated as *A*, *B*, and *C*, respectively, is shown in figure 14. Here the nos. 1, 2, 3, and 4 indicate the sectors where the dot signal of that number is heard with the maximum intensity. The small round dots represent the layout of the four antennas, differently located with respect to the points of the compass in each case. Thus, assume a pilot to be lost. From the beacon identification letter, which, let us say, is D (— ..), he finds he is receiving the "*B*" radio range. He also finds from his beacon course signal that he is in a 65-cycle or *A* (. —) quadrant. When the 1- and 2-dot quadrant and course cardioid identification is heard (see fig. 14 at (*a*)), the 1- and 2-dot signals are somewhere near equal in intensity, thus placing the pilot in region *FG* or *HI* and confirming the indication given by the beacon course signal that the pilot is in a 65-cycle or *A* (. —) quadrant. When the 3- and 4-dot signals are heard, (see fig. 14 at (*b*)), the 3 dots are barely audible, while the 4 dots are very loud. This immediately places the pilot definitely southeast of the "B" beacon in region *FG*.

Even though the beacon may have bent courses as shown, the identification method holds good, since a different combination of

strong and weak signals will always be received on each different course and quadrant.

In a few special cases where the four courses are aligned approximately along the lines of direction to the TL antennas, it is necessary to send only the two cardioid signals, the dot and 2 dots. With but two identification signals, there are two opposite courses shown at *A*, figure 8, along the line to antennas 26 and 28, along which there is no differentiation in the identification signal, the dot and 2 dots being about equal in intensity on each course. However, the pilot can

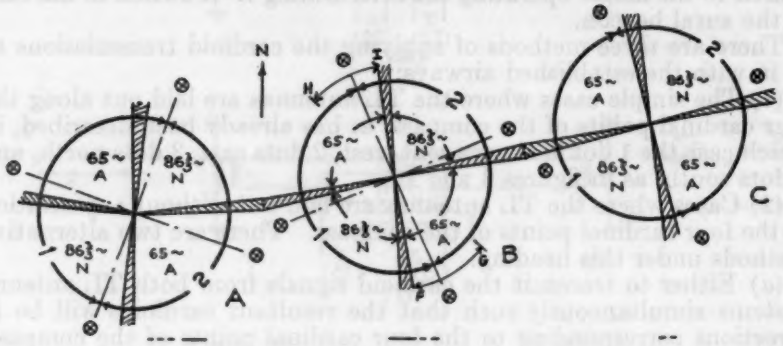


FIGURE 14.—*A chart as might be furnished to pilots using the quadrant and course identification signals.*

determine which of the two courses he is on by deviating to the right and noting which off-course signal predominates. Thus, if his compass shows he is flying north and he obtained an increase in the *N* or 86⅔-cycle signal when deviating to the right, he is on the course extending south of the beacon, because if he had been flying north and deviated to the right and obtained an increase in the A or 65-cycle signal, he would have been on the course north of the beacon.

A simple set of rules which might be followed in all cases, having given the location of the four antennas with respect to the points of the compass, would be:

(1) When the antenna system is laid out such that the lines of direction between diagonally opposite antennas coincide with the 4 cardinal points of the compass, then the 1-dot signal shall be sent in a westerly direction, 2 dots east, 3 dots north, and 4 dots south.

(2) When the antenna system is laid out such that lines between diagonally opposite antennas do not coincide with the four cardinal points of the compass, then the 1-dot signal will be sent in a westerly direction along the line of direction of the two diagonally opposite antennas extending the most nearly east and west. In the special case where the antenna system is laid out such that the lines between diagonally opposite antennas are at an angle of 45° with respect to the four cardinal points of the compass, then the 1-dot signal shall be sent in the northwest direction.

(3) The 2-, 3-, and 4-dot signals shall be sent in directions corresponding to the following degrees of azimuth going clockwise around the beacon from the direction in which the 1-dot signal is sent—2 dots, 180°; 3 dots, 90°; 4 dots, 270°; and in the order—1 dot-2 dots, then 3 dots-4 dots.

The author wishes to express appreciation to H. Diamond for valuable suggestions as to the urgent needs for and requirements of some form of quadrant identification, and to F. G. Kear for research in the design and application of phasing sections to the TL antenna system for the production of the cardioid signals.

WASHINGTON, June 20, 1933.

U.S. Department of Commerce, Bureau of Standards

RESEARCH PAPER RP594

*Part of Bureau of Standards Journal of Research, Vol. 11, September 1933*

# EFFECTS OF PARTICLE SIZE OF A POTTER'S "FLINT" AND A FELDSPAR IN WHITEWARE

By R. F. Geller, D. N. Evans, and A. S. Creamer

ABSTRACT

A feldspar and a potter's flint (crushed quartz) of commercial grade were separated by means of an air elutriator into four fractions. Each fraction contained particles grading from the finest originally present to maximum diameters of 10, 20, 35, and 75 microns, respectively. In addition, fractions containing particles varying from 35 to 75 microns were separated and a portion of the original feldspar was reground to produce a material composed of particles of 35 micron maximum diameter. The specific surface in $cm^2/g$ was calculated for each fraction from data obtained by microscopic count.

Various combinations of the several fractions of flint and of feldspar were incorporated in whiteware bodies. Specimens of these bodies were heated at 1150°, 1200°, 1250°, 1300° and 1350° C., and tested for linear shrinkage, apparent porosity, strength in bending, and linear thermal expansion. Shrinkage and porosity results were compared with the specific surface values of the flint and feldspar in the respective bodies. Relative fusion and solution in the body was estimated by microscopic examination.

The data obtained indicate the possibility of vitrifying commercial ceramic whiteware with more finely ground materials, and without the use of auxiliary fluxes, at temperatures significantly lower than are now required in the industry.

CONTENTS

| | Page |
|---|---|
| I. Introduction | 328 |
| II. Materials and methods | 329 |
| 1. Clays | 329 |
| 2. Flint | 329 |
| (*a*) Chemical purity | 329 |
| (*b*) Particle-size fractions | 329 |
| (*c*) Solubility | 329 |
| 3. Feldspar | 330 |
| (*a*) Chemical purity | 330 |
| (*b*) Particle-size fractions | 330 |
| (*c*) Solubility | 331 |
| 4. Bodies | 331 |
| (*a*) Compositions | 331 |
| (*b*) Preparation of specimens | 331 |
| (*c*) Methods of test | 332 |
| III. Properties of bodies | 334 |
| 1. Shrinkage during drying | 334 |
| 2. Shrinkage during heating | 334 |
| 3. Apparent porosity after heating | 334 |
| 4. Transverse strength | 336 |
| 5. Linear thermal expansion | 337 |
| (*a*) Bodies 1 to 12, inclusive | 337 |
| (1) Specimens heated at 1350° C | 337 |
| (2) Specimens heated at 1250° C | 337 |
| (3) Specimens heated at 1150° C | 337 |
| (*b*) Bodies 18 to 24, inclusive | 337 |

III. Properties of bodies—Continued. Page
6. Fusion and solution ..... 338
(*a*) Specimens heated at 1350° C ..... 338
(*b*) Specimens heated at 1250° C ..... 339
(*c*) Specimens heated at 1150° C ..... 339
IV. Summary ..... 339
V. Conclusions ..... 340

## I. INTRODUCTION

Success in the manufacture of ceramic clay ware must depend on forming the desired structure by a process of fusion and solution at elevated temperatures. The rate at which this process will proceed is a function not only of temperature but also of the surface areas of the materials. Therefore a study was undertaken of some effects of variations in particle size and corresponding variations in specific surface (area per unit weight) of potter's "flint" and feldspar. This paper is a report of one phase of the study and is confined to ceramic whiteware bodies in which the mean particle sizes of one "flint" (crushed quartz) and of one feldspar were varied.

Flint and feldspar as supplied to the pottery trade are so finely divided that only a small fraction is retained by the no. 325 sieve. Therefore some equipment other than sieves is necessary, not only for determining particle size distribution but also for separating finer sizes of particles in sufficient quantity to study their effects in specimens comparable with commercial products.

The necessary equipment has been supplied by the development of air elutriators [1] capable of making separations of particles at diameters as small as $10\mu$,[2] and of producing as much as 250 grams of $<10\mu$ material in an hour of operating time.

TABLE 1.—*Chemical compositions of batch materials and of feldspar particle-size fractions*

| | Kaolin [a] | Ball clay [a] | Flint [b] | Feldspar fractions [a] | | | | |
|---|---|---|---|---|---|---|---|---|
| | | | | <75μ | 35 to 75μ | <35μ | <20μ | <10μ |
| | *Percent* | *Percent* | *Percent* | *Percent* | *Percent* | *Percent* | *Percent* | *Percent* |
| $SiO_2$ | 45.3 | 51.8 | ..... | 65.6 | 65.6 | 65.6 | 65.8 | 65.3 |
| $Al_2O_3$ | 39.1 | 28.9 | ..... | [c] 18.4 | [c] 18.7 | [c] 18.7 | [c] 18.8 | [c] 18.7 |
| $K_2O$ | .15 | ..... | ..... | 13.4 | 13.2 | 13.4 | 13.4 | 13.4 |
| $Na_2O$ [d] | .10 | ..... | ..... | 2.0 | 2.1 | 2.0 | 2.2 | 1.8 |
| $Fe_2O_3$ | .27 | 1.03 | [e] 0.02 | ..... | ..... | ..... | ..... | ..... |
| $TiO_2$ | 1.54 | 1.47 | ..... | ..... | ..... | ..... | ..... | ..... |
| Nonvolatile residue | ..... | ..... | .25 | ..... | ..... | ..... | ..... | ..... |
| Ignition loss | 13.7 | 15.6 | .13 | ..... | ..... | ..... | ..... | ..... |
| Total | 100.16 | 98.80 | .38 | 99.4 | 99.6 | 99.7 | 100.2 | 99.2 |

[a] Analyses by J. F. Klekotka.
[b] Analysis by F. W. Glaze.
[c] Determined as $R_2O_3$; includes $Al_2O_3$, $Fe_2O_3$, $TiO_2$ and $P_2O_5$.
[d] Determined by difference from combined chlorides of K and Na.
[e] Included in nonvolatile residue.

[1] Constructed by L. A. Wagner of the Bureau of Standards following the principles described by J. C. Pearson and W. H. Sligh in B.S.Tech. Paper No. 48, 1915.
[2] $1\mu$ (micron) equals 0.0001 cm or 0.00003937 inch.

## II. MATERIALS AND METHODS

### 1. CLAYS

The kaolin (Georgia "soft") and the ball clay (Kentucky No. 4) were washed through a no. 325 sieve, dried, and recrushed to pass a no. 20 sieve. The chemical compositions are given in table 1.

### 2. FLINT

#### (a) CHEMICAL PURITY

The nature and amount of impurities in the flint (Pennsylvania crushed quartz) are given in table 1. The several particle size fractions used in this study were not analyzed chemically because the purity of the original material precluded the possibility of significant variations among them.

#### (b) PARTICLE-SIZE FRACTIONS

The several fractions were obtained in the following manner. The original material was first treated in the air elutriator and particles approximately 60$\mu$ and less in maximum diameter were "blown over." The residue was then sieved dry through a no. 325 sieve,[3] the portion passing the sieve added to the portion blown over by the elutriator, and the combined sample labeled as the "$<75\mu$ fraction".[4] A portion of this $<75\mu$ fraction was elutriated further to obtain a fraction composed of particles having diameters between the limits 35$\mu$ and 75$\mu$. Three other portions were elutriated to eliminate particles larger than 35$\mu$, 20$\mu$, and 10$\mu$ diameters, respectively. The particle diameter distribution of the $<75\mu$ fraction with respect to total surface area is shown in figure 1. In table 2 are given the particle diameter distribution by weight, and the calculated values for average diameter "$D$", equaling $\Sigma nd^3$ divided by $\Sigma nd^2$,[5] and specific surface $\pi nD^2$, in cm$^2$ per g, of each fraction. In these calculations, which are based on the assumption that all particles are spheres, "$n$" equals the total number of particles of any given estimated diameter "$d$" as determined by microscopic count.

#### (c) SOLUBILITY

Portions of the 35$\mu$ to 75$\mu$ and the $<10\mu$ fractions were agitated with distilled water for 48 hours and permitted to settle from suspension for 24 hours. The suspensions were then filtered through especially made filters of $Al_2O_3$ and evaporated to dryness. There was no weighable residue from 200 ml of filtrate from the 35$\mu$ to 75$\mu$ suspension, but the residue from the $<10\mu$ suspension filtrate indicated a "solubility" of 0.022 g/l. All of the residue was not in true solution, but examination with the ultramicroscope showed the amount of suspended material to be extremely small. This residue appeared to contain no silica since treatment with HF produced no significant reduction in weight.

[3] Although the openings of the U.S. Standard no. 325 sieve are theoretically 44$\mu\pm$2.72$\mu$, they will pass particles of crushed quartz or feldspar (normally very irregular in shape) having maximum dimensions of as much as 75$\mu$. The preliminary separation of particles less than 60$\mu$ in diameter, by means of the air elutriator, expedited the sieving operation appreciably.

[4] The portion retained by the sieve, which constituted not more than 5 percent of the initial sample, was discarded.

[5] Theodore Hatch, Jour. Franklin Inst., 215 (1), p. 27 (Jan. 1933).

TABLE 2.—*Calculated average diameter and specific surface of flint and feldspar particle size fractions, and particle diameter distribution by weight and by area*

| Nominal diameter limits of fraction | Diameter | | | Specific surface of fraction[c] in $cm^2/g$ | | Particle diameter distribution. Percentage of initial sample | | | |
|---|---|---|---|---|---|---|---|---|---|
| | Max[a] | Av. $(D)=\frac{\Sigma nd^3}{\Sigma nd^2}$ | | Flint | Feldspar | By weight[b] | | By area[c] | |
| | | Flint | Feldspar | | | Flint | Feldspar | Flint | Feldspar |
| μ | μ | μ | μ | $cm^2$ | $cm^2$ | *Percent* | *Percent* | *Percent* | *Percent* |
| Sd[d] | 35 | | 4.8 | | 4,800 | | | | |
| <10 | 12 | 4.6 | 3.1 | 5,000 | 7,500 | 25 | 20 | 63 | 58 |
| <20 | 30 | 7.0 | 6.7 | 3,200 | 3,500 | 45 | 40 | 80 | 78 |
| <35 | 40 | 11 | 14 | 2,200 | 1,850 | 80 | 80 | 92 | 87 |
| <75 | 80 | 14 | 15 | 1,660 | 1,450 | 95 | 95 | 98 | 96 |
| 35 to 75 | 80 | 51 | 50 | 450 | 470 | 15 | 15 | 7 | 9 |

[a] Particles having diameters greater than the "nominal" maximum diameter did not, for any fraction exceed 5 percent by weight of the total. This applies to both flint and feldspar.
[b] Based on separations by air elutriation.
[c] Calculated from microscopic count.
[d] Portion of original sample which was reground.

## 3. FELDSPAR

### (a) CHEMICAL PURITY

A feldspar of highest purity was selected from those commercially available[6] because impurities may segregate in certain of the particle-

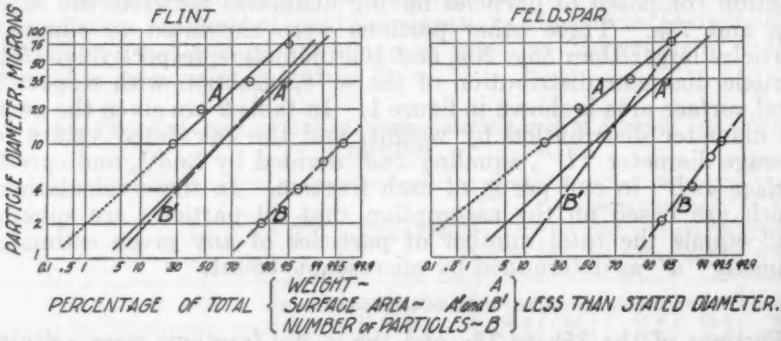


FIGURE 1.—*Logarithmic probability curves showing the calculated particle diameter distributions with respect to total surface area (curves A′ and B′) for the <75μ fractions of flint and feldspar which are practically equivalent to the intial samples.*

Curves *A′* are calculated from curves *A* which show the particle diameter distributions with respect to total weight as obtained by air elutriator separation. Curves *B′* are calculated from curves *B* which show the particle diameter distribution with respect to total number of particles as obtained by microscopic count. Thus, feldspar particles 4μ and less in diameter constituted approximately 3 percent of the total sample by weight, 18 percent by area as calculated from curve *A*, 37 percent by area as calculated from curve *B*, and 97 percent by microscopic count of particles. For further information on this method of calculating particle distribution see reference in footnote 5, page 329.

size fractions provided they are not in solid solution and are present in appreciable percentages. The chemical composition of each of the fractions used is given in table 1.

### (b) PARTICLE-SIZE FRACTIONS

The fractions (table 1) were obtained in the same manner as described for the flint. In addition, part of the original feldspar

[6] The material used is from the same source as feldspar no. 19 in the paper by Geller and Creamer in the Jour. Amer. Cer. Soc., vol. 14 (1), p. 30 (Jan. 1931).

sample (designated in tables 2 and 3 by *S*) was ground dry in a ball mill for 34 hours. This grinding reduced the material to particles of less than 35$\mu$ maximum diameter. Particle diameter distribution of the <75$\mu$ fraction, with respect to total surface area, is shown in figure 1. The average diameter, specific surface, and percentage by weight and area of the initial sample are given, for the respective fractions, in table 2.

### (c) SOLUBILITY

The "solubility" or, more properly, the relative hydrolysis [7] of the feldspar was obtained with the same methods as described for the flint. The results, calculated to grams per liter and given to the nearest 0.005 g, are as follows: 35$\mu$ to 75$\mu$ fraction, 0.025 g; <75$\mu$ fraction, 0.050 g; <35$\mu$ fraction, 0.050 g; <20$\mu$ fraction, 0.065 g; *S* (reground), 0.070 g; <10$\mu$ fraction, 0.120 g. In the case of the feldspar, as of the flint, examination with the ultramicroscope showed that only an extremely small amount of material in the filtrate was present in suspension.[8] The following chemical composition was determined for residue from the hydrolysis of the <10$\mu$ fraction: silica, 19.5 percent; $Al_2O_3$ and MgO, not detectable; $Ca(OH)_2$, 4.4 percent; NaOH and KOH (by difference), 76.1 percent.

TABLE 3.—*Batch compositions of bodies and particle size fractions of flint and feldspar used in each body*

[Nominal diameter limits of feldspar and flint particles [1]]

| Body no. | 1 | 2 | 3 | 4 | 5 | 6 | 7 | 8 | 9 | 10 | 11 | 12 | 18 | 20 | 21 | 22 | 23 | 24 |
|---|---|---|---|---|---|---|---|---|---|---|---|---|---|---|---|---|---|---|
| | $\mu$ | $\mu$ | $\mu$ | $\mu$ | $\mu$ | $\mu$ | $\mu$ | $\mu$ | $\mu$ | $\mu$ | $\mu$ | $\mu$ | $\mu$ | $\mu$ | $\mu$ | $\mu$ | $\mu$ | $\mu$ |
| Flint | 10 | 20 | 35 | 75 | 75 | 75 | 75 | 10 | 20 | 35 | 35 to 75 | 75 | 10 | 35 to 75 | 10 | 35 to 75 | (Ball clay) | |
| Feldspar | 75 | 75 | 75 | 75 | 10 | 20 | 35 | 10 | 20 | 35 | 35 to 75 | *S* [2] | 10 | 10 | (Ball clay) | | 10 | 35 to 75 |
| Batch compositions: 15 percent ball clay. 35 percent kaolin. 35 percent flint. 15 percent feldspar. | | | | | | | | | | | | | 50 percent flint. 50 percent feldspar. | | 50 percent flint. 50 percent ball clay. | | 50 percent feldspar. 50 percent ball clay. | |

[1] Values in the table designate the nominal diameter limits of each fraction. For further details see table 2.
[2] Portion of original sample which was reground.

## 4. BODIES

### (a) COMPOSITIONS

The body compositions are given in table 3.

The mixtures of clay, flint, and feldspar designated as bodies 1 to 12, inclusive, approximate an average between American earthenware and hotel china compositions. Bodies 18 to 24, inclusive, were subsequently prepared to find additional data bearing on the differences in thermal expansion of bodies 8 and 11 heated to 1,150° C.

### (b) PREPARATION OF SPECIMENS

Specimens of bodies 1 to 12, inclusive, were prepared by wet-mixing the ingredients for approximately 4 hours and 20 minutes (18,000 revolutions) in a ball mill, using no stones. The resultant "slips" were passed over a magnetic separator, through a no. 80

[7] The term "hydrolysis", as applied to feldspar, is suggested by H. G. Byers (unpublished data), Bur. Chem. and Soils, U.S.Dept.Agr.
[8] For more extensive data on the leaching of silica and feldspar by water, and by acid and salt solutions, see Cushman and Hubbard, U.S. Dept. Agr. Bull. 28 (1907), Lenher and Truog, J.Amer.Chem.Soc. 38, 1058 (1916), and Joseph and Hancock, J.Chem.Soc. (Brit.) 123, 2022 (1923).

sieve, and dried on plaster to a plastic consistency. These plastic masses [9] were aged in a damp closet for 1 week, then hand kneaded and extruded as rods one half inch in diameter and 6 inches long. A sufficient number of rods were prepared to permit determinations of shrinkage, water absorptivity, and strength on from 10 to 12 specimens of each body from each heat treatment. In addition, specimens for thermal-expansion determinations were molded in the form of disks about 2 cm in diameter, 0.3 cm in thickness, with a hole through the center about 0.7 cm in diameter; and having three small equally spaced cones or "feet" protruding from each side. The average height varied between 0.50 and 0.75 cm. Specimens of each body were heated in a laboratory kiln, using gas as fuel, at five different temperatures, namely, 1,150°, 1,200°, 1,250°, 1,300°, and 1,350° C. For the final 200° the temperature was raised at the rate of 20° per hour and the maximum temperature was maintained for 45 minutes.

The only specimens prepared of bodies 18 to 24, inclusive, were discs for thermal expansion determinations. Since bodies 18 and 20 (flint-feldspar mixtures) were not self-bonding, gum tragacanth was used as a binder. All of these bodies were heated for 1 hour at 1,150° C. in an electrically heated furnace.

### (c) METHODS OF TEST

The linear shrinkage was determined by measuring the distance, after drying and after heating, between two gage marks which had been pressed 100 mm apart into the freshly extruded rods. Percentage values are based on the original distance between gage marks.

The water absorptivity, or apparent porosity, of the rods after heating was calculated from the dry weight, the weight after saturating by immersing in water and "autoclaving" for 5 hours at a steam pressure of 150 lb./in.$^2$, and the bulk volume. The bulk volume was calculated from the weight in air and the weight when suspended in mercury.

To determine the transverse strength a span of 4 inches was used for all of the no. 1 bodies, and for all of the no. 8 bodies except those heated to 1,150° C. A span of 4½ inches was used for all others. The load was applied at midspan and the strengths calculated in terms of modulus of rupture.

Thermal expansions were determined by the interferometer method,[10] using a heating rate of 2° to 3° C. per minute.

The relative fusion and solution which had taken place in the body structures after the several heat treatments was estimated by miscroscopic examinations of thin sections.

[9] In order to produce optimum workability of each body (nos. 1 to 12, inclusive) it was necessary to vary the water content, known also as the "tempering water", from 20 percent in body 11 to 34 percent in body 8. At best, bodies 1, 2, 8, and 9 were very difficult to knead and extrude while bodies 5 and 6 appeared but slightly better. Careful comparisons of the workability of bodies 18 to 24, inclusive, were not made. The general observation that workability is decreased by using very fine fractions of flint and feldspar applied to all of the bodies.

[10] G. E. Merritt, B.S. Research Paper No. 515, 1933.

FELDSPAR and FLINT
FLINT
CONSTITUENT: FELDSPAR

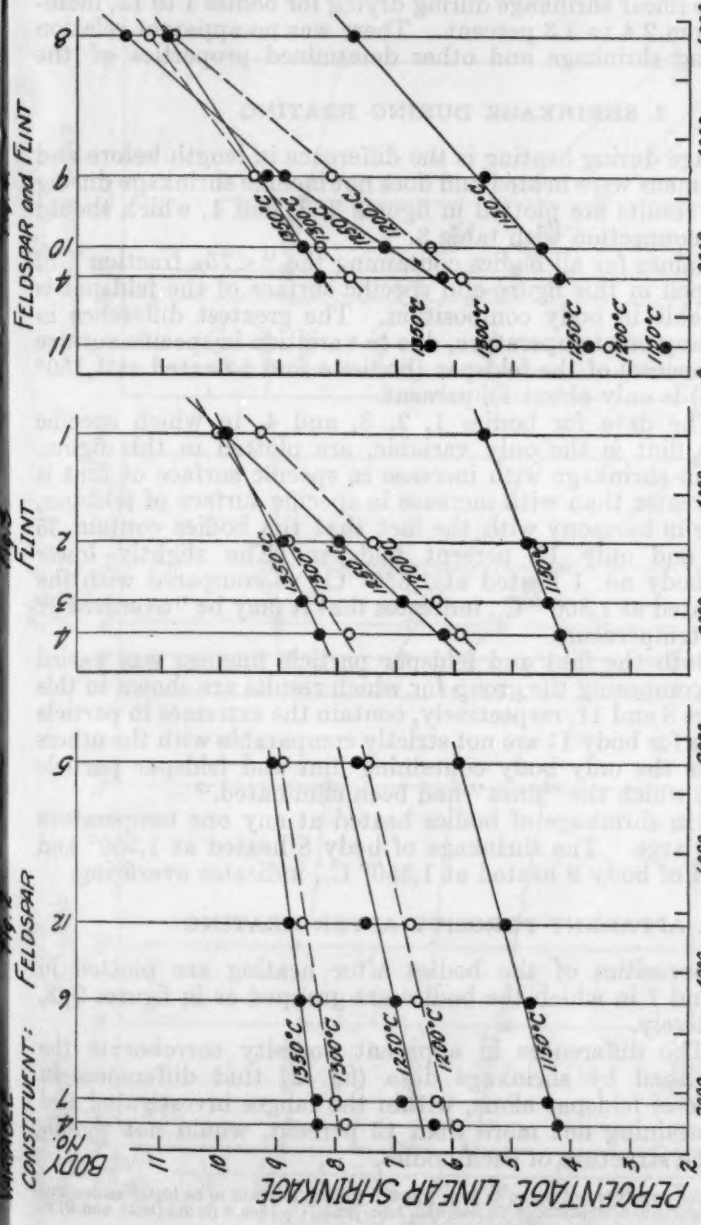


FIGURES 2, 3, and 4.—*The relation between percentage linear shrinkage during heating and the specific surface (in cm²/g) of the variable constituent in the several bodies the numbers of which are given at the upper part of the graph. The temperatures accompanying the curves indicate the maximum temperatures to which the respective groups of bodies were heated. Since the mean diameter (and specific surface) of both the feldspar and flint fractions was varied in the bodies for which data are given in figure 4, the specific surface values were calculated as the weighted average for the feldspar and flint.*

## III. PROPERTIES OF BODIES

### 1. SHRINKAGE DURING DRYING

The average linear shrinkage during drying for bodies 1 to 12, inclusive, varied from 2.4 to 3.3 percent. There was no apparent relation between drying shrinkage and other determined properties of the bodies.

### 2. SHRINKAGE DURING HEATING

The shrinkage during heating is the difference in length before and after the specimens were heated and does not include shrinkage during drying. The results are plotted in figures 2, 3, and 4, which should be studied in connection with table 3.

Figure 2. Values for all bodies containing the "$<75\mu$ fraction" of flint are grouped in this figure and specific surface of the feldspar is the only variable in body composition. The greatest difference in shrinkage, at any one temperature, due to variation in specific surface (or particle fineness) of the feldspar (bodies 4 and 5 heated at 1,150° and 1,200° C.) is only about 1½ percent.

Figure 3. The data for bodies 1, 2, 3, and 4, in which specific surface of the flint is the only variable, are plotted in this figure. The increase in shrinkage with increase in specific surface of flint is appreciably greater than with increase in specific surface of feldspar, which effect is in harmony with the fact that the bodies contain 35 percent flint and only 15 percent feldspar. The slightly lower shrinkage of body no. 1 heated at 1,350° C., as compared with the same body heated at 1,300 ° C., indicates that it may be "overfired"[11] at the higher temperature.

Figure 4. Both the flint and feldspar particle fineness was varied in the bodies composing the group for which results are shown in this figure. Bodies 8 and 11, respectively, contain the extremes in particle sizes. Results for body 11 are not strictly comparable with the others because this is the only body containing flint and feldspar particle fractions from which the "fines" had been eliminated.[12]

Differences in shrinkage of bodies heated at any one temperature are relatively large. The shrinkage of body 8 heated at 1,300° and 1,350° C., and of body 9 heated at 1,350° C., indicates overfiring.

### 3. APPARENT POROSITY AFTER HEATING

Apparent porosities of the bodies after heating are plotted in figures 5, 6, and 7 in which the bodies are grouped as in figures 2, 3, and 4, respectively.

Figure 5. The differences in apparent porosity corroborate the evidence furnished by shrinkage data (fig. 2) that differences in specific surface of feldspar alone, within the ranges investigated and for bodies containing not more than 15 percent, would not significantly alter the structure of such bodies.

[11] That is, a vesicular structure had begun to form which is a condition held to be highly undesirable because of decreased mechanical strength; H. H. Sortwell, Jour. Amer. Cer. Soc. 6 (8) 915 (1923), and R. F. Geller, Bull. Amer. Cer. Soc. 12 (1) 18 (1933).

[12] Specific surface increases so rapidly with decreasing particle size, and the finest particles are so difficult to see and to measure, that the calculated specific surface values for the fractions containing "fines" are probably systematically lower than the values for the $35\mu$ to $75\mu$ fractions when compared with the respective true values. Such an assumption would account for the fact that results for body 11 (figs. 4 and 7) are not in better alignment with results for the other bodies.

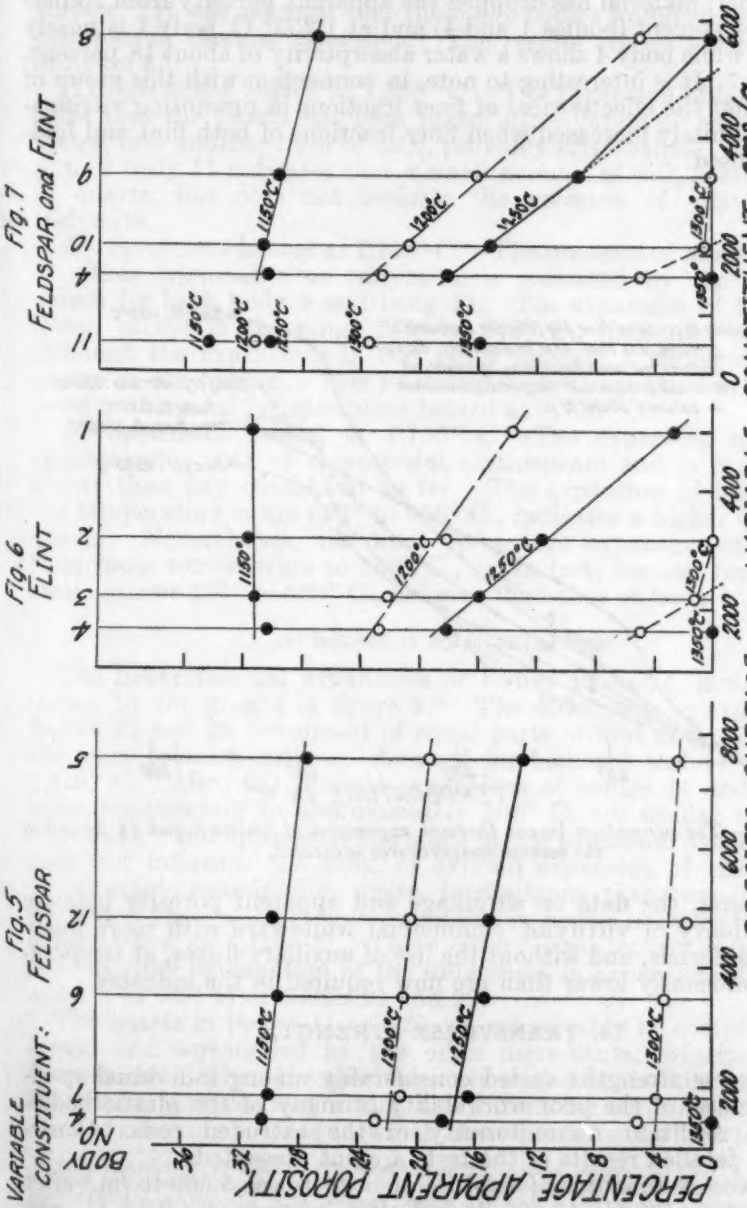


FIGURES 5, 6, and 7.—*The relation between percentage apparent porosity after heating and the specific surface (in cm²/g) of the variable constituent in the several bodies. The bodies are grouped, and the graphs compiled, in the same manner as in figures 2, 3, and 4, respectively. After heating at 1,350° C. all of the specimens, excepting those of body 11 (fig. 7), showed no measureable porosity; also, after heating at 1,300° C. body 1 (fig. 6) and body 8 (fig. 7) showed no porosity.*

Figure 6. This group of bodies, in which specific surface of the flint is the only variable, shows interesting differences after having been heated to 1,200° C. and higher temperatures. At 1,200° C., for example, the substitution of $<10\mu$ flint for $<75\mu$ (or practically commercial) material has dropped the apparent porosity from 23 percent to 14 percent (bodies 1 and 4) and at 1,250° C. body 1 is nearly vitrified, while body 4 shows a water absorptivity of about 18 percent.

Figure 7. It is interesting to note, in connection with this group of bodies, that the effectiveness of finer fractions in promoting vitrification is definitely increased when finer fractions of both flint and feldspar are used.

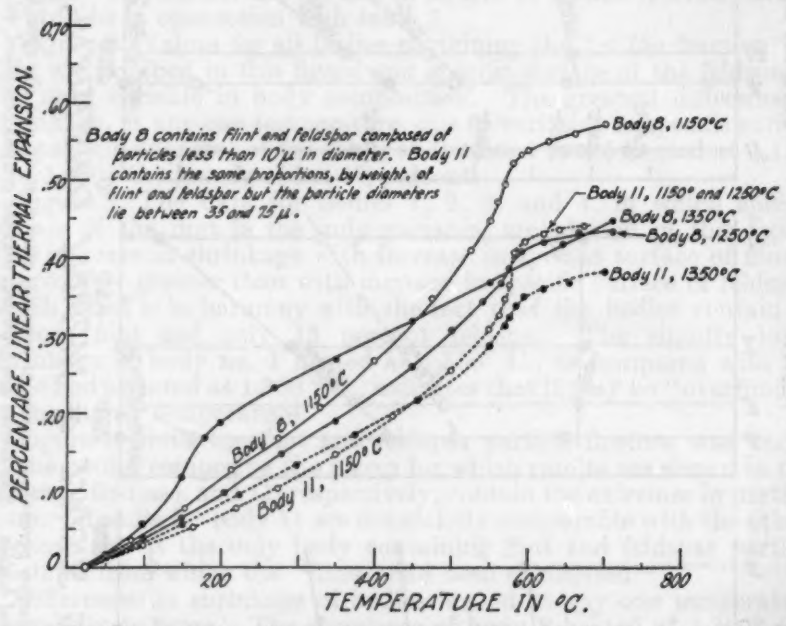


FIGURE 8.—*The percentage linear thermal expansion of bodies 8 and 11 heated to the several temperatures indicated.*

In general, the data on shrinkage and apparent porosity indicate the possibility of vitrifying commercial whiteware with more finely ground materials, and without the use of auxiliary fluxes, at temperatures significantly lower than are now required in the industry.

### 4. TRANSVERSE STRENGTH

Transverse strengths varied considerably among individual specimens because of the poor workability of many of the plastic bodies and the resultant nonuniformity of the extruded rods. Consequently, detailed results of the tests are not presented.

The average modulus of rupture of body 8 was 5,600 lb./in.$^2$ after heating at 1,150° C., 10,000 lb./in.$^2$ after heating at 1,250° C., and 10,800 lb./in.$^2$ after heating at 1,350° C. Equivalent values for body 11 were 1,900, 2,300, and 4,300 lb./in.$^2$, respectively. These values represent the extremes.

## 5. LINEAR THERMAL EXPANSION

### (a) BODIES 1 TO 12, INCLUSIVE

The only specimens of bodies 1 to 12 tested were those of bodies 8 and 11 which contain the fractions of highest and lowest specific surface. It was assumed that these two bodies would show, also, the extremes in thermal expansion. The results are shown graphically in figure 8.

(1) Specimens heated at 1,350° C.—The expansion of body 8 indicates that the quartz has been taken into solution or has been converted into another form of $SiO_2$, probably cristobalite. The expansion of body 11 indicates that a small amount of $SiO_2$ is still present as quartz, but does not indicate the presence of cristobalite or tridymite.

(2) Specimens heated at 1,250° C.—The presence of quartz, but not of either cristobalite or tridymite, is indicated by the expansion values for both body 8 and body 11. The expansion of body 11 is lower, except in the range 550° to 600° C., than that of body 8, although the expansions in this range indicate a higher content of quartz in the former. This relatively higher expansion of body 8 is more pronounced for specimens heated at 1,150° C.

(3) Specimens heated at 1,150° C.—The expansion of body 8 approximates that of commercial earthenware and is considerably higher than any considered so far. The expansion of body 11 for the temperature range 550° to 600° C., indicates a higher content of quartz. Nevertheless, the total percentage expansion of body 11 from room temperature to 700° C., or, in fact, for any temperature range except 550° to 600° C., is lower than that of body 8.

### (b) BODIES 18 TO 24, INCLUSIVE

The linear thermal expansions of bodies 18 to 24, inclusive, are shown by the graphs in figure 9.[13] The differences in expansion of bodies 21 and 22 (composed of equal parts of flint and clay), are of the same relative order as observed for bodies 8 and 11 heated at 1,150° C. Also, the thermal expansions of bodies 11 and 22 from room temperature to approximately 500° C. are similar to that of clay alone [14] and apparently the much higher expansion of the quartz [15] does not influence the bulk, or over-all expansion of the bodies.[16] Petrographic examination shows, furthermore, that very little reaction takes place at clay-quartz contacts in bodies heated at temperatures as low as 1,150° C. These observations, collectively, suggest the following explanation of the differences in expansion of bodies 8 and 11, as well as of bodies 21 and 22:

The quartz in bodies 11 and 22 can conceivably be completely dispersed and surrounded by the other ingredients, principally clay. Consequently, when the specimens are cooled in the kiln or furnace, the quartz particles may shrink away from the surrounding mass of the body leaving a space in which these particles are free to expand

[13] Specimens made of flint and 35μ to 75μ feldspar could not be tested because they were too friable. Furthermore, it was reasonably certain that the difference in the degree of fusion between a "35μ to 75μ fraction" of feldspar, and that of a "<10μ fraction", heated at 1,150° C. would not alter the thermal expansion sufficiently to explain the facts regarding bodies 8 and 11. See footnote 6, page 330.

[14] This refers to clay which has not been heated sufficiently to cause formation of mullite and cristobalite. See W. Steger, Ber. d. Deut. Ker. Gesell. 13 (9) 412, 1932, and R. A. Heindl, B.S.Jour. Research, vol. 8 (RP410), p. 199, 1932.

[15] R. B. Sosman, The Properties of Silica, p. 363, The Chem. Cat. Co., 1927.

[16] A similar phenomenon has been observed in connection with clay refractories, J. B. Austin and R. H. H. Pierce, Jr., Jour. Amer. Cer. Soc. 16 (2) 104 (1933).

and contract to a limited amount and therefore have only a limited influence on the bulk or overall expansion. In bodies 8 and 21, however, it is conceivable that the total differential contraction is not sufficient for the quartz to free itself, and therefore the quartz can exert a relatively greater influence on the bulk expansion.

Applying this hypothesis to explain the fact that bodies 18 and 20 have the same expansion curve, it is necessary to assume that the bond between the flint and the feldspar was sufficient to prevent even the large flint particles from freeing themselves in the cooling process.

The curves for bodies 23 and 24 apparently indicate that the presence of flint in the body is necessary to cause the difference in expansion of bodies 8 and 11.

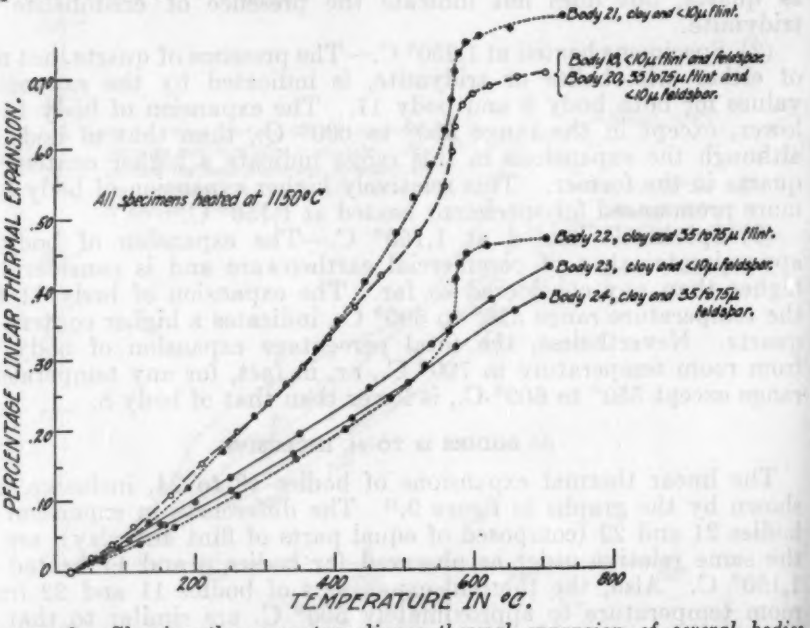


FIGURE 9.—*Showing the percentage linear thermal expansion of several bodies heated at 1,150° C. and containing 50 percent each of clay and flint, flint and feldspar, or clay and feldspar. This group of bodies was tested to obtain further information on the cause of the differences in expansion of bodies 8 and 11 heated to 1,150° C. (fig. 8).*

## 6. FUSION AND SOLUTION

### (a) SPECIMENS HEATED AT 1,350° C.

All of the $<10\mu$, and nearly all of the $<20\mu$, feldspar had become diffused through the body. Larger particles of feldspar had lost their sharp outline and were mottled in appearance, indicating the presence of mullite.

A small quantity of the finest particles of quartz (about 10 percent of the body) could be seen in body 8, although the thermal expansion data did not indicate its presence. Larger particles showed wide solution rims of low index of refraction.

It could be seen plainly that development of mullite had taken place in larger clay particles.

(b) SPECIMENS HEATED AT 1,250° C.

No grains of feldspar could be detected in bodies containing the $<10\mu$ fraction, but a considerable number were distinguishable in bodies containing the $<20\mu$ fraction. Larger particles showed fairly sharp outlines. The mottled appearance was distinct in portions of $35\mu$ to $75\mu$ particles and was quite uniform in particles of less than $35\mu$ diameter.

The larger quartz particles showed very narrow solution rims, and appreciably less of the very finest particle fraction had dissolved as compared with specimens heated at 1,350° C.

(c) SPECIMENS HEATED AT 1,150° C.

Even the coarsest particles of feldspar, although completely fused to glass, maintained sharp outlines; the finest ($<10\mu$) particles could be detected in considerable quantities. None of the quartz particles of sufficient size to be identified showed solution rims and probably not more than 10 percent of the $<10\mu$ fraction (body 8) had dissolved.

## IV. SUMMARY

A feldspar and a potter's flint (crushed quartz) of commercial grade were separated by means of an air elutriator into fractions, and in addition a portion of the original feldspar was reground.

The calculated specific surface, based on data obtained by microscopic count, varies from 450 $cm^2/g$ for the 35 to 75 micron flint fraction to 7,500 $cm^2/g$ for the less than 10 micron feldspar fraction. The relative solubility of even the finest particle-size fractions of flint is probably negligible (0.04 g per liter) while the solubility of the feldspar varied from 0.025 g per liter for the 35 to 75 micron fraction to 0.120 g per liter for the finest fraction.

In general, the workability is decreased by using the very fine fractions of flint and of feldspar. There is comparatively little difference in linear shrinkage during drying; the extremes were 2.4 and 3.3 percent.

Varying the specific surface of feldspar only, does not greatly affect the shrinkage during heating at any one temperature; the maximum increase was from 5.9 percent to 7.5 percent. The effect on apparent porosity is also relatively small; the maximum reduction was from 18.4 percent to 13 percent. This indicates, for a body containing only 15 percent feldspar, that feldspar of less than 10 microns diameter can be substituted for one of the same chemical composition but of average present-day commercial fineness without greatly altering the ultimate structure of the body. The effects of varying the mean particle size, or specific surface, of flint only is more pronounced; the maxima were from 6.4 percent to 10 percent increase in linear shrinkage and from 18.5 percent to 2.8 percent reduction in apparent porosity. The greater effectiveness of the flint is in harmony with the fact that the bodies contain 35 percent flint and only 15 percent feldspar. Using increasingly finer fractions of both flint and feldspar produced a maximum increase in shrinkage from 6 percent to 11.6 percent and a maximum reduction in porosity from 18 percent to zero percent.

Transverse strengths varied between the extreme modulus of rupture values of 5,600 and 1,900 lb./in.$^2$ respectively for bodies heated

at 1,150 ° C., and 10,800 and 4,300 lb./in.$^2$ for the same bodies heated at 1,350° C.

Linear thermal-expansion determinations warrant the generalization that thermal expansion may be influenced greatly by extremes in particle size of flint and feldspar. The use of flint containing no particles of less than 35 microns diameter may produce bodies of unusually low expansion when compared with bodies of similar composition but containing much finer flint.

The effects of particle-size variations on relative fusion and solution in the body structures were well defined when observed microscopically.

## V. CONCLUSIONS

The data obtained indicate the possibility of vitrifying commercial ceramic whiteware with more finely ground materials, and without the use of auxiliary fluxes, at temperatures significantly lower than are now required in the industry. Further studies of the effects of particle sizes of flint and feldspar in ceramic whiteware bodies, particularly with regard to the development of bodies which can be used advantageously on a commercial scale, are believed justified.

WASHINGTON, July 24, 1933.

UNITED STATES DEPARTMENT OF COMMERCE, BUREAU OF STANDARDS

RESEARCH PAPER RP595

*Part of Bureau of Standards Journal of Research, Vol. 11, September 1933*

# COMPARISON OF HIGH VOLTAGE X-RAY TUBES

By Lauriston S. Taylor, George Singer, and C. F. Stoneburner

ABSTRACT

A comparison of the X-ray output as a function of the applied voltage has been made for 2 thin glass X-ray tubes, 5 thick glass tubes, and 1 metal-centered tube on several generators of different voltage wave form. Thin glass tubes show about 15 percent greater output than thick glass tubes on constant potential, while the metal-centered tube gave about 15 percent less output. At any given effective (rms) voltage, the outputs of all glass tubes on all generators were nearly the same, and equal to the output on a constant potential of the same value. Likewise, at a given effective voltage, the quality (full absorption curve) was the same for all tubes on all generators.

Outputs of all tubes at a given peak voltage varied over a range of 25 percent between tubes and between different generators. The metal-centered tube output varied widely between half and full wave rectification at equal peak voltages. The same tube, however, gave the same output at any given effective voltage supplied by any generator.

CONTENTS

| | Page |
|---|---|
| I. Introduction | 341 |
| II. Experimental results | 342 |
| 1. Tubes and generators employed | 342 |
| 2. Output on constant potential | 344 |
| 3. X-ray output per average milliampere | 344 |
| 4. X-ray output per effective milliampere | 345 |
| 5. Measurements on metal-centered tube (T5) | 349 |
| 6. Relationship of X-ray quality to voltage measurements | 350 |

## I. INTRODUCTION

Previous papers from the Bureau of Standards X-ray laboratory[1 2 3 4] have dealt with the relationship between the applied X-ray tube voltage and the intensity and quality of the emitted radiation measured under given filtrations and other conditions. These showed for a wide variety of applied voltage wave forms that, regardless of the peak voltage, the resultant X-ray qualities as given by a full absorption curve are alike for any given effective voltage; also the outputs per effective milliampere [5] for a given tube operated on

[1] L. S. Taylor and K. L. Tucker, B.S.Jour. Research, vol. 9, p. 333, 1932. Also Amer. Jour. Roent.
[2] L. S. Taylor, G. Singer, and C. F. Stoneburner, B.S.Jour. Research, vol. 9, p. 561, 1932.
[3] L. S. Taylor, Strahlentherapie.
[4] L. S. Taylor, G. Singer, and C. F. Stoneburner, B.S.Jour. Research, vol. 11, p. 293, 1933.
[5] See footnote no. 2.

the various voltage wave forms are nearly the same at any given effective voltage. As a consequence, the quality (and intensity, to a certain extent) of all radiations is expressible in terms of two readily measured quantities, the effective tube voltage and effective tube current.

This previous work was carried out, using thin-walled glass Coolidge tubes which are free from certain inherent disadvantages present in other tubes. In order that the relationship between quantity, quality, and effective tube voltage might be more completely generalized, however, it is, of course, necessary to investigate the effect with the other types of tubes and generators.

Most prominent among the newer tubes are the several American makes of thick-walled pyrex tubes, and the foreign tubes of the metal-centered type. In operating the thick-walled tubes on a fluctuating voltage, it is found that the output changes (usually decreased) some 20 percent during the first few minutes of operation, even though the average tube current and transformer primary (rms) voltage are held constant.[6] [7] This is caused by current and voltage wave-form change arising from the interaction of the transformer and tube, which change in turn is caused by a high electrostatic charge on the tube walls acting as a charged grid when the tube is cold but which is dissipated as the glass heated up. It was then found [7] that by maintaining the effective tube voltage and current constant during the transition period, a change in output no longer occurred. That is, output readings for any effective voltage and current are characteristic of the tube, irrespective of accumulated charge on the glass walls. On the other hand, using the customary peak voltage and average current measurements, sufficient time must also be allowed to permit the tube to reach a steady state before making output measurements.

While this grid action is not present in the metal-centered type of tube another difficulty in arriving at an adequate comparison of tubes is introduced through the elimination of stem radiation from the ionization readings. With the common glass tube, stem radiation may amount to 10 to 20 percent of the total, and this, in general, [8] is of a considerably softer quality than the focal spot radiation.[9] [10]

In view of the above described tube differences, the principal purpose of this investigation was to further compare the operation of several typical X-ray tubes on a group of typical X-ray generators.

## II. EXPERIMENTAL RESULTS

### 1. TUBES AND GENERATORS EMPLOYED

The arrangement of the equipment is the same as in our recent studies of generators.[11] The tube was in a lead box 4 by 4 by 7 feet, lined with one fourth inch of lead (fig. 1), with a fixed insulating support insuring a uniform distance from the center of the target to the ionization chamber. In addition to the box being well ventilated, a strong blast of air could be directed against the tube walls.

[6] M. J. Gross, Radiology, vol. 20, p. 14, 1933.
[7] L. S. Taylor and C. F. Stoneburner, B.S.Jour. Research, vol. 10, p. 233, 1933.
[8] W. D. Coolidge and C. N. Moore, G. E. Rev., p. 272, April 1917.
[9] E. Lorenz, Proc. Nat. Acad. Sci., vol. 14, p. 582, 1928.
[10] L. S. Taylor and G. Singer, B.S.Jour. Research, vol. 6, p. 219, 1931.
[11] See footnote no. 4, p. 341.

Simultaneous measurements were made of the effective (rms) tube voltage and current, peak voltage, average voltage and average current in the high tension circuit. The average and effective voltage were measured by means of a 150-megohm coronaless shielded resistor [12] used as a voltmeter multiplier. As before, to avoid possible uncertainties in the comparison of tubes, the aerial system was kept the same for all generators. Tubes and generators could be changed within a minute's time. The results have been checked repeatedly over a period of several months.

Radiation emerged from the box through a 10-cm aperture forming a beam about 14.5 cm in diameter at the ionization chamber, thus giving similar to conditions used clinically. A fixed filter of 0.557 mm Cu + 1.0 mm Al was placed over the aperture with the copper toward

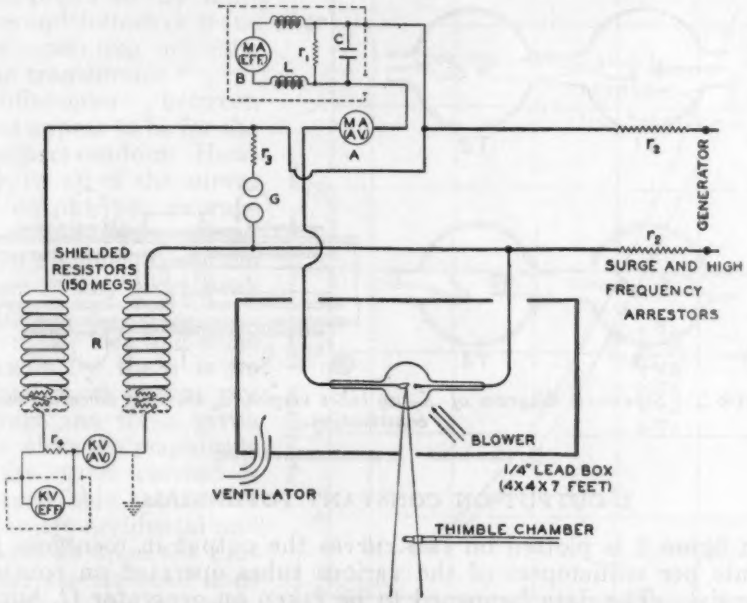


FIGURE 1.—*Diagram showing arrangement of apparatus used in the comparison of X-ray tubes.*

the tube. Ionization measurements were made in air with a calibrated thimble chamber at a distance of 50 cm from the target center, particular care being taken to avoid the inclusion of any spurious (scattered) radiation, particularly back-scattering and scattering from the diaphragm. The only difference between this arrangement and the one previously used in our generator comparisons is in the diameter of the beam at the point of measurement. In the earlier work (with thin-walled tubes) the beam diameter was 5.5 cm, as compared with 14.5 cm in this work. The resulting difference in measured ionization was 9 ± 0.4 percent at all voltages and is attributable to the inclusion of more stem radiation in the larger beam. The measurements given here for thin-walled tubes are our earlier values increased by 9 percent which change renders the results in this paper directly comparable with our earlier work. The following high

[12] L. S. Taylor, B.S.Jour. Research, vol. 5, p. 609, 1930.

voltage generators, as previously designated, were used: (B) Mechanical rectifier, double high-tension transformer in single tank, rectifies 20 electrical degrees of each half cycle; (C) Constant potential, commercial, 2 percent ripple per ma; (D) Half-wave kenotron rectifier; (E) Full-wave kenotron rectifier; (F) Constant potential (B.S. Standard), 0.2 percent ripple per ma.

The following X-ray tubes (fig. 2) were used: *T1*, (2 tubes) thin glass, massive target; *T2*, (2 tubes) thick glass, massive target; *T3*, (2 tubes) thick glass, disc target; *T4*, (1 tube) thick glass, disc target; *T5*, (1 tube) metal centered, line focus, water cooled.

It may be stated here that all tubes of the same make and type gave practically the same output on any one generator so the results obtained with one tube only of each type are given.

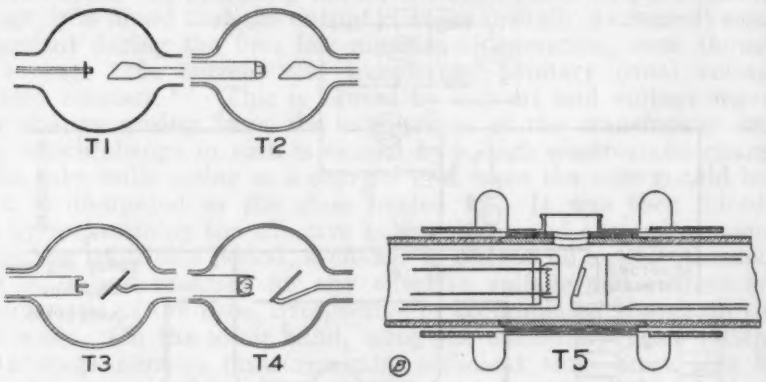


FIGURE 2.—*Schematic diagram of X-ray tubes employed, showing essential details of construction.*

[A, glass tubes. B, metal-centered tube]

## 2. OUTPUT ON CONSTANT POTENTIAL

In figure 3 is plotted on two curves the output in roentgens per minute per milliampere of the various tubes operated on constant potential. The data happened to be taken on generator C, but as pointed out previously there is no appreciable difference between the outputs using generators (C) and (F), although the ripplage of (F) is only about a tenth that of (C). The lower curve for the thick-walled tubes (*T2*, *T3*, and *T4*) clearly shows no appreciable difference between the outputs per ma at any given voltage. The upper curve for the thin-walled tube (*T1*) shows a considerably higher output than the thick-walled at all voltages—ranging from about 17 percent at 105 kv to 14 percent at 145 kv. A decrease in relative output with increased voltage is to be expected, since at the higher voltages, the radiation being harder, the absorption in the thick glass walls becomes relatively less.

## 3. X-RAY OUTPUT PER AVERAGE MILLIAMPERE

As in our previous study of X-ray generators, output curves obtained under the more common criteria of control, are given first to show the limitations therein. In comparing the tubes operated on different generators, it is least confusing to group on one graph the

outputs of all the tubes on one particular generator. Figures 4, 5, and 6 show the output per average ma, for the full-wave (E), half-wave (D), and mechanical rectifier (B), respectively, as a function of the peak voltage. The upper curve in all three figures is for tube *T3* on the constant potential generator (C).

It is evident from the curves that there is a considerable difference between the outputs of individual tubes when operated on the same generator. At 180 kv (peak) the maximum difference on the full-wave rectifier is about 28 percent; on the half-wave rectifier about 32 percent, and on the mechanical rectifier about 35 percent. Part of the difference is attributable to differences in the transformer design, but earlier studies have shown that there is not necessarily any similarity between the outputs produced by half-wave and full-wave rectifiers operating on the same transformer.[13]

Differences between tubes appear to be for the most part random. However, in all of the curves the output per average ma of tube *T3* is predominantly higher than the others at any given peak voltage.

It is also seen that while occasionally there is no difference in output per average ma for a given tube when the magnitude of the tube current is changed, this appears to be largely accidental and dependent upon the particular circuit conditions for which the measurements were made.

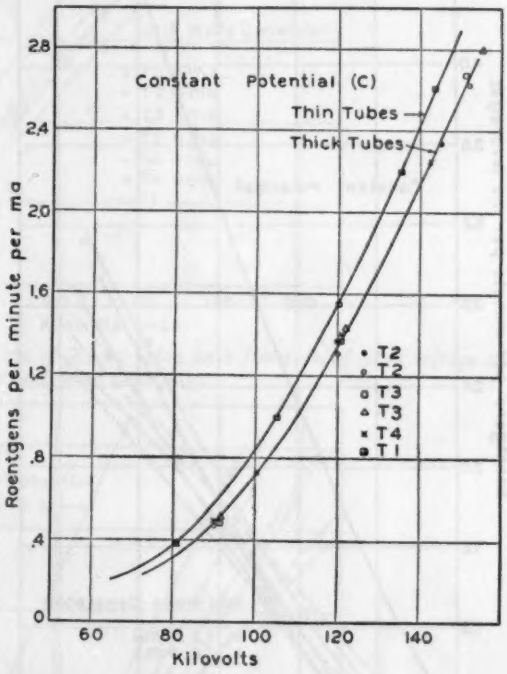


FIGURE 3.—*Output of X-ray tubes on constant potential.*

It should be emphasized that the basing of any general conclusions regarding the relative efficiency of tubes based on measurements of peak voltage and average tube current is unsafe. Depending upon the generator and tube current, such a wide range of outputs is obtainable under supposedly the same conditions as to render the results almost meaningless.

## 4. X-RAY OUTPUT PER EFFECTIVE MILLIAMPERE

Earlier investigations with thin-walled tubes operated on a group of representative generators, showed a much closer agreement in output at any given values of the effective tube current and effective voltage.

[13] See footnote no. 4, p. 341.

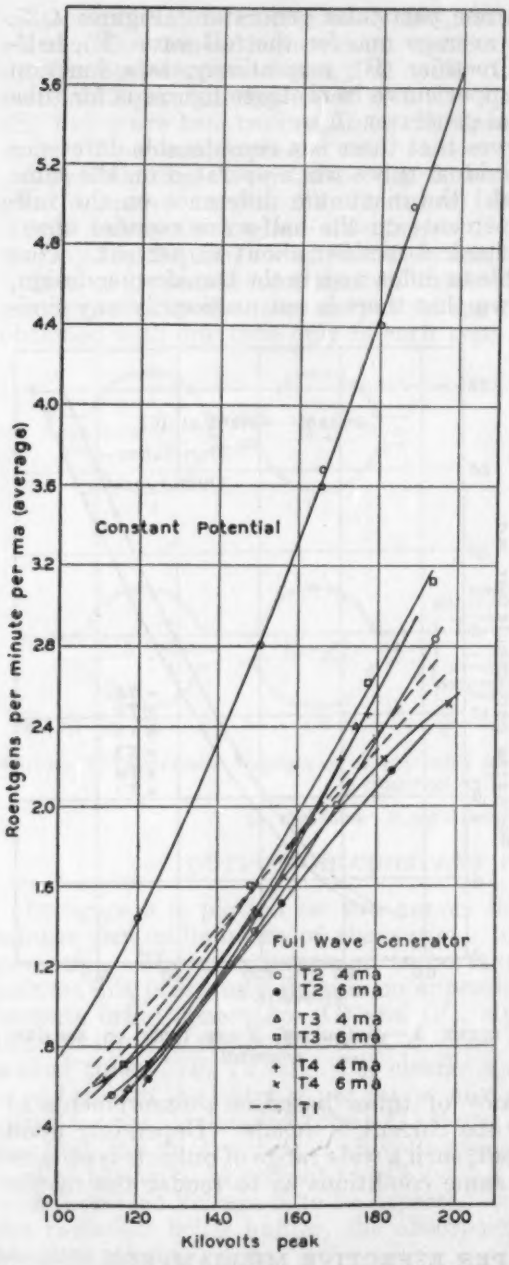


FIGURE 4.—*Output per average ma of X-ray tubes as a function of peak voltage on full-wave generator.*

The curves in figures 7, 8, and 9 likewise show a close relationship for the thick-walled tubes on full-wave (E), half-wave (D), and mechanical rectifier (B), respectively. Data plotted for the thin tube are taken as before from a recent paper and corrected as noted above to the larger field area used in this study. The lower broken-line curve in figures 7 to 9 is for constant potential on the thick tubes and is taken from figure 3.

In figure 7 for the full-wave generator (E) the points for the various tubes are scattered somewhat at random about the constant potential curve; in general the outputs per effective milliampere are approximately the same. The upper broken-line curve is for constant potential (from fig. 3) on the thin tube (*T1*) and the two adjacent curves are for the same tube on the full-wave generator. The separation between the two constant potential curves is to be ascribed to the difference in filtration of the thin and thick glass walls.

In figure 8, for the half-wave generator, it is again seen that the outputs per effective milliampere are grouped fairly closely and at random about the constant potential curve. To obtain these curves, the actual meter readings of the voltage and current were corrected, as in our earlier work, by the factors $\sqrt{2}$ and $\sqrt{1/2}$, respectively, in order to make proper allowance for the suppressed half wave.[14] The two full-line curves for the

[14] See footnote no. 4, p. 341.

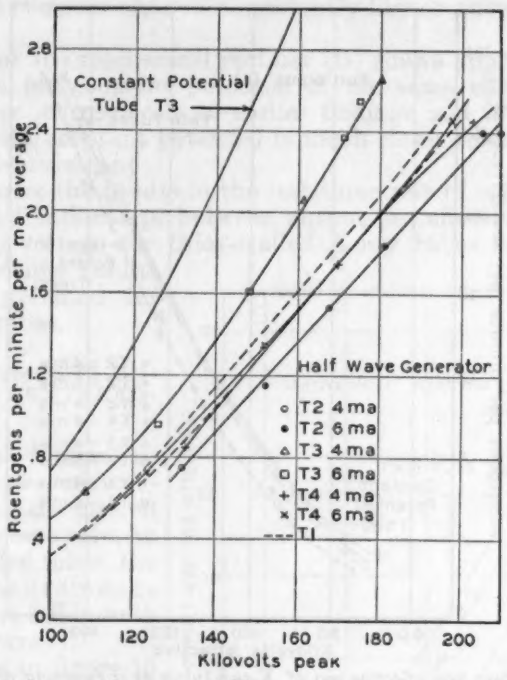


FIGURE 5.—*Output per average ma of X-ray tubes as a function of peak voltage on on half-wave generator.*

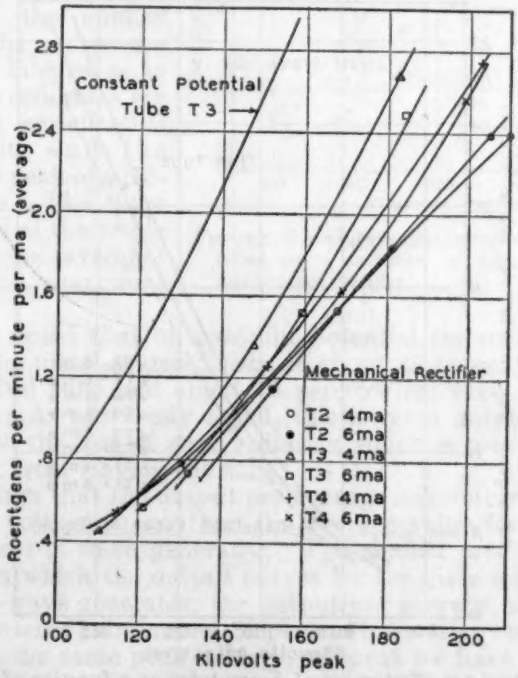


FIGURE 6.—*Output per average ma of X-ray tubes as a function of peak voltage on mechanical rectifier.*

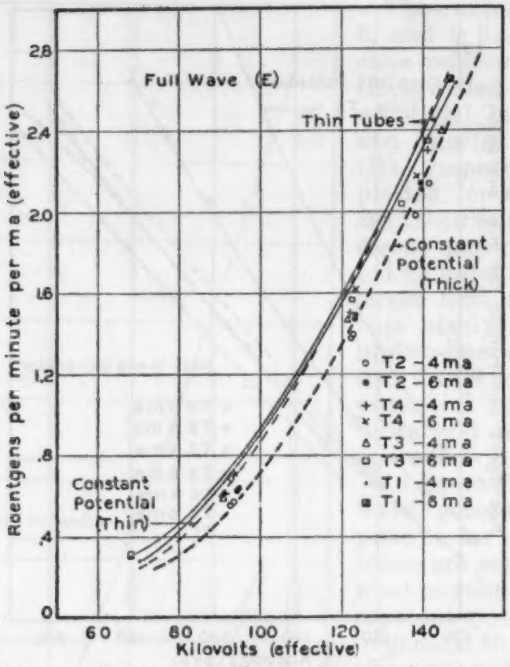


FIGURE 7.—*Output per effective ma of X-ray tubes as a function of effective voltage on full-wave rectifier.*

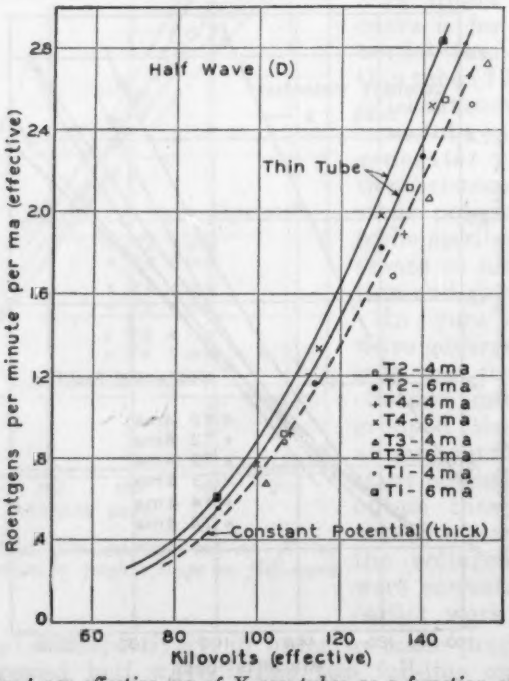


FIGURE 8.—*Output per effective ma of X-ray tubes as a function of effective voltage on half-wave rectifier.*

thin tube (*T1*) again show a consistently higher output at a given voltage.

Figure 9 for the mechanical rectifier (B) shows appreciably higher outputs than for constant potential of the same effective voltage. This, however, corresponds to earlier findings and in any case the agreement with constant potential is much closer than by any other method of measurement.

To summarize the results in the last three sets of curves, it may be said that the relationships between output per effective milliampere and effective voltage for thick-walled X-ray tubes follows closely the more detailed results previously presented for thin-walled tubes.

## 5. MEASUREMENTS ON METAL-CENTERED TUBE (T5)

Due to the fundamentally different construction of the metal-centered tube (*T5*) as compared with the glass-walled tubes, the output measurements thereon do not fall in with the other curves.

The curves in figure 10 show for this tube the output per milliampere as a function of the applied voltage. The curves are individually labeled as to whether the ordinates are for average or effective tube current, and the abscissae for peak or effective voltage. The tube was operated at the single current of 4 ma (average) which is its maximum rating.

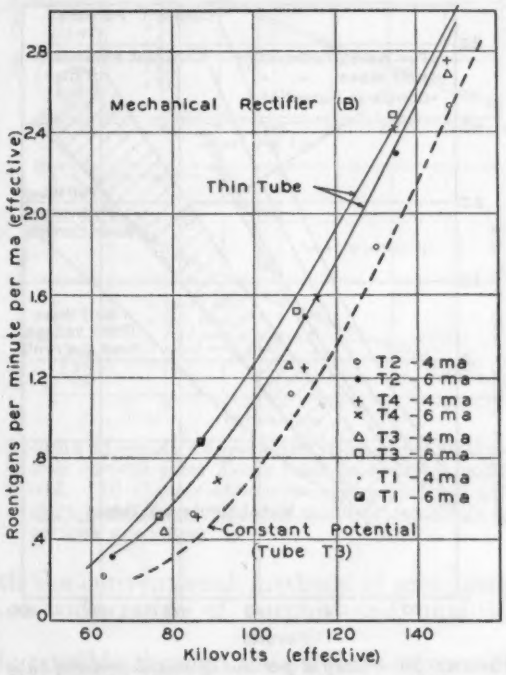


FIGURE 9.—*Output per effective ma of X-ray tubes as a function of effective voltage on mechanical rectifier.*

It will be noted that on constant potential the output per milliampere of the metal-centered tube is about 35 percent less than for the thin-walled tube and about 16 percent less than for the thick-walled tube. As previously noted, this lowered output is probably due partly to the loss of stem radiation which is prevented, by the metal shield, from leaving the tube.

It is also seen that the output per average milliamper as a function of the peak voltage is less than the average value for all the other tubes on the full-wave generator. The shaded area indicates the region within which the output curves for the glass-walled tubes lie. For the half-wave generator, the output per average milliampere for the metal-centered tube is some 30 percent lower than on the full-wave generator at the same peak voltage, whereas we have shown before

that for glass-walled tubes the difference introduced by use of the two types of wave form has comparatively little effect on the output per milliampere. This great decrease in output on the half-wave generator is due to the wave distortion introduced by the current limiting characteristics of such tubes.

As contrasted to the behavior of this tube on half- and full-wave generators when controlled by average current and peak voltage, it is found that the output per effective milliampere, as a function of the effective voltage, follows closely the output for constant potential. On this basis of comparison then the X-ray output for this tube (*T5*) is the same for all generators and thus conforms to the results found with glass tubes.

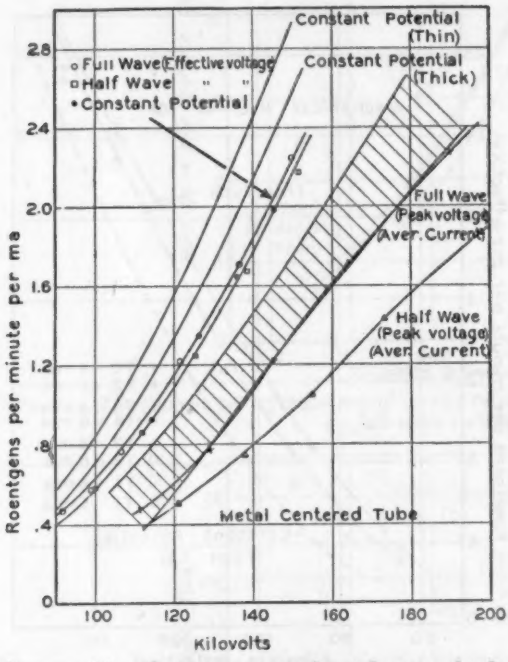


FIGURE 10.—*Output per ma of metal-centered tube on different generator.*

## 6. THE RELATIONSHIP OF X-RAY QUALITY TO VOLTAGE MEASUREMENTS

It has been shown by Silberstein [15] that radiations having the same complete absorption curves in copper (or aluminum) have likewise the same effective spectral distribution. Also, we have shown in recent studies, using thin-walled tubes, that radiations produced by the same effective voltage (by whatever voltage wave form, including constant potential) yield very closely the same full copper-absorption curve, regardless of the peak voltage.

This is corroborated by the semilogarithmic copper-absorption curves in figure 11. Curves A are for the tubes *T1* to *T5* operated on a constant potential of 141.4 kv. It is seen that at least after an initial filtration of 0.28 mm of copper, the absorption curves, and hence the quality, are all alike within reasonable limits. Tubes *T1* and *T4* do, however, appear to give a very slightly softer radiation than *T2* and *T3* which is to be expected since the latter tubes have the heaviest walls of the group.

Curves B show similar results for tubes *T3* on all generators, and tube *T5* on constant potential and full-wave rectifiers, all at 141.4 kv (effective) but at very different peak voltages. The two curves are identical with those in A and show that again the qualities are essentially the same on all generators at a given effective voltage. (The

[15] L. Silberstein, Phil. Mag., ser. 7, vol. 15, p. 375, 1933.

measured value of the effective voltage for the half-wave generator of 100 kv for the full cycle, was corrected by the factor $\sqrt{2}$ to give the true value during the useful half cycle.) Tube *T5* appears to yield a slightly harder radiation than the glass tubes, on both constant potential and full-wave rectification. This is probably due to the loss of the softer stem radiation which cannot contribute to the final result as in the case of the other tubes.

Our earlier conclusion is thus corroborated that (1) the quality of any X-ray beam may be adequately specified in terms of the constant voltage necessary to produce the same absorption curve, and (2) the qualities of the X-ray beams produced by any tube, in conjunction with different generators, are the same for a given effective (rms) voltage applied to the tube; (3) while there are necessarily small differences in output, due to such factors as wall thickness or elimination of stem radiation, these sources are readily recognized and allowances made therefor; and (4) with the conventional methods of measuring tube voltage and current, a wide range of outputs and qualities are obtainable.

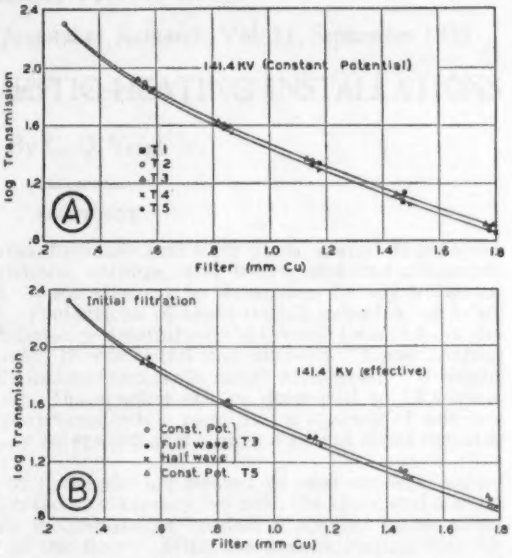


FIGURE 11.—(*A*) *Copper-absorption curves obtained with various glass X-ray tubes on constant potential.* (*B*) *Copper-absorption curves obtained with thick glass X-ray tube and metal centered tube on various generators.*

This work has been made possible through the cordial cooperation of the American manufacturers of X-ray tubes and equipment, to whom we express our appreciation.

WASHINGTON, May 10, 1933.

U.S. Department of Commerce, Bureau of Standards

RESEARCH PAPER RP596

*Part of Bureau of Standards Journal of Research, Vol. 11, September 1933*

# FIRE HAZARD OF DOMESTIC HEATING INSTALLATIONS

By G. Q. Voigt

**ABSTRACT**

Tests were conducted with stoves, furnaces, and their pipes, spaced at different distances from unprotected partitions, ceilings, and floors, and the maximum temperatures thereon measured, in an attempt to determine by experimental means the fire hazard involved. Protections of sheet metal, asbestos, or brick were then applied and the closest distance determined that would be safe from the standpoint of ignition of the wood. It was found that stoves for house heating should be spaced not less than 24 inches from walls faced with wood. If bright sheet metal is applied to the walls, the spacing can be decreased to 12 inches. Similarly, plastered wood stud partitions, while requiring a spacing of not less than 18 inches if unprotected, may be spaced at 9 inches if bright sheet metal is applied.

If stoves are without ashpits or if ashpits are heated to near redness, an air space of 5 inches or more was indicated as necessary between the stove and a wood floor, in addition to ¼-inch thick incombustible insulation applied under sheet metal over the exposed portion of the floor. With the firebox resting directly on the floor, temperatures high enough to cause ignition of wood were transmitted through a 4-inch brick base.

Tests with smokepipes indicated that a clearance of 12 inches from ceiling or joists was adequate. Where smokepipes pass through combustible partitions, either a ventilated air space of not less than 4 inches, or 2 inches of insulation all around the pipe, was found necessary.

Furnaces for hot-water installations and their pipes were found to present little hazard to adjacent construction as fired with either coal, oil, or gas. The hazard from warm-air heating ducts was found to be moderate, protections being required only where they enter floors or partitions relatively close to the furnace. In the case of the "pipeless" furnace the down-draft of cold air around the warm-air duct protects the adjacent construction, the hazard with this equipment resulting mainly from placing combustible materials on the warm-air register or locating the latter beneath or too close to partitions.

Tests with a gas range having an oven without insulation indicated that 6-inch separation between the side of the oven and a wood partition gives reasonably safe conditions.

**CONTENTS**

| | Page |
|---|---|
| I. Introduction | 354 |
| II. Tests to determine smokepipe hazards | 355 |
| 1. Equipment and testing methods | 355 |
| 2. Results of tests | 356 |
| III. Tests with smokepipe thimbles | 358 |
| 1. Description of thimbles | 358 |
| 2. Results of tests | 358 |
| IV. Tests with warm-air furnaces | 359 |
| 1. Equipment | 359 |
| 2. Temperatures of ducts | 360 |

Page
V. Floor protections ---- 362
1. Testing equipment ---- 362
2. Results of tests ---- 362
VI. Tests with wall protections ---- 364
1. Equipment and testing methods ---- 364
2. Results of tests ---- 364
VII. Gas ranges ---- 367
1. Testing methods ---- 367
2. Results ---- 367
VIII. General summary and conclusions ---- 367
1. Smokepipes ---- 370
2. Smokepipe thimbles ---- 370
3. Warm-air ducts ---- 370
4. Floor protection ---- 371
5. Wall protection ---- 371
6. Scope of application of results ---- 372
IX. Acknowledgments ---- 372

## I. INTRODUCTION

An annual fire loss for the country, as a whole, of about $20,000,000 is reported as caused by stoves, furnaces, boilers, and their pipes, or between 9 and 10 percent of the loss from all known causes. If heating installations are responsible for the same proportion of these fires, the causes of which could not be ascertained, the total fire loss per year from such installations would be about $45,000,000. Such fires result from placing stoves, furnaces, and other heating equipment too near combustible walls, partitions, and ceilings, or from absence of adequate protection for floors. Definite information on the required spacings of heating equipment from unprotected combustible construction and on the protections needed for closer spacings has been lacking, the requirements in building codes being based largely on the judgment of men experienced in fire protection and fire underwriting.

Tests were undertaken to determine the practicability of evaluating the fire hazards of such installations by laboratory methods. In such tests it is not necessary to introduce conditions which actually result in ignition, since the temperatures to which adjacent combustible materials are heated, are a measure of the hazard.

For a proper degree of safety, temperatures on exposed wood construction frequently exceeding 125° C. (257° F.) should probably be avoided, although apparently no decided hazard is involved if they occasionally reach 150° C. (302° F.). The determination of experimental conditions and general planning of the tests were based in part on information obtained in a survey of fires from such equipment occurring in the District of Columbia during the period 1928 to 1930. The information was obtained from reports on such fires, inspections of the premises affected, and inspection and tests of installations considered hazardous.

The tests were confined to domestic househeating and cooking equipment, and were made with the types most commonly used. Smokepipes, stoves, and furnaces were tested in relation to the fire hazard to adjacent partitions, ceilings, and platforms. Several types of protection for such combustible constructions were tested in cases where it appeared that such protection was necessary to avoid unduly large spacings between the construction and the appliance. The practical aspects have been kept in mind throughout

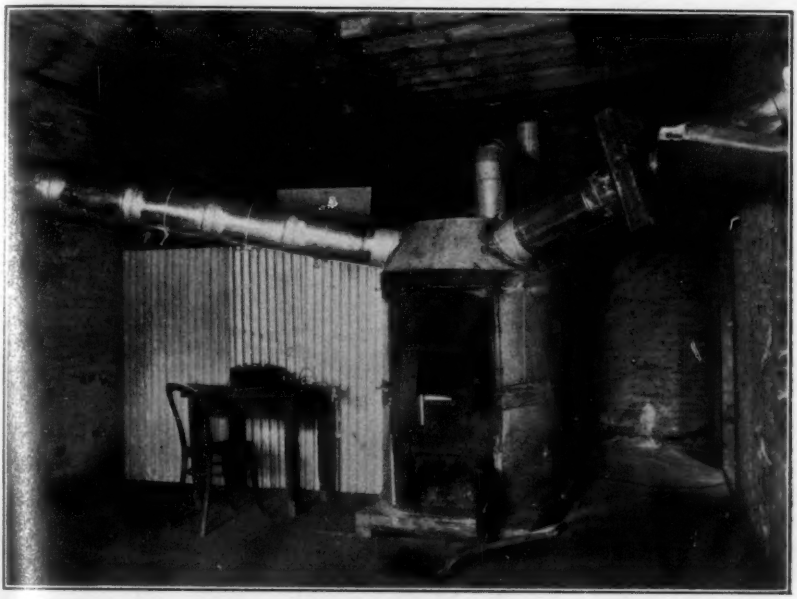

FIGURE 1.—*Warm-air heating unit.*

UNIV. OF WASH.

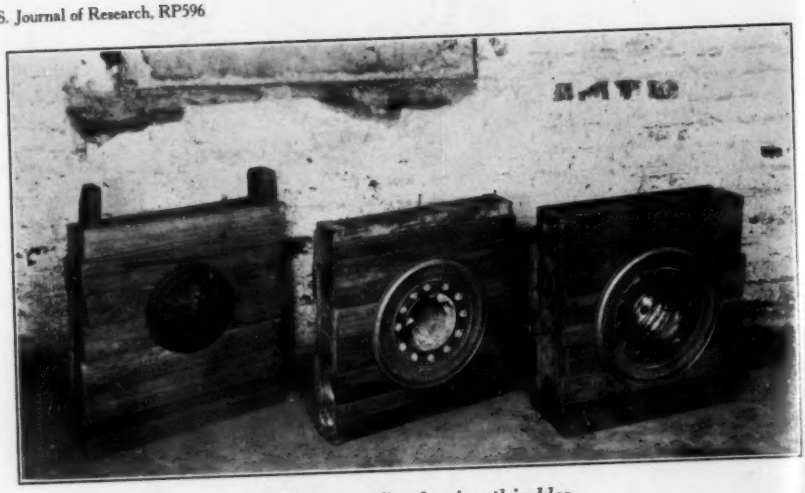

FIGURE 4.—*Smokepipe thimbles.*

so that compliance with any requirements based on the results of these tests can be had at minimum inconvenience and expense.

## II. TESTS TO DETERMINE SMOKEPIPE HAZARDS

### 1. EQUIPMENT AND TESTING METHODS

The tests in this and all succeeding series were conducted within a chamber 15 by 29 feet in plan with ceiling height of about 10 feet. To eliminate chance effects of drafts, all the shutters of the chamber were kept closed except the one in the end farthest away from the equipment tested, which was kept partially open to supply the air necessary for the best combustion conditions and also to regulate the temperature of the room.

Preliminary tests made on several types of commonly used stoves and heaters indicated that the highest smokepipe temperatures were obtained when a sheet-metal stove with 6-inch smokepipe was used, with 12-inch lengths of oak fireplace wood as fuel. This stove was oval-shaped in plan, 23 by 15 inches, and 22½ inches high, with a 3-inch diameter draft opening at the bottom. A circular cover on the top was opened partly to give the draft required for maximum smokepipe temperatures. The cast-iron removable legs spaced the stove base 5 inches above the wood floor platform. The distance from platform to ceiling was 8 feet 8 inches. The 6-inch smokepipe rising vertically from the stove was turned by an elbow, the distance between the top of the elbow and the ceiling or joists being varied by changing the vertical rise. The smokepipe temperatures were measured on the horizontal pipe immediately adjacent to the elbow. At a horizontal distance of 11 feet from the rear of the stove the smokepipe was again turned vertically into a chimney in the roof of the chamber, above which it was allowed to project about 2 feet.

Temperatures were measured with iron-constantan thermocouples of no. 24-gage wire. The welded junctions were placed at the center of a circular coil of the wire, the approximate coiled length being 200 or more diameters of the wire used. These were fastened on the top exterior surface of the smokepipe under a thin sheet of mica about 0.002 inch thick by asbestos cord tied around the pipe. Vertically above each of these locations were fastened thermocouples under thin sheets of mica, one on the surface of the wood joist, which was 8 inches deep, and others on either side of the joist on the lower side of the ceiling boards.

Further tests were made with a warm-air furnace having an 8-inch smokepipe spaced 12 inches from the exposed construction. The furnace fire box was 20 inches in diameter and the outer jacket of 26-gage galvanized steel was 40 inches in diameter. At the bottom rear of this jacket a recirculating opening for air intake, 8 by 24 inches, was made. The fire was started by paper and wood and thereafter semibituminous coal, in lumps and powdered form combined, was used as fuel. A view of the equipment is shown in figure 1.

Temperatures were also measured on smokepipes of some installations in service. These measurements were confined chiefly to oil and gas burners recently installed in former coal-fired central heating units.

## 2. RESULTS OF TESTS

Temperature data are given in table 1 and figures 2 and 3 for tests with the exposed construction spaced 6, 10, 12, 18, and 24 inches above the smokepipes. The temperatures shown by the upper curves are those obtained on the smokepipe. The lowest curve represents the room temperature during the test. The intermediate curves give the

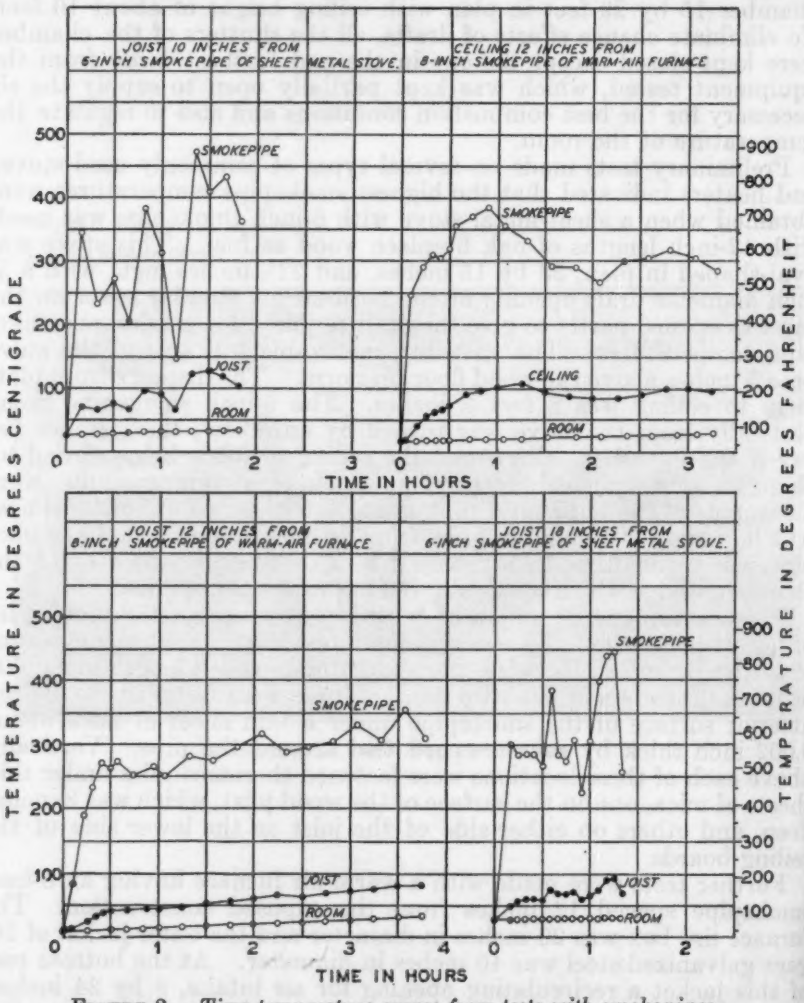
JOIST 10 INCHES FROM 6-INCH SMOKEPIPE OF SHEET METAL STOVE.
CEILING 12 INCHES FROM 8-INCH SMOKEPIPE OF WARM-AIR FURNACE
JOIST 12 INCHES FROM 8-INCH SMOKEPIPE OF WARM-AIR FURNACE
JOIST 18 INCHES FROM 6-INCH SMOKEPIPE OF SHEET METAL STOVE.
SMOKEPIPE
JOIST
CEILING
ROOM
TEMPERATURE IN DEGREES CENTIGRADE
TEMPERATURE IN DEGREES FAHRENHEIT
TIME IN HOURS

FIGURE 2.—*Time-temperature curves from tests with smokepipes.*

temperatures measured on the surface adjacent to the smokepipe. Tests of longer durations than those shown indicated that substantially no higher temperatures resulted. The maximum temperature measured on the surface of the smokepipe was 483° C. (901° F.) This is appreciably above the ignition temperature of most common combustible materials and hence it is apparent that fires may occur readily when combustibles are in contact with or very near to smokepipes.

The maximum smokepipe temperatures obtained with oil and gas conversion burners in hot water house heating systems were much lower than those obtained with the wood and coal-fired stoves and

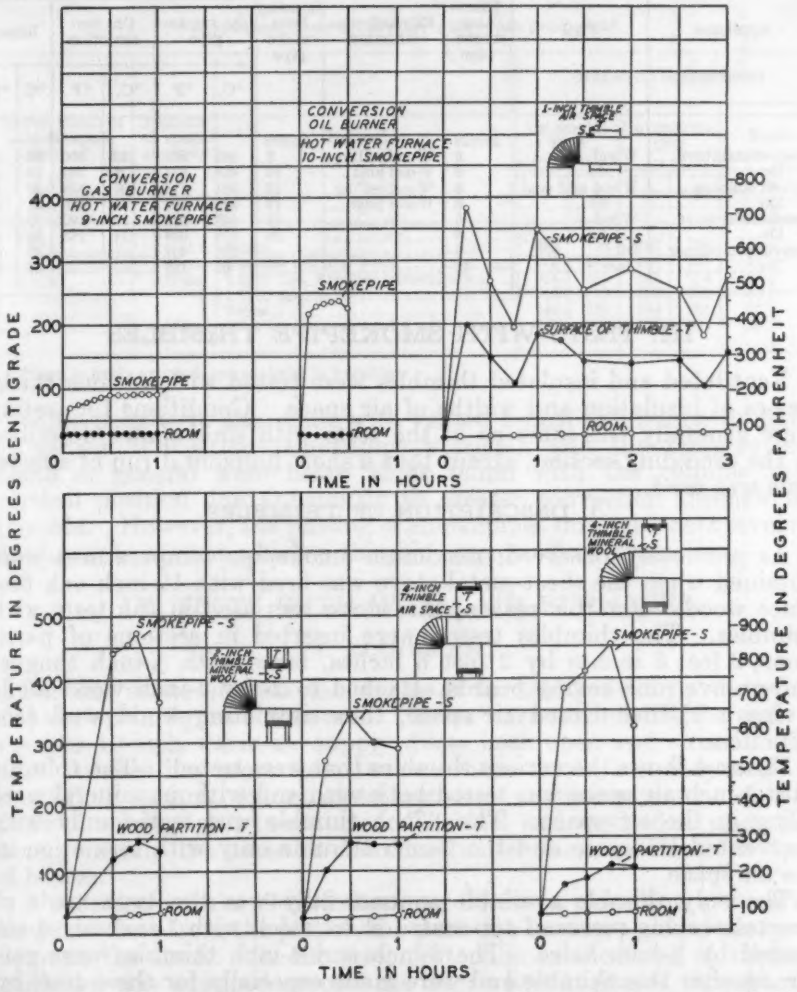


FIGURE 3.—*Time-temperature curves from tests with smokepipes and thimbles.*

warm-air furnaces, even though rate of gas and oil input was increased beyond that attained in normal operation. Temperatures measured on smokepipes of coal-fired hot-water installations and not herein reported, were also relatively low, indicating that the type of heating equipment as well as the fuel used are important in this connection.

TABLE 1.—*Temperature data from smokepipe tests*

| Appliance | Fuel | Diameter smokepipe | Exposed construction | Spacing from smokepipe | Maximum temperatures | | | | | |
|---|---|---|---|---|---|---|---|---|---|---|
| | | | | | On smokepipe | | On construction | | Room | |
| | | | | | °C. | °F. | °C. | °F. | °C. | °F. |
| | | *Inches* | | *Inches* | | | | | | |
| Sheet-metal stove | Wood | 6 | Wood ceiling | 6 | 483 | 901 | 152 | 306 | 30 | 86 |
| Do | do | 6 | Wood joist | 10 | 468 | 874 | 126 | 259 | 28 | 82 |
| Hot-air furnace | Wood and coal | 8 | Wood ceiling | 12 | 381 | 718 | 109 | 228 | 29 | 84 |
| Do | do | 8 | Wood joist | 12 | 353 | 667 | 81 | 178 | 31 | 88 |
| Sheet-metal stove | Wood | 6 | do | 18 | 448 | 838 | 88 | 190 | 29 | 84 |
| Do | do | 6 | do | 24 | 318 | 604 | 74 | 165 | 28 | 82 |
| Conversion burner | Oil | 9 | | | 236 | 457 | | | 23 | 73 |
| Do | Gas | 10 | | | 92 | 198 | | | 27 | 81 |

## III. TESTS WITH SMOKEPIPE THIMBLES

Ventilated and insulated thimbles were tested with various thicknesses of insulation and widths of air space. Conditions for testing were generally the same as in the tests with smokepipes described in the preceding section, except that a short horizontal run of smokepipe was used.

### 1. DESCRIPTION OF THIMBLES

As previously observed, maximum smokepipe temperatures were obtained when the sheet-metal stove was fired with 12-inch oak fireplace wood. For this reason, this stove was used in the tests with thimbles. The thimbles tested were inserted in sections of partitions, 2 feet 6 inches by 2 feet 6 inches, faced with ¾-inch tongue-and-groove pine ceiling boards attached to 2- by 4-inch wood studs giving a 3¾-inch closed air space, thus simulating wood stud construction.

Figure 4 shows the various thimbles that were tested. The thimble with 4-inch air space was tested both with and without mineral wool filling in the air space. The 1-inch thimble was tested only with the vented air space and the 2-inch thimble only with insulation in the air space.

The only thimble available commercially was the type made of two telescoping pieces of tin-coated sheet steel, with 1-inch air space vented by ½-inch holes. The 2-inch and 4-inch thimbles were patterned after this thimble and were made especially for these tests by a local tinsmith. The 2-inch thimble had ¾-inch-diameter vent holes, and the 4-inch thimble had 1-inch holes. All thimbles were made to receive a 6-inch smokepipe.

### 2. RESULTS OF TESTS

Table 2 and figure 3 give the maximum temperatures measured on the combustible material nearest the stovepipe and in contact with the thimble. When only the vented air space was used the resulting temperatures appeared rather excessive so resort was had to insulation. Mineral wool was inserted in the air space to a density of about 8 lbs. per cubic foot. In some tests with the 4-inch thimble

a 1-inch cylindrical tile sleeve was placed over the smokepipe within the thimble.

TABLE 2.—*Results of tests with smokepipe thimbles*

[Appliance: Sheet-metal stove with 6-inch smokepipe]

| Radial width of annular space (inches) | Thimble air space (inches) | Insulation | Maximum temperatures | | | | | |
|---|---|---|---|---|---|---|---|---|
| | | | On smoke-pipe | | On construction | | Room | |
| | | | °C. | °F. | °C. | °F. | °C. | °F. |
| 1 | [1] 1 | None | 382 | 720 | 198 | 388 | 21 | 70 |
| 2 | None | 2 inches mineral wool | 473 | 883 | 144 | 291 | 31 | 88 |
| 4 | None | 1 inch tile, 3 inches mineral wool | 364 | 687 | 101 | 214 | 26 | 79 |
| 4 | 3 | 1 inch tile | 304 | 579 | 150 | 302 | 30 | 86 |
| 4 | 4 | None | 346 | 655 | 144 | 291 | 27 | 81 |
| 4 | None | 4 inches mineral wool | 426 | 799 | 105 | 221 | 29 | 84 |

[1] Thimble freely exposed, not enclosed in partition.

Some tests were also made with vented 1-inch and 2-inch thimbles in horizontal position (smokepipe vertical), and the temperatures found in general were below those found with the thimble in a vertical position due apparently to greater convection through the thimble. However, the passing of smokepipes through floors involves fire hazards against which a thimble cannot afford protection.

## IV. TESTS WITH WARM-AIR FURNACES

### 1. EQUIPMENT

For one series of tests the warm-air furnace previously described and shown in figure 1 was used. Tests were made with the ends of the two 10-inch warm-air supply ducts both open and closed. The usual furnace has more than two warm-air ducts, but they may be shut off to such an extent as to introduce conditions comparable to those obtaining with two ducts. The fuel and method of operation were generally the same as described under section II for this type of heater.

A partition with a 10-inch diameter hole was placed on one warm-air duct 3 feet from the jacket, the partition having a closed air space between the studs. In one test, protection in the form of asbestos millboard was wrapped around the duct where it passed through the partition.

The "pipeless" furnace data were obtained with an installation in a dwelling. The fire box was 24 inches in diameter and the outer sheet-metal jacket was 30 by 36 inches at the floor level. Wood fuel was used followed by hard coal, and finally a combination of the two. The radiation dome during a portion of the test became visibly red.

## 2. TEMPERATURES OF DUCTS

Table 3 and figure 5 give the temperatures at the several locations indicated, in tests with the warm-air furnace. These charts show that the temperature of the air within the ducts near the furnace is

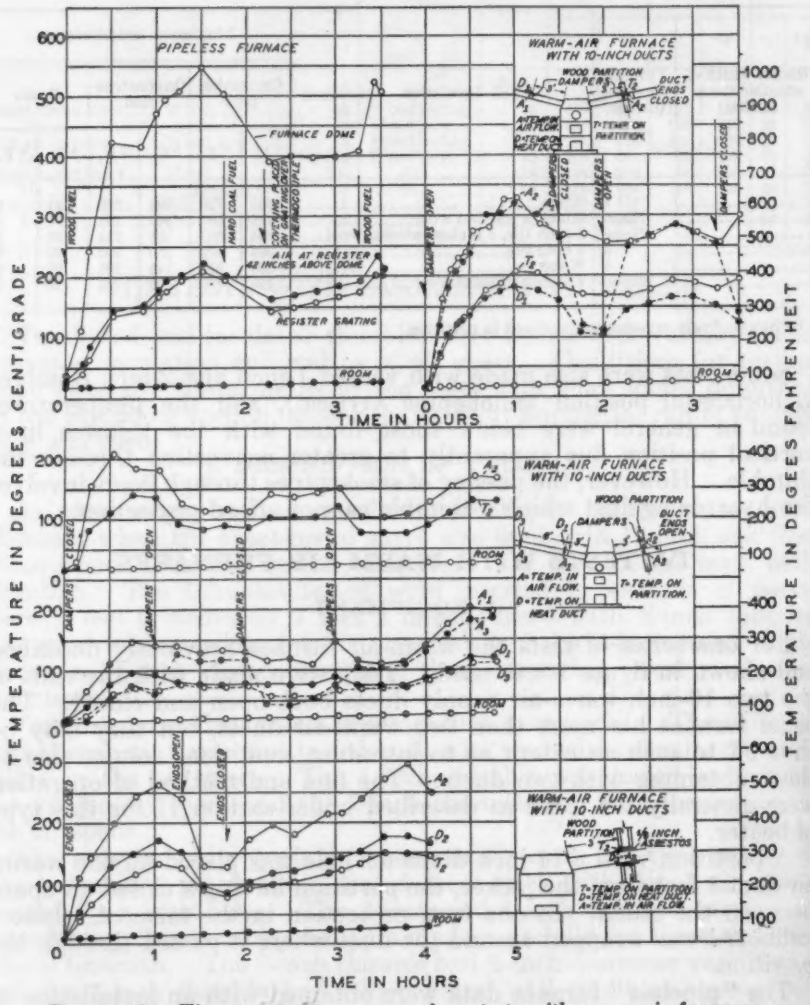


FIGURE 5.—*Time-temperature curves from tests with warm-air furnaces.*

sufficiently high to cause ignition of combustible material. The temperature gradient of the air within the duct was small when dampers were open, and whereas with dampers closed the temperature of the air in the duct near the furnace was higher, it decreased sharply with increased distance from the furnace.

TABLE 3.—*Results of tests with warm-air furnace*

[Appliance: Warm-air furnace with 10-inch circular ducts]

| Ends of ducts | Damper | Maximum temperatures | | | | | | | | | | | |
|---|---|---|---|---|---|---|---|---|---|---|---|---|---|
| | | Air in duct | | | On exterior surface of duct | | | On wood partition | | | | Room | |
| | | Distance | °C. | °F. | Distance | °C. | °F. | Insulation on duct | Distance | °C. | °F. | °C. | °F. |
| | | *Feet* | | | *Feet* | | | | *Feet* | | | | |
| Closed | Open | 3 | 328 | 622 | 3 | 182 | 360 | None | 3 | 208 | 406 | 27 | 81 |
| Open | do | 3 | 202 | 396 | 3 | 120 | 248 | None | 3 | 132 | 270 | 27 | 81 |
| Do | do | 9 | 183 | 361 | 9 | 112 | 234 | None | | | | 27 | 81 |
| Do | Closed | 9 | 75 | 167 | 9 | 70 | 158 | None | | | | 27 | 81 |
| Closed | Open | 3 | 207 | 567 | 3 | 178 | 352 | ⅛-inch asbestos millboard. | 3 | 148 | 298 | 27 | 81 |

The difference between the temperature of the heated air within the duct and that on the exterior surface of the duct became greater as the temperature in the air flow increased. This same effect existed but to a smaller degree, between the partition temperature and that of the exterior of the protected duct in proximity thereto. Temperatures obtaining with protection around the duct where it passes through a partition are shown in figure 5, when asbestos millboard one eighth inch thick and weighing about one half lb./ft.$^2$ was wrapped around the duct.

Figure 5 and table 4 show the temperatures measured at given locations on a "pipeless" furnace system. Due to the passage of cold air downward around the outside of the central heating duct, the temperatures in the space around the central warm air duct were all below the hazardous range. The maximum temperature recorded on the register grating 2 inches outside the periphery of the central warm air heating duct and at point of contact with the wood flooring, was 50° C. (122° F.). The condition most likely to introduce hazards occurs when furniture, rugs, or clothing are placed on the warm-air register, or when combustible partitions are located in or too close to the warm-air flow. Temperatures in the air flow at the floor level reached 233° C. (451° F.).

TABLE 4.—*Results of tests with "pipeless" furnace*

| Fuel | Maximum temperatures | | | | | | | |
|---|---|---|---|---|---|---|---|---|
| | Radiating dome | | Warm air at register | | Register grating | | Room | |
| | °C. | °F. | °C. | °F. | °C. | °F. | °C. | °F. |
| Wood | 547 | 1,017 | 222 | 432 | 209 | 409 | 21 | 70 |
| Hard coal | [1] 408 | 766 | [1] 191 | 376 | 173 | 344 | 26 | 79 |
| Wood and coal | 523 | 973 | 233 | 451 | 200 | 392 | 26 | 79 |

[1] Register partly covered by wood board producing slight banking of air flow.

## V. FLOOR PROTECTIONS

### 1. TESTING EQUIPMENT

The base supporting the heating equipment was 4 by 4 feet and made of ¾-inch tongue and groove pine boards nailed to three 2- by 4-inch wood joists. For the tests with asbestos and sheet metal protection the boards were in single thickness with the joists set edgewise. The other protection was of clay common bricks set on edge, the thickness inclusive of the mortar being 4 inches. The boards were applied in double layer to the joists laid flatwise. The air space between the boards and the concrete floor was either open, closed at the ends, or filled with dry sand. The thermocouples were placed on the bottom of the stove and also next to the wooden flooring over which the protection was placed. The sheet-metal stove described under section II, fired with wood, was used in all tests for which temperature data are reported.

### 2. RESULTS OF TESTS

Observations with the cast-iron coal stove with legs and having an ash box integral with the stove, indicated no hazard to a wood floor separated by an air space from the bottom of the stove. The same was true for a water-jacketed heater that was tested.

With the sheet-metal stove raised 5 inches above the floor and the floor protected with ⅛-inch thick asbestos millboard under black iron, a temperature of 175° C. (347° F.) was reached on the wood (table 5). With the 5-inch air space and the ¼-inch asbestos protection under sheet metal, the temperatures on the surface of the floor reached a maximum of 120° C. (248° F.) (fig. 6). The results with the brick protection are also given in table 5 and figure 6. With the double board floor no very decided difference in temperature on its upper surface was found for open, closed, and filled spaces beneath it. The fires in the sheet-metal stove in direct contact with the brick can be taken also as representative of a moderate condition of fire exposure to constructions beneath braziers and fireplaces.

TABLE 5.—*Results of tests with floor protections*

[Appliance: Sheet-metal stove without ash pit]

| Spacing inches | Protection | Maximum temperatures | | | | | |
|---|---|---|---|---|---|---|---|
| | | On stove base | | On construction | | Room | |
| | | ° C. | ° F. | ° C. | ° F. | ° C. | ° F. |
| 5 | 1 sheet 20-gage black iron. Two ⅛-inch sheets asbestos millboard. | 399 | 750 | 120 | 248 | 28 | 82 |
| Stove base on iron | 1 sheet 20-gage black iron | | | 202 | 396 | 30 | 86 |
| 5 | 1 sheet 20-gage black iron. One ⅛-inch sheet asbestos. | | | 175 | 347 | 22 | 72 |
| 8¾ | do | | | 116 | 241 | 24 | 75 |
| Stove base on brick | 4 inches of brick on wood platform. Open air space below platform and stove not sanded around bottom. | 495 | 923 | 182 | 360 | 16 | 61 |
| Do | 4 inches of brick on wood platform. Closed air space below platform and stove not sanded around bottom. | 495 | 923 | 173 | 343 | 21 | 70 |
| Do | 4 inches of brick on wood platform. Open air space below platform and stove sanded around bottom. Ashes in stove before test. | 342 | 648 | 182 | 360 | 23 | 73 |
| Do | 4 inches of brick on wood platform. Open air space below platform and stove sanded around bottom. No ashes in stove before test. | 475 | 887 | 242 | 468 | 17 | 63 |
| Do | 4 inches of brick on wood platform. Closed air space below platform and stove sanded around bottom. | 481 | 898 | 224 | 435 | 26 | 79 |
| Do | 4 inches of brick on wood platform. Air space filled with sand and stove sanded around bottom. | 622 | 1,152 | 243 | 469 | 26 | 79 |

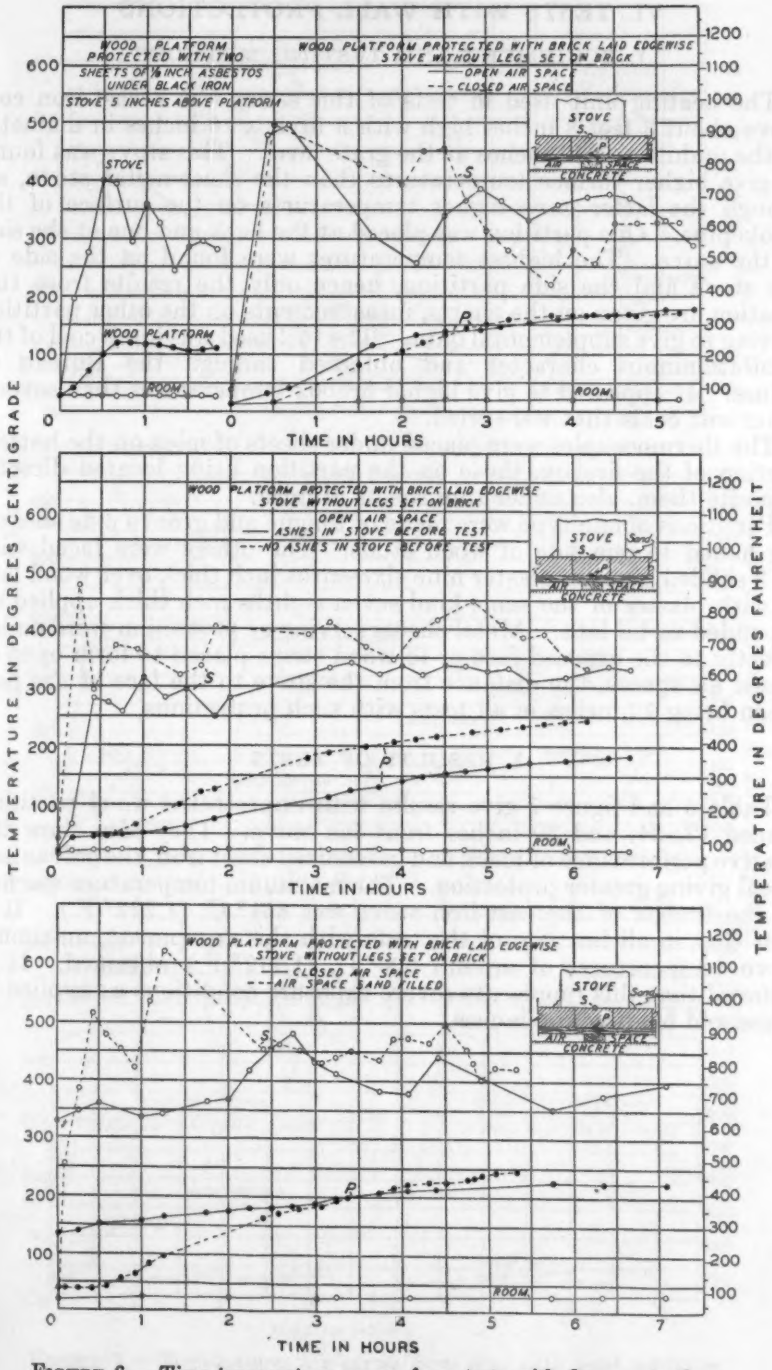


FIGURE 6.—*Time-temperature curves from tests with floor protections.*

## VI. TESTS WITH WALL PROTECTIONS

### 1. EQUIPMENT AND TESTING METHODS

The heating unit used in tests of this series was a cast-iron coal stove about 3 feet 8 inches high with a firebox 16 inches in diameter at the middle and 12 inches at the grate level. This stove was found to give higher surface temperatures than the sheet-metal stove, although the latter gave higher temperatures on the surface of the smokepipe. One partition was placed at the back and one at the side of the stove. The highest temperatures were found on the side of the stove and the side partition, hence only the results from this location are given on the charts, measurements on the other partition serving to give supplemental data. The fuel used was lump coal of the semibituminous character and obtained through the Bureau of Mines. It appeared to give higher firebox temperatures than several other soft coals that were tried.

The thermocouples were placed under sheets of mica on the hottest portion of the firebox, those on the partition being located directly opposite them, also under thin sheets of mica.

Partitions of one type were made of tongue and groove pine sheathing nailed to one side of wood studs. The others were faced with 1 : 3 sanded gypsum plaster nine sixteenths inch thick over wood lath or with plaster of the same kind seven eighths inch thick applied on expanded metal lath. Metal sheets serving as protection were nailed directly to the exposed face or to wood strips placed to form open or closed air spaces, the distance from the stove to the face of the partition being 12 inches in all tests with such protections.

### 2. RESULTS OF TESTS

Table 6 and figure 7 give results with unprotected wood partition spaced 12, 24, and 30 inches from the stove. They also show the relative performance of black and galvanized sheet iron, the galvanized metal giving greater protection. The maximum temperature reached on the firebox of the cast-iron stove was 661° C. (1,222° F.). It is seen that in all but two of the tests with this equipment, maximum stove temperatures of around 600° C. (1,112° F.) obtained. It is believed that this represents severe exposure conditions as applied to household heating appliances.

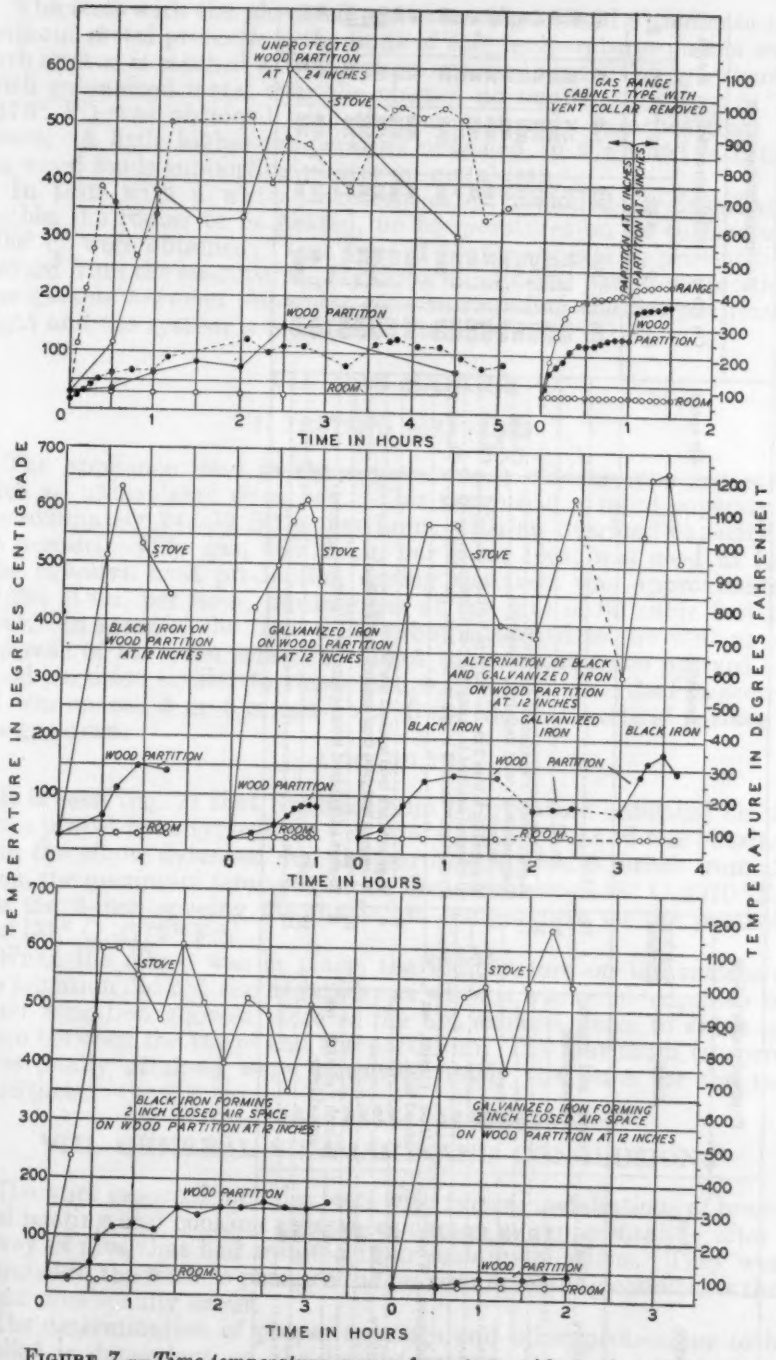
UNPROTECTED WOOD PARTITION AT 24 INCHES
STOVE
WOOD PARTITION
ROOM
GAS RANGE CABINET TYPE WITH VENT COLLAR REMOVED
PARTITION AT 6 INCHES
PARTITION AT 3 INCHES
RANGE
WOOD PARTITION
ROOM
TIME IN HOURS
TEMPERATURE IN DEGREES CENTIGRADE
TEMPERATURE IN DEGREES FAHRENHEIT
STOVE
BLACK IRON ON WOOD PARTITION AT 12 INCHES
GALVANIZED IRON ON WOOD PARTITION AT 12 INCHES
ALTERNATION OF BLACK AND GALVANIZED IRON ON WOOD PARTITION AT 12 INCHES
BLACK IRON
GALVANIZED IRON
BLACK IRON
WOOD PARTITION
ROOM
TIME IN HOURS
STOVE
BLACK IRON FORMING 2 INCH CLOSED AIR SPACE ON WOOD PARTITION AT 12 INCHES
GALVANIZED IRON FORMING 2 INCH CLOSED AIR SPACE ON WOOD PARTITION AT 12 INCHES
WOOD PARTITION
ROOM
TIME IN HOURS

FIGURE 7.—*Time-temperature curves from tests with wood partition.*

TABLE 6.—*Results of tests with wall protections*

| Appliance | Fuel | Exposed construction | | Protection | Air space | Maximum temperatures | | | | | |
|---|---|---|---|---|---|---|---|---|---|---|---|
| | | Kind | Spacing (inches) | | | On stove | | On construction | | Room | |
| | | | | | | °C. | °F. | °C. | °F. | °C. | °F. |
| Cast-iron stove | Coal | Tongue and groove wood partition. | 12 | None | | 536 | 997 | 213 | 415 | 26 | 79 |
| Do | do | do | 24 | do | | 602 | 1,116 | 148 | 298 | 31 | 88 |
| Do | do | do | 30 | do | | 659 | 1,218 | 116 | 241 | 34 | 93 |
| Do | do | do | 12 | 20-gage black iron against partition | | 661 | 1,222 | 177 | 351 | 29 | 84 |
| Do | do | do | do | 20-gage black iron 1 inch from partition | Closed | 521 | 970 | 115 | 239 | 33 | 91 |
| Do | do | do | do | do | Open | 607 | 1,125 | 92 | 198 | 27 | 81 |
| Do | do | do | do | 20-gage black iron 2 inches from partition | Closed | 602 | 1,116 | 148 | 298 | 27 | 81 |
| Do | do | do | do | 20-gage galvanized iron against partition | | 615 | 1,139 | 85 | 185 | 27 | 81 |
| Do | do | do | do | 20-gage galvanized iron 2 inches from partition | Closed | 635 | 1,175 | 44 | 111 | 27 | 81 |
| Sheet-metal stove | Wood | ⅛-inch plaster on wood lath. | do | | | 307 | 585 | 148 | 298 | 30 | 86 |
| Do | do | do | 6 | | | 366 | 691 | 189 | 372 | 27 | 81 |
| Cast-iron stove | Coal | do | 9 | 20-gage black iron against partition | | 628 | 1,162 | 189 | 372 | 37 | 99 |
| Do | do | do | 9 | 20-gage galvanized iron against partition | | 618 | 1,144 | 81 | 178 | 38 | 100 |
| Do | do | do | 18 | None | | 634 | 1,173 | 159 | 318 | 44 | 111 |
| Do | do | ⅛-inch plaster on metal lath. | 9 | 20-gage galvanized iron against partition | | 610 | 1,130 | 74 | 165 | 39 | 102 |
| Do | do | do | 12 | None | | 618 | 1,144 | 195 | 383 | 30 | 86 |
| Do | do | do | 18 | do | | 593 | 1,099 | 144 | 291 | 32 | 90 |

The tests with the plastered partitions (figs. 8 and 9) indicate that without metal protection, the limit of safe temperatures on the wood lath or stud is reached with the stove spaced 18 inches away, whereas, with galvanized metal over the plaster, no temperature over 81° C. (178° F.) was obtained with the partition only 9 inches from the stove. A little higher temperature obtained on the wood lath than on wood studs supporting plaster on metal lath.

In tests with a water-jacketed heater, intended for installation within the rooms to be heated, no temperatures on its surface over 100° C. were obtained. This type of heater appears to present little hazard from the standpoint of ignition of adjacent partitions provided the gaskets between the water coils surrounding the fire pot remain tight and the system is maintained full of water.

## VII. GAS RANGES

### 1. TESTING METHODS

The appliance used in these tests was a cabinet-type gas range with an uninsulated oven box. This range had a rated capacity of approximately 24,000 B.t.u. per hour, with an overload capacity of 50 percent. City gas, 600 B.t.u. per cubic foot, was used as fuel. The effective heat production during the tests was approximately 32,200 B.t.u. per hour, burning gas at the rate of 60 cubic feet per hour. In some of the tests a 90° elbow attached to the vent at the top rear of the oven served to direct the exhaust gases upward. A wood partition similar to those used in the tests described in section VI was spaced 3 or 6 inches away from the rear vertical surface of the gas oven.

### 2. RESULTS

It is seen (fig. 7) that the maximum temperature indicated on the range proper for a typical run was 225° C. (437° F.) and was obtained with the elbow detached and the partition spaced 3 inches from the oven, the maximum temperature on the wood being 188° C. (370° F.). For the 6-inch spacing the maximum temperature on the partition was 133° C. (272° F.).

When the elbow was in place, the temperature on the surface of the partition did not rise as rapidly as when it was removed, since the latter condition allowed more of the hot exhaust gases to enter the space between the range and the partition. The maximum temperatures finally attained were, however, nearly the same for the two conditions.

## VIII. GENERAL SUMMARY AND CONCLUSIONS

The work reported includes tests with typical installations of household heating and cooking appliances chosen as representative after a survey of fires that had resulted from such installations. They were operated in the tests to produce the maximum heating conditions that might occasionally occur.

The determination of proper spacings and other protections to be applied is dependent on the hazard certain attained temperatures represent. The combustible material usually exposed is wood in the form of building members or finish or as wood lath under plaster.

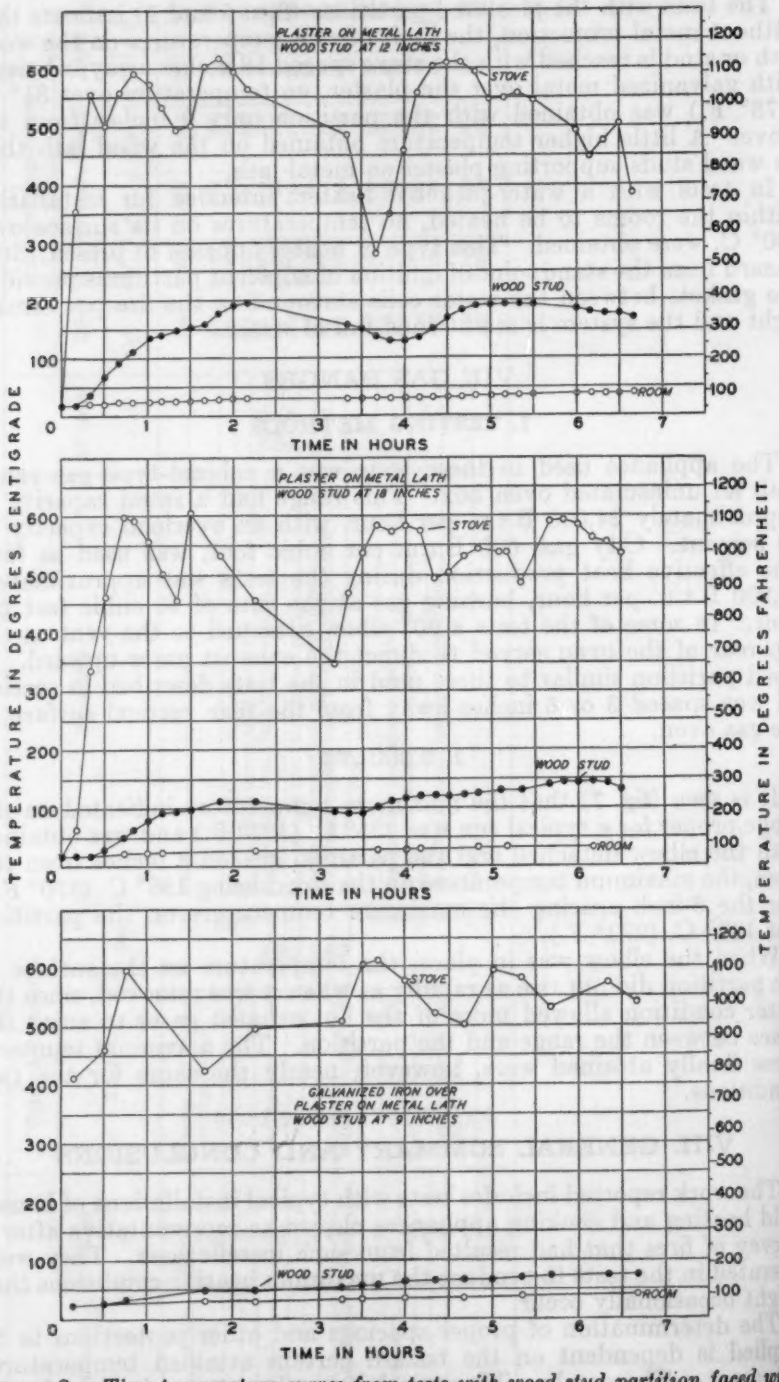


FIGURE 8.—*Time-temperature curves from tests with wood stud partition faced with plaster on metal lath.*

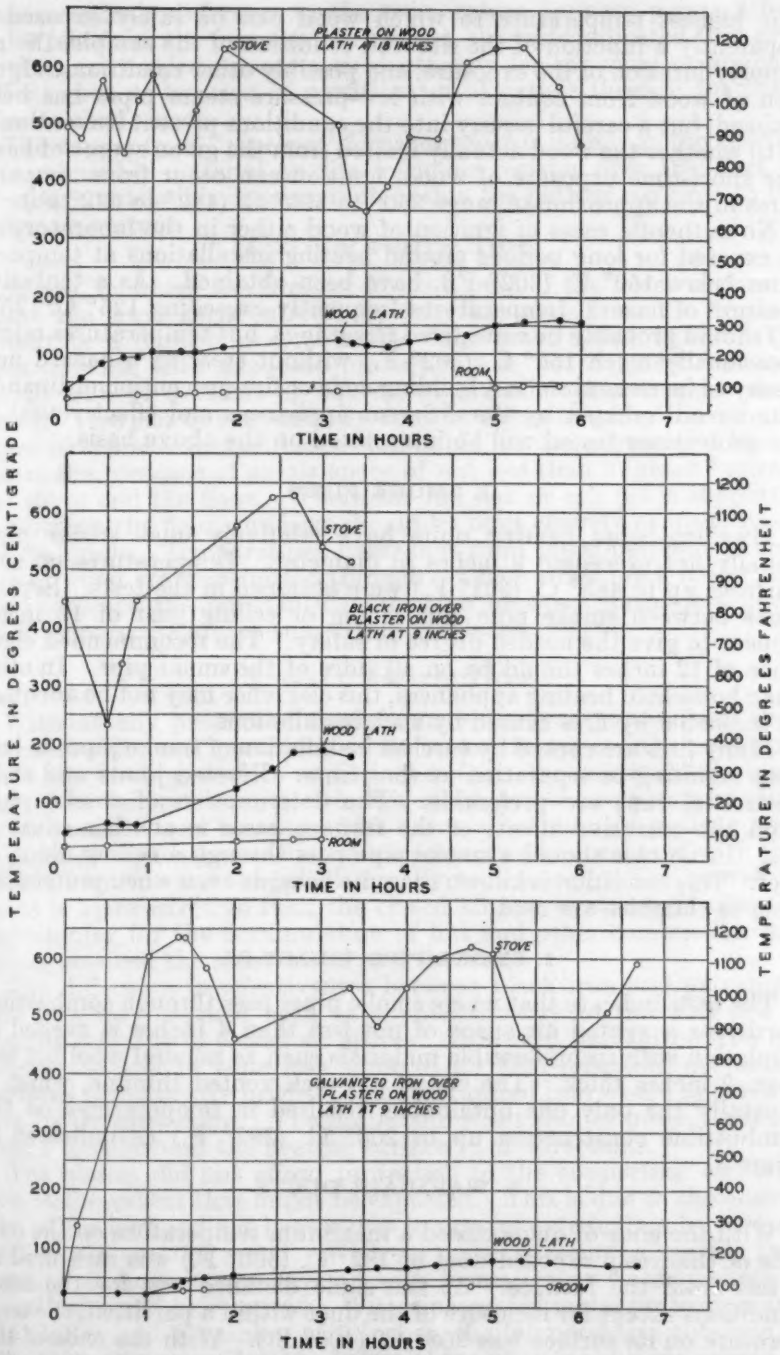


FIGURE 9.—*Time-temperature curves from tests with wood stud partitions faced with plaster on wood lath.*

The highest temperature to which wood can be safely exposed is apparently a function of the size and condition of the sample, the air supply, duration of the exposure, and possibly other conditions. Ignition of wood from contact with low-pressure steam pipes has been claimed, but a careful inquiry into the conditions present leaves doubt as to whether the wood actually ignited from the given source of heat. For short-time exposure of wood, ignition can occur from temperatures in the approximate range 250° to 300° C. (482° to 572° F.).

No authentic cases of ignition of wood either in the laboratory or as exposed for long periods around heating installations at temperatures below 150° C. (302° F.), have been obtained. As a tentative measure of hazard, temperatures frequently exceeding 125° C. (257° F.) should probably be considered hazardous, but temperatures might occasionally reach 150° C. (302° F.) without creating a hazard necessary to be recognized in a building code or fire-prevention ordinance. The hazard created by the different appliances and effectiveness of the protections tested will be interpreted on the above basis.

### 1. SMOKE PIPES

Dwelling-house heating units have relatively small smoke pipes usually not exceeding 9 inches in diameter. Temperatures on such surfaces up to 483° C. (901° F.) were obtained in the tests. Separations between smoke pipe and ceiling or ceiling joist of 12 inches appear to give the needed degree of safety. The recommended clearance of 12 inches should be on all sides of the smoke pipe. In other than household heating appliances, this clearance may not be adequate as indicated by fires caused by such installations.

Many fires are caused by careless installation of smoke pipes in long runs resulting in separation at the joints. Riveted joints and short horizontal runs are preferable. The deterioration of smoke pipes from the corrosive effects of the furnace gases is another cause of fire. In no case should a smoke pipe pass through a ceiling, floor, or roof. This condition is known to invite hazards even when protections such as thimbles are used.

### 2. SMOKE-PIPE THIMBLES

The tests indicate that where smoke pipes pass through combustible partitions a vented air space of not less than 4 inches is needed or insulation with incombustible materials such as mineral wool not less than 2 inches thick. The use of a 1-inch vented thimble, which is generally the only one obtainable, resulted in temperatures on the combustible construction up to 200° C. (392° F.) as indicated in figure 3.

### 3. WARM-AIR DUCTS

With the ends of ducts closed a maximum temperature on the outside of the freely exposed duct of 182° C. (360° F.) was measured at 3 feet from the furnace. At the same distance and for the same conditions except for inclosure of the duct within a partition, the temperature on its surface was 208° C. (406° F.). With the ends of the ducts closed there was a decided fall in temperature of the duct with increase in distance from the furnace. With the ends open the maximum temperature on the duct did not exceed 120° C. (248° F.), but

there was little difference in the temperature between points 3 feet and 9 feet from the furnace. In general, the tests indicated that protections are needed on warm-air ducts only for the more severe conditions such as location of partitions or of outlets through the floor, close to the furnace.

The danger from "pipeless" furnaces consists mainly in the placing of combustible material on the warm-air register over the duct or locating combustible constructions within the path or too close to the warm-air current.

### 4. FLOOR PROTECTION

Stoves, in which the fire box forms a part of the lower surface or where the lower surfaces are heated by hot coals from the fire box, constitute a hazard to combustible floor construction below. The tests indicate that adequate protection can be obtained with one fourth inch of asbestos or equivalent material placed under sheet metal. This can be conveniently done by filling in under the crimped edges of the sheet-metal bases obtainable for the purpose. This assumes the presence of an air space of not less than 5 inches between the stove and the floor. Where the fire box or ash pit is supported directly on the floor, the base should be built entirely of incombustible materials. Temperatures hazardous from the standpoint of ignition of wood are transmitted through a 4-inch thick brick base. The tests indicate the possibility of ignition of wood forms left under brick or concrete arches supporting fireplaces.

### 5. WALL PROTECTION

Without any protection a minimum spacing of stoves from combustible walls and partitions of 24 inches is apparently necessary. With the heating surface at 12 inches from the construction, black iron gives fair protection, although much better protection is given by galvanized iron because of its lower absorption of radiant heat. A closed air space gives some added protection as compared with that afforded by the metal applied directly to the wall. The vented air space is more effective than the closed air space, although affording opportunity for the accumulation of lint and other combustible materials between the sheet metal and the wall.

The difference in effectiveness between black iron and galvanized iron was very marked both as applied directly to the wall and as forming one side of closed air spaces. However, galvanized iron will deteriorate and in time lose some of its heat-reflecting properties. Surfaces permanently brighter than galvanized iron would apparently give better protection. The protecting sheet should project not less than 1 foot beyond the heating surface in all directions.

The plaster did not afford protection to the supporting construction to the extent that might be expected. This is due to the absorption of the long radiant heat waves to greater extent than by surfaces such as zinc-coated metal. With no metal covering, a spacing from heating equipment, not covered with insulation or water jackets, of 18 inches would be required. With zinc-coated metal protection over the plaster and a spacing of 9 inches, the temperatures obtained on the wood were considerably below those that can be considered as hazardous.

The tests with a gas range having an oven without insulation indicated that a 6-inch separation between the side of the oven and a wood partition gives reasonably safe conditions. Fires have been known to result from spacing the oven 1 inch from the wall. The tests indicated excessive wall temperatures where the oven was spaced 3 inches from the wall.

### 6. SCOPE OF APPLICATION OF RESULTS

The results apply mainly to heating devices of the types and sizes used in private dwellings. For larger heating units, smoke pipes, and air ducts, the results may not apply without modification. With increase in the area of the heating surface higher maximum temperatures on the exposed surface would be expected for the same temperature on the heating surface. There is also possibility that the temperature of the appliance as well as of the smoke outlets and ducts may be higher for the larger installation. In general, however, the larger installations do not present a decided hazard because of the insulation applied over the heating units and their segregation within fire-resistive enclosures.

No attempt has been made to cover the hazards of portable heating and cooking devices such as portable oil stoves, gas stoves, electric heaters, and hot plates. The hazard of such devices is caused not only by the temperatures to which the nearby construction is exposed but also by the possibility of breakage of fuel-supply lines and overturning or damage to the equipment.

## IX. ACKNOWLEDGMENTS

Acknowledgment is made to Mr. G. Haller for assistance in the survey and for information relative to many pertinent fire hazards encountered by him as fire inspector in the District of Columbia. Acknowledgment is also made to Mr. S. H. Ingberg, chief, fire-resistance section of the Bureau of Standards, for valuable suggestions in planning the tests.

WASHINGTON, July 17, 1933

U.S. Department of Commerce, Bureau of Standards

RESEARCH PAPER RP597

*Part of Bureau of Standards Journal of Research, Vol. 11, September 1933*

# A CONTINUOUS RECORDER OF RADIO FIELD INTENSITIES[1]

By K. A. Norton and S. E. Reymer.

ABSTRACT

A recorder of received radio field intensities is described which is used for making continuous records with no attention from operating personnel during periods of at least 24 hours. A bridge arrangement is described which makes feasible the operation of the recorder from a commercial alternating voltage supply. Sample records of received field intensities from several American broadcasting stations are also shown, to illustrate the flexibility of the recording method used and also to illustrate some interesting properties of broadcast transmissions which have been shown by the use of this recorder.

The recorder described in this paper was developed at the Bureau of Standards for the purpose of making continuous records of received field intensities of radio stations. Several of these recorders have been constructed and are in continuous use for recording the received intensities of broadcasting and other stations.

The apparatus has the following characteristics: (*a*) It has a wide frequency range, 540 to 20,000 kilocycles per second; (*b*) all operating voltages are obtained from the 110-volt 60-cycle power supply; (*c*) the scale of the recorder can be made to accommodate the radio-frequency voltage range from 1 to 300,000 microvolts, or any reasonable portion of that range, e.g., 300 to 1,000; (*d*) the scale of the recorder is very nearly logarithmic over the entire intensity range, making possible a uniform percentage accuracy for all portions of the range measured (this feature is of the greatest importance in field intensity measurements since the diurnal variation of radio field intensities may be as much as 100,000 to 1 for a distant station); (*e*) indications are independent of small variations in line voltage and temperature; (*f*) the cost is small, since the parts used are commercially available, having been designed and constructed for other purposes; (*g*) it requires a minimum of attention from the operating personnel, calibrations being required, for a large part of the frequency range, only once in 48 hours; (*h*) it is portable, as shown by transportation of two of the recorders in a truck more than 3,000 miles, and use during and after the trip.

The method used in recording is as follows. A potentiometer recorder [2] (such as is used for recording temperature, humidity, etc.)

[1] Read at U.R.S.I. meeting at Washington, April 27, 1933.

[2] The Brown potentiometer recorder was used, although the Leeds and Northrup potentiometer recorders have been used successfully also.

was used to record the plate resistance of a vacuum tube used as the first intermediate-frequency amplifier in a superheterodyne receiving set. A broadcast receiving set [3] was employed which incorporated an automatic volume control. To cover the frequency band from 1,500 to 20,000 kc, a high-frequency converter was used in conjunction with the broadcast receiving set. The circuit arrangement of the potentiometer recorder is shown in figure 1. It may be seen that it is a wheatstone bridge, the recorder operating in such a manner as to automatically adjust the slide wire $S$ (having a maximum resistance of 50 ohms) for zero current in the galvanometer $G$. The 250-v. direct current is obtained from the power supply of the receiving set, and $R_3$ is made large enough (about 250,000 ohms) so that the voltage across the slide wire in the recorder is about 50 mv. $R_p$ is the plate resistance of the vacuum tube used for measurement. In order to change the intensity range of the recorder it is only

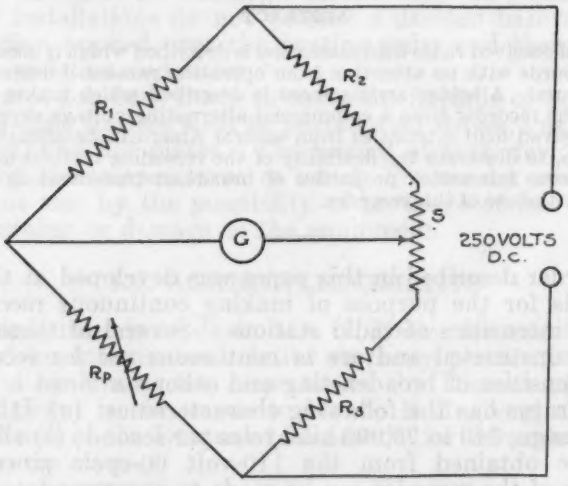


FIGURE 1.—*Bridge used in recorder.*

necessary to vary $R_1$ and $R_2$. These resistors are variable between the limits 0 to 50 ohms and 0 to 175 ohms, respectively. An approximate relation between $R_p$ and the radio-frequency voltage $E$ impressed across the input terminals of the receiving set was found experimentally to be:

$$R_p \cong C \log E \qquad (1)$$

It was found that $R_p$ was very sensitive to small changes in the power-supply voltage, a 5 percent variation causing an apparent 100 percent change in the recorded value of $E$. These variations were effectively eliminated by replacing $R_3$ by the plate resistance of a tube similar to that used for $R_p$.[4] Since the ratio $R_p/R_3$ is independent of line voltage, the recorder no longer responds to power-supply voltage variations. This independence of line voltage for this ratio of plate resistances does not require an exact match of tube characteris-

[3] A Fada KW superheterodyne receiver was used, primarily because it was well shielded and had an appropriate automatic volume control.

[4] This modification was suggested by L. V. Berkner of the radio section.

tics. The sensitivity of the receiving set did not change appreciably with 5 percent variations in the supply voltage so that the function as given in (1) is independent of such variations. The final circuit arrangement of the receiving set and recorder is given in figure 2.

The recorder is calibrated by removing the antenna and applying a local voltage from a standard radio-frequency generator across the antenna and ground terminals of the receiving set (or converter in the case of the higher frequencies). A measurement is occasionally made of the ratio of the voltage across the input terminals introduced by the standard generator and that produced by a known field intensity acting on the antenna; the absolute value of this field intensity is measured by a field-intensity set. In ordinary calibrations of the recorders, it is only necessary to have the standard radio-frequency generator accurate for relative values, the absolute value of the field intensity being checked occasionally as mentioned. One precaution may be mentioned in using this method. It is necessary that the internal impedance of the standard generator be small compared to the input impedance of the receiving set; if this is not the case it will be necessary to make corrections for this shunting impedance in order to keep the relative values of the local voltage correct.

In figure 3 are given several different calibrations of the recorder in terms of microvolts applied to the receiving set. All of these different voltage ranges were obtained simply by varying the resistances $R_1$ and $R_2$. In general, it was found necessary to increase the range for the higher frequencies for two reasons: First, because the intensities on those frequencies vary over a wide range, and, second, the fading is so rapid that the recorder (which changes its balance point only once every 3 seconds) could not follow the variations when the intensity range was decreased. The maximum amount of balancing each 3 seconds amounts to about 8 percent of the total scale value. In this connection it may be mentioned that the recorder is usually run at the rate of 2 inches of record paper per hour but may be run at rates of from 1 to 6 in. per hour; on the frequencies above 2,000 kc it has been found desirable to run the recorder at a rate of 6 in. per hour in order to resolve the rapid fading characteristic of such frequencies.

A temperature variation of $\pm 3°$ C. was found to have a slight effect on the accuracy of the records, especially on the higher broadcast frequencies (1,100 to 1,500 kc), this effect being due primarily to a drift of the heterodyne oscillator. In order to keep this effect at a minimum, the intermediate-frequency band-pass may be broadened, provided the overall selectivity of the receiving set will allow this for the particular existing conditions of interference on neighboring frequencies. On the lower broadcast frequencies (540 to 1,100 kc) it was found that a 6° C. temperature change did not appreciably affect the records. By using a frequency of 575 kc for the intermediate frequency for the converter, the high frequencies also are free from effects of temperature variations. The temperature of the building in which the apparatus is housed is thermostatically controlled to about $\pm 3°$ C. The effect of temperature variation is thus eliminated.

Figure 4 is a photograph of the receiving set and recorder as used for the frequencies between 1,500 and 20,000 kc. Figure 5 is a photograph of several recorders as used for various frequencies in the broad-

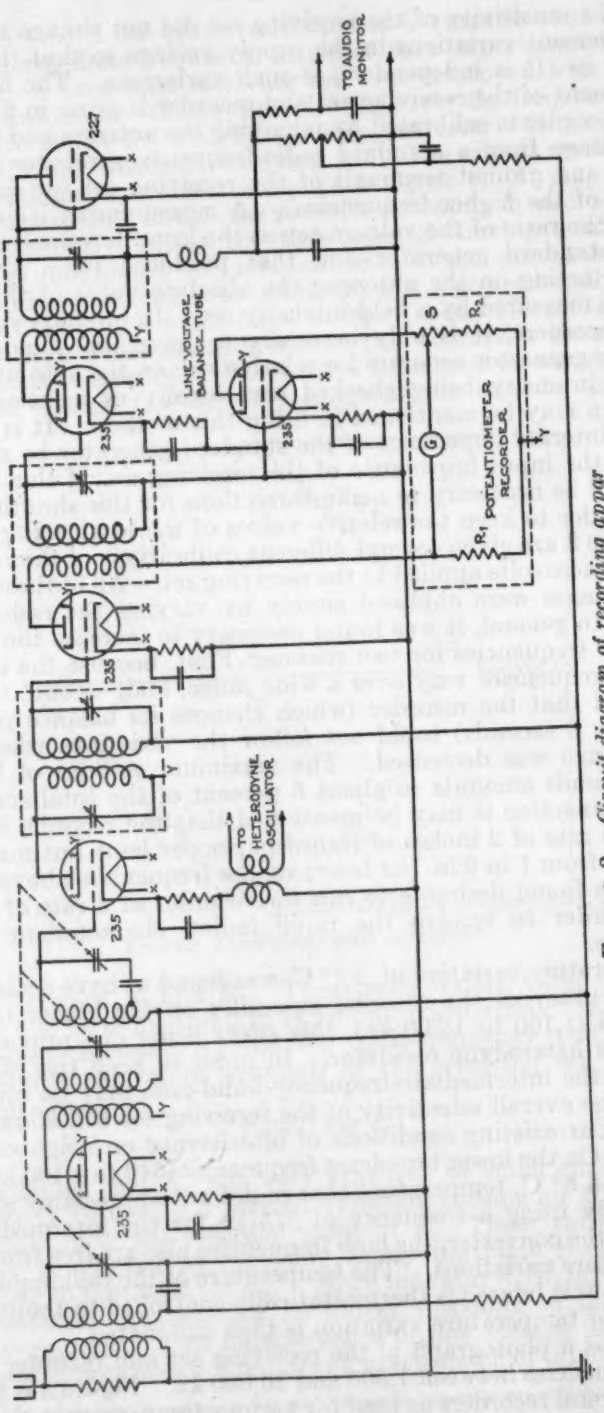


FIGURE 2.—*Circuit diagram of recording appar*

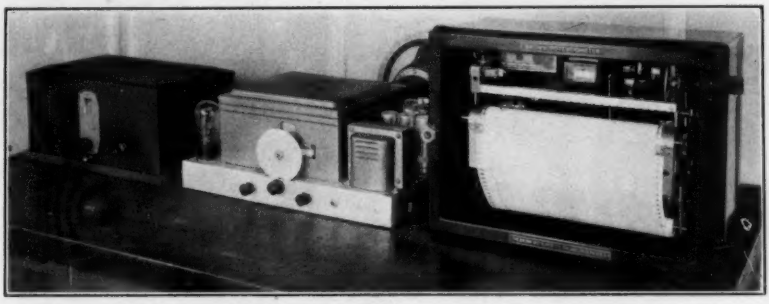

FIGURE 4.—*Field intensity recorder used for frequencies from 1,500 to 20,000 kc.*

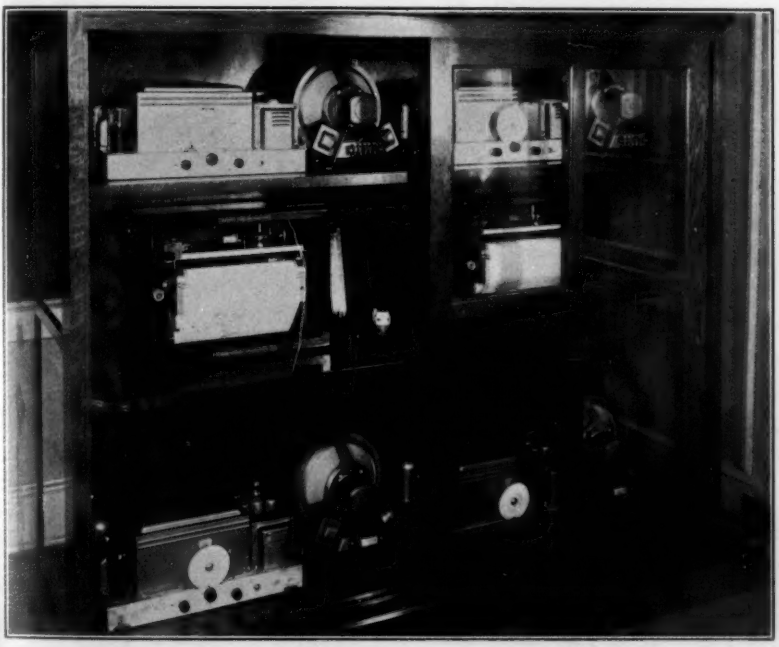

FIGURE 5.—*Field intensity recorders used for broadcast frequencies, 550 to 1,500 kc.*

UNIV. OF MICH.

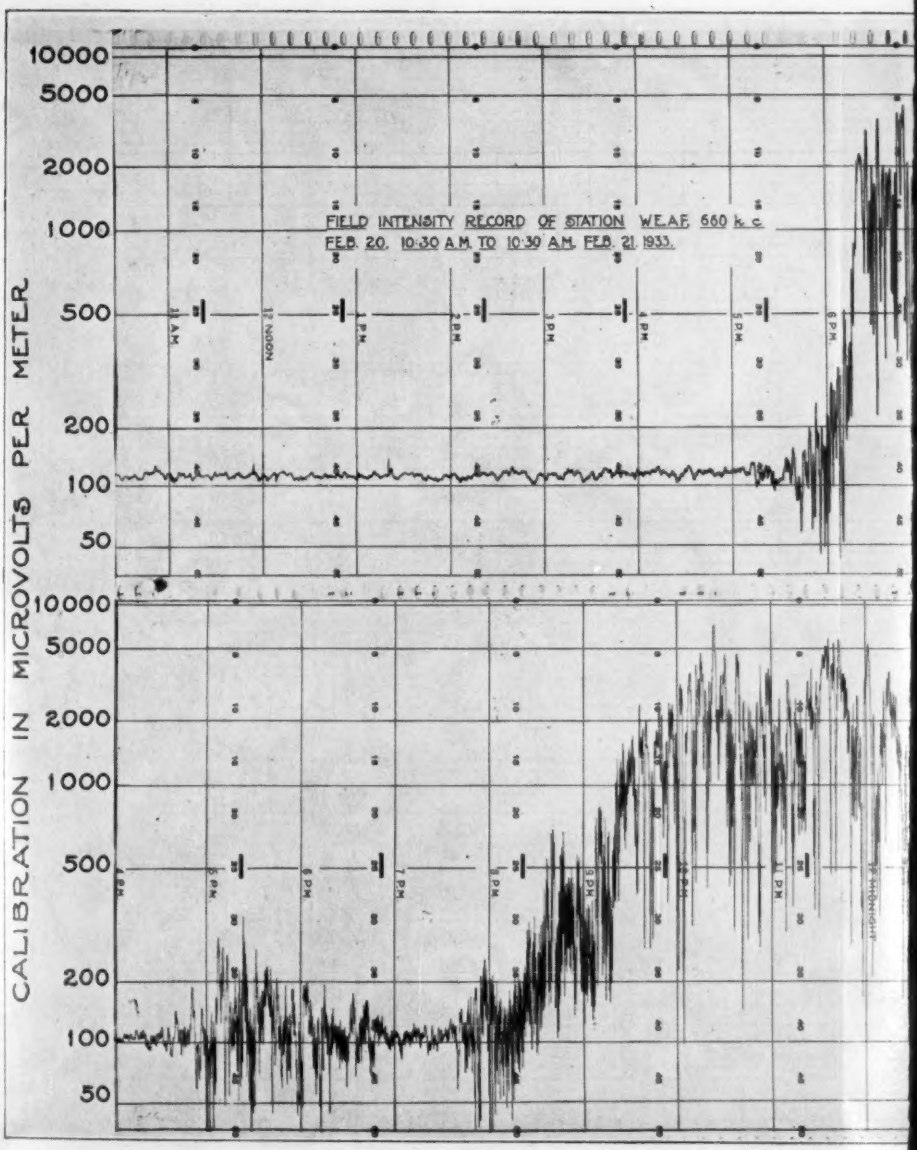


FIGURE 6.—*Field intensity reco*

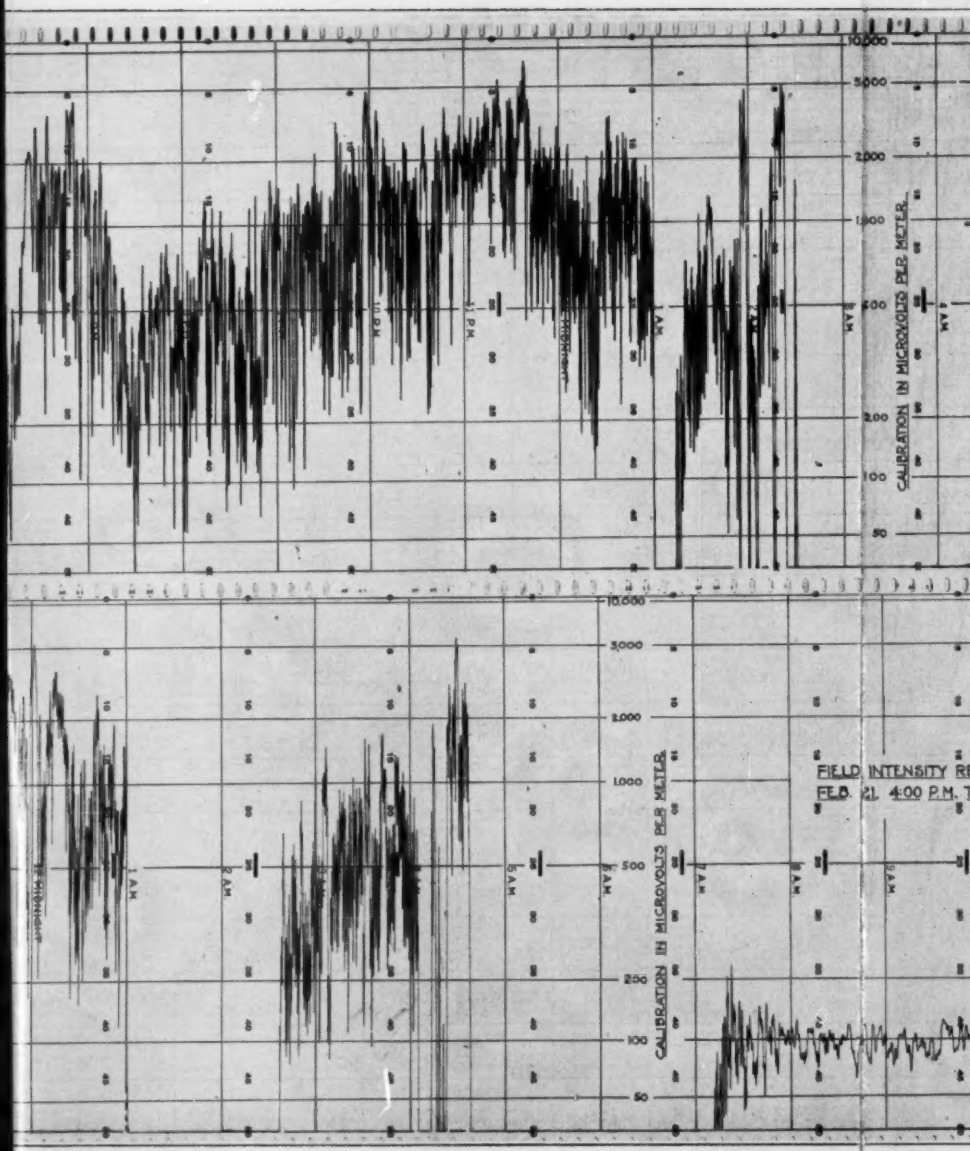


*records of station WEAF, New York, N.Y., frequency 660 kc, power 50 kw, distance 353 km.*

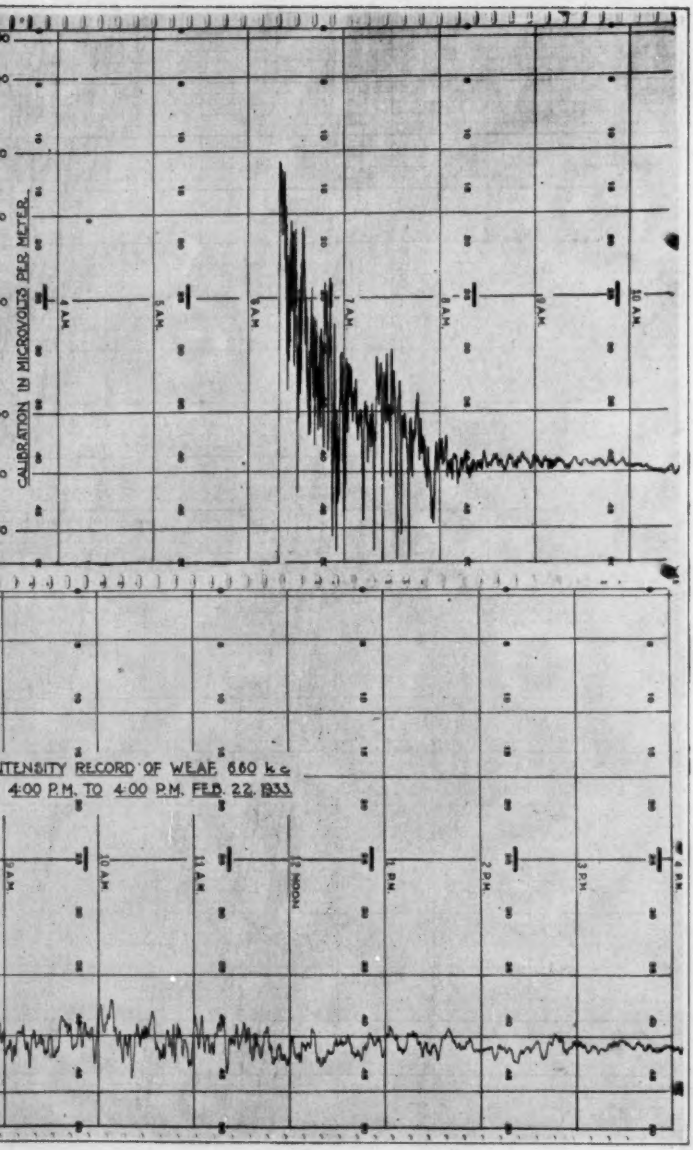


*353 km.*

UNIV OF MICH.

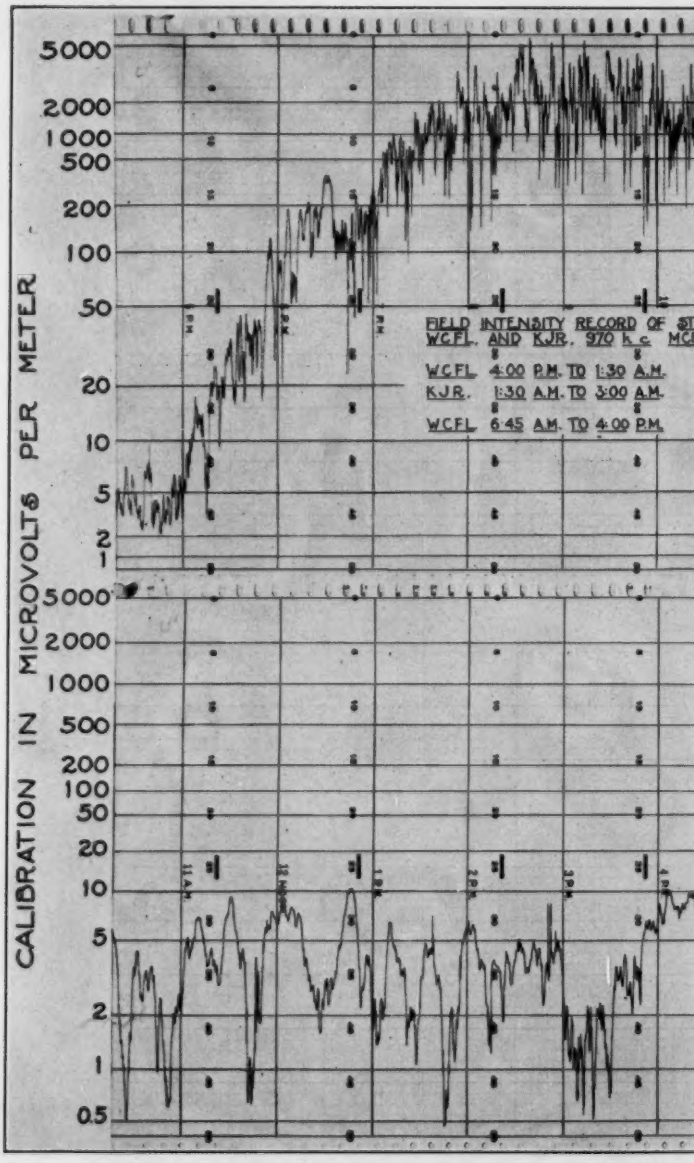


FIGURE 7.—*Field intensity records of stations WCFL, Chicago, Ill.,*

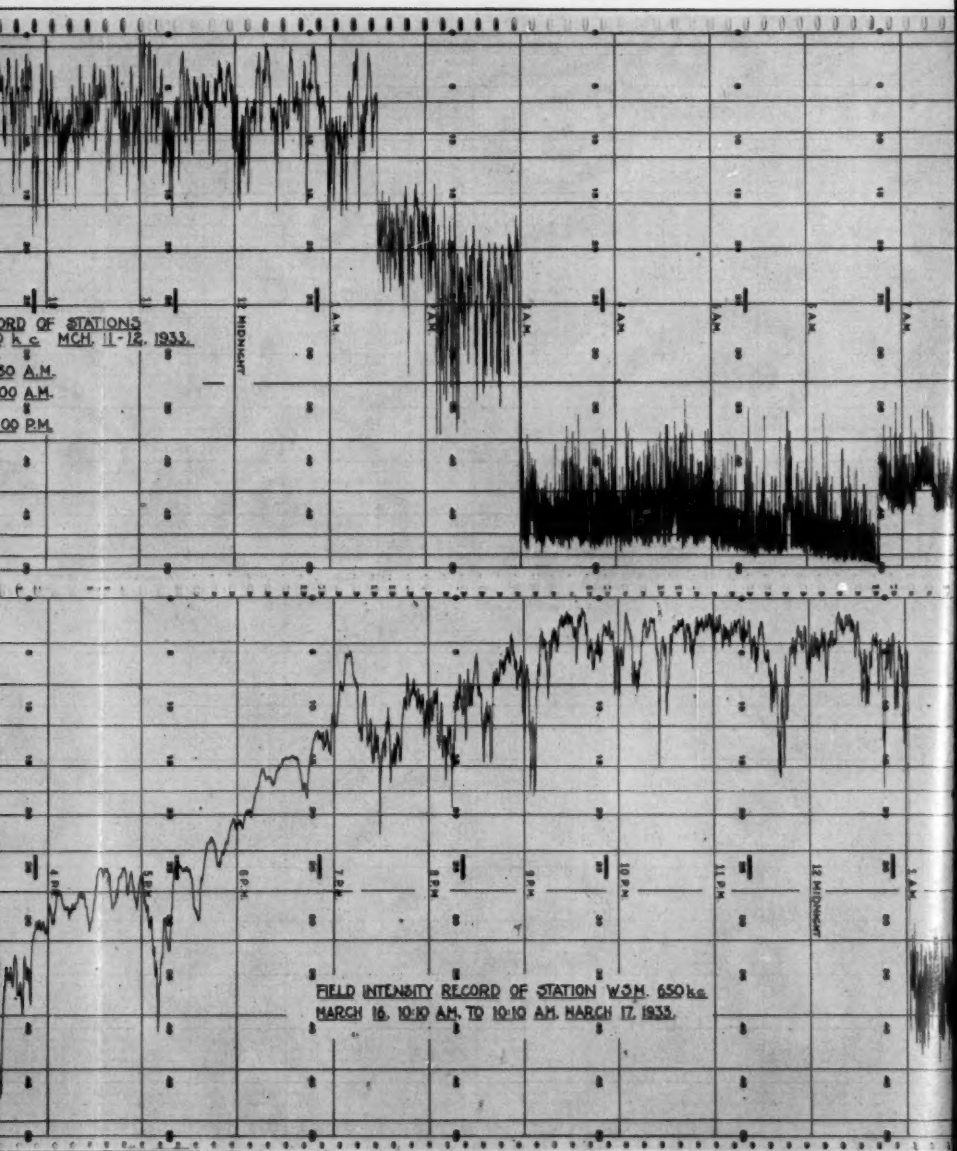


*cago, Ill., frequency 970 kc, power 1.5 kw, distance 988 km; KJR, Seattle, Wash., frequency 97*
*power 50 kw, distance 928 km.*

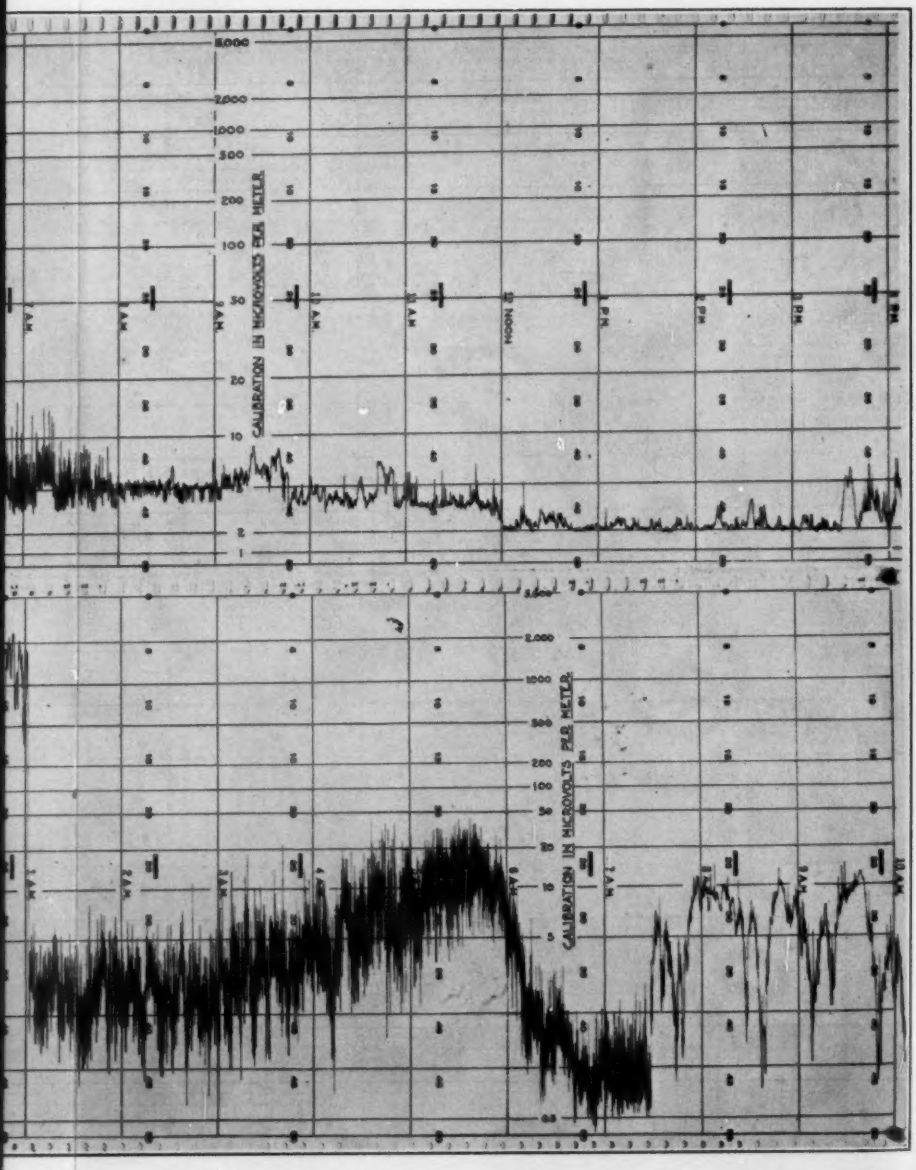


*ncy 970 kc, power 5 kw, distance 3,750 km; and WSM, Nashville, Tenn., frequency 650 kc,*

cast frequency band. Lead-cable transmission lines are used to connect the receiving sets to vertical antennas.

Some examples of the records obtained are given in figures 6 and 7. The field-intensity scales are given by the numbers at the left and by the horizontal lines. Time is given in eastern standard time for hourly intervals along the middle of the records. Table 1 gives the location, frequency, power, and distance (from the receiving station) of the broadcasting stations recorded.

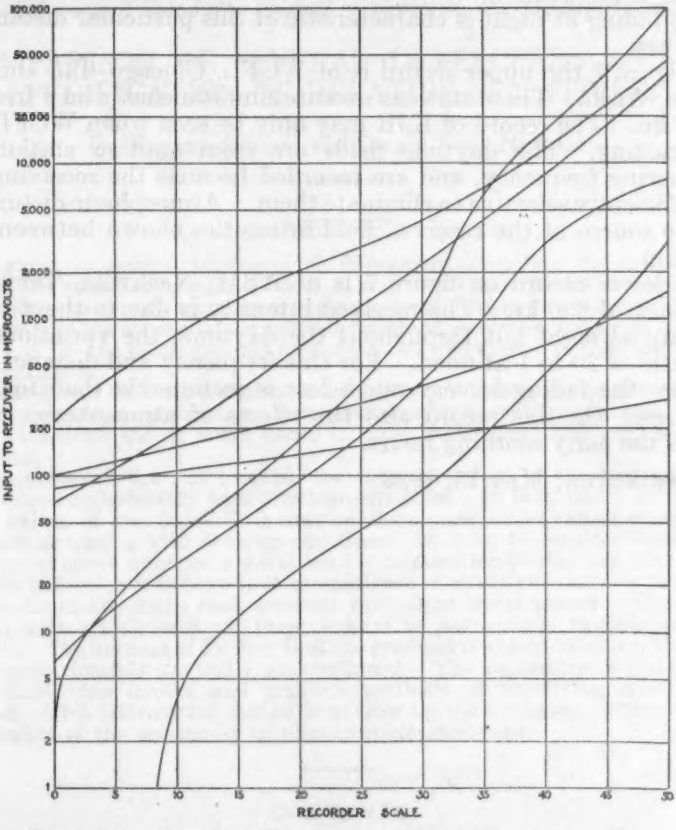


FIGURE 3.—*Sample calibrations of the field intensity recorder.*

TABLE 1

| Station | Location | Frequency | Power | Distance |
|---|---|---|---|---|
| | | *kc* | *kw* | *km* |
| WEAF | Bellmore, Long Island, N.Y. | 660 | 50 | 353 |
| WCFL | Chicago, Ill. | 970 | 1½ | 988 |
| KJR | Seattle, Wash. | 970 | 5 | 3,750 |
| WSM | Nashville, Tenn. | 650 | 50 | 928 |

Figure 6 shows two 24-hour records of station WEAF, located on Long Island. In the upper record the relative steadiness of the day field intensity indicates that it consists primarily of a ground wave.

The fact that the apparatus used recorded the ground wave as a substantially straight line indicates its freedom from line voltage and temperature fluctuations. It will be noticed that the scale of the recorder is approximately logarithmic, making possible an equal percentage accuracy for all parts of the range. Over a period of several months no field intensities have been received for this station greater than 10 mv per meter. At 7:30 p.m. there is a decrease in the field intensity following the rise shown. The dip appears on most of the records of this station, which extend over a period of about 6 months. Severe fading at night is characteristic of this particular distance and frequency.

In figure 7 the upper record is of WCFL, Chicago, Ill., and KJR, Seattle, Wash. These stations operate simultaneously on a frequency of 970 kc. The record of KJR may only be seen when WCFL is not broadcasting. The daytime fields are from another station on a neighboring frequency, and are recorded because the receiving set is not sufficiently selective to eliminate them. Atmospheric disturbances are the source of the received field intensities shown between 3 and 6:45 a.m.

The lower record on figure 7 is of WSM, Nashville, Tenn., on a frequency of 650 kc. The received intensity is due to the sky wave, not only at night but throughout the daytime, the variations being in a ratio of 20 to 1 at noon. For this frequency and distance, about 930 km, the fading is very much less objectionable than for nearer distances. On this record also the effects of atmospherics may be seen in the early morning hours.

WASHINGTON, May 15, 1933.

U.S. Department of Commerce, Bureau of Standards

RESEARCH PAPER RP598

*Part of Bureau of Standards Journal of Research, vol. 11, September 1933*

# A COMPARISON OF SEVERAL DEVELOPERS AND THE SPECIFICATION OF RELATIVE SENSITIVITY

By Raymond Davis and Gerald Kent Neeland

ABSTRACT

In a study of several photographic developers, including the international sensitometric standard, *p*-aminophenol, it was found that the latter agent is not as satisfactory as certain metol-hydroquinone developers in two respects: (1) The "toe" region of the characteristic curve is increased, accompanied by an increased inertia; and (2) the recommended formula is not well chosen in that the solution is supersaturated.

It is also found that the presence of soluble bromide in some developers gives, with some emulsions at least, an increased sensitivity with prolonged development. This effect should prove useful in those cases where high contrast is not detrimental.

It was observed that, in general, the ratio of values of the two sensitivity indices varied considerably with development time. In fact, under certain conditions, values of one index ($1/i$) may be decreasing while values of the other ($1/E_m$) are increasing with development time. In order to consider these apparently contradictory changes a definition for relative sensitivity has been set up. From this definition it follows that comparisons of sensitivity may be made only when the emulsions have each received equivalent development. The type of emulsion with which each of these indices is particularly applicable is also indicated. The findings of Luther, that the gradient of the curve above the inertia point is approximately one half $\gamma$, are confirmed. The application of this constant to coordinate the inertia and gradient methods of specifying sensitivity is discussed. This information should help clear up the confusion surrounding the measurement of the sensitivity of photographic emulsions.

CONTENTS

| | Page |
|---|---|
| I. Introduction | 380 |
| II. Sensitometric characteristics measured | 380 |
| 1. Inertia and fog correction | 381 |
| III. Reproducibility of the measurements | 383 |
| IV. Developers studied | 385 |
| 1. Metol-hydroquinone | 386 |
| (*a*) Without bromide | 386 |
| (*b*) The effect of soluble halides and other fog preventatives | 388 |
| (*c*) The keeping qualities of metol-hydroquinone compared with *p*-aminophenol | 391 |
| 2. *p*-aminophenol | 393 |
| 3. Other developing agents | 398 |
| (*a*) Hydroquinone | 400 |
| (*b*) Metol | 400 |
| (*c*) Glycin | 400 |

Page
V. The relation between the "inertia gradient" and gamma ..... 402
VI. Discussion ..... 403
1. *p*-aminophenol ..... 403
2. Soluble bromide ..... 404
3. Inertia versus gradient ..... 405
4. The international sensitivity index ..... 407
VII. Acknowledgments ..... 407

## I. INTRODUCTION

From the standpoint of international standardization, the chief purpose of photographic sensitometry is to make possible a universally recognized system for expressing the properties of photographic materials. While several modes of expression have been proposed from time to time, the system which appears to be the most flexible and complete is that based on the density versus log-exposure graph devised by Hurter and Driffield. This method of expression was developed many years ago, and its use in representing the characteristics of photographic emulsions is widespread, although some workers prefer the less laborious systems based on the threshold sensitivity obtained by visual inspection of the sensitive material after exposure, etc.

In the last few years, particularly since the advent of sound in motion pictures, there has been an increasing demand for a standard sensitometric system not only for motion-picture work, but also for use by amateur and professional photographers. Here the expression of emulsion properties by the "H&D" graph is the most satisfactory and complete method so far devised.

It is the shape and position of this "H&D" or "characteristic" curve which, of course, determines the values of the quantities representing various properties of the emulsion, such as contrast, sensitivity, etc. As is well known, the shape of this curve depends to some extent upon the developer. The choice of an international standard developer for sensitometric purposes is therefore important since it influences the results obtained when different emulsions are compared.

In this paper we have endeavored to bring out the relative merits of several developers, particularly with regard to their effect on the shape of the characteristic curve.

## II. SENSITOMETRIC CHARACTERISTICS MEASURED

In order to obtain the effect of different developers on sensitivity values, certain sensitometric quantities were measured [1] under constant or comparable conditions with each developer. Several types of emulsions were employed, but where direct comparisons of developers are made, the emulsions are of the same brand and batch, i.e., the same emulsion number. The quantities measured are: (1) Contrast, measured by $\gamma$ (the slope of the straight-line portion of the characteristic curve); (2) minimum density, $D_{min.}$; defined as the least density which could be obtained with a given emulsion under the particular processing conditions. This would be equal to the sum of the densities of the support, gelatin and the fog on an unexposed

[1] Strips of the sensitive material were exposed in a sensitometer and families of characteristic curves constructed using substantially the same procedure as described in B.S.Jour., Research, vol. 7 (R.P. 355), p. 195, 1931. As in that paper, all such curves were plotted directly from the observed densities with no attempt at smoothing or fog correction. (See p. 381.)

portion in most cases; with certain emulsions, due to a fog-reversal effect in the "toe" region of the characteristic curve, $D_{min.}$ will be less than the foregoing sum and may be defined as the least density obtainable by any exposure; (3) sensitivity [2] or "speed", measured both by the "inertia", and by the exposure value of the "minimum useful gradient", $E_m$. The inertia is the exposure value of the intersection of the extended straight-line section of the characteristic curve with a horizontal line representing the minimum density. $E_m$ is the exposure value of the point on the characteristic curve where the gradient is a certain value. The value of gradient to be taken as the "minimum useful" depends on several factors which need not be discussed here. We have taken a value of 0.2 in this work, since this value has been used by other investigators and, as we have shown in previous work, the shape of sensitivity versus development-time curves is not much altered by change in the gradient.

In most cases these four magnitudes were derived for each of six periods of development ranging from 1 to 18 minutes at a temperature of $20° \pm 0.5°$ C. With the exception of the experiments with stand-development, all test strips were brush developed. Table 1 describes the emulsions used. The subscripts after the designation A indicate different batches of the same brand of emulsion. Plate $A_1$ had been kept on hand about 16 months before being used and consequently gives a greater fog than either $A_2$ or $A_3$, as the succeeding tables show. Plate $A_2$ was used within 1 to 5 months and plate $A_3$ within a month after being received from the manufacturer.

TABLE 1.—*Types of plates used*

| Types of plates used | | Types of plates used | |
|---|---|---|---|
| Plate designation | Type of emulsion | Plate designation | Type of emulsion |
| $A_1$ | Ordinary "medium speed" | D | Ordinary "process." |
| $A_2$ | do | E | Ordinary (experimental emulsion containing 1 percent AgI). |
| $A_3$ | do | | |
| B | Ordinary "medium speed", contrasty. | F | Ordinary (experimental emulsion containing 4 percent AgI). |
| C | Orthochromatic "high speed" soft | G | Orthochromatic "medium speed." |

## 1. INERTIA AND FOG CORRECTION

Considerable confusion surrounding the comparison of photographic emulsions in terms of sensitivity arises from the uncertainty regarding the desirability of correcting the densities for fog in the procedure for obtaining the inertia. In a recent publication treating the subject of sensitometry in a tutorial way, Jones [3] has discussed methods of fog correction. However, we do not believe that the conditions under which a correction should be made were sufficiently emphasized. We would like to repeat that in sensitometric work, the results of which are to be applied in a practical way, no correction, in the strict sense of the word, should be made for fog.

In order to make our position more clear, it will be well to go back to the method of plotting the characteristic curve itself. That is, in

[2] See the definition for and the comparison of these and other methods in B.S.Jour. Research, vol. 7 (R.P. 355), p. 495, 1931.

[3] Photographic Sensitometry, Jour. Soc. Motion Picture Engrs, vol. 17, nos. 10 and 11, and vol. 18, nos. 1 and 3, 1931–32.

the present work, the various sensitometric quantities have been obtained from characteristic curves where density is plotted against log-exposure and no correction is made for fog. This is because it is the uncorrected curves which are effective when the negative is examined visually or when it is used to make a positive.[4] Thus, in all practical sensitometry only these uncorrected or effective characteristic curves need be considered.

Such curves differ considerably in shape from those derived from densities, from each of which there has been subtracted an amount equal to the estimated fog component of that particular density. Formulas for making this estimation have been proposed by Wilsey,[5] Pritchard,[6] and others.

It is beyond the scope of this paper to discuss the merits of these formulas. However, it may be said that their use would, at best, present the characteristic curve which *might have been* were there no fog.

Just as plotting the uncorrected densities against log-exposure gives effective scale and contrast, so does this procedure give the *effective inertia* of the material. That is, the effective sensitivity value for the material may be obtained from reciprocal inertia if the uncorrected density is plotted against log-exposure, *provided that the inertia is taken as the exposure value of the intersection of the produced straight-line portion of the curve with a line parallel to the log-exposure axis at a distance above equal to* $D_{min}$.[7]

To show that this method is necessary to obtain the effective inertia of the material, it will be convenient to present again the "hypothetical case" discussed in a previous paper.[8] Here uncorrected densities are plotted against log-exposure and we have two emulsions, A and B, such that each value of exposure results in a density for A which is greater than that of B by a constant amount. In other words, the curves are identical in shape but one is raised above the other. Consequently, if "inertias" are obtained from the intercept on the log-exposure axis, the sensitivity of A will be indicated as being higher than B. On the other hand, it is clear that if the method which we have recommended is followed, the sensitivity value will be the same for both emulsions. It seems only logical that the effective sensitivity of these emulsions should be indicated as the same, since it is obvious that by proper regulation of the printing exposure identical prints could be made from both. The fact that the densities of the one are higher than corresponding values of the other need be of no concern; it is merely as if a uniform density had been placed under one of two identical negatives—only the printing time would be affected.

A little consideration will show that this procedure is mathematically equivalent to the subtraction of a value equal to $D_{min}$ from each of the observed densities before plotting as was Hurter and Driffield's procedure. *This procedure does not necessarily assume that*

[4] This assumes, of course, that the photographic and visual densities are the same. Where this is not true, a correction would be applied to the visual densities. Obviously, this is not to be confused with a correction for fog.

[5] Fog Corrections in Photographic Densities, R. B. Wilsey, Phot. Jour., vol. 65, p. 454, September 1925.

[6] The Fog Correction of Photographic Densities: A Sensitometric Study, H. A. Pritchard, Phot. Jour., vol. 67, p. 447, 1927.

[7] This method of obtaining the effective inertia is not new, having been used by several workers, particularly Carlton and Crabtree in Some Properties of Fine-Grain Developers for Motion Picture Film. Trans. Soc. Motion Picture Engrs., vol. 13, no. 38 p. 406, 1929.

[8] A Note on the "Speed" of Photographic Emulsions, by R. Davis and G. K. Neeland, Jour. Opt. Soc. Amer., vol. 21, no. 7, July 1931.

*the fog component of all densities is a constant. In fact, no assumption is made regarding the fraction of each density which is due to fog.* In Hurter and Driffield's procedure the inertia is taken as the exposure value of the intersection of the extended straight-line portion of the curve with the log-exposure axis itself.

It may be argued that by the use of a suitable fog correction formula the sensitivity values of the two materials considered in the "hypothetical case" might turn out to be the same. Even if this were the case, this method of obtaining sensitivity values does not offer any advantages on the basis of logic over that which we have described, and, in addition, has the considerable disadvantage of not representing the effective characteristic curve.

## III. REPRODUCIBILITY OF THE MEASUREMENTS

The exactness with which the sensitivity indexes may be reproduced is an important factor in determining their merit although it is not, as a rule, available. Tables 2 and 3, in which the technique used was the same as that throughout the paper, give a good idea of the reproducibility attained in the present work. Here the densities of the test strips were read but once and no attempt was made to "smooth" the data.

Table 2 shows the reproducibility of—the individual densities; $\gamma$; $D_{min.}$; the two indexes, $1/i$ and $1/E_m$; and the various derived quantities; all obtained at one time of development.

TABLE 2.—*Shows the reproducibility of the densities, $\gamma$, $D_{min.}$, and 2 indexes of sensitivity, $1/i$ and $1/E_m$ where 5 separate (brush) developments (test strips I–V) were made from 1 batch of (metol-hydroquinone) developer. The 5 strips were developed the same day, the time of development being 6 minutes at a temperature of 20° C. Plate $A_1$ was used*

| Test strip | Densities of squares indicated | | | | | | | | | | | $\gamma$ | $D_{min.}$ | $1/i$ | $1/E_m$ |
|---|---|---|---|---|---|---|---|---|---|---|---|---|---|---|---|
| | 1 | 2 | 3 | 4 | 5 | 6 | 7 | 8 | 9 | 10 | 11 | | | | |
| I | 0.34 | 0.37 | 0.43 | 0.53 | 0.66 | 0.84 | 1.04 | 1.23 | 1.42 | 1.62 | 1.85 | 0.99 | 0.32 | 28 | 55 |
| II | .37 | .39 | .45 | .55 | .68 | .86 | 1.07 | 1.26 | 1.47 | 1.68 | 1.90 | 1.00 | .33 | 28 | 52 |
| III | .37 | .39 | .45 | .55 | .70 | .88 | 1.08 | 1.28 | 1.49 | 1.70 | 1.92 | 1.04 | .34 | 27 | 60 |
| IV | .36 | .39 | .44 | .55 | .69 | .87 | 1.09 | 1.29 | 1.50 | 1.69 | 1.92 | 1.04 | .34 | 26 | 52 |
| V | .34 | .37 | .43 | .53 | .67 | .85 | 1.07 | 1.26 | 1.46 | 1.65 | 1.85 | 0.98 | .32 | 30 | 58 |
| Average | .36 | .38 | .44 | .54 | .68 | .86 | 1.07 | 1.26 | 1.47 | 1.67 | 1.89 | 1.01 | .33 | 28 | 55 |
| Deviations: | | | | | | | | | | | | | | | |
| I | .02 | .01 | .01 | .01 | .02 | .02 | .03 | .03 | .05 | .05 | .04 | .02 | .01 | 0 | 0 |
| II | .01 | .01 | .01 | .01 | | | | | | .01 | .01 | .01 | ----- | 0 | 3 |
| III | .01 | .01 | .01 | .01 | .02 | .02 | .01 | .02 | .02 | .03 | .03 | .03 | .01 | 1 | 5 |
| IV | ----- | .01 | ----- | .01 | .01 | .01 | .02 | .03 | .03 | .02 | .03 | .03 | .01 | 2 | 3 |
| V | .02 | .01 | .01 | .01 | .01 | .01 | ----- | | .01 | .02 | .04 | .03 | .01 | 2 | 3 |
| Mean deviation | .012 | .010 | .008 | .010 | .012 | .012 | .012 | .016 | .022 | .026 | .030 | .024 | .008 | 1.0 | 2.8 |
| Percent mean deviation | 3.3 | 2.6 | 1.8 | 1.9 | 1.8 | 1.4 | 1.1 | 1.3 | 1.5 | 1.6 | 1.6 | ----- | | | |
| Average percent mean deviation | ----- | | | | | 1.8 | | | | | | 2.4 | 2.4 | 3.6 | 5.1 |

Table 3 gives additional data on the reproducibility of the 4 characteristics, in this case obtained at each of 6 times of development. $D_{min.}$ is the most reproducible and $\gamma$ next. It would seem that the reproducibility was least with the low and the high times of development.

TABLE 3.—*Shows the reproducibility of $\gamma$, $D_{min.}$ and 2 indexes of sensitivity, $1/i$ and $1/E_m$, where the numbers under these headings give the time of development in minutes. Separate developments were made on different days in 6 batches of developer. Values are given at 6 times of (brush) development ranging from 1 to 18 minutes at a temperature of 20° C. Plate $A_2$ was used. A metol-hydroquinone developer having a formula (that of experiment 26) slightly different from that of table 2 was employed*

| Developer | $\gamma$ | | | | | | $D_{min.}$ | | | | | | $1/i$ | | | | | | $1/E_m$ | | | | | |
|---|---|---|---|---|---|---|---|---|---|---|---|---|---|---|---|---|---|---|---|---|---|---|---|---|
| | 1 | 2 | 3 | 6 | 12 | 18 | 1 | 2 | 3 | 6 | 12 | 18 | 1 | 2 | 3 | 6 | 12 | 18 | 1 | 2 | 3 | 6 | 12 | 18 |
| Batch I | 0.27 | 0.53 | 0.73 | 1.05 | 1.31 | 1.42 | 0.06 | 0.09 | 0.12 | 0.26 | 0.48 | 0.59 | 89 | 71 | 69 | 60 | 58 | 56 | 44 | ----- | ----- | ----- | ----- | ----- |
| Batch II | .29 | .56 | .70 | 1.02 | 1.29 | 1.27 | .06 | .09 | .12 | .27 | .47 | .59 | 81 | 72 | 81 | 66 | 58 | 62 | 50 | 115 | ----- | ----- | 120 | 110 |
| Batch III | .28 | .58 | .71 | 1.00 | 1.26 | 1.32 | .06 | .09 | .12 | .25 | .47 | .56 | 65 | 52 | 65 | 63 | 55 | 62 | 36 | 115 | 125 | 125 | 100 | 96 |
| Batch IV | .28 | .55 | .70 | 1.01 | 1.32 | 1.43 | .06 | .09 | .12 | .24 | .46 | .57 | 63 | 62 | 68 | 65 | 55 | 55 | 36 | 115 | 125 | 125 | 110 | 125 |
| Batch V | .25 | .51 | .65 | 1.00 | 1.38 | 1.32 | .06 | .09 | .13 | .28 | .48 | .64 | 96 | 78 | 89 | 68 | 54 | 59 | 66 | 110 | 125 | 120 | 115 | 115 |
| Batch VI | --- | --- | .69 | 1.02 | 1.38 | 1.42 | --- | --- | .13 | .29 | .52 | .64 | -- | -- | 83 | 62 | 49 | 55 | -- | --- | 145 | 120 | 130 | 130 |
| Average | .27 | .55 | .70 | 1.02 | 1.32 | 1.36 | .06 | .09 | .12 | .26 | .48 | .60 | 79 | 67 | 76 | 64 | 55 | 58 | 46 | 114 | 130 | 122 | 115 | 115 |
| Deviations: | | | | | | | | | | | | | | | | | | | | | | | | |
| Batch I | .00 | .02 | .03 | .03 | .01 | .06 | .00 | .00 | .00 | .00 | .00 | .01 | 10 | 4 | 7 | 4 | 3 | 2 | 2 | ----- | ----- | ----- | ----- | ----- |
| Batch II | .02 | .01 | .00 | .00 | .03 | .09 | .00 | .00 | .00 | .01 | .01 | .01 | 2 | 5 | 5 | 2 | 3 | 4 | 4 | 1 | ----- | ----- | 5 | 5 |
| Batch III | .01 | .03 | .01 | .02 | .06 | .04 | .00 | .00 | .00 | .01 | .01 | .04 | 14 | 15 | 11 | 1 | 0 | 4 | 10 | 1 | 5 | 3 | 15 | 19 |
| Batch IV | .01 | .00 | .00 | .01 | .00 | .07 | .00 | .00 | .00 | .02 | .02 | .03 | 16 | 5 | 8 | 1 | 0 | 3 | 10 | 1 | 5 | 3 | 5 | 10 |
| Batch V | .02 | .04 | .05 | .02 | .06 | .04 | .00 | .00 | .01 | .02 | .00 | .04 | 17 | 11 | 13 | 4 | 1 | 1 | 20 | 4 | 5 | 2 | 0 | 0 |
| Batch VI | --- | --- | .01 | .00 | .06 | .06 | --- | --- | .01 | .03 | .04 | .04 | -- | -- | 7 | 2 | 6 | 3 | -- | ----- | 15 | 2 | 15 | 15 |
| Mean | .01 | .02 | .02 | .01 | .04 | .06 | .00 | .00 | .00 | .02 | .01 | .03 | 12 | 8 | 8 | 2 | 2 | 3 | 9 | 2 | 8 | 2 | 8 | 10 |
| Percent mean | 3.7 | 3.6 | 2.9 | 1.0 | 3.0 | 4.4 | 0.0 | 0.0 | 0.0 | 7.7 | 2.1 | 5.0 | 15 | 12 | 11 | 3.1 | 3.6 | 5.2 | 20 | 1.8 | 6.2 | 1.6 | 7.0 | 8.7 |
| Average percent mean | | | 3.1 | | | | | | 2.5 | | | | | | | 8.3 | | | | | | 7.6 | | |

The reproducibility of the two indexes, $1/i$ and $1/E_m$, is approximately the same since table 2 shows $1/i$ to be less variable, while table 3 indicates the reverse. This may seem strange in view of the fact that the values of $1/i$ depend on $D_{min.}$ and $\gamma$, each of which depends in turn on the individual densities themselves. The explanation for this unexpected inaccuracy of $1/i$ doubtless lies in graphical errors, principally a shift in the $\gamma$-line parallel to its true position thus changing the inertia value without affecting the value of $\gamma$.

It may also be seen from these tables that the values of the sensitivity indexes are not reproducible to more than two figures under the conditions of these experiments.[9] Doubtless it would be possible to secure greater reproducibility than this from the average of several determinations of each quantity. This procedure would usually involve an unnecessary amount of labor but unless this is done, we do not believe that the use of more than two significant figures is justified. However, this is, of course, no objection to the use of the usual indexes $10/i$ or $10/E_m$. We have used $1/i$ and $1/E_m$ here merely to eliminate useless zeros from the tables.

## IV. DEVELOPERS STUDIED

In the past (and to a considerable extent at present) pyrogallol developers have been used for sensitometric work; but in practice "pyro" has been largely replaced by combinations of metol and hydroquinone. This substitution is probably responsible for the growing tendency to use metol-hydroquinone is sensitometry as well. For this reason, considerable attention has been given to these agents in the present work.

However, the Eighth International Congress of Photography (1931) has adopted, as an international standard for sensitometric use, a certain *p*-aminophenol developer, the characteristics of which have been discussed by Sheppard and Trivelli.[10] The principal reasons given for adopting *p*-aminophenol in place of pyrogallol or a metol-hydroquinone combination were "that it was of single definite constitution, readily purified and reproduced. It gave a neutral gray silver deposit, was only slightly affected by soluble bromide, and gave, so far as experience indicated, undistorted characteristic curves."

At the above mentioned congress, the German sensitometric committee (in connection with a proposed standard method of sensitivity determination),[11] suggested the use of a certain metol-hydroquinone solution as an alternative for *p*-aminophenol.

The sodium sulphite used in these experiments was the anhydrous salt containing, by analysis, 99.2 percent $Na_2SO_3$. The use of potassium metabisulphite instead of sodium sulphite has been recommended by the German sensitometric committee on the ground that it is easier to obtain commercially in a pure form. However, no difficulty was found in obtaining a consistently good grade of sodium sulphite (97 to 99 percent $Na_2SO_3$) on the American market. On the other hand, potassium metabisulphite (ordinarily about 90 percent

[9] The accuracy with which the values of $1/E_m$ may be obtained depends to a considerable extent on the magnitude of the ratio of the apertures in the sector wheel of the sensitometer. The wheel used by Hurter and Driffield had apertures in the ratio of powers of two; that used in these experiments had two thirds this ratio.

[10] A Comparison of Some Developers for Sensitometric Standardization, Proc. of Seventh Int. Cong. of Phot., p. 174, 1928.

[11] Detailed consideration of this method is deferred to another time since it is under consideration by the American national committee of the Ninth International Congress of Scientific and Applied Photography.

$K_2S_2O_5$) is subject to greater variation in strength than sodium sulphite. That used in experiment 55 contained, by analysis, 93 percent $K_2S_2O_5$.

The amount of carbonate is given in the tables in grams per liter of the monohydrated salt theoretically 85.5 percent $Na_2CO_3$. The samples used here contained, by analysis, 87.2 percent $Na_2CO_3$. The monohydrate form was used because of its greater stability, since it approaches equilibrium with average atmospheric humidity more closely than the other forms of carbonate. The potassium carbonate used in experiment 55 contained 99.7 percent $K_2CO_3$. This salt is quite definitely hygroscopic which is an objection to its use.

### 1. METOL-HYDROQUINONE

#### (a) WITHOUT BROMIDE

It was thought desirable to consider first a series of these developers without bromide in order not to confuse its effect with that of the other constituents. Table 4, therefore, deals with the effect of different concentrations (in grams per liter) of sodium sulphite (under heading S) and monohydrated sodium carbonate (under C). The concentrations of metol (under M) and hydroquinone (under Q) were held constant at 2 and 5 grams per liter, respectively, throughout the series of experiments given in this table.

TABLE 4.—*The data for metol-hydroquinone*

4551—33—6

TABLE 4.—*The data for metol-hydroquinone developers, showing the effects of varying concentrations of sodium sulphite and sodium carbonate. The letters under the title "Formula" head columns giving quantities in grams per liter of metol (M); hydroquinone (Q); sodium sulphite (S); and monohydrated sodium carbonate (C)*

| Identification | | Formula | | | | $\gamma$ | | | | | | $D_{min.}$ | | | | | | 1/i | | | | | | $1/E_m$ | | | | | | Values at $\gamma=1$ | | |
|---|---|---|---|---|---|---|---|---|---|---|---|---|---|---|---|---|---|---|---|---|---|---|---|---|---|---|---|---|---|---|---|---|
| Experiment No. | Plate | M | Q | S | C | 1 | 2 | 3 | 6 | 12 | 18 | 1 | 2 | 3 | 6 | 12 | 18 | 1 | 2 | 3 | 6 | 12 | 18 | 1 | 2 | 3 | 6 | 12 | 18 | 1/i | $1/E_m$ | $i/E_m$ |
| 1 | $A_1$ | 2 | 5 | 10 | 10 | 0.50 | 0.90 | 1.09 | 1.51 | 1.58 | ---- | 0.16 | 0.25 | 0.31 | 0.48 | 0.86 | ---- | 19 | 17 | 19 | 17 | 20 | -- | 36 | 48 | 46 | 50 | 50 | 43 | 18 | 47 | 2.6 |
| 2 | $A_1$ | 2 | 5 | 20 | 10 | .50 | .81 | 1.06 | 1.33 | 1.38 | 1.34 | .18 | .27 | .34 | .53 | .86 | 1.15 | 25 | 23 | 20 | 21 | 25 | 25 | 35 | 40 | 44 | 46 | 46 | 44 | 20 | 43 | 2.1 |
| 3 | $A_1$ | 2 | 5 | 40 | 10 | .50 | .83 | 1.00 | 1.33 | 1.30 | 1.27 | .18 | .31 | .40 | .57 | .86 | 1.09 | 22 | 19 | 21 | 21 | 24 | 25 | 30 | 48 | 48 | 42 | 48 | 48 | 21 | 48 | 2.3 |
| 4 | $A_1$ | 2 | 5 | 80 | 10 | .40 | .74 | .96 | 1.44 | 1.56 | 1.49 | .18 | .35 | .46 | .75 | 1.11 | 1.41 | 20 | 19 | 19 | 17 | 18 | 17 | 23 | 42 | 42 | 42 | 50 | 50 | 19 | 42 | 2.2 |
| 5 | $A_1$ | 2 | 5 | 160 | 10 | .29 | .49 | .72 | 1.02 | 1.29 | 1.29 | .12 | .23 | .34 | .59 | .91 | 1.14 | 25 | 27 | 22 | 23 | 21 | 22 | 13 | 36 | 44 | -- | 40 | 44 | 23 | 42 | 1.8 |
| 6 | $A_1$ | 2 | 5 | 20 | 1 | .10 | .27 | .44 | .82 | 1.06 | 1.15 | .05 | .08 | .12 | .23 | .43 | .56 | 10 | 14 | 14 | 14 | 16 | 18 | -- | 6 | 16 | 38 | 55 | 42 | 15 | 50 | 3.3 |
| 7 | $A_1$ | 2 | 5 | 20 | 5 | .37 | .67 | .84 | 1.16 | 1.27 | 1.44 | .13 | .24 | .30 | .49 | .77 | 1.04 | 20 | 19 | 21 | 23 | 25 | 25 | 23 | 40 | 48 | 42 | 44 | 46 | 22 | 45 | 2.0 |
| 8 | $A_1$ | 2 | 5 | 20 | 10 | .55 | .89 | 1.13 | 1.36 | 1.22 | 1.20 | .17 | .26 | 34 | .53 | .81 | 1.08 | 22 | 21 | 18 | 20 | 30 | 29 | 33 | 50 | 50 | 55 | 50 | 44 | 20 | 50 | 2.5 |
| 9 | $A_1$ | 2 | 5 | 20 | 50 | .77 | 1.09 | 1.45 | 1.53 | 1.51 | 1.48 | .23 | .32 | .44 | .73 | 1.17 | 1.50 | 22 | 21 | 17 | 20 | 22 | 25 | 42 | 44 | 42 | 46 | -- | 40 | 21 | 43 | 2.0 |
| 10 | $A_1$ | 2 | 5 | 20 | 100 | .81 | 1.12 | 1.34 | 1.29 | 1.18 | 1.10 | .21 | .35 | .44 | .65 | 1.02 | 1.32 | 19 | 18 | 17 | 23 | 28 | 29 | 48 | 44 | 44 | 48 | 48 | 46 | 18 | 45 | 2.5 |

Experiments 1 to 5 show that if the sulphite content of the developer is increased from a minimum of about 10 grams per liter there results first an increase in fog and a slight decrease in $\gamma$; when the concentration becomes sufficient to exert appreciable solvent action on the silver halide both quantities are considerably reduced. It was further found that the amount of 20 grams per liter is ample where the carbonate content is low (5 to 20 grams per liter). With high carbonate the keeping quality is not good. Variations in the strength of sodium sulphite ordinarily encountered are insufficient to affect appreciably the properties of the developer.

The carbonate concentration of the developer is important, since it affects the velocity of development, the maximum obtainable value of $\gamma$, the aerial oxidation of the solution, and the physical condition of the emulsion after development. However, the effect of the slight variations in the water content of the carbonate on the velocity will be small.

If sensitivity comparisons are made at equal values of $\gamma$, as they should be, small changes in the rate of development will not affect the sensitivity values. Low carbonate concentrations enhance the keeping qualities of the developer, thus reducing the aerial oxidation (important in brush or tray development) as well as having less tendency to soften the emulsion.

Experiments 6 to 10 (table 4) show that the rate of development was, of course, raised by increasing the carbonate content. It was found that below 10 grams per liter the fog (included in values of $D_{min.}$) at a given value of $\gamma$ increased slightly for values in the vicinity of $\gamma = 1$. However, a concentration of 5 grams per liter was selected for the succeeding experiments because it gave slower and therefore more reproducible development with very good keeping qualities.

#### (b) THE EFFECT OF SOLUBLE HALIDES AND OTHER FOG PREVENTATIVES

In the preceding experiments, the change in sensitivity due to variation in the sulphite or carbonate concentration was comparatively small. However, when a soluble bromide is added to a developer, it is seen that the sensitivity values are considerably altered. This effect is brought out by the results of the series of experiments 11 to 33. Here the concentration, in grams per liter, of metol was 2; hydroquinone, 5; sodium sulphite, 20; and monohydrated sodium carbonate, 5 throughout. The concentration of potassium bromide (in grams per liter) is given under heading B, table 5. Experiments were made with six kinds of plates, including two experimental emulsions made by the photographic emulsion laboratory. In all cases, except with the process plate, D, the addition of potassium bromide was without much effect on $\gamma$; reduced the fog; and caused a decrease in values of both sensitivity indexes for short times of development, but *considerably increased sensitivity values with prolonged development* (i.e., at the higher values of $\gamma$). The variation of the index $1/E_m$ is best illustrated by sensitivity versus development-time curves such as shown in figure 1.

TABLE 5.—*The data for a series of metol-hydroquinone developers showing the effects of potassium bromide, (B); potassium iodide, (I); sodium chloride, (Cl); sodium fluoride, (F); and 6-nitrobenziminazol, (6N)*

| Identification | | Formula | | | | | | $\gamma$ | | | | | | $D_{min.}$ | | | | | | $1/i$ | | | | | | $1/E_m$ | | | | | | Values at $\gamma=1$ | | |
|---|---|---|---|---|---|---|---|---|---|---|---|---|---|---|---|---|---|---|---|---|---|---|---|---|---|---|---|---|---|---|---|---|---|---|
| Experiment no. | Plate | M | Q | S | C | B | Other | 1 | 2 | 3 | 6 | 12 | 18 | 1 | 2 | 3 | 6 | 12 | 18 | 1 | 2 | 3 | 6 | 12 | 18 | 1 | 2 | 3 | 6 | 12 | 18 | $1/i$ | $1/E_m$ | $i/E_m$ |
| 11 | B | 2 | 5 | 20 | 5 | 0 | 0 | 0.35 | 0.70 | 1.00 | 1.56 | 1.89 | 1.92 | 0.05 | 0.08 | 0.10 | 0.25 | 0.57 | 0.79 | 62 | 46 | 44 | 37 | 34 | 30 | 48 | 96 | 91 | 100 | 79 | 66 | 44 | 91 | 2.0 |
| 12 | B | 2 | 5 | 20 | 5 | .5 | 0 | .38 | .75 | .95 | 1.54 | 2.10 | 2.26 | .05 | .06 | .06 | .09 | .22 | .40 | 28 | 30 | 41 | 38 | 37 | 36 | 22 | 60 | 76 | 110 | 150 | 160 | 41 | 77 | 1.9 |
| 13 | B | 2 | 5 | 20 | 5 | 1.0 | 0 | .29 | .61 | .91 | 1.44 | 2.04 | 2.19 | .05 | .06 | .06 | .07 | .12 | .22 | 26 | 36 | 37 | 39 | 41 | 43 | 18 | 50 | 66 | 100 | 150 | 155 | 37 | 73 | 2.0 |
| 14 | B | 2 | 5 | 20 | 5 | 2.0 | 0 | .25 | .69 | .97 | 1.45 | 1.96 | 1.89 | .05 | .05 | .06 | .06 | .09 | .14 | 16 | 21 | 27 | 36 | 43 | 59 | 7 | 30 | 55 | 87 | 145 | 165 | 28 | 57 | 2.0 |
| 15 | B | 2 | 5 | 20 | 5 | 4.0 | 0 | --- | .61 | .91 | 1.40 | 2.20 | 1.90 | .05 | .07 | .07 | .08 | .09 | .12 | -- | 14 | 20 | 32 | 43 | 83 | -- | 21 | 35 | 69 | 115 | 250 | 22 | 42 | 1.9 |
| 16 | C | 2 | 5 | 20 | 5 | 0 | 0 | .31 | .54 | .66 | .95 | 1.06 | .95 | .12 | .17 | .21 | .36 | .66 | 1.05 | 69 | 79 | 98 | 87 | 85 | 65 | 50 | 110 | 110 | 125 | 145 | 135 | 86 | 135 | 2.7 |
| 17 | C | 2 | 5 | 20 | 5 | 4 | 0 | --- | .54 | .60 | .90 | 1.04 | .99 | .06 | .09 | .13 | .17 | .29 | .41 | -- | 24 | 54 | 72 | 105 | 130 | -- | 30 | 74 | 130 | 165 | 200 | 94 | 150 | 2.7 |
| 18 | C | 2 | 5 | 20 | 5 | 8 | 0 | --- | --- | .53 | .88 | 1.01 | 1.03 | .07 | .07 | .09 | .15 | .22 | .31 | -- | -- | 26 | 45 | 93 | 120 | -- | -- | 33 | 100 | 170 | 185 | 93 | 170 | 2.9 |
| 19 | D | 2 | 5 | 20 | 5 | 0 | 0 | .97 | 1.71 | 2.12 | 3.00 | 3.26 | 2.84 | .05 | .09 | .13 | .35 | 1.00 | 1.70 | 6.0 | 5.2 | 5.8 | 5.9 | 6.8 | 8.1 | 12 | 17 | 18 | 23 | 29 | 29 | 6.0 | 12 | 2.0 |
| 20 | D | 2 | 5 | 20 | 5 | 2 | 0 | .71 | 1.75 | 2.19 | 3.10 | 3.95 | 4.45 | .05 | .06 | .06 | .06 | .09 | .16 | 3.1 | 3.1 | 3.6 | 4.8 | 5.8 | 6.5 | 4.2 | 6.2 | 8.3 | 14 | 23 | 23 | 3.1 | 4.8 | 1.5 |
| 21 | D | 2 | 5 | 20 | 5 | 8 | 0 | --- | 1.51 | 1.83 | 2.63 | 3.20 | 3.29 | --- | .05 | .05 | .06 | .07 | .09 | ----- | 1.6 | 2.4 | 3.8 | 5.6 | 6.8 | ----- | 4.7 | 5.5 | 11 | 13 | 20 | ----- | ----- | ----- |
| 22 | E | 2 | 5 | 20 | 5 | 0 | 0 | .40 | .78 | 1.05 | 1.62 | 2.22 | 2.32 | .05 | .06 | .07 | .14 | .35 | .65 | 15 | 15 | ----- | 16 | 14 | 17 | 11 | 22 | 24 | 25 | ---- | 29 | 15 | 19 | 1.3 |
| 23 | E | 2 | 5 | 20 | 5 | 4 | 0 | --- | .67 | 1.00 | 1.87 | 2.66 | 2.77 | .05 | .05 | .05 | .06 | .07 | .09 | ----- | 6.8 | 8.5 | 11 | 13 | 17 | ----- | 9.6 | 14 | 21 | 26 | 42 | 8.5 | 14 | 1.6 |
| 24 | F | 2 | 5 | 20 | 5 | 0 | 0 | .27 | .54 | .72 | 1.02 | 1.28 | 1.28 | .06 | .06 | .07 | .16 | .35 | .52 | 25 | 29 | 30 | 27 | 21 | 20 | 11 | 55 | 50 | 52 | 46 | ---- | 27 | 50 | 1.9 |
| 25 | F | 2 | 5 | 20 | 5 | 4 | 0 | --- | .47 | .71 | 1.18 | 1.84 | 1.63 | .05 | .05 | .05 | .05 | .07 | .09 | ---- | 9.1 | 14 | 17 | 14 | 26 | ----- | 11 | 22 | 36 | 46 | 76 | 15 | 28 | 1.9 |
| 26 [a] | $A_2$ | 2 | 5 | 20 | 5 | 0 | 0 | .27 | .55 | .70 | 1.02 | 1.32 | 1.36 | .06 | .09 | .12 | .26 | .48 | .50 | 79 | 67 | 76 | 64 | 55 | 58 | 46 | 114 | 130 | 122 | 113 | 115 | 64 | 123 | 1.9 |
| 27 | $A_2$ | 2 | 5 | 20 | 5 | 1 | 0 | .27 | .63 | .78 | 1.13 | 1.34 | 1.35 | .06 | .09 | .13 | .17 | .35 | .47 | 32 | 43 | 59 | 72 | 74 | 65 | 12 | 72 | 120 | 130 | 135 | 115 | 67 | 127 | 1.9 |
| 28 | $A_2$ | 2 | 5 | 20 | 5 | 2 | 0 | --- | .51 | .68 | 1.03 | 1.41 | 1.32 | .05 | .08 | .09 | .13 | .22 | .33 | ----- | 43 | 55 | 68 | 71 | 79 | ----- | 58 | 100 | 130 | 175 | 195 | 68 | 130 | 1.9 |
| 29 | $A_2$ | 2 | 5 | 20 | 5 | 4 | 0 | --- | .48 | .64 | .96 | 1.27 | 1.30 | .06 | .06 | .08 | .10 | .16 | .25 | ----- | 26 | 43 | 51 | 69 | 79 | ----- | 32 | 69 | 105 | 170 | 170 | 53 | 113 | 2.1 |
| 30 | $A_2$ | 2 | 5 | 20 | 5 | 8 | 0 | --- | .35 | .63 | .97 | 1.27 | 1.46 | .06 | .06 | .08 | .10 | .14 | .20 | ----- | 16 | 26 | 51 | 74 | 78 | ----- | 9.6 | 33 | 110 | 170 | 200 | 53 | 116 | 2.2 |
| 31 [b] | $A_2$ | 2 | 5 | 20 | 5 | 0 | 0 | .17 | .47 | .57 | .86 | 1.24 | 1.25 | .07 | .11 | .13 | .24 | .40 | .49 | 110 | 68 | 78 | 69 | 51 | 54 | ----- | 105 | 110 | 110 | 105 | 96 | 62 | 108 | 1.7 |
| 32 [b] | $A_2$ | 2 | 5 | 20 | 5 | 0 | 0 | --- | ---- | .57 | .80 | 1.27 | 1.51 | --- | --- | .14 | .23 | .38 | .48 | ---------- | | 60 | 66 | 50 | 44 | ---------- | | 100 | 97 | 91 | 91 | 60 | 95 | 1.6 |
| 33 [b] | $A_2$ | 2 | 5 | 20 | 5 | 3 | 0 | --- | ---- | .48 | .74 | 1.06 | 1.33 | --- | --- | .09 | .11 | .15 | .22 | ---------- | | 55 | 87 | 89 | 79 | ---------- | | 110 | 170 | 175 | 130 | 88 | 174 | 2.0 |
| 34 | $A_2$ | 2 | 5 | 20 | 5 | 0 | I .25 | .21 | .46 | .61 | .92 | 1.19 | 1.27 | .06 | .07 | .09 | .16 | .31 | .41 | 39 | 55 | 65 | 79 | 81 | 79 | 13 | 55 | 79 | 115 | 125 | 125 | 79 | 118 | 1.5 |
| 35 | $A_2$ | 2 | 5 | 20 | 5 | 0 | .50 | .19 | .44 | .56 | .80 | 1.01 | 1.20 | .05 | .06 | .08 | .12 | .22 | .33 | 27 | 38 | 49 | 72 | 81 | 85 | ----- | 33 | 50 | 100 | 120 | 120 | 81 | 120 | 1.8 |
| 36 | $A_2$ | 2 | 5 | 20 | 5 | 0 | 1.00 | --- | .33 | .42 | .65 | .83 | .83 | .05 | .06 | .06 | .09 | .14 | .21 | ----- | 27 | 36 | 51 | 59 | 69 | ----- | 19 | 36 | 66 | 91 | 100 | ---------- | | |
| 37 | $A_2$ | 2 | 5 | 20 | 5 | 0 | 2.00 | --- | ---- | .27 | .43 | .48 | .51 | --- | .05 | .05 | .06 | .12 | .14 | ----- | 14 | 25 | 40 | 48 | 45 | ---------- | | 12 | 38 | 52 | 55 | ---------- | | |
| 38 | $A_2$ | 2 | 5 | 20 | 5 | 0 | Cl 1 | .24 | .52 | .60 | .88 | 1.22 | 1.31 | .06 | .09 | .12 | .24 | .44 | .59 | 81 | 69 | 69 | 69 | 62 | 62 | 28 | 100 | 125 | 120 | 120 | 120 | 67 | 120 | 1.8 |
| 39 | $A_2$ | 2 | 5 | 20 | 5 | 0 | 10 | .29 | .57 | .70 | 1.03 | 1.28 | 1.34 | .06 | .10 | .13 | .27 | .48 | .60 | 83 | 65 | 74 | 65 | 62 | 63 | 46 | 100 | 125 | 91 | 110 | 120 | 66 | 94 | 1.4 |
| 40 | $A_2$ | 2 | 5 | 20 | 5 | 0 | 40 | .27 | .58 | .70 | (c) | (c) | (c) | .06 | .12 | .17 | (c) | (c) | (c) | 89 | 62 | 71 | (c) | (c) | (c) | 40 | 115 | 125 | (c) | (c) | (c) | (c) | (c) | (c) |
| 41 | $A_2$ | 2 | 5 | 20 | 5 | 0 | F 2 | .27 | .56 | .71 | 1.03 | 1.36 | 1.42 | .06 | .09 | .11 | .26 | .47 | .61 | 87 | 62 | 71 | 60 | 50 | 51 | 42 | 115 | 130 | 120 | 96 | 98 | 61 | 121 | 2.0 |
| 2 | $A_2$ | 2 | 5 | 20 | 5 | 0 | 6N .064 | .25 | .47 | .63 | .96 | 1.36 | 1.41 | .05 | .06 | .07 | .09 | .19 | .30 | 43 | 66 | 78 | 91 | 68 | 65 | 23 | 91 | 105 | 160 | 190 | 170 | 89 | 163 | 1.8 |

[a] Average of several determinations (values from table 3).

[b] Stand (tank) development.

[c] Dichroic fog precluded measurements.

The experimental emulsions, plates E and F, differed in the proportion of AgI, which was 1 percent in the former and 4 percent in the latter. They were made by the same general process and with the same gelatin. Comparison of experiments 22 and 24, where development was without bromide, show that the concentration of iodide present in the emulsion caused a noticeable difference in the sensitivity versus development-time relations. As the iodide concentration of the developer was decreased, the maximum of the sensitivity versus development-time curve was moved to higher times of development. The addition of soluble bromide to the developer (experiments 23

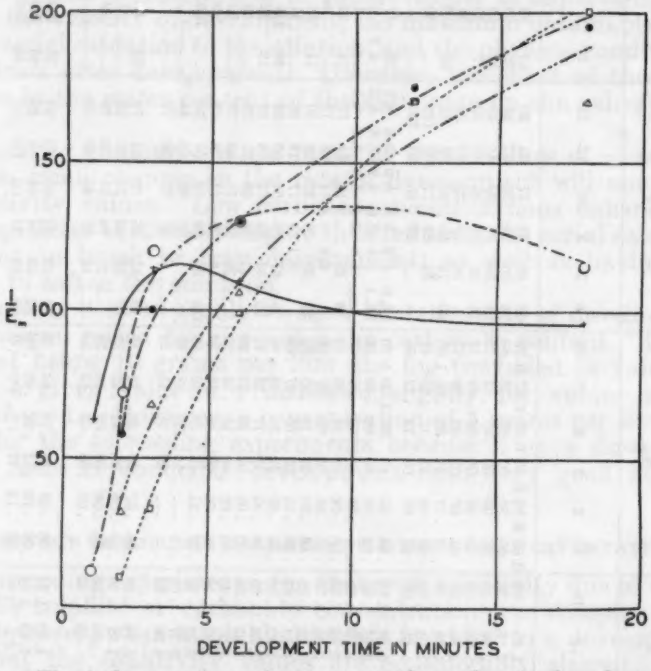


FIGURE 1.—*The influence of varying concentrations of potassium bromide in a metol-hydroquinone developer on the sensitivity versus development-time curves of plate $A_2$. Data are from experiments 26 to 30, table 4. The curve without bromide is marked +; that for 1 gram per liter is marked 0; 2 grams per liter .; 4 grams per liter △; and for 8 grams per liter □.*

and 25) increased the sensitivity values at 18 minutes development with both emulsions.

Experiments 31 to 33 show that the sensitivity increase with bromide also occurs with stand development. It should be noted that experiment 32 repeats 31, omitting the first two development times and gives an idea of the reproducibility which we obtained with this form of development. However, tank development is unsuitable for most sensitometric purposes.

Salts of the other halogens were investigated for similar effects. Experiments 34 to 37 with plate $A_2$ show the effect of varying concentrations of potassium iodide (I). Increasing the iodide concentration in the developer moved the maximum of the sensitivity versus development-time curve for $1/_t$ to higher times of development.

With concentrations of 0.5 grams per liter and less, it gave greater values than were obtained with the control developer (experiment 26). The effect on the curves for $1/E_m$ was similar except that values exceeding those for the control were not obtained. This indicates a change in the shape of the characteristic curve. The higher the iodide concentration the more difficult fixation becomes. There is not much improvement from a fog standpoint, taking into consideration the considerably reduced velocity of development. Experiments 38 to 40 show the effect of varying sodium chloride (Cl); experiment 41, sodium fluoride (F); and experiment 42, 6-nitrobenziminazole. The first two gave negative results.[12] The addition of 6-nitrobenziminazole to emulsions as a fog preventative was patented by Wulff, and its use for this purpose in developers was studied by Trivelli and Jensen.[13] This substance did show an increase in sensitivity similar to that obtained on prolonged development with bromide.

The last three columns of tables 4 to 10 give the respective values of the sensitivity indexes $1/_t$ and $1/E_m$ at $\gamma=1$, and also their ratio. These values (table 5) show that an increase in sensitivity, over that obtained with the control developer, takes place at $\gamma=1$ only with plates $A_2$ and C. The constancy of the ratio $1/E_m$ indicates that (except with the process plate D) there is no appreciable change in the shape of the "toe" region of the characteristic curve with change in bromide content.

In general, the importance of the bromide effect will be greatest where high contrast and high sensitivity are both desirable, such as in astronomical photography, spectography, and oscillography.

### (c) THE KEEPING QUALITY OF METOL-HYDROQUINONE COMPARED WITH *p*-AMINOPHENOL

Carlton and Crabtree[14] have shown that the Eastman D-76 (metol-hydroquinone) borax developer is subject to a considerable increase in the rate of development after standing for 49 days. As they stated, "for sensitometric purposes, a developer is needed whose rate of development does not change with keeping." Tests were therefore made (experiments 43 to 46, table 6) to determine the change with time of standing of a (single solution) metol-hydroquinone developer, (the formula of experiment 26), and in the standard *p*-aminophenol developer. Strips of plate $A_3$ having equal sensitometric exposures were developed for a series of times (all in the same day) in quantities of each developer which were made up, on the one hand, a few hours before use (experiments 43 and 45), and on the other, in quantities of the same developers which had stood for about 6 weeks at room temperature in half-empty, stoppered bottles (experiments 44 and 46). The resulting values show that the change in both developers was very slight. While the aged standard developed was quite discolored, the aged metol-hydroquinone solution was colorless before using. The first showed no change within the experimental error. The 6-weeks old metol-hydroquinone solution gave slightly greater values of $\gamma$. With both developers the change on standing for a reasonable length of time is quite negligible for most sensitometric purposes.

[12] See table no. 5, p. 389.
[13] Antifogging Agents in Developers, Jour. Franklin Institute, vol. 210, p. 287, 1930.
[14] Some Properties of Fine-Grain Developers for Motion Picture Film, Trans. Soc. Mot. Pict. Engrs., vol. 13, no. 38, p. 406, 1929.

TABLE 6.—*Data obtained on the keeping qualities of metol-hydroquinone and the standard p-aminophenol developer*

| Identification | | Formula | | | | | γ | | | | | | $D_{min.}$ | | | | | | 1/i | | | | | | $1/E_m$ | | | | | | Values at γ=1 | | |
|---|---|---|---|---|---|---|---|---|---|---|---|---|---|---|---|---|---|---|---|---|---|---|---|---|---|---|---|---|---|---|---|---|---|
| Experiment No. | Plate | M | Q | S | C | P.A.P. | 1 | 2 | 3 | 6 | 12 | 18 | 1 | 2 | 3 | 6 | 12 | 18 | 1 | 2 | 3 | 6 | 12 | 18 | 1 | 2 | 3 | 6 | 12 | 18 | 1/i | $1/E_m$ | $i/E_m$ |
| 43 | $A_3$ | 2 | 5 | 20 | 5 | 0 | 0.23 | 0.49 | 0.70 | 0.95 | 1.20 | 1.31 | 0.06 | 0.08 | 0.12 | 0.24 | 0.44 | 0.56 | 83 | 78 | 62 | 74 | 63 | 63 | 46 | 120 | 135 | 125 | 105 | 115 | 72 | 121 | 1.7 |
| 44[a] | $A_3$ | 2 | 5 | 20 | 5 | 0 | .27 | .57 | .75 | 1.04 | 1.28 | 1.34 | .05 | .09 | .11 | .25 | .45 | .59 | 89 | 68 | 69 | 66 | 59 | 62 | 46 | 120 | 135 | 120 | 115 | 105 | 66 | 123 | 1.9 |
| 45 | $A_3$ | 0 | 0 | 50 | 57.3 | 7.25 | .30 | .53 | .74 | .93 | 1.07 | 1.09 | .06 | .08 | .09 | .16 | .31 | .38 | 56 | 65 | 51 | 59 | 52 | 56 | 44 | 96 | 105 | 145 | 140 | 135 | 55 | 142 | 2.6 |
| 46[a] | $A_3$ | 0 | 0 | 50 | 57.3 | 7.25 | .27 | .45 | .74 | .97 | 1.02 | 1.03 | .06 | .08 | .09 | .18 | .31 | .40 | 78 | 59 | 54 | 56 | 62 | 65 | 50 | 96 | 110 | 145 | 145 | 135 | 58 | 145 | 2.5 |

[a] Developing solutions kept 6 weeks before use.

### 2. *p*-AMINOPHENOL

In table 7 are the data for a series of experiments with *p*-aminophenol developers, including comparisons with several metol-hydroquinone solutions. The column headings are the same as in table 4 and, in addition, the quantities of *p*-aminophenol in grams per liter are given under the heading *p*-aminophenol and the quantity of potassium metabisulphite under M-B. In experiment 55, the developer was that proposed by the German committee containing 50 grams per liter of anhydrous potassium carbonate.

TABLE 7.—*Results of a series of experiments comparing the international standard p-aminophenol developer with several metol-hydro-quinone and p-aminophenol-hydroquinone developers. The headings are the same as in table 4 and in addition the quantity of p-aminophenol in grams per liter is given under P.A.P.; of potassium metabisulphite under M-B; and of potassium bromide under B*

| Identification | | Formula | | | | | | $\gamma$ | | | | | | $D_{min.}$ | | | | | | $1/i$ | | | | | | $1/E_m$ | | | | | | Values at $\gamma=1$ | | |
|---|---|---|---|---|---|---|---|---|---|---|---|---|---|---|---|---|---|---|---|---|---|---|---|---|---|---|---|---|---|---|---|---|---|---|
| Experiment no. | Plate | M | Q | S | C | B | P.A.P. | 1 | 2 | 3 | 6 | 12 | 18 | 1 | 2 | 3 | 6 | 12 | 18 | 1 | 2 | 3 | 6 | 12 | 18 | 1 | 2 | 3 | 6 | 12 | 18 | $1/i$ | $1/E_m$ | $i/E_m$ |
| 47 | $A_2$ | 0 | 0 | 50 | 57.3 | 0 | 7.25 | 0.29 | 0.59 | 0.76 | 1.12 | 1.37 | 1.41 | 0.09 | 0.11 | 0.14 | 0.23 | 0.36 | 0.42 | 69 | 59 | 58 | 50 | 42 | 37 | 40 | 100 | 130 | 155 | 155 | 160 | 53 | 147 | 2.8 |
| 48 | $A_2$ | 0 | 0 | 50 | 100 | 0 | 7.25 | .23 | .47 | .73 | 1.01 | 1.49 | 1.59 | .08 | .11 | .15 | .23 | .36 | .42 | 91 | 71 | 55 | 41 | 31 | 27 | 40 | 120 | 115 | 135 | 135 | 135 | 41 | 135 | 3.3 |
| 49 | $A_2$ | 0 | 0 | 50 | 57.3 | 0 | 7.25 | .32 | .61 | .89 | 1.47 | 1.78 | 1.75 | .09 | .12 | .16 | .27 | .38 | .45 | 63 | 43 | 33 | 21 | 19 | 20 | 52 | 89 | 98 | 98 | 125 | 130 | 31 | 98 | 3.2 |
| 50 | $A_2$ | 0 | 0 | 50 | 57.3 | 1 | 7.25 | .28 | .62 | .80 | 1.17 | 1.52 | 1.61 | .06 | .09 | .11 | .15 | .24 | .28 | 36 | 32 | 36 | 35 | 29 | 26 | 25 | 60 | 79 | 100 | 120 | 105 | 35 | 90 | 2.6 |
| 51 | $A_2$ | 0 | 0 | 50 | 57.3 | 2 | 7.25 | .32 | .56 | .74 | 1.20 | 1.15 | 1.11 | .05 | .09 | .10 | .12 | .19 | .23 | 18 | 29 | 34 | 30 | 42 | 42 | 6 | 43 | 72 | 100 | 96 | 87 | 32 | 78 | 2.4 |
| 52 | $A_2$ | 0 | 0 | 50 | 57.3 | 4 | 7.25 | ... | .53 | .71 | 1.10 | 1.41 | 1.45 | .05 | .08 | .08 | .11 | .15 | .17 | .. | 18 | 26 | 30 | 31 | 30 | .. | 32 | 42 | 76 | 96 | 100 | 29 | 51 | 1.8 |
| 53 | B | 2 | 5 | 20 | | 5 | 0 | .38 | .69 | 1.04 | 1.49 | 2.16 | 2.47 | .09 | .12 | .16 | .31 | .59 | .79 | 30 | 32 | 28 | 28 | 20 | 18 | 34 | 54 | 68 | 66 | 54 | 55 | 29 | 66 | 2.3 |
| 54 | B | 0 | 0 | 50 | 57.3 | 0 | 7.25 | .44 | .93 | 1.18 | 1.95 | 2.36 | 2.35 | .09 | .10 | .13 | .25 | .44 | .57 | 30 | 21 | 12 | 13 | 12 | 13 | 37 | 60 | 66 | 74 | 68 | 74 | 18 | 62 | 3.4 |
| | | | | | | | M-B | | | | | | | | | | | | | | | | | | | | | | | | | | | |
| 55 | $A_2$ | 2 | 5 | 0 | 50[a] | 1 | 15 | .50 | .87 | 1.12 | 1.17 | 1.28 | 1.29 | .06 | .07 | .09 | .15 | .37 | .48 | 55 | 62 | 60 | 76 | 68 | 68 | 76 | 125 | 130 | 185 | 115 | 110 | 61 | 127 | 2.1 |
| | | | | | | | P.A.P. | | | | | | | | | | | | | | | | | | | | | | | | | | | |
| 56 | $A_2$ | 0 | 0 | 50 | 57.3 | 0 | 7.25 | .27 | .53 | .73 | 1.03 | 1.09 | .95 | .06 | .10 | .13 | .21 | .35 | .45 | 110 | 76 | 63 | 52 | 55 | 72 | 58 | 105 | 135 | 145 | 125 | 110 | 53 | 144 | 2.7 |
| 57 | $A_2$ | 0 | 0 | 25 | 57.3 | 0 | 7.25 | .34 | .70 | .85 | 1.20 | 1.31 | 1.47 | .06 | .09 | .11 | .20 | .31 | .40 | 85 | 54 | 54 | 42 | 41 | 49 | 72 | 115 | 135 | 145 | 140 | 130 | 49 | 139 | 2.8 |
| 58 | G | 2 | 5 | 20 | 5 | 0 | 0 | .22 | .45 | .68 | .96 | 1.23 | 1.26 | .08 | .12 | .17 | .30 | .53 | .76 | 110 | 110 | 96 | 100 | 85 | 76 | 40 | 140 | 160 | 150 | 140 | 135 | 98 | 149 | 1.5 |
| 59 | G | 0 | 0 | 50 | 57.3 | 0 | 7.25 | .27 | .55 | .69 | 1.01 | 1.10 | 1.07 | .08 | .12 | .16 | .27 | .47 | .70 | 100 | 76 | 78 | 66 | 60 | 51 | 51 | 120 | 145 | 160 | 140 | 125 | 66 | 160 | 2.4 |
| 60 | G | 0 | 5 | 20 | 5 | 0 | 1.692 | ... | .16 | .31 | .64 | 1.01 | 1.13 | .06 | .08 | .12 | .22 | .35 | .56 | ... | 150 | 110 | 93 | 76 | 68 | .. | ... | 66 | 115 | 130 | 87 | 93 | 130 | 1.4 |
| 61 | G | 0 | 5 | 20 | 20 | 0 | 1.692 | .20 | .45 | .69 | 1.02 | 1.33 | 1.12 | .08 | .13 | .17 | .34 | .60 | .88 | 120 | 89 | 105 | 71 | 62 | 66 | .. | 115 | 130 | 125 | 120 | 105 | 73 | 125 | 1.7 |
| 62 | G | 0 | 2.750 | 20 | 10 | 0 | 3.638 | .14 | .33 | .52 | .85 | 1.26 | 1.12 | .07 | .14 | .19 | .35 | .60 | .86 | 125 | 105 | 85 | 87 | 68 | 66 | .. | 93 | 110 | 125 | 115 | 93 | 80 | 121 | 1.5 |

[a] 50 grams per liter of anhydrous $K_2CO_3$.

Experiments 47 to 48 in which the quantity of carbonate is approximately doubled show that the velocity of development is not greatly altered by this change in alkalinity. This insensitivity to carbonate variation, together with the good keeping qualities discussed in the previous section, constitute good points of this developing agent. The sensitivity versus development-time relations for $1/i$ were altered by increasing carbonate; that is, with 50 grams per liter, the sensitivity values decreased by one half in 18 minutes; but with 100 grams per liter values (at 18 minutes' development) were decreased to one third that at 1-minute development. On the other hand, values of $1/E_m$ did not increase with time of development as much with 100 grams as with 50 grams per liter, showing that a change in the shape of the characteristic curve had taken place.

The action of potassium bromide on the standard developer (experiments 49 to 52) differs from its effect on metol-hydroquinone in that values of neither of the sensitivity indexes in the case of the bromided solutions rise above those for the unbromided even after 18 minutes development. Nor did it appear as though such an increase would occur with further development before the dichroic fog, due to prolonged development with bromide, would become objectionable.

It is interesting to compare experiment 54 (table 7) in which the international standard *p*-aminophenol developer [15] was used, with experiment 53 using the metol-hydroquinone control developer (formula of experiment 26)—the same emulsion being used in both experiments. Values of $1/E_m$ show that the sensitivity is much the same on this basis for the two developers (ratio of values at $\gamma=1$ being 0.94); but values of $1/i$ for the standard are, in general, considerably lower (ratio of values at $\gamma=1$ being 0.62). This indicates a condition at once apparent on inspection of the characteristic curves of plate B given in figure 2;[16] that is, as compared with metol-hydroquinone, the *p*-aminophenol increases the length of the "toe" chiefly at the expense of the straight-line portion of the curve accompanied by decreasing values of $1/i$.

This effect of para-aminophenol is somewhat at variance with the findings of Sheppard and Trivelli.[17] [18] However, in their work, data comparing metol-hydroquinone and *p*-aminophenol developers are shown for only one emulsion and further it would appear that a separate batch of emulsion was used with each developer. Thus, the variation between batches for the same developer being about the same as that between different developers, no very definite conclusions as to the latitude [19] or length of "toe" seem justified.

Further data comparing metol-hydroquinone and *p*-aminophenol on another emulsion (plate G) are given in experiments 58 and 59 and illustrated in figure 3.

[15] According to information received after most of the experimental work in this paper was concluded, the quantity of *p*-aminophenol specified by the formula for the international standard developer is 7.275 instead of 7.250 grams per liter, as in the formula recommended by Sheppard and Trivelli at the seventh congress (see footnote, p. 385). The effect on emulsion characteristics of the 25 mg difference between the two formulas would obviously be quite negligible.

[16] The experiments, the results of which are shown in this figure, were repeated using a longer log-exposure scale so as to include the "shoulder" of the curve. It was found that the "shoulder" begins just at the last ordinate shown on this graph in the case of both developers. This should reassure the reader as to the reliability of values of $1/i$ for the standard developer.

[17] A Comparison of Some Developers for Sensitometric Standardization, Proc. 7th Int. Cong. of Phot., p. 174, July 1928.

[18] Verification of our findings with *p*-aminophenol was made by Carroll, Hubbard, and Kretchman; of the photographic emulsion laboratory of this Bureau using experimental emulsions. They also report the same difficulty in getting the developing agent into solution which is referred to later in this paper.

[19] The exposure range of the straight portion of the characteristic curve.

The effect was also observed with the metol developers, table 9, and figure 4. This raises an objection to the use of either of these substances alone as standard developing agents.

It was thought possible to straighten the characteristic curves by adding hydroquinone. The latter has this effect when combined with metol. A comparison of the metol-hydroquinone control, the standard *p*-aminophenol developer, and a *p*-aminophenol-hydroquinone combination containing an amount of *p*-aminophenol equivalent to 2 grams of metol, is given in experiments 58, 59, and 60, respectively. Notice that values of the ratio $i/E_m$ (a measure of the

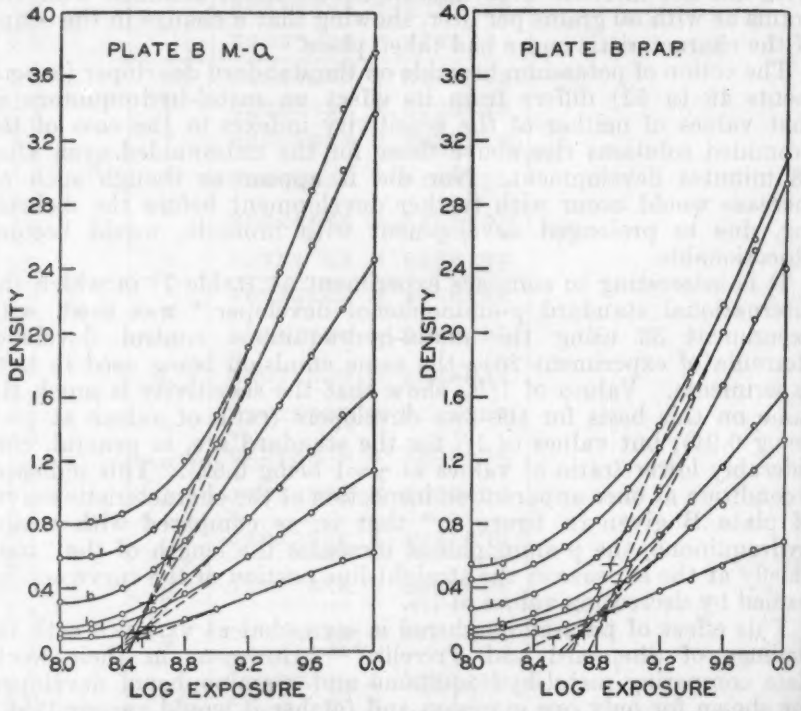


FIGURE 2.—*Comparison of families of characteristic curves obtained with metol-hydroquinone (data from experiment 58) and the standard p-aminophenol developer (experiment 54).*

distortion of the curve) are practically the same, 1.5 and 1.4 for metol-hydroquinone and *p*-aminophenol-hydroquinone, respectively.

The velocity of development for this *p*-aminophenol-hydroquinone combination is low; however, it can be made comparable with the metol-hydroquinone control by increasing the alkalinity as illustrated in experiment 61. This does not appreciably increase the length of the "toe" of the curve.

For comparison purposes, another *p*-aminophenol-hydroquinone combination is given in which each of the developing agents have concentrations of M/40 the combination being M/20 as used by Nietz and others. This also gives characteristic curves having good straight-line sections.

It is of interest to point out that the metol-hydroquinone developer recommended by the German sensitometric committee gave characteristic curves with good straight-line sections, although it is somewhat

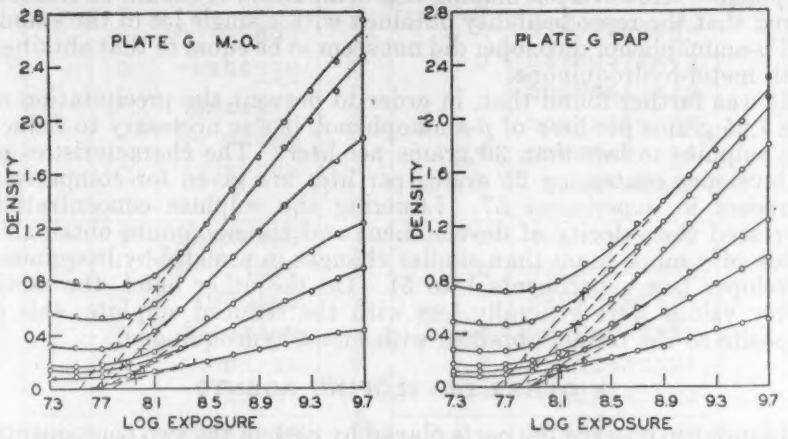


FIGURE 3.—*Further comparison of families of characteristic curves obtained with metol-hydroquinone (data from experiment 58) and the standard p-aminophenol developer (experiment 59). As in figure 2, the curves for the standard developer have definitely longer "toe" portions.*

more rapid in action than necessary. (For a comparison of this developer with the standard see experiments 55 and 56.)

One of the principal difficulties which were experienced with *p*-aminophenol was that of getting the developing agent to remain in

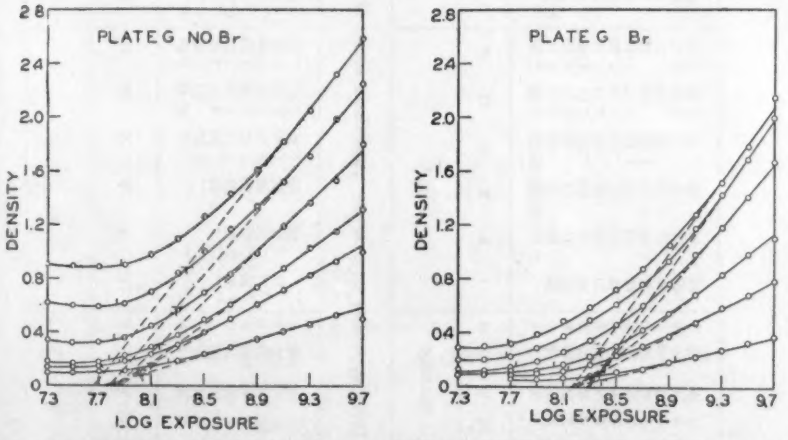


FIGURE 4.—*Showing the effect on the characteristic curve of adding potassium bromide to a metol developer. Note that the maximum value of $1/E_m$ is greater for the bromided developer and also that, as compared with the curves for metol-hydroquinone in figure 3, these curves have greater length of "toe."*

solution. That is, the 50 grams per liter of sulphite seem to be sufficient to throw the developing agent out of solution at 20°C. If the developer is heated the *p*-aminophenol will be dissolved, but it slowly precipitates out again on standing. Two samples were tried

and the same difficulty encountered with each. Some idea of the reproducibility of the two lots may be had by comparing experiment 45, the original lot, with experiment 56 which was made with a later shipment. However, in making this comparison it should be remembered that the reproducibility obtained with a single lot of the standard *p*-aminophenol developer did not seem to be equal to that obtained with metol-hydroquinone.

It was further found that, in order to prevent the precipitation of the 7.25 grams per liter of *p*-aminophenol, it was necessary to reduce the sulphite to less than 30 grams per liter. The characteristics of a developer containing 25 grams per liter are given for comparison purposes in experiment 57. Lowering the sulphite concentration increased the velocity of development and the maximum obtainable value of $\gamma$ much more than similar changes in a metol-hydroquinone developer (see experiments 1 to 5). On the other hand, the sensitivity values were generally less with the reduced sulphite; this is opposite to the results obtained with metol-hydroquinone.

### 3. OTHER DEVELOPING AGENTS

In order to observe the parts played by each of the two components, the metol-hydroquinone experiments 6 to 10, table 4, were repeated, eliminating first the metol (table 8, experiments 63 to 67) and then the hydroquinone (table 9, experiments 71 to 75).

TABLE 8.—*Data obtained with hydroquinone developer*

TABLE 8.—*Data obtained with hydroquinone developers*

| Identification | | Formula | | | | γ | | | | | | $D_{min.}$ | | | | | | 1/i | | | | | | $1/E_m$ | | | | | | Values at γ=1 | | |
|---|---|---|---|---|---|---|---|---|---|---|---|---|---|---|---|---|---|---|---|---|---|---|---|---|---|---|---|---|---|---|---|---|
| Experiment No. | Plate | Q | S | C | B | 1 | 2 | 3 | 6 | 12 | 18 | 1 | 2 | 3 | 6 | 12 | 18 | 1 | 2 | 3 | 6 | 12 | 18 | 1 | 2 | 3 | 6 | 12 | 18 | 1/i | $1/E_m$ | $i/E_m$ |
| 63 | $A_1$ | 5 | 20 | 1 | 0 | ---- | ---- | ---- | ---- | 0.48 | 0.69 | ---- | ---- | ---- | ---- | 0.08 | 0.35 | -- | -- | -- | -- | 8 | 11 | -- | -- | -- | -- | 9 | 22 | -- | -- | --- |
| 64 | $A_1$ | 5 | 20 | 5 | 0 | ---- | ---- | ---- | 0.65 | .92 | 1.08 | ---- | ---- | ---- | 0.25 | 1.20 | 1.72 | -- | -- | -- | 14 | 10 | 10 | -- | -- | -- | 32 | 26 | 28 | 10 | 27 | 2.7 |
| 65 | $A_1$ | 5 | 20 | 10 | 0 | ---- | ---- | 0.49 | .84 | 1.07 | 1.01 | ---- | ---- | 0.06 | .71 | 1.49 | 1.88 | -- | -- | 7 | 11 | 13 | 14 | -- | -- | 7 | 33 | 36 | 30 | 13 | 35 | 3.1 |
| 66 | $A_1$ | 5 | 20 | 50 | 0 | 0.16 | 0.46 | .63 | 1.11 | 1.29 | 1.07 | 0.06 | 0.37 | .63 | 1.11 | 1.54 | 1.90 | 12 | 16 | 17 | 12 | 15 | 14 | -- | 40 | 33 | 28 | 29 | 26 | 14 | 29 | 2.1 |
| 67 | $A_1$ | 5 | 20 | 100 | 0 | .19 | .41 | .60 | 1.12 | 1.29 | 1.22 | .11 | .38 | .49 | .74 | 1.08 | 1.30 | 32 | 24 | 29 | 18 | 18 | 20 | -- | 32 | 29 | 30 | 40 | 32 | 20 | 30 | 1.5 |
| 68 | $A_2$ | 20 | 40 | 50 | 2 | ---- | .28 | .69 | 1.27 | 1.47 | 1.80 | .05 | .05 | .07 | .15 | .42 | .55 | -- | 25 | 44 | 49 | 44 | 32 | -- | 23 | 83 | 125 | 115 | 120 | 47 | 106 | 2.3 |
| 69 | $A_2$ | 20 | 40 | 100 | 2 | .19 | .47 | .82 | 1.40 | 1.47 | 1.48 | .05 | .06 | .09 | .19 | .41 | .55 | 25 | 60 | 46 | 37 | 36 | 36 | -- | 83 | 100 | 125 | 100 | 96 | 40 | 108 | 2.7 |
| 70 | $A_2$ | 20 | 40 | 100 | 6 | ---- | .42 | .65 | 1.35 | 1.61 | 1.64 | .05 | .05 | .06 | .10 | .18 | .34 | -- | 27 | 39 | 41 | 47 | 46 | -- | 26 | 55 | 145 | 165 | 145 | 40 | 105 | 2.6 |

TABLE 9.—*Data obtained with metol developers showing effects of varying the concentrations of metol and sodium carbonate*

| Identification | | Formula | | | | γ | | | | | | $D_{min.}$ | | | | | | 1/i | | | | | | $1/E_m$ | | | | | | Values at γ=1 | | |
|---|---|---|---|---|---|---|---|---|---|---|---|---|---|---|---|---|---|---|---|---|---|---|---|---|---|---|---|---|---|---|---|---|
| Experiment no. | Plate | M | S | C | B | 1 | 2 | 3 | 6 | 12 | 18 | 1 | 2 | 3 | 6 | 12 | 18 | 1 | 2 | 3 | 6 | 12 | 18 | 1 | 2 | 3 | 6 | 12 | 18 | 1/i | $1/E_m$ | $i/E_m$ |
| 71 | $A_1$ | 2 | 20 | 1 | 0 | ---- | 0.20 | 0.36 | 0.63 | 0.96 | 1.06 | ---- | 0.05 | 0.09 | 0.18 | 0.35 | 0.47 | -- | 19 | 15 | 19 | 18 | 20 | -- | 8 | 17 | 35 | 52 | 52 | 19 | 52 | 2.7 |
| 72 | $A_1$ | 2 | 20 | 5 | 0 | 0.28 | .43 | .59 | .96 | 1.11 | 1.11 | 0.10 | .15 | .24 | .38 | .58 | .75 | 34 | 34 | 28 | 20 | 22 | 27 | 29 | 40 | 38 | 40 | 44 | 46 | 20 | 41 | 2.0 |
| 73 | $A_1$ | 2 | 20 | 10 | 0 | .27 | .51 | .64 | .92 | 1.21 | 1.22 | .12 | .17 | .24 | .40 | .67 | .79 | 31 | 25 | 23 | 20 | 19 | 21 | 38 | 39 | 46 | 33 | 48 | 48 | 20 | 37 | 1.8 |
| 74 | $A_1$ | 2 | 20 | 50 | 0 | .30 | .49 | .62 | .91 | 1.07 | 1.06 | .12 | .19 | .25 | .44 | .67 | .85 | 33 | 26 | 23 | 36 | 21 | 25 | 26 | 40 | 38 | 33 | 46 | 48 | 29 | 40 | 2.1 |
| 75 | $A_1$ | 2 | 20 | 100 | 0 | .25 | .40 | .51 | .83 | 1.13 | 1.16 | .12 | .17 | .24 | .42 | .68 | .85 | 39 | 32 | 27 | 18 | 17 | 19 | 29 | 30 | 32 | 32 | 42 | 40 | 18 | 38 | 2.1 |
| 76 | $A_1$ | 8 | 20 | 5 | 0 | .23 | .44 | .61 | .82 | 1.11 | 1.24 | .08 | .12 | .18 | .29 | .47 | .61 | 20 | 18 | 17 | 25 | 24 | 21 | 6 | 20 | 28 | 46 | 46 | 50 | 24 | 46 | 1.9 |
| 77 | $A_1$ | 8 | 20 | 10 | 0 | .48 | .72 | .90 | 1.16 | 1.07 | 1.16 | .13 | .20 | .25 | .41 | .66 | .90 | 19 | 21 | 17 | 16 | 26 | 26 | 29 | 40 | 35 | 38 | 44 | 58 | 17 | 37 | 2.2 |
| 78 | $A_1$ | 8 | 20 | 50 | 0 | .68 | 1.00 | 1.13 | 1.03 | .92 | .76 | .18 | .27 | .34 | .59 | 1.02 | 1.46 | 18 | 13 | 13 | 19 | 30 | 28 | 36 | 38 | 33 | 46 | 66 | 38 | 13 | 38 | 2.9 |
| 79 | $A_1$ | 8 | 20 | 100 | 0 | .56 | .91 | 1.12 | .98 | .82 | .81 | .18 | .26 | .35 | .61 | 1.13 | 1.57 | 16 | 13 | 11 | 16 | 23 | 22 | 32 | 32 | 33 | 44 | 58 | 44 | 12 | 32 | 2.7 |
| 80 | G | 8 | 20 | 10 | 0 | .30 | .56 | .71 | .94 | 1.15 | 1.27 | .09 | .12 | .18 | .31 | .59 | .89 | 91 | 96 | 79 | 69 | 51 | 44 | 59 | 140 | 170 | 155 | 145 | 135 | 61 | 151 | 2.5 |
| 81 | G | 8 | 20 | 10 | 3 | .24 | .51 | .76 | 1.16 | 1.40 | 1.34 | .06 | .08 | .09 | .11 | .17 | .29 | 42 | 49 | 50 | 43 | 39 | 42 | 115 | 72 | 93 | 185 | 215 | 210 | 46 | 148 | 3.2 |

(a) HYDROQUINONE

These hydroquinone developers produced, in some instances, about as much fog as image. The sensitivity was considerably reduced, the rate of development was low, and the shape of the characteristic curve changed considerably with alkalinity as evidenced by the change in values of the ratio $i/E_m$ from 2.7 to 1.5. This is undoubtedly due to the low concentration of the developing agent, since, as is well known, hydroquinone developers can be made which, with sufficient alkali—as in experiments 68 to 70—will give at least as great contrast as the combination. Experiment 70 indicates that the sensitivity increase produced by soluble bromide also takes place with hydroquinone developers.

(b) METOL

While the metol developers gave lower values of $\gamma$ than the metol-hydroquinone combination, it was thought that the hydroquinone content might be dispensed with entirely with no disadvantage if the quantity of metol and carbonate were sufficiently increased; but it was found in experiments 76 to 79, that even four times the previous concentration of metol was not alone sufficient to give values of $\gamma$ equal to those obtained with the combination.

Comparison of experiments 80 and 81 shows that with the index $1/E_m$, sensitivity values were obtained with the bromided solution in excess of those with the control. Values of $1/i$ were lower for the developer containing bromide due to the increased distortion of the curve (corresponding to a change in values of the ratio $i/E_m$ from 2.5 to 3.2). In order to visualize this effect families of characteristic curves are presented in figure 4 obtained with 2 metol developers differing only in that 1 contained 3 grams per liter of potassium bromide.

The principal objection to using this agent alone is its tendency to increase the "toe" at the expense of the straight-line portion of the characteristic curve. This is indicated by the relatively high values of $i/E_m$ for $\gamma = 1$, and is obvious on inspection of the characteristic curves.

(c) GLYCIN

While it was found that metol-hydroquinone and certain hydroquinone developers gave characteristic curves with reasonably short "toe" portions, the use of the latter is objectionable principally because of its tendency to fog and because the large amount of alkali required to give reasonably rapid development impairs the keeping qualities.

The use of metol-hydroquinone as a standard has been criticized because of the use of two developing agents instead of one. Although this objection does not seem to be serious, it was thought that it might be of interest to investigate some of the possibilities of glycin as a developer. This agent has a reputation for good keeping qualities and low aerial fog.

Increasing the carbonate content with this agent did not affect the velocity of development in a very definite manner. This negative result also occurred in the first group of metol developers (experiments 72 to 75) but not with the second (experiments 76 to 79) having a higher concentration of metol. With the highest concentrations of carbonate the maximum value of $\gamma$ obtained with glycin was not as great as with lower concentrations. This effect was also observed with metol-hydroquinone (experiment 10).

TABLE 10.—*Data obtained with glycin (G) and pyrogallol (P). The quantities are in grams per liter. The symbol M-B represents potassium meta-bisulphite*

| Identification | | Formula | | | | $\gamma$ | | | | | | $D_{min}$ | | | | | | $1/i$ | | | | | | $1/E_m$ | | | | | | Values at $\gamma=1$ | | |
|---|---|---|---|---|---|---|---|---|---|---|---|---|---|---|---|---|---|---|---|---|---|---|---|---|---|---|---|---|---|---|---|---|
| Experiment no. | Plate | G | S | C | B | 1 | 2 | 3 | 6 | 12 | 18 | 1 | 2 | 3 | 6 | 12 | 18 | 1 | 2 | 3 | 6 | 12 | 18 | 1 | 2 | 3 | 6 | 12 | 18 | $1/i$ | $1/E_m$ | $i/E_m$ |
| 82 | $A_2$ | 5 | 50 | 25 | 0 | ---- | 0.29 | 0.44 | 0.75 | 1.04 | 1.20 | 0.05 | 0.06 | 0.09 | 0.22 | 0.38 | 0.49 | -- | 27 | 46 | 72 | 78 | 68 | -- | 13 | 52 | 160 | 140 | 110 | 78 | 155 | 2.0 |
| 83 | $A_2$ | 5 | 50 | 50 | 0 | ---- | .24 | .39 | .72 | 1.13 | 1.31 | .05 | .05 | .09 | .18 | .34 | .47 | -- | 71 | 89 | 93 | 79 | 65 | -- | 25 | 66 | 155 | 160 | 115 | 88 | 158 | 1.8 |
| 84 | $A_2$ | 5 | 50 | 100 | 0 | ---- | .24 | .41 | .69 | 1.07 | 1.36 | .06 | .07 | .09 | .18 | .32 | .42 | -- | 60 | 59 | 85 | 68 | 52 | -- | 21 | 66 | 115 | 135 | 130 | 73 | 130 | 1.8 |
| 85 | $A_2$ | 5 | 50 | 150 | 0 | ---- | .14 | .23 | .56 | .94 | 1.18 | .05 | .06 | .08 | .15 | .25 | .34 | -- | 105 | 98 | 68 | 59 | 48 | -- | -- | 32 | 110 | 120 | 115 | 56 | 119 | 2.1 |
| 86 | $A_2$ | 10 | 25 | 25 | 0 | ---- | .32 | .43 | .88 | 1.20 | 1.25 | .05 | .07 | .13 | .25 | .45 | .52 | -- | 38 | 66 | 54 | 50 | 47 | -- | 28 | 68 | 91 | 79 | 91 | 53 | 87 | 1.6 |
| 87 | $A_2$ | 10 | 25 | 25 | 1 | ---- | -- | -- | .79 | 1.20 | 1.23 | -- | -- | -- | .09 | .15 | .23 | -- | -- | -- | 27 | 45 | 52 | -- | -- | -- | 66 | 105 | 115 | 36 | 86 | 2.4 |
| 88 | $A_2$ | 10 | 25 | 25 | 2 | ---- | -- | -- | .84 | 1.25 | 1.25 | -- | -- | -- | .06 | .12 | .18 | -- | -- | -- | 14 | 30 | 45 | -- | -- | -- | 32 | 110 | 115 | 20 | 62 | 3.1 |
| 89 | $A_2$ | 10 P | 25 | 25 | 4 M-B* | ---- | -- | -- | -- | 1.12 | 1.34 | -- | -- | -- | .05 | .09 | .12 | -- | -- | -- | -- | 21 | 30 | -- | -- | -- | -- | 72 | 115 | -- | -- | -- |
| 90 | $A_2$ | 6 | 9 | 7.5 | 1.2 | 0.18 | .34 | .54 | .89 | 1.30 | 1.55 | .06 | .09 | .10 | .19 | .38 | .51 | 89 | 120 | 91 | 69 | 43 | 32 | -- | 100 | 105 | 125 | 125 | 79 | 63 | 125 | 2.0 |

* Different lot from that used in experiment 55, table 7.

It is evident that the effect of carbonate on the sensitivity versus development-time curve for the index $1/i$ has been to shift the maximum to lower times of development. On the other hand, with the exception of the lowest concentration, the maximum of the curve for $1/E_m$ occurs at a constant time of development (12 minutes). This indicates a change in the shape of the characteristic curve which is not clearly shown by the ratio $i/E_m$ for $\gamma=1$.

In addition, this developing agent, under the conditions of these experiments, was found to be much more sensitive to bromide than those previously considered.[20] The sensitivity values at $\gamma=1$ decrease markedly with increasing bromide, but the data show higher sensitivity values on the basis of $1/E_m$ with bromide and seem to indicate that values of $1/i$ would also exceed those for the unbromided developers if the development were sufficiently prolonged. However, the shape of the curve is altered so markedly with bromide (as is evidenced by the change in the ratio $i/E_m$ from 1.6 to 3.1, experiments 86 to 88) that this developer is quite unsuitable for most sensitometric purposes.

## V. THE RELATION BETWEEN THE "INERTIA GRADIENT" AND GAMMA

In studying the shape of the "toe" or "underexposure" region of the characteristic curve, Luther[21] found the following relations to hold quite closely. These are (1), "*in the underexposure portion all characteristic curves of the same gamma are geometrically similar*"; and (2), "*The slope of the characteristic curve at the inertia exposure is about one half of* $\gamma$". His data included 42 determinations for 8 emulsions using 4 developers. Values of $\gamma$ ranged from 0.7 to 3.5. The average value of $G_i/\gamma$ was 0.48; the extremes being 0.38 and 0.58.

In order to test Luther's second relation, 17 experiments were selected from tables 4 to 7, and from the curves values of the gradient at a point directly above the inertia were determined. These experiments were chosen so as to include a variety of developers and characteristic curve shapes. The details of the selection are as follows:

Experiments 6 and 7, plate $A_1$, developed with metol-hydroquinone with 1 and 5 grams of monohydrated sodium carbonate per liter. These curves are differently shaped as is shown in table 4 by values of $i/E_m$ or 3.3 and 2, respectively. Experiments 11 and 14, plate B, developed with metol-hydroquinone, without bromide, and with 2 grams per liter of potassium bromide, respectively. Experiments 16 and 17, plate C, developed with metol-hydroquinone without bromide, and with 4 grams per liter of potassium bromide, respectively. Experiments 19 and 20, plate D, developed with metol-hydroquinone without bromide, and with 2 grams per liter of potassium bromide, respectively. Experiments 22 and 24, plates E and F (experimental emulsions containing 1 and 4 percent, respectively, of silver iodide), developed with metol-hydroquinone. Experiments 45, 47, and 59, plates $A_3$, $A_2$, and G, respectively, developed with the standard *p*-aminophenol developer. Experiment 58, plate G, devel-

[20] Nietz (Theory of Development, Monographs on the Theory of Photography from the Research Laboratory of the Eastman Kodak Co., no. 2, 1922) has assigned to glycin a reduction potential of 1.6 relative to hydroquinone as 1.

[21] "The Underexposure Period of the Characteristic Curve", The Physical Chemistry of the Photographic Process, General Discussion of the Faraday Society, p. 340, May 1923.

oped with metol-hydroquinone. Finally, experiments 60, 61, and 62, plate G, with a series of *p*-aminophenol-hydroquinone developers.

The resulting values of $G_i$ and $G_i/\gamma$ are given in table 11. From a total of 99 determinations the average value of $G_i/\gamma$ was 0.50, the extremes being 0.31 and 0.63. This range is slightly greater than that of Luther. It should be noted, however, that a greater range of values of $\gamma$ was employed; namely, from 0.14 to 4.45. Examination of the table shows no certain systematic variation of $G_i/\gamma$, with time of development, with the composition of the developer, or with the type of emulsion. Particularly interesting is the fact that the values are not affected by soluble bromide in the developer or by changes in the length of the "toe" of the characteristic curve. The individual values of $G_i/\gamma$ in the table have, in some instances, rather wide departures from the mean. This is to be expected since these values depend upon graphical determinations of $\gamma$, inertia and the gradient $G_i$. In table 3, it is shown that the average mean deviation for $1/i=8.3$ percent, for $1/E_m$, 7.6 percent, and for $\gamma$, 3.1 percent. From a consideration of these factors, it is not surprising that large deviations in $G_i/\gamma$ may occasionally occur. While the ratio cannot be strictly considered a constant, it is highly improbable that the agreement is an accident. This ratio is at least a useful approximation of the facts under a wide range of conditions.

TABLE 11.—*Shows the relation between $\gamma$ and the gradient of the characteristic curve at a point directly above the inertia, $G_i$. Luther found that the average value of the ratio $G_i/\gamma$ was about 0.5*

| Experiment no. | 1 | | | 2 | | | 3 | | | 6 | | | 12 | | | 18 | | |
|---|---|---|---|---|---|---|---|---|---|---|---|---|---|---|---|---|---|---|
| | $G_i$ | $\gamma$ | $G_i/\gamma$ | $G_i$ | $\gamma$ | $G_i/\gamma$ | $G_i$ | $\gamma$ | $G_i/\gamma$ | $G_i$ | $\gamma$ | $G_i/\gamma$ | $G_i$ | $\gamma$ | $G_i/\gamma$ | $G_i$ | $\gamma$ | $G_i/\gamma$ |
| 6 | ---- | 0.10 | ---- | 0.17 | 0.27 | 0.63 | 0.24 | 0.44 | 0.55 | 0.45 | 0.82 | 0.55 | 0.54 | 1.06 | 0.51 | 0.68 | 1.15 | 0.59 |
| 7 | 0.21 | .37 | 0.57 | .36 | .67 | .54 | .44 | .84 | .52 | .54 | 1.16 | .47 | .57 | 1.27 | .45 | .59 | 1.44 | .41 |
| 11 | .13 | .35 | .37 | .34 | .70 | .49 | .48 | 1.00 | .48 | .82 | 1.56 | .53 | .95 | 1.89 | .50 | 1.00 | 1.92 | .52 |
| 14 | .15 | .25 | .60 | .38 | .69 | .55 | .49 | .97 | .51 | .83 | 1.45 | .57 | .98 | 1.96 | .50 | 1.06 | 1.89 | .56 |
| 16 | .14 | .31 | .45 | .31 | .54 | .57 | .27 | .66 | .41 | .43 | .95 | .45 | .45 | 1.06 | .42 | .57 | .95 | .60 |
| 17 | ---- | ---- | ---- | .25 | .54 | .46 | .27 | .60 | .45 | .43 | .90 | .48 | .44 | 1.04 | .42 | .41 | .99 | .41 |
| 19 | .45 | .97 | .46 | .80 | 1.71 | .47 | .95 | 2.12 | .45 | 1.44 | 3.00 | .48 | 1.34 | 3.26 | .41 | 1.37 | 2.84 | .48 |
| 20 | .35 | .71 | .49 | .74 | 1.75 | .42 | .99 | 2.19 | .45 | 1.51 | 3.10 | .49 | 1.87 | 3.95 | .47 | 1.94 | 4.45 | .44 |
| 22 | .18 | .40 | .45 | .33 | .78 | .42 | .51 | 1.05 | .49 | .77 | 1.62 | .48 | 1.28 | 2.22 | .58 | 1.02 | 2.32 | .44 |
| 24 | .17 | .27 | .63 | .31 | .54 | .57 | .34 | .72 | .47 | .55 | 1.02 | .54 | .62 | 1.28 | .48 | .71 | 1.28 | .55 |
| 45 | .17 | .30 | .57 | .25 | .53 | .47 | .38 | .74 | .51 | .45 | .93 | .48 | .56 | 1.07 | .52 | .58 | 1.09 | .53 |
| 47 | .18 | .29 | .62 | .33 | .59 | .56 | .41 | .76 | .54 | .53 | 1.12 | .47 | .66 | 1.34 | .49 | .72 | 1.41 | .51 |
| 58 | .11 | .22 | .50 | .24 | .45 | .53 | .33 | .68 | .49 | .43 | .96 | .45 | .59 | 1.23 | .48 | .60 | 1.26 | .48 |
| 59 | .16 | .27 | .59 | .30 | .55 | .55 | .38 | .69 | .55 | .53 | 1.01 | .52 | .60 | 1.10 | .55 | .62 | 1.07 | .58 |
| 60 | ---- | ---- | ---- | .05 | .16 | .31 | .15 | .31 | .48 | .28 | .64 | .44 | .47 | 1.01 | .47 | .49 | 1.13 | .43 |
| 61 | .11 | .20 | .55 | .26 | .45 | .58 | .26 | .69 | .38 | .47 | 1.02 | .46 | .60 | 1.33 | .45 | .54 | 1.12 | .48 |
| 62 | .08 | .14 | .57 | .17 | .33 | .52 | .32 | .52 | .62 | .41 | .85 | .48 | .55 | 1.26 | .44 | .56 | 1.12 | .50 |
| Group average | ---- | ---- | .53 | ---- | ---- | .51 | ---- | ---- | .49 | ---- | ---- | .49 | ---- | ---- | .48 | ---- | ---- | .50 |
| Grand average | ---- | ---- | ---- | ---- | ---- | ---- | ---- | ---- | .50 | ---- | ---- | ---- | ---- | ---- | ---- | ---- | ---- | ---- |

## VI. DISCUSSION

### 1. *p*-AMINOPHENOL

It has been pointed out that both *p*-aminophenol and metol seem to affect the characteristic curve in such a way as to increase the length of the "toe" chiefly at the expense of the lower portion of the straight-line section. This furnishes a strong objection to the use of either of these developing agents singly, as standards.

It has been shown that the tendency of *p*-aminophenol and metol to distort the characteristic curve may be corrected by using either one of these agents in conjunction with hydroquinone.

It was also observed that, with some developers which increase the "underexposure" or "toe" region of the characteristic curve (experiments 49, 53, 56, and 59, table 7), values of $1/E_m$ increase with time of development while the values of $1/i$ decrease.

With the *p*-aminophenol developer the maximum value of $1/i$ would occur at the lowest practicable time of development. But it is clear that maximum sensitivity is not obtained at this short time of development. Thus the characteristic decrease of values of $1/i$ with increasing development time when using solutions of this type constitutes a strong argument against the use of this index to obtain the maximum value.[22] However, it might be said here that the principle of taking the maximum value of any index to represent the sensitivity of the emulsion is open to serious objection since it often falls at values of $\gamma$ which are either much higher or much lower than those desired in practical work with the same emulsions and developers. This is particularly true with bromided developers.

The recommended *p*-aminophenol developer formula seems to be in need of modification. We have been unable to get the developing agent into solution without heat and on standing at a temperature of 20° C. it slowly crystallizes out, indicating super saturation. This trouble could be avoided by reducing the concentration of either the *p*-aminophenol or the sulphite or by increasing the alkalinity.

### 2. SOLUBLE BROMIDE

It was observed that the addition of potassium bromide to the developing solution not only causes a decrease in values of the sensitivity indexes $1/i$ and $1/E_m$ with the shorter development times but also, with some emulsions at least, if the time is sufficiently prolonged, values result which are greater than those obtainable with the same developer without bromide. That this increase occurs has been seldom pointed out although it is recognized in practice in some so-called "maximum energy" developers [23] containing high concentrations of bromide. Nietz [24] has made a considerable study of the effect of bromide in photographic developers. He expresses the effect on sensitivity by a downward shift of the intersection point of the extended straight lines of a family of characteristic curves. That is, the intersection point for the bromide-free developer usually is located on the log-exposure axis, while for the same developer plus bromide, it is located at some point vertically below. Values of inertia were obtained from the intersection of the extended straight lines with the log-exposure axis and not with the $D_{min}$ line. Under these conditions it is, of course, geometrically impossible to indicate an increase in sensitivity with bromide.

[22] Obviously, the use of the index $1/i$, where $I$ is the exposure value of the intersection of the produced straight-line portion of the curve with the zero density line (no correction being made for fog or support), which has been erroneously called the inertia by some workers, also suffers from this same fault in addition to those discussed in RP355 (see footnote p. 381).

[23] Such as, for example, the Eastman D-82 developer, and the hydroquinone-caustic soda developer used by Davidson (Conditions Governing the Behavior of Silver Bromide Grain During Development, Phot. Jour., vol. 66, p. 230, May 1926.)

[24] See footnote, p. 402.

Incidentally, Nietz stated that he used emulsions which were relatively free from fog and obtained a common intersection point[25] without recourse to a fog correction.

### 3. INERTIA VERSUS GRADIENT

In the course of these experiments with different developers, we have found that in several cases the change in the values of $1/i$ and $1/E_m$ with development—time is opposite in sign.

It may appear that under these conditions either one index or the other is in error. Such a suspicion arises from the imperfect conception as to just what we consider constitutes relative sensitivity. In other words, relative sensitivity must be defined before one may judge which index better measures it. In practice, it is often stated that the relative sensitivity of two emulsions is the ratio of the exposures required to give the same picture with each emulsion. An ideal definition results by replacing the expression "the same picture" by "identical-shaped characteristic curves." That is, the brightness differences in the subject are represented by equal density differences in each negative. Under ideal conditions the two characteristic curves are identical in shape, but one is displaced from the other by a certain horizontal distance. In this case, the relative sensitivity is the ratio of exposures required to give the same density in excess of $D_{min.}$ This ratio will be the same regardless of the value of density chosen. But in actual practice it is seldom that any two curves could be made to coincide completely by any horizontal or vertical shift. If we choose curves having the same values of $\gamma$, the ratio of exposures required to give the same density in excess of $D_{min.}$ will be a constant for values lying on the straight-line portions of both curves and will be equal to the ratio of the inertias. However, it is clear, that as the straight-line portions of either or both of the curves become shorter, the range of densities for which the inertias measure the relative sensitivity decreases with a single density as a limit when the straight-line portion of one of the curves reaches the vanishing point. That is, the farther the curve departs from the $\gamma$-line, the less applicable becomes the ratio of inertias. Some straight line is required which more closely follows the curve. One such line is the mean gradient line as defined by Jones[26] in connection with the characteristic curves of printing papers. It extends from the point taken as the minimum useful gradient in the "toe" to the corresponding point in the "shoulder" of the curve. The relative sensitivity of 2 emulsions will then be the ratio of the exposure values of any 2 points on the mean gradient lines at equal density distances above $D_{min.}$ where the emulsions have both been developed to the same mean gradient, $\phi$ and will be equal to the ratio of the 2 values of the sensitivity index, $1/E_m$.

This method is somewhat more complicated than is needed when the plates have reasonably long straight-line portions and are developed to equal values of $\gamma$. In such cases, practically the same relative speed will be indicated by the use of either index. However, Jones

[25] S. E. Sheppard (Characteristics and Anomalies of Emulsions on Development—Part 1, Phot. Jour., vol. 66, p. 190, 1926) has made a study of various emulsions in connection with this intersection point. He finds that in certain types of emulsion there may be two or more points of intersection. He would then divide emulsions into two main groups: (1) The normal or orthophotic, those having one intersection point, and (2) abnormal or anorthophotic, those having more than one intersection point.

[26] The Contrast of Photographic Printing Paper, Jour. of Franklin Institute, vol. 202, p. 204, 1926.

and Russell,[27] and Luther [28] have shown some examples where the relative sensitivity would not be the same for both indexes and doubtless there are others. This situation will probably occur most frequently when the emulsions differ considerably in sensitivity. That is, as the sensitivity of the two emulsions becomes more nearly the same, their relative sensitivity obtained (on a basis of equal values of $\gamma$) by $1/i$ and by $1/E_m$ will become more nearly alike. However, it is often desirable in practice to know the relative sensitivity of, say, a "moderately slow" contrasty plate and a soft "high-speed" plate. Here the two curves may be of quite different types, so that at the same value of $\gamma$ it may be impossible to select a ratio of exposures which would bring the curves into coincidence over an appreciable range. In this case it would be necessary to resort to comparisons of sensitivity, using the index $1/E_m$ on the basis of equal mean gradients, as we have described.

It will be noted that in the ideal case we have considered that the curves needed only a horizontal shift in order to be brought into coincidence. This is because a vertical shift of the curve is without significance insofar as sensitivity is concerned; for, as stated, two identical curves at different distances above the log exposure axis are to be considered of equal sensitivity so long as they are not horizontally displaced from each other.

Returning to the variation in the ratio $i/E_m$ with development time, in view of what has been said, it is not surprising that values of the two indexes should, under certain conditions, vary in opposite directions. It simply indicates a change in shape of the characteristic curve. The comparison of the relative sensitivity of two members of a family of curves is not, according to our definition, strictly possible, since the curves differ in shape so that they cannot be made to coincide by any sidewise motion along the log exposure axis.

To sum up, then, comparison of the sensitivity of emulsions having definite straight-line portions should be made using the index $1/i$, values being obtained at an arbitrarily determined standard value of $\gamma$, ($\gamma_s$). Comparison of emulsions not having characteristic curves with definite straight-line portions with each other or with those of the above type should be made using the index $1/E_m$ values being obtained at a certain arbitrarily determined value of mean gradient $\phi_s$.

At this point mention should be made of a possible application of Luther's relation, that the gradient of the characteristic curve directly above the inertia is one half $\gamma$. Our data seem to check very well with those of Luther, so that if the value of $\gamma$ chosen be sufficiently low, such as 0.8, it would be possible to take half this value, $\gamma_s/2 = G_t$, as an "inertia gradient", the corresponding sensitivity index being $1/E_t$. In this case identical sensitivity values would be indicated by both the indexes $1/i$ and $1/E_t$. This plan would forestall the confusion of a dual system of sensitivity values such as would result when both $1/i$ and $1/E_m$ are used.

[27] The Expression of Plate Speed in Terms of Minimum Useful Gradient by L. A. Jones and M. E. Russell, Proc. 7th Int. Cong. Phot., p. 130; July 1928.

[28] See footnote p. 402.

### 4. THE INTERNATIONAL SENSITIVITY INDEX

In this paper an attempt has been made to clear up the confusion surrounding the comparison of photographic sensitivity and to indicate a procedure which would cover both normal and freak emulsions with the hope that the next international congress can adopt a standard method utilizing the "H&D" graph. If some such procedure is adopted, a separate and distinct name should be given to the resulting sensitivity values in place of the vague term "H&D speed." This would avoid the unjustified comparison of values obtained by different systems.

It may readily be seen that if there is adopted a system of measurement such as we have recommended, involving a dual index, emulsions without a straight-line section would be given a sensitivity value obtained by the index $1/E_m$, at a certain standard value of mean gradient. The normal emulsions would be given a value of $1/i$ obtained at a certain standard value of $\gamma$, and a value of $1/E_m$ obtained at the standard mean gradient. This would not only make possible their comparison with "freak" emulsions but also would mark them as having superior properties.

## VII. ACKNOWLEDGMENTS

The authors are indebted to Dr. B. H. Carroll, of the photographic emulsion laboratory of this Bureau, for the analysis of chemicals used in these experiments, and for supplying the two experimental emulsions containing known amounts of iodide.

WASHINGTON, July 12, 1933.

U.S. Department of Commerce, Bureau of Standards

RESEARCH PAPER RP599

*Part of Bureau of Standards Journal of Research, vol. 11, September 1933*

# THE SECOND SPECTRUM OF KRYPTON

By T. L. deBruin,[1] C. J. Humphreys, and William F. Meggers

ABSTRACT

The second spectrum of krypton (Kr II) characteristic of once ionized krypton atoms ($Kr^+$) has been selected from various krypton spectra excited in Geissler tubes by noting intensity changes accompanying variations of capacity and inductance in the electrical circuit. This description and analysis of the Kr II spectrum includes estimates of relative intensities and wave-length measurements for 1,050 lines extending from 2,080.53 A in the ultraviolet to 10,659.5 A in the infrared. Most of these lines (71 percent) have been classified as combinations of 128 energy levels, 112 of which have been more or less definitely identified with quantum numbers and electron configurations. Zeeman effects are quoted for 102 lines. In addition, 51 lines in the extreme ultraviolet (575.92 to 964.93 A) are classified as transitions from excited states to the normal ones.

The $s^2p^5$ electron configuration of the normal $Kr^+$ ion is represented by a doublet P term with level separation 5,371 $cm^{-1}$, and the excited states are described by doublet and quartet terms arising from the addition of *ns*, *np*, *nd*, *nf* electrons to the $s^2p^4$ group constituting the outer structure of the doubly charged ion ($Kr^{++}$). An absolute value of 198,182 $cm^{-1}$ is derived for the ground level $s^2p^5\,{}^2P_{3}{}^{1}/_{2}$, which fixes the ionization potential of $Kr^+$ atoms at approximately 24.4 volts.

CONTENTS

| | | Page |
|---|---|---|
| I. | Introduction | 409 |
| II. | Wave-length measurements | 410 |
| III. | Analysis of the Kr II spectrum | 413 |
| | 1. Theoretical terms | 413 |
| | 2. Absolute terms, ionization potential of $Kr^+$ | 414 |
| | 3. Identification of experimental terms | 415 |
| | 4. Classification of Kr II lines | 416 |

## I. INTRODUCTION

The authors have published two papers describing and analyzing the first spectrum of krypton,[2] Kr I. In these, reference was made to the fact that the spectral terms which represent the excited states of the neutral Kr atom result from the interaction of the series electron with the electron group which characterizes the normal state of the $Kr^+$ ion. Various states of this ion determine the second spectrum of krypton, Kr II, and it is the purpose of the present paper to give our description and analysis of this second spectrum.

Runge [3] was the first to call attention to the fact that krypton emits two different line spectra, one without leyden jar and spark

[1] Laboratory "Physica" of the University of Amsterdam.
[2] William F. Meggers, T. L. deBruin, and C. J. Humphreys, B.S.Jour. Research, vol. 3 (RP89), p. 129, 1929; vol. 7 (RP364), p. 643, 1931.
[3] C. Runge, Astrophys. J., vol. 10, p. 73, 1899.

gap in the secondary circuit of an induction coil, the other with leyden jar and spark gap. He published the wave lengths for 16 lines (4,274.09 to 7,601.47 A) in the first spectrum and 31 lines (3,654.11 to 5,419.38 A) in the second. A more complete and accurate determination of wave lengths for both spectra of krypton was completed in 1903 by Baly.[4] He gave 74 lines (3,502.69 to 6,456.65 A) for the first spectrum and 733 lines (2,418.13 to 5,871.12 A) for the second, but the stronger lines are common to both lists and some in each are identifiable with xenon. Moreover the so-called "second spectrum of krypton" is not strictly identical with what is now known as the Kr II spectrum, because the condensed, disruptive discharge produces several stages of ionization, so that although the Kr II spectrum is the most prominent, many Kr III lines and possibly also some Kr IV lines appear in the spectrum. Methods of separating these successive spectra, and theoretical interpretations of their structures have been developed in recent years. They will be discussed below.

Krypton spectra excited in electrodeless discharges were described in 1924 by L. Bloch, E. Bloch, and G. Déjardin.[5] Nearly 800 lines are listed; they range in wave length from 2,227.96 to 6,907 A and represent the stronger lines from neutral atoms and from three successive stages of ionization. This list contains a number of lines not previously reported by other observers, but the wave lengths of these new lines are recorded only to 0.1 A in the ultraviolet and to 1 A in the visible spectrum.

The various spectra of krypton in the extreme ultraviolet were observed by Abbink and Dorgelo.[6]

Examination of the above-mentioned data enabled Kichlu[7] to make a partial analysis of the Kr II spectrum. He recognized the ground term as an inverted doublet P with level separation of 5,371 $cm^{-1}$, but was unable to specify the nature of most of the other levels because Zeeman-effect data were lacking. This last deficiency was removed by Bakker, Zeeman, and deBruin[8] who recently published Zeeman effect observations for 91 Kr II lines (3,150.92 to 4,857.20 A) which permitted correction and extension of Kichlu's term analysis. In the meantime we had completed an entirely new and greatly improved description of the second spectrum of Krypton which made it possible to extend the analysis still further. Now many of the theoretically predicted terms have been identified and most of the observed lines have been classified.

## II. WAVE-LENGTH MEASUREMENTS

Our experience with Kr II spectra was very similar to that with Kr I spectra. In both cases a preliminary description was first made with Geissler tubes used side-on, and later revised and extended with tubes used end-on, because it was found that the latter tubes emitted a brighter spectrum, thus permitting the study of fainter lines and more precise measurement of wave lengths. Values for 91 lines from our preliminary Kr II list were quoted by Bakker and deBruin, but

[4] E. C. C. Baly, Phil. Trans., vol. 202, p. 183, 1904.
[5] L. Bloch, E. Bloch, and G. Déjardin, Ann. de Phys. (10), p. 461, 1924.
[6] J. H. Abbink and H. B. Dorgelo, Zeits. f. Phys., vol. 47, p. 221, 1928.
[7] P. K. Kichlu, Proc. Roy. Soc. London, vol. 120 A, p. 643, 1928.
[8] C. J. Bakker and P. Zeeman, Proc. Amsterdam, vol. 32, p. 565, 1931. C. J. Bakker and T. L. deBruin, Zeits. f. Phys., vol. 69, p. 36, 1931.

none of the remainder have been published. The wave lengths and intensities presented below represent mainly the new observations with the brighter source and with a higher powered spectrograph.

The tube used in making the last observations was obtained from Robert Goetze, Leipzig; it has two cylindrical electrodes connected by a capillary of 11 cm length and about 1 mm bore, the viewing end of the capillary being enclosed in a thin-walled glass bulb of 2.5 cm diameter. This glass was fairly transparent to ultraviolet; it transmitted the spectrum to about 2,500 A. For producing the spark spectra this tube was operated by ac transformers, with secondary voltages of 10,000 to 40,000, a spark gap of 5 to 10 mm being connected in series and mica condensers of 0.006 $\mu$f capacity in parallel with the tube. In addition, various amounts of self-induction (0.0002 to 0.0005 H) were inserted in the circuit for some exposures to determine which lines belonged to the higher stages of ionization.

The spectrographs employed for the study of the Kr II spectra were described in our second publication on the Kr I spectrum (RP364). Spark spectra emitted by the end-on tube were photographed with the Rowland grating (20,000 lines per inch) in the interval 2,500 to 8,900 A, and with the Anderson grating (7,500 lines per inch) beyond 8,000 A. The range from 2,000 to 3,000 A was photographed with a Hilger $E_1$ quartz spectrograph, a tube of fused quartz, filled in our laboratory with krypton gas purchased from the Linde Gesellschaft für Eismaschinen, München, being used side-on for these observations.

Eastman 33 photographic plates were used exclusively in our first observations which covered the range 2,080 to 9,361 A. The plates were sensitized to waves longer than 4,800 A by bathing in solutions of pinaverdol, pinacyanol, dicyanin, rubrocyanin, and neocyanin. The exposure times ranged from 1 to 4 hours when the tube was operated without self-inductance, but it was necessary to double or triple the time to obtain about the same record of Kr II lines when self-inductance was placed in the circuit.

During the past year new types of infrared sensitive plates were announced by the Eastman Kodak Co.,[9] and several of these have been employed to improve and extend our observations of krypton spectra in the region of longer waves. The interval 7,400 to 9,200 A was investigated with mesocyanine plates (P type of sensitizing) and the infrared beyond 8,500 A with xenocyanine plates (Q type of sensitizing). With the latter plate we succeeded in extending the long wave limit of observed Kr II lines from 9,361 to 10,659 A and many new lines were thus added to our list. Results for the Kr I spectrum recorded in the infrared on P and Q sensitized plates have already been published.[10]

Wave-length measurements were made relative to international secondary standards in the arc spectrum of iron which was photographed, both in place and in time, between the Kr II exposures with and without self-inductance. The stronger Kr I lines which have been compared with the primary standard by interferometer measurements also appeared with great intensity in the Kr II spectrograms, but on account of their tendency to appear diffuse and unsymmetrical in the spark discharge they were not used as wave length standards. Practically all of the lines were measured on two or more spectrograms,

[9] C. E. K. Mees, J. Opt. Soc. Am., vol. 22, p. 204, 1932.
[10] William F. Meggers and C. J. Humphreys. B.S.Jour. Research (RP540), vol. 10, p. 427, 1933.

the number of observations reaching 4 or 5 in overlapping regions. When all of the measurements were compiled, they constituted a formidable list in which earlier experience had shown that many spurious lines, impurities, ghosts, and various stages of ionization were present. All Rowland ghosts were first eliminated, and Lyman ghosts were sought but not found. Then a considerable number of lines identifiable with argon spectra and a few belonging to xenon were stricken from the list. Finally, the Kr I lines characteristic of neutral krypton atoms and those which must be ascribed to Kr III and Kr IV spectra were identified; the remainder are believed to represent the Kr II spectrum characteristic of once ionized krypton atoms. Among these Kr II lines there exists a remarkable variety of types; while the majority of lines appear to be reasonably sharp and symmetrical, a considerable number are hazy (*h*), some being very hazy and wide (H), and many of the hazy lines are unsymmetrical, some being shaded to red (*l*) and others to violet (*v*).

In the case of sharp lines the probable error of wave-length determinations is usually less than 0.01 A, but the error may be several times as great for hazy and unsymmetrical lines. An effort was made to measure the center of gravity in every case, and the spectral regularities which were found later show that this procedure was justified; it will be seen that the spectral term combinations represent even the hazy lines within 1 part in 100,000, on the average. It will be noticed also that these hazy lines usually involve high energy states in which the electrons are probably influenced by electric fields of neighboring ions so that the unusual character of the lines may be presumed to be due to Stark effect.

Now, it is necessary to discuss in more detail just how the Kr II spectrum is recognized in the presence of several other krypton spectra. Two methods of differentiating between successive spectra are availalbe—one depends entirely on the effects of varying the conditions of discharge in the ordinary Geissler tube and the other is based on the behavior of lines in the electrodeless discharge when the electrical potential is varied. The latter method was employed by L. Bloch, E. Bloch, and G. Dejardin;[11] we have chosen the former. It is well known that uncondensed discharges, either dc or ac, through Geissler tubes of krypton excite the so-called "first spectrum" which has been shown to consist only of Kr I lines characteristic of neutral krypton atoms. Condensed, disruptive discharges through the same tube excite the so-called "second spectrum" which is much more complex than the first. This increase in complexity is due, at least in part, to the presence of neutral atoms, ionized atoms, twice-ionized atoms, and possibly even higher stages of ionization so that the observed spectrum is really a mixture of several spectra. The Kr I spectrum persists under all conditions (except complete and permanent ionization), but since it has been completely described before, it is readily identified.

The insertion of self-inductance in the discharge circuit has a remarkable effect on the spectra of krypton; it decreases the brightness of the tube; but if this is compensated by a longer exposure, it is found that some of the lines are enhanced, the majority maintain more or less the same intensity, while a considerable number are greatly reduced in strength, and some entirely suppressed. In gen-

[11] L. Bloch, E. Bloch, and G. Dejardin, Ann. de Phys. (10), vol. 2, p. 241, 1924.

eral, these groups represent in succession the Kr I, Kr II, Kr III, and Kr IV spectra. The effect of self-inductance on line intensity is so marked that a difference is observed between low and high energy states in one and the same spectrum, so that the transition between spectra is not abrupt and occasionally lines are encountered which cannot be positively assigned to one spectrum or the next. The same uncertainty arises in the method of line length in the electrodeless discharge as studied by L. Bloch, E. Bloch, and G. Dejardin, but comparison of the results obtained independently from these two different methods shows very satisfactory agreement.

## III. ANALYSIS OF THE Kr II SPECTRUM

### 1. THEORETICAL TERMS

The neutral atoms of any of the rare gases, Ne, A, Kr, Xe, Rn, have in the unexcited state, the configuration of a closed shell with 2 $s$ and 6 $p$ electrons, symbolized by $s^2p^6$, and, according to Hund's theory,[12] the term which characterizes the normal state is a single level, $^1S_0$, in the first spectrum. The simple ions of these gases are characterized by the electron group $s^2p^5$, giving rise to an inverted doublet term, $^2P°_{1½, 0½}$, in the second spectrum. This doublet term is of great importance in the structural analysis of rare gas spectra because the terms representing the excited states of the neutral atoms arise from the interaction of the series electron with the $s^2p^5$ group of the ions. With the exception of $^1S_0$, all of the spectral terms involved in the production of the first spectrum of a rare gas result from the addition in turn of $ns$, $np$, $nd$, and $nf$ electrons to the $^2P°_{1½, 0½}$ term of the ion. These two levels are the convergence limits of all the term series thus obtained. The presence of two series limits in these spectra was first indicated by Paschen,[13] who found in his analysis of the Ne I spectrum that certain groups of terms converged to one limit while others converged to another one separated from the first by about 780 cm$^{-1}$. This displacement was first interpreted by Grotrian,[14] who recognized the 2 series limits as 2 different states of the neon ion. These states were later identified [15] with the $^2P°_{1½, 0½}$ term above referred to, and a strictly analogous state of affairs has since been found to exist in the spectra of the succeeding rare gases, A,[16], Kr,[17] and Xe.[18] The ground doublet separations are 782, 1,431, 5,371, and 10,540 cm$^{-1}$ for Ne II, A II, Kr II, and Xe II spectra, respectively.

Now in addition to the ground doublet associated with the $s^2p^5$ configuration of a rare gas ion, many other spectral terms occur to produce the rather complex second spectrum. All of these remaining terms are associated with the electron group $s^2p^4$ of the doubly charged ion. The configuration $s^2p^4$ gives rise to $^1S$, $^1D$, and $^3P$ terms in the third spectrum, and the various terms (except $^2P°$ from $s^2p^5$ and $^2S$ from $sp^6$) of the second spectrum are derived from the addition

[12] F. Hund, Linienspectren und periodisches system der Elemente, p. 144, Julius Springer, Berlin, 1923.
[13] Paschen, Ann.d. Phys., vol. 60, p. 405, 1919; vol. 63, p. 201, 1920.
[14] W. Grotrian, Zeits.f.Physik, vol. 8, p. 116, 1921.
[15] T. L. deBruin, Zeits.f.Phys. vol. 44, p. 157, 1927. Kichlu Proc. Phys. Soc., London, vol. 39, p. 424, 1927. K. T. Compton and J. C. Boyce, J. Frank. Inst. vol. 205, p. 497, 1928.
[16] K. T. Compton, J. C. Boyce, and H. N. Russell, Phys. Rev., vol. 32, p. 179, 1928. T. L. de Bruin, Proc. Roy. Akad. Sciences, Amsterdam, vol. 33, p. 198, 1930.
[17] P. Kichlu, Proc. Roy. Soc., London, vol. A120, p. 643, 1928.
[18] C. J. Humphreys, T. L. de Bruin, and W. F. Meggers, B.S.Jour. Research, vol. 6 (RP275), p. 287, 1931.

of *ns*, *np*, *nd*, probably *nf*, and possibly *ng* electrons to the low terms characteristic of the doubly charged ion. The terms which may be theoretically expected to account for the second spectrum of a rare gas are shown for the specific case of Kr II in table 1, where the term correlation with electron configuration and convergence limits is illustrated.

Throughout the remainder of this paper we have represented the spectral terms by a complete notation which includes electron configuration and term symbol.[19] Terms resulting from the interaction of a series electron with the atom core are represented by the outer electron configuration of the core, the limiting term toward which the series converges (in parenthesis), the running electron, and the term symbol, in the order named.

TABLE 1.—*Electron configurations and spectral terms for Kr* II

| Electron configuration | Term limit $^3P$ | Term limit $^1D$ | Term limit $^1S$ |
|---|---|---|---|
| $s^2p^5$ | $^2P^\circ$ | | |
| $s^2p^4.5s$ | $^2P$, $^4P$ | $^2D$ | $^2S$ |
| $s^2p^4.5p$ | $^2S^\circ$, $^2P^\circ$, $^2D^\circ$, $^4S^\circ$, $^4P^\circ$, $^4D^\circ$ | $^2P^\circ$, $^2D^\circ$, $^2F^\circ$ | $^2P^\circ$ |
| $s^2p^4.4d$ | $^2P$, $^2D$, $^2F$, $^4P$, $^4D$, $^4F$ | $^2S$, $^2P$, $^2D$, $^2F$, $^2G$ | $^2D$ |
| $s^2p^4.5d$ | $^2P$, $^2D$, $^2F$, $^4P$, $^4D$, $^4F$ | $^2S$, $^2P$, $^2D$, $^2F$, $^2G$ | $^2D$ |
| $s^2p^4.6s$ | $^2P$, $^4P$ | $^2D$ | $^2S$ |
| $s^2p^4.6p$ | $^2S^\circ$, $^2P^\circ$, $^2D^\circ$, $^4S^\circ$, $^4P^\circ$, $^4D^\circ$ | $^2P^\circ$, $^2D^\circ$, $^2F^\circ$ | $^2P^\circ$ |
| $s^2p^4.4f$ | $^2D^\circ$, $^2F^\circ$, $^2G^\circ$, $^4D^\circ$, $^4F^\circ$, $^4G^\circ$ | $^2P^\circ$, $^2D^\circ$, $^2F^\circ$, $^2G^\circ$, $^2H^\circ$ | $^2F^\circ$ |
| $s^2p^4.5f$ | $^2D^\circ$, $^2F^\circ$, $^2G^\circ$, $^4D^\circ$, $^4F^\circ$, $^4G^\circ$ | $^2P^\circ$, $^2D^\circ$, $^2F^\circ$, $^2G^\circ$, $^2H^\circ$ | $^2F^\circ$ |
| $s^2p^4.5g$ | $^2F$, $^2G$, $^2H$, $^4F$, $^4G$, $^4H$ | $^2D$, $^2F$, $^2G$, $^2H$, $^2I$ | $^2G$ |
| $sp^6$ | $^2S$ | | |

## 2. ABSOLUTE TERMS, IONIZATION POTENTIAL OF $Kr^+$

The absolute term values have been estimated by applying the Rydberg series formula to the first two series members of the sequence $s^2p^4.ns$. The value of the level $5s^4P_{2\frac{1}{2}}$ so obtained is 85,352 $cm^{-1}$. All other terms have been fixed relative to this value. The combination $s^2p^5.^2P^\circ_{1\frac{1}{2}} - s^2p^4.5s.^4P_{2\frac{1}{2}}$ gives a line at 112,830 $cm^{-1}$ in the ultraviolet spectrum described by Abbink and Dorgelo.[20] Hence, the ground level $s^2p^5.^2P^\circ_{1\frac{1}{2}}$ is located at 198,182 $cm^{-1}$, corresponding with an ionization potential of 24.4 volts. Déjardin [21] in an experimental investigation of the critical potentials of the rare atmospheric gases determined the ionization potential of $Kr^+$ at $28.25 \pm 0.05$ volts.

A suggested explanation of the rather large discrepancy between Déjardin's value and ours is that the Rydberg series formula has been applied to only the first two members of the $s^2p^4.ns.^4P_{2\frac{1}{2}}$ sequence. Although this series has been extended to three members, it is not very regular, so that the value of the level, $5s.^4P_{2\frac{1}{2}}$, estimated from the first two members seems to be as reliable an approximation as could reasonably be made. It did not appear justifiable to apply any

[19] See Report on notation for atomic spectra. Phys. Rev., vol. 33, p. 900, 1929.
[20] J. H. Abbink and H. B. Dorgelo, Zeits.f.Phys., vol. 47, p. 221, 1928.
[21] Déjardin, Ann. de Phys. (10), vol. 2, p. 241, 1924.

of the 3-constant formulas. The sequence chosen is represented by a Rydberg formula more closely than any of the others of which more than one member is known, which is to be expected since the terms arise from the binding of an *s*-electron. In making a choice of level sequences among those arising from the same configuration $ns.^4P_{2\frac{1}{2}}$ was selected since it converges to the limit $s^2p^4.^3P_2$ of $Kr^{++}$, according to Hund's rules of correlation. Kichlu's [22] estimation of the value 214,000 $cm^{-1}$ for $s^2p^5.^2P^\circ_{1\frac{1}{2}}$ was obtained from the two known members of the $s^2p^4.np^2P^\circ_{1\frac{1}{2}}$ sequence, viz, $s^2p^5.^2P^\circ_{1\frac{1}{2}}$ and $s^2p^4.5p.^2P^\circ_{1\frac{1}{2}}$.

### 3. IDENTIFICATION OF EXPERIMENTAL TERMS

A total of 128 levels has been found in Kr II of which 112 have been identified. The character of 52 of these has been established by the published Zeeman-effect observations of Bakker, Zeeman, and deBruin.[23] Unpublished Zeeman-effect observations, which Bakker, Zeeman, and deBruin have permitted us to use, give the observed patterns of combinations of 10 levels in addition to those reported, although 3 of these levels are still unidentified or uncertain.

Table 2 contains a complete list of the known terms of Kr II. These are separated into the odd and even sets, and grouped within these divisions according to electron configurations, beginning with the lowest energy states. All observed *g* values are listed and compared with the corresponding Landé values. The table also indicates the observed term combinations.

The discovery of the ground level separation 5,371 $cm^{-1}$ by Kichlu has been mentioned. This doublet $s^2p^5.^2P^\circ_{1\frac{1}{2}, 0\frac{1}{2}}$ combines with the even terms arising from the $s^2p^4.ns$ and $s^2p^4.nd$ configurations giving lines in the Schumann region. Most of the krypton spark lines observed by Abbink and Dorgelo [24] have been identified as such combinations. All classified extreme ultraviolet lines are given in table 3.

The even terms also combine with terms arising from $s^2p^4.5p$, accounting for a great majority of the classified lines in the region covered by the description here reported. Additional combinations of the levels of the even terms establish three additional groups of odd levels near 30,000, 25,000, and 15,000 $cm^{-1}$. The first two groups were originally regarded as $s^2p^4.6p$ levels converging, respectively, to the $^3P$ and $^1D$ limits. Such an interpretation is possible based upon a Rydberg extrapolation of the second series members. Other considerations indicate, however, that these levels may belong to terms arising from $s^2p^4.5f$. The hazy character of many of the lines supports this interpretation. Furthermore, the ultraviolet multiplet in the vicinity of 47,000 $cm^{-1}$ suggests a $^4D - {}^4F$ combination. There is no certain evidence from Zeeman effects. The interpretation of these levels as belonging to the $s^2p^4.5f$ configuration has been finally accepted with reservations. No interpretation is indicated of the group at 15,000 $cm^{-1}$, but the possibility that these levels may be third series members is suggested.

Practically all of the even levels have been interpreted. Combinations of the second series members lie in accessible spectral regions and in most cases have been observed. Some assistance in the identification is obtained by use of a Rydberg table for spark spectra to

[22] P. K. Kichlu, Proc. Roy. Soc. London, vol. 120A, p. 643, 1928.
[23] See footnote 8, p. 410.
[24] J. H. Abbink and H. B. Dorgelo, Zeits.f.Phys., vol. 47, p. 221, 1928.

extrapolate the higher series members. The $s^2p^4(^3P)$ *ns* term series have been extended to three members. A group of levels at about 19,300 cm$-1$ combines with the terms interpreted as $s^2p^4.5f\,^4F°$ and $^2F°$. It is sugges ed that these may belong to the term $s^2p^4.5g.\,^4G$, although the identification is uncertain because the lines are very hazy and the measurements, therefore, are not to be regarded as very accurate. Three unidentified even levels remain, the one at 65,209.50 cm$-1$ involving especially strong combinations. It is of the same magnitude and combines in the same way as the $s^2p^4.4d$ terms but there is no vacancy for a level with $j$ equal to 2½.

Apart from Zeeman analysis some information as to the character of the terms is to be obtained by comparison of the similarly constituted spectra, Ne II and A II. That is, the location of spectroscopically similar terms and probable magnitudes of level separations may be predicted to a reasonably close approximation by extrapolation.

The character of the lines tells us something as to the identity of the combining levels. Thus, lines arising from the combinations of low levels are sharp. High level lines are hazy or unsymmetrically broadened, due to Stark effect or the perturbations of levels lying close together as discussed below. A group of lines due to different combinations of one level react alike to inductance in the circuit. The two features of this spectrum which add most to the uncertainty in the identifications are the irregularity of spectral series, and the very complete development of intersystem combinations. Thus, if the selection rules relating to parity and inner quantum numbers are satisfied, we may expect relatively strong combinations of terms of different multiplicity, also of terms converging to different limits.

## 4. CLASSIFICATION OF Kr II LINES

The present state of our knowledge concerning spectral lines characteristic of once ionized krypton atoms is displayed in tables 3 and 4. Table 3 presents data in the extreme ultraviolet from the publication by Abbink and Dorgelo,[25] but only the lines for which a classification was found are quoted, since some of the remainder may represent impurities or higher stage spectra. Our own observations of the Kr II spectrum are given in table 4, in which estimated intensities, measured wave lengths, vacuum wave numbers, term combinations, observed and computed Zeeman patterns, appear in successive columns. Many of the intensity numbers are followed by symbols representing the character of the line. These symbols have the following meaning: $h$ = hazy, H = very hazy, $w$ = wide, $l$ = shaded to longer waves, $v$ = shaded to shorter waves. The classified lines are represented in column 4 by term combinations, symbols for the energy levels as shown in the term table (table 2) being used throughout, except for levels the identification of which is unknown or uncertain.

The computed Zeeman effects are derived from the observed $g$ values shown in table 2. Comparison with the corresponding patterns derived from Landé $g$ values can easily be made by reference to tables of theoretical Zeeman effects published by Kiess and Meggers.[26]

Table 4 contains a total of 1,050 lines, and of these 750, or 71 percent, have been classified. Our efforts to make the analysis more

[25] J. H. Abbink and H. B. Dorgelo, Zeits.f.Phys., vol. 47, p. 221, 1928.
[26] C. C. Kiess and W. F. Meggers, B.S.Jour. Research (RP23), vol. 1, p. 641, 1928.

nearly complete have yielded many additional levels but unless they could be checked by several combinations or otherwise plausibly established they have been discarded as unreal. Only one level, 19,339.61, based on a single combination has been retained, because if its quantum numbers are assumed to be correct it can have no other combinations, but it explains one of the strongest remaining lines, 9,293.82 A, 500 HL.

Attention has been called to the fact that many of the Kr II lines are hazy and unsymmetrical, and it has been supposed that this is an evidence of Stark effect. Now we wish to point out that the unsymmetrical shading of lines in this spectrum appears to be due mainly to the mutual perturbation of levels of opposite parity which have nearly the same energy value.

A striking example of such perturbation is found in the levels $s^2p^4(^1D)5p^2P^\circ_{1½}=47{,}978.52$ and $s^2p^4(^1D)4d^2D_{1½}=48{,}002.13$. The former is odd, the latter even, and their difference is 23.61 $cm^{-1}$, which corresponds with a wave length of 420$\mu$ or 0.42 mm. When the former (47,978.52) combines with (even) terms of low energy content the lines are shaded to violet ($v$) and when it combines with high (even) terms the lines are shaded to red ($l$). The neighboring level (48,002.13) combines with both low and high odd terms with lines shading toward red and violet, respectively, that is, in the opposite sense from lines involving 47,978.52. Thus, the mutual effect of these perturbing levels suggests a repulsion between them.

Similarly, the (odd) levels $s^2p^4(^1D)5p^2P^\circ_{0½}=45{,}941.03$ and $s^2p^4(^1D)5p^2D^\circ_{1½}=45{,}990.14$ are perturbed by the adjacent (even) level $s^2p^4(^1D)4d^2P_{0½}=45{,}995.30$ and all lines involving these levels are shaded either to lower or to higher frequencies in the same way as those discussed in the previous example.

Practically all of the lines involving the above-mentioned perturbing levels are shaded in one direction or the other, the only exceptions being those for which dissymmetry could not be detected on account of faintness or nearness to other lines.

Lines which have been identified as originating with twice ionized krypton atoms, and among which regularities have been found and interpreted, will be described later in a note on the Kr III spectrum

TABLE 2.—*Krypton II term table*

ODD TERMS

| Configuration and limit | Symbol | Term value | Differences | g-values | | Term combinations |
|---|---|---|---|---|---|---|
| | | | | Landé | Observed | |
| $s^2p^4$ | $^2P_{1½}$ | 198,182.00 | −5,371 | | | $sp^6.{}^2S$; $s^2p^4(^3P)5s^4P$, $^2P$; $s^2p^4(^1D)$ $5s$ $^2D$ $s^2p^4(^1S)5s^2S$; $s^2p^4(^3P)6s^4P$; $s^2p^4(^1S)6s^2S$; $s^2p^4(^3P)7s^4P$; $s^2p^4(^3P)4d^4F$, $^4D$, $^4P$, $^2F$, $^2D$, $^2P$; $s^2p^4(^1D)4d^2F$, $^2D$, $^2P$; $s^2p^4(^1S)$ $4d^2D$; $s^2p^4(^3P)5d^4F$, $^4D$, $^4P$, $^2D$; 59,686.98; 65,209.50. |
| | $^2P_{0½}$ | 192,811.00 | | | | |
| $s^2p^4(^3P)$ | $5p\ ^4P_{2½}$ | 64,256.35 | −362.79 | 1.60 | 1.58 | $sp^6.{}^2S$; $s^2p^4(3P)5s^4P$, $^2P$; $s^2p^4(^1S)5s^2S$; $s^2p^4(^3P)6s^4P$, $^2P$; $s^2p^4(^1D)6s^2D$; $s^2p^4$ $(^1S)6s^2S$; $s^2p^4(^3P)7s^4P$; $s^2p^4(^3P)4d^4D$; $s^2p^4(^1D)4d^2F$, $^2D$, $^2P$; $s^2p^4(^1S)4d^2D$; $s^2p^4(^3P)5d^4F$, $^4D$, $^4P$, $^2F$, $^2D$, $^2P$; 31,180.55. |
| | $^4P_{1½}$ | 63,893.56 | −1,494.59 | 1.73 | 1.67 | |
| | $^4P_{0½}$ | 62,398.97 | | 2.67 | 1.98 | |

TABLE 2.—*Krypton II term table*—Continued

ODD TERMS—Continued

| Configuration and limit | Symbol | Term value | Differences | g-values | | Term combinations |
|---|---|---|---|---|---|---|
| | | | | Landé | Observed | |
| | $^4D_{1/2}$ | 62,398.82 | | 1.43 | 1.43 | $s^2p^6\,{}^2S$; $s^2p^4(^3P)5s\,{}^4P$, $^2P$; $s^2p^4(^1D)5s\,{}^2D$; $s^2p^4(^3P)6s\,{}^4P$, $^2P$; $s^2p^4(^1D)6s\,{}^2D$; $s^2p^4(^1S)6s\,{}^2S$; $s^2p^4(^3P)7s\,{}^4P$; $s^2p^4(^3P)4d\,{}^4D$; $s^2p^4(^1D)4d\,{}^2G$, $^2D$, $^2P$; $s^2p^4(^1S)4d\,{}^2D$; $s^2p^4(^3P)5d\,{}^4F$, $^4D$, $^4P$, $^2F$, $^2D$, $^2P$; $s^2p^4(^1D)5d\,{}^2G\,{}^2P$; 31,180.55. |
| | $^4D_{3/2}$ | 62,111.00 | −287.82 | 1.37 | 1.23 | |
| | $^4D_{5/2}$ | 59,800.65 | −2,310.35 | 1.20 | 1.26 | |
| | $^4D_{7/2}$ | 58,018.75 | −1,781.90 | 0.00 | 0.00 | |
| | $^4S_{3/2}$ | 56,459.28 | | 2.00 | 1.54 | $s^2p^6\,{}^2S$; $s^2p^4(^3P)5s\,{}^4P$, $^2P$; $s^2p^4(^1D)5s\,{}^2D$; $s^2p^4(^3P)6s\,{}^4P$, $^2P$; $s^2p^4(^1D)6s\,{}^2D$; $s^2p^4(^1S)6s\,{}^2S$; $s^2p^4(^3P)7s\,{}^4P$, $^2P$; $s^2p^4(^3P)4d\,{}^4D$, $^4P$; $s^2p^4(^1D)4d\,{}^2D$, $^2P$; $s^2p^4(^3P)5d\,{}^4F$, $^4D$, $^4P$, $^2F$, $^2D$, $^2P$; $s^2p^4(^1D)5d\,{}^2F$, $^2P$; 31,180.55. |
| $s^2p^4(^3P)$ $5p$ | $^2P_{1/2}$ | 58,044.85 | 1,033.79 | 1.33 | 1.26 | $s^2p^6\,{}^2S$; $s^2p^4(^3P)5s\,{}^4P$, $^2P$; $s^2p^4(^1D)5s\,{}^2D$; $s^2p^4(^3P)6s\,{}^4P$, $^2P$; $s^2p^4(^1D)6s\,{}^2D$; $s^2p^4(^1S)6s\,{}^2S$; $s^2p^4(^3P)7s\,{}^4P$, $^2P$; $s^2p^4(^3P)4d\,{}^4F$, $^4D$, $^4P$; $s^2p^4(^1D)4d\,{}^2D$, $^2P$; $s^2p^4(^3P)5d\,{}^4F$, $^4D$, $^4P$, $^2F$, $^2D$, $^2P$; $s^2p^4(^1D)5d\,{}^2P$; $s^2p^4(^1S)4d\,{}^2D$; 31,180.55. |
| | $^2P_{3/2}$ | 59,078.64 | | 0.67 | 1.78 | |
| | $^2D_{3/2}$ | 58,063.01 | −1,876.69 | 1.20 | 1.34 | $s^2p^6\,{}^2S$; $s^2p^4(^3P)5s\,{}^4P$, $^2P$; $s^2p^4(^1D)5s\,{}^2D$; $s^2p^4(^3P)6s\,{}^4P$, $^2P$; $s^2p^4(^1D)6s\,{}^2D$; $s^2p^4(^1S)6s\,{}^2S$; $s^2p^4(^3P)7s\,{}^4P$, $^2P$; $s^2p^4(^3P)4d\,{}^4F$, $^4D$, $^4P$; $s^2p^4(^1D)4d\,{}^2D$, $^2P$; $s^2p^4(^1S)4d\,{}^2D$; $s^2p^4(^3P)5d\,{}^4F$, $^4D$, $^4P$, $^2F$, $^4D$, $^2P$; $s^2p^4(^1D)5d\,{}^2P$; 31,180.55. |
| | $^2D_{5/2}$ | 56,186.32 | | 0.80 | 1.33 | |
| | $^2S_{1/2}$ | 55,818.45 | | 2.00 | 1.50 | $s^2p^6\,{}^2S$; $s^2p^4(^3P)5s\,{}^4P$, $^2P$; $s^2p^4(^1D)5s\,{}^2D$; $s^2p^4(^3P)6s\,{}^4P$, $^2P$; $s^2p^4(^1D)6s\,{}^2D$; $s^2p^4(^1S)6s\,{}^2S$; $s^2p^4(^3P)7s\,{}^4P$, $^2P$; $s^2p^4(^3P)4d\,{}^4D$; $s^2p^4(^1D)4d\,{}^2P$; $s^2p^4(^3P)5d\,{}^4F$, $^4D$, $^4P$, $^2F$, $^2D$, $^2P$; $s^2p^4(^1D)5d\,{}^2P$. |
| | $^3F_{2/2}$ | 48,477.45 | | 1.14 | 1.14 | $s^2p^4(^3P)5s\,{}^4P, {}^2P$; $s^2p^4(^1D)5s\,{}^2D$; $s^2p^4(^1D)6s\,{}^2D$; $s^2p^4(^3P)4d\,{}^4F$, $^4D$, $^4P$, $^2F$, $^2D$, $^2P$; $s^2p^4(^1S)4d\,{}^2D$; $s^2p^4(^3P)5d\,{}^4F$, $^4D$, $^4P$, $^2D$; $s^2p^4(^1D)5d\,{}^2G$, $^2F$, $^2D$; 59686.98. |
| | $^3F_{3/2}$ | 49,008.58 | 531.13 | 0.86 | 0.86 | |
| $s^2p^4(^1D)$ $5p$ | $^3P_{1/2}$ | 47,978.52 | | 1.33 | 1.33 | $s^2p^6\,{}^2S$; $s^2p^4(^3P)5s\,{}^4P$, $^2P$; $s^2p^4(^1D)5s\,{}^2D$; $s^2p^4(^3P)6s\,{}^4P^2, P$; $s^2p^4(^1D)6s\,{}^2D$; $s^2p^4(^1S)6s\,{}^2S$; $s^2p^4(^3P)7s\,{}^4P$; $s^2p^4(^3P)4d\,{}^4F$, $^4D$, $^4P$, $^2F$, $^2D$, $^2P$; $s^2p^4(^1S)4d\,{}^2D$; $s^2p^4(^3P)5d\,{}^4F$, $^4D$, $^4P$, $^2F$, $^2D$, $^2P$; $s^2p^4(^1D)5d\,{}^2F$, $^2D$, $^2P$; 59686.98; 65209.50. |
| | $^3P_{0/2}$ | 45,941.03 | −2037.49 | 0.67 | 0.70 | |
| | $^3D_{1/2}$ | 45,865.80 | | 1.20 | 1.20 | $s^2p^4(^3P)5s\,{}^4P$, $^2P$; $s^2p^4(^1D)5s\,{}^2D$; $s^2p^4(^1D)6s\,{}^2D$; $s^2p^4(^3P)7s\,{}^4P$, $^2P$; $s^2p^4(^1D)4d\,{}^2D$, $^2P$; $s^2p^4(^3P)4d\,{}^4F$, $^4D$, $^4P$, $^2F$, $^2D$, $^2P$; $s^2p^4(^1S)4d\,{}^2D$; $s^2p^4(^3P)5d\,{}^4F$, $^4D$, $^4P$, $^2F$, $^2D$, $^2P$; $s^2p^4(^1D)5d\,{}^2F$, $^2D$, $^2P$; 59686.98; 65209.50. |
| | $^3D_{2/2}$ | 45,990.14 | 124.34 | 0.80 | 0.80 | |
| $s^2p^4(^1S)$ $5p$ | $^2P_{1/2}$ | 29,242.65 | | 0.67 | 0.90 | $s^2p^4(^1S)5s\,{}^2S$; $s^2p^4(^3P)4d\,{}^4F$, $^4P$, $^2F$, $^2D$, $^2P$; $s^2p^4(^1D)4d\,{}^2D$, $^2P$; 65209.50. |
| | $^2P_{3/2}$ | 29,919.10 | 676.45 | 1.33 | 1.24 | |
| $s^2p^4(^3P)$ $5f$ | $^4G_{11/2}$ | | | | | |
| | $^4G_{9/2}$ | | | | | |
| | $^4G_{7/2}$ | | | | | |
| | $^4G_{5/2}$ | | | | | |
| | $^4F_{9/2}$ | 30,096.51 | | | | $s^2p^4(^1D)\ 5s\,{}^2D$; $s^2p^4(^3P)4d\ {}^4F$, $^4D$, $^4P$, $^2F$, $^2D$, $^2P$; $s^2p^4(^1D)4d\ {}^2F$, $^2D$, $^2P$; 65209.50. |
| | $^4F_{7/2}$ | 30,064.00 | −32.51 | | | |
| | $^4F_{5/2}$ | 29,998.80 | −62.50 | | | |
| | $^4F_{3/2}$ | 29,796.88 | −201.92 | | | |
| | $^4D_{7/2}$ | | | | | |
| | $^4D_{5/2}$ | | | | | |
| | $^4D_{3/2}$ | 29,463.10 | | | | $s^2p^4(^1S)5s\,{}^2S$; $s^2p^4(^3P)4d\ {}^4D$, $^4P$, $^2D$, $^2P$; $s^2p^4(^1D)4d\ {}^2P$. |
| | $^4D_{1/2}$ | | | | | |
| | $^4G_{11/2}$ | | | | | |
| | $^4G_{9/2}$ | | | | | |
| | $^2F_{7/2}$ | 29,921.57 | | | | $s^2p^4(^1D)\ 5s\,{}^2D$; $s^2p^4(^3P)4d\ {}^4F$, $^4D$, $^4P$, $^2F$, $^2D$, $^2P$; $s^2p^4(^1D)4d\ {}^2F$, $^2D$, $^2P$; 65209.50. |
| | $^2F_{5/2}$ | 29,719.47 | −202.10 | | | |
| | $^2D_{5/2}$ | | | 0.80 | 1.02 | $s^2p^4(^1S)\ 5s\,{}^2S$; $s^2p^4(^3P)4d\ {}^4D$, $^4P$, $^2F$, $^2D$, $^2P$; $s^2p^4(^1D)4d\ {}^2D$, $^2P$; 65209.50. |
| | $^2D_{3/2}$ | 29,551.64 | | | | |
| $s^2p^4(^1D)$ $5f$ | $^3H_{11/2}$ | | | | | |
| | $^3H_{9/2}$ | | | | | |
| | $^3G_{11/2}$ | | | | | |
| | $^3G_{9/2}$ | | | | | |
| | $^3F_{9/2}$ | 25 050.97 | | | | $s^2p^4(^3P)6s\,{}^2P$; $s^2p^4(^3P)4d\,{}^4F, {}^4P, {}^2F$, $^2D$, $^2P$; $s^2p^4(^1D)4d\,{}^2D$, $^2P$; $s^2p^4(^3P)5d\,{}^4D$; 59686.98; 65209.50. |
| | $^3F_{7/2}$ | 25,025.58 | −25.39 | | | |
| | $^3D_{3/2}$ | 25,408.63 | | | | $s^2p^4(^1D)5s\,{}^2D$; $s^2p^4(^2P)4d\,{}^4F?$, $^4P$, $^2F$, $^2D$, $^2P$; $s^2p^4(^1D)4d\,{}^2F$, $^2D$, $^2P$; 65209.50. |
| | $^3D_{1/2}$ | 25,467.28 | 58.65 | | | |

TABLE 2.—*Krypton II term table*—Continued

ODD TERMS—Continued

| Configuration and limit | Symbol | Term value | Differences | g-values | | Term combinations |
|---|---|---|---|---|---|---|
| | | | | Landé | Observed | |
| $s^2p^4(^1D)$ | $5f\,{}^2P_{1½}$ | 24,494.12 | | | | $s^2p^4(^3P)6s\,{}^4P$; $s^2p^4(^3P)4d\,{}^4F?$, $^4P$, $^2F?$, $^2D$, $^2P$; $s^2p^4(^1D)4d\,{}^2D$, $^2P$; 65209.50. |
| | $5f\,{}^2P_{0½}$ | 23,679.00 | −815.12 | | | |
| $s^2p^4(^1S)$ | $5f\,{}^2F_{2½}$ | | | | | |
| | $5f\,{}^2F_{1½}$ | | | | | |
| | $j$ | | | | | |
| | 1½ | 32,026.50? | | | | $s^2p^4(^1D)5s\,{}^2D$; $s^2p^4(^1S)5s\,{}^2S$; $s^2p^4(^3P)4d\,{}^2F$, $^2D$; $s^2p^4(^1D)4d\,{}^2D$, $^2P$. |
| | 2½ | 29,691.33 | | | | $s^2p^4(^1D)5s\,{}^2D$; $s^2p^4(^3P)4d\,{}^4F$, $^2F$. |
| | 1½ | 27,294.47 | | | | $s^2p^4(^1S)5s\,{}^2S$; $s^2p^4(^1D)4d\,{}^2P$. |
| | 2½ | 26,886.30 | | | | $s^2p^4(^1D)5s\,{}^2D$; $s^2p^4(^3P)4d\,{}^4F$, $^2F$, $^2D$. |
| | 2½ | 26,795.68 | | | | $s^2p^4(^1D)5s\,{}^2D$; $s^2p^4(^3P)4d\,{}^2F$, $^2D$; $s^2p^4(^1D)4d\,{}^2G?$. |
| | 3½ | 26,622.00 | | | | $s^2p^4(^1D)5s\,{}^2D$; $s^2p^4(^3P)4d\,{}^2F$; 65,209.50. |
| | 2½ | 25,447.85 | | | | $s^2p^4(^1D)5s\,{}^2D$; $s^2p^4(^3P)4d\,{}^2P$; $s^2p^4(^1D)4d\,{}^2G?$, $^2D$. |
| | 1½ | 15,717.15 | | | | $s^2p^4(^1S)6s\,{}^2S$; $s^2p^4(^3P)5d\,{}^4D?$, $^4P$; $s^2p^4(^1D)4d\,{}^2P$, $^2D$. |
| | 0½? | 15,702.73 | | | | $s^2p^4(^1S)6s\,{}^2S$; $s^2p^4(^3P)6s\,{}^4P$, $^2P$; $s^2p^4(^3P)5d\,{}^4D?$, $^4P$; $s^2p^4(^1D)4d\,{}^2P$, $^2D$. |
| | 1½ | 15,370.10 | | | | $s^2p^4(^3P)6s\,{}^2P$; $s^2p^4(^3P)5d\,{}^4D$; $s^2p^4(^1D)4d\,{}^2P$, $^2D$. |
| | 2½ | 15,340.81 | | | | $s^2p^4(^3P)5d\,{}^4D$, $^2F$, $^2P$; $s^2p^4(^1D)4d\,{}^2P$, $^2D$. |
| | 1½ | 15,216.41 | | | | $s^2p^4(^3P)5d\,{}^4D?$; $s^2p^4(^1D)4d\,{}^2P$, $^2D$. |
| | 2½ | 14,873.45 | | | | $s^2p^4(^1S)6s\,{}^2S$; $s^2p^4(^1D)4d\,{}^2P$, $^2D$. |

EVEN TERMS

| | | | | | | |
|---|---|---|---|---|---|---|
| $s^2p^4$ | $^3S_{1½}$ | 89,179.94 | | | | $s^2p^3$. $^2P°$; $s^2p^4(^2P)5p\,{}^4D°$, $^4P°$, $^4S°$; $^2D°$, $^2P°$, $^2S°$; $s^2p^4$ $(^1D)$ $5p\,{}^2P°$. |
| $s^2p^4(^3P)$ | $5s\,{}^4P_{2½}$ | 85,352.00 | | 1.60 | 1.60 | $s^2p^3$. $^2P°$; $s^2p^4(^3P)5p\,{}^4D°$, $^4P°$, $^4S°$, $^2D°$, $^2P°$, $^2S°$; $s^2p^4(^1D)5p\,{}^2F°$, $^2D°$, $^2P°$. |
| | $5s\,{}^4P_{1½}$ | 83,088.29 | −2,263.71 | 1.73 | 1.54 | |
| | $5s\,{}^4P_{0½}$ | 80,577.27 | −2,511.02 | 2.67 | 2.64 | |
| | $5s\,{}^2P_{1½}$ | 79,705.93 | | 1.33 | 1.52 | $s^2p^3$. $^2P°$; $s^2p^4(^3P)5p\,{}^4D°$, $^4P°$, $^4S°$, $^2D°$, $^2P°$, $^2S°$; $s^2p^4(^1D)5p\,{}^2F°$, $^2D°$, $^2P°$. |
| | $5s\,{}^2P_{0½}$ | 77,178.13 | −2,527.80 | 0.67 | 0.70 | |
| $s^2p^4(^1D)$ | $5s\,{}^2D_{2½}$ | 70,318.77 | | 1.20 | 1.20 | $s^2p^3$. $^2P°$; $s^2p^4(^3P)5p\,{}^4D°$, $^4S°$, $^2D°$, $^2P°$, $^2S°$; $s^2p^4(^1D)5p\,{}^2F°$, $^2D°$, $^2P°$; $s^2p^4(^3P)5f\,{}^4F°$, $^2F°$; $s^2p^4(^1D)5f\,{}^2F°$, $^2D°$; 29691.33; 26886.30; 26795.68; 26622.00; 25447.85. |
| | $5s\,{}^2D_{1½}$ | 70,582.81 | 264.04 | 0.80 | 0.80 | |
| $s^2p^4(^1S)$ | $5s\,{}^2S_{0½}$ | 52,368.39 | | 2.00 | 2.00 | $s^2p^3$. $^2P°$; $s^2p^4(^3P)5p\,{}^4P°$; $s^2p^4(^1S)5p\,{}^2P°$; $s^2p^4(^3P)5f\,{}^2D°$, $^2D°$; 32026.50. |
| $s^2p^4(^3P)$ | $4d\,{}^4F_{4½}$ | 72,179.43 | | | | $s^2p^3$. $^2P°$; $s^2p^4(^3P)5p\,{}^2D°$, $^2P°$; $s^2p^4(^1D)5p\,{}^2F°$, $^2D°$, $^2P°$; $s^2p^4(^1S)5p\,{}^2P°$; $s^2p^4(^3P)5f\,{}^4F°$, $^2F°$; $s^2p^4(^1D)5f\,{}^2F°$, $^2D°?$, $^2P°?$; 29,691.33; 26,886.30. |
| | $4d\,{}^4F_{3½}$ | 70,250.80 | −1,928.63 | | | |
| | $4d\,{}^4F_{2½}$ | 68,483.02 | −1,767.78 | | | |
| | $4d\,{}^4F_{1½}$ | 68,438.44 | −44.58 | | | |
| | $4d\,{}^4D_{3½}$ | 77,970.41 | | | | $s^2p^3$. $^2P°$; $s^2p^4(^3P)5p\,{}^4D°$, $^4P°$, $^4S°$, $^2D°$, $^2P°$, $^2S°$; $s^2p^4(^1D)5p\,{}^2F°$, $^2D°$, $^2P°$; $s^2p^4(^1P)5f\,{}^4F°$, $^4D°$, $^2F°$, $^2D°$. |
| | $4d\,{}^4D_{2½}$ | 77,753.35 | −217.06 | | | |
| | $4d\,{}^4D_{1½}$ | 77,179.90 | −573.45 | | | |
| | $4d\,{}^4D_{0½}$ | 76,400.72 | −779.18 | 0.00 | 0.00 | |
| | $4d\,{}^4P_{2½}$ | 66,804.76 | | | | $s^2p^3$. $^2P°$; $s^2p^4(^3P)5p\,{}^4D°$, $^4S°$, $^2D°$; $s^2p^4(^1D)5p\,{}^2F°$, $^2D°$, $^2P°$; $s^2p^4(^1S)5p\,{}^2P°$; $s^2p^4(^3P)5f\,{}^4F°$ $^4D°$, $^2F°$, $^2D°$; $s^2p^4(^1D)5f\,{}^2F°$, $^2D°$, $^2P°$. |
| | $4d\,{}^4P_{1½}$ | 67,286.72 | 481.96 | | | |
| | $4d\,{}^4P_{0½}$ | 67,667.41 | 380.69 | | | |
| | $4d\,{}^2F_{3½}$ | 66,548.14 | | | | $s^2p^3$. $^2P°$; $s^2p^4(^1D)5p\,{}^2F°$, $^2D°$, $^2P°$; $s^2p^4(^1S)5p\,{}^2P°$; $s^2p^4(^3P)5f\,{}^4F°$, $^4D°$, $^2F°$, $^2D°$; 29,691.33, 26,886.30, 26,795.68, 26,622.00, 32,026.50. |
| | $4d\,{}^2F_{2½}$ | 61,082.02 | −5,466.12 | | | |
| | $4d\,{}^2D_{2½}$ | 63,613.18 | | | | $s^2p^3$. $^2P°$; $s^2p^4(^1D)5p\,{}^2F°$, $^2D°$, $^2P°$; $s^2p^4(^1S)5p\,{}^2P°$; $s^2p^4(^3P)5f\,{}^4F°$, $^4D°$, $^2F°$, $^2D°$; $s^2p^4(^1D)5f\,{}^2F°$, $^2D°$, $^2P°$; 32,026.50; 26,886.30; 26, 795.68. |
| | $4d\,{}^2D_{1½}$ | 65,214.72 | 1,601.54 | | | |
| | $4d\,{}^2P_{1½}$ | 63,558.83 | | | | $s^2p^3$. $^2P°$; $s^2p^4(^1D)5p\,{}^2F°$, $^2D°$, $^2P°$; $s^2p^4(^1S)5p\,{}^2P°$; $s^2p^4(^3P)5f\,{}^4F°$, $^4D°$, $^2F°$, $^2D°$; $s^2p^4(^1D)5f\,{}^2F°$, $^2D°$, $^2P°$; 25,447.85. |
| | $4d\,{}^2P_{0½}$ | | | | | |

TABLE 2.—*Krypton II term table*—Continued

EVEN TERMS—Continued

| Configuration and limit | Symbol | Term value | Differences | g-values | | Term combinations |
|---|---|---|---|---|---|---|
| | | | | Landé | Observed | |
| | $^2G_{4½}$ | 51, 289. 68? | | | | $s^2p^4(^3p)5p^4D^\circ$; $s^2p^4$ $(^3P)5f^4F^\circ$?; 26,795.68; 25,447.85. |
| | $^2G_{3½}$ | | | | | |
| | $^2F_{3½}$ | 48, 321. 73? | −953. 97 | | | $s^2p^4(^3P)5p^4P^\circ$?; $s^2p^4(^3P)5f^4F^\circ$, $^2F^\circ$; $s^2p^4(^1D)5f^2F^\circ$, $^2D^\circ$. |
| | $^2F_{2½}$ | 47, 367. 76? | | | | |
| | $^2D_{2½}$ | 48, 666. 10 | −663. 97 | | | $s^2p^5$ $^2P^\circ$; $s^2p^4(^3P)5p^4D^\circ$, $^4P^\circ$, $^2D^\circ$, $^2P^\circ$; $s^2p^4(^1S)$ $5p^2P^\circ$; $s^2p^4(^3P)5f^4F^\circ$, $^2F^\circ$, $^2D^\circ$; $s^2p^4$ $(^1D)5f^2F^\circ$, $^2D^\circ$, $^2P^\circ$; 32026.50; 25447.85; 15717.15; 15702.73; 15340.81; 15370.10; 15216.41; 14873.45. |
| $s^2p^4(^1D)$ | $^2D_{1½}$ | 48, 002. 13 | | | | |
| | $^2P_{1½}$ | 46, 354. 00 | −358. 70 | | | $s^2p^5$ $^2P^\circ$; $s^2p^4(^3P)5p^4D^\circ$, $^4P^\circ$, $^4S^\circ$, $^2D^\circ$, $^2P^\circ$, $^2S^\circ$; $s^2p^4(^1S)5p^2P^\circ$; $s^2p^4$ $(^3P)5f^4F^\circ$, $^4D^\circ$, $^2F^\circ$, $^2D^\circ$; $s^2p^4(^1D)$ $5f^2F^\circ$, $^2D^\circ$, $^2P^\circ$; 32026.50; 15717.15; 15702.73; 15340.81; 15370.10; 15216.41; 14873.45. |
| | $^2P_{0½}$ | 45, 995. 30 | | | | |
| | $^2S_{0½}$ | | | | | |
| $s^2p^4(^1S)$ | $^2D_{2½}$ | 26, 211. 39 | | 1. 20 | 1. 20 | $s^2p^5$ $^2P^\circ$; $s^2p^4(^3P)5p^4D^\circ$, $^2D^\circ$, $^2P^\circ$; $s^2p^4$ $(^1D)5p^2F^\circ$, $^2D^\circ$, $^2P^\circ$; 15,340.81. |
| | $^2D_{1½}$ | 26, 130. 11 | −81. 28 | 0. 80 | 0. 80 | |
| | $^4P_{2½}$ | 41, 102. 93 | | 1. 60 | 1. 60 | $s^2p^5$ $^2P^\circ$; $s^2p^4(^3P)5p^4D^\circ$, $^4P^\circ$, $^4S^\circ$, $^2D^\circ$, $^2P^\circ$, $^2S^\circ$; $s^2p^4(^1D)5p^2P^\circ$; $s^2p^4(^1S)5p^2P^\circ$. |
| | $^4P_{1½}$ | 40, 296. 59 | −806. 34 | 1. 73 | 1. 39 | |
| $s^2p^4(^3P)$ | $^4P_{0½}$ | 36, 304. 63 | −3, 991. 96 | 2. 67 | 2. 34 | |
| | $^2P_{1½}$ | 36, 122. 97 | | 1. 33 | 1. 33 | $s^2p^4(^3P)5p^4D^\circ$, $^4P^\circ$, $^4S^\circ$, $^2D^\circ$, $^2P^\circ$, $^2S^\circ$; $s^2p^4(^1D)5p^2F^\circ$; $s^2p^4(^1D)5f^2F^\circ$?; 15,702.73; 15,370.10. |
| | $^2P_{0½}$ | 35, 615. 84 | −507. 13 | 0. 67 | 0. 92 | |
| $s^2p^4(^1D)$ | $^2D_{2½}$ | 27, 610. 88 | | 0. 80 | 1. 00 | $s^2p^4(^3P)5p^4D^\circ$, $^4P^\circ$, $^4S^\circ$, $^2D^\circ$, $^2P^\circ$, $^2S^\circ$; $s^2p^4(^1D)5p^2F^\circ$, $^2D^\circ$, $^2P^\circ$; 15,340.81. |
| | $^2D_{1½}$ | | | | | |
| $s^2p^4(^1S)$ | $^2S_{0½}$ | 33, 742. 84? | | 2. 00 | 1. 94 | $s^2p^5$ $^2P^\circ$; $s^2p^4(^3P)5p^4D^\circ$, $^4P^\circ$, $^4S^\circ$, $^2D^\circ$, $^2P^\circ$, $^2S^\circ$; $s^2p^4(^1D)5p^2P^\circ$; 15,717.15; 15,702.73; 14, 873.45. |
| | $^4F_{4½}$ | 35, 973. 16 | | 1. 33 | 1. 33 | $s^2p^5$ $^2P^\circ$; $s^2p^4(^3P)5p^4D^\circ$, $^4P^\circ$, $^4S^\circ$, $^2D^\circ$, $^2P^\circ$, $^2S^\circ$; $s^2p^4(^1D)5p^2P^\circ$. |
| | $^4F_{3½}$ | 35, 650. 09 | −323. 07 | 1. 24 | 1. 17 | |
| | $^4F_{2½}$ | 33, 104. 65 | −2, 545. 44 | 1. 03 | 1. 12 | |
| | $^4F_{1½}$ | 31, 134. 87 | −1, 969. 78 | 0. 40 | 0. 52 | |
| | $^4D_{3½}$ | 36, 896. 69 | | 1. 43 | 1. 40 | $s^2p^5$ $^2P^\circ$?; $s^2p^4(^3P)5p^4D^\circ$, $^4P^\circ$, $^4S^\circ$, $^2D^\circ$, $^2P^\circ$, $^2S^\circ$; $s^2p^4(^1D)5p^2P^\circ$; $s^2p^4(^1D)5f^2F^\circ$; 15,702.73; 15,340.81; 15,370.10; 15,216.41. |
| | $^4D_{2½}$ | 36, 730. 17 | −136. 52 | 1. 37 | 1. 37 | |
| | $^4D_{1½}$ | 36, 380. 08 | −350. 09 | | | |
| | $^4D_{0½}$ | 35, 148. 52 | −1, 231. 56 | 0. 00 | 0. 88 | |
| $s^2p^4(^3P)$ | $^4P_{2½}$ | 37, 168. 44 | | 1. 60 | 2. 47 | $s^2p^5$ $^2P^\circ$; $s^2p^4(^3P)5p^4D^\circ$, $^4P^\circ$, $^4S^\circ$, $^2D^\circ$, $^2P^\circ$, $^2S^\circ$; $s^2p^4(^1D)5p^2F^\circ$, $^2P^\circ$; $s^2P^4(^1D)$ $5f^2F^\circ$; 15,717.15; 15,702.73; 15,340.81. |
| | $^4P_{1½}$ | 36, 772. 71 | −395. 73 | | | |
| | $^4P_{0½}$ | 37, 385. 32 | 612. 61 | 2. 67 | 2. 07 | |
| | $^2F_{3½}$ | 32, 784. 28 | | 1. 14 | 1. 24 | $s^2p^4(^3P)5p^4D^\circ$, $^4P^\circ$, $^4S^\circ$, $^2D^\circ$, $^2P^\circ$; $s^2p^4(^1D)$ $5p^2F^\circ$, $^2P^\circ$; 15,340.81. |
| | $^2F_{2½}$ | 30, 663. 09 | −2, 121. 19 | 0. 86 | 1. 04 | |
| | $^2D_{2½}$ | 28, 477. 15 | | 1. 20 | 1. 15 | $s^2p^5$ $^2P^\circ$; $s^2p^4(^3P)5p^4D^\circ$, $^4P^\circ$, $^4S^\circ$, $^2D^\circ$, $^2P^\circ$, $^2S^\circ$; $s^2p^4(^1D)5p^2F^\circ$, $^2D^\circ$, $^2P^\circ$. |
| | $^2D_{1½}$ | 30, 268. 89 | 1, 791. 74 | 0. 80 | 1. 18 | |
| | $^2P_{1½}$ | 33, 040. 09 | | 1. 33 | 1. 40 | $s^2p^4(^3P)5p^4D^\circ$, $^4P^\circ$, $^4S^\circ$, $^2D^\circ$, $^2P^\circ$, $^2S^\circ$; $s^2p^4(^1D)5p^2P^\circ$. |
| | $^2P_{0½}$ | 31, 228. 69 | −1, 811. 40 | 0. 67 | 0. 51 | |
| | $^2G_{4½}$ | 21, 589. 03 | | 1. 11 | 1. 11 | $s^2p^4(^3P)5p^4D^\circ$?; $s^2p^4(^1D)5p^2F^\circ$. |
| | $^2G_{3½}$ | 22, 290. 26 | 701. 23 | 0. 89 | 0. 89 | |
| | $^2F_{3½}$ | 20, 273. 00 | | 1. 14 | 1. 14 | $s^2p^4(^3P)5p^4S^\circ$; $s^2p^4(^1D)5p^2F^\circ$, $^2D^\circ$, $^2P^\circ$. |
| | $^2F_{2½}$ | 20, 471. 72 | 198. 72 | 0. 86 | 0. 89 | |
| $s^2p^4(^1D)$ | $^2D_{2½}$ | 19, 861. 37 | | 1. 20 | 1. 20 | $s^2p^4(^1D)5p^2F^\circ$, $^2D^\circ$, $^2P^\circ$. |
| | $^2D_{1½}$ | 22, 071. 04 | 2, 209. 67 | | | |
| | $^2P_{1½}$ | 20, 498. 17 | | 1. 33 | 1. 18 | $s^2p^4(^3P)5p^4D^\circ$, $^4S^\circ$, $^2D^\circ$, $^2P^\circ$, $^2S^\circ$; $s^2p^4(^1D)5p^2D^\circ$, $^2P^\circ$. |
| | $^2P_{0½}$ | 19, 394. 37 | −1, 103. 80 | | | |
| | $^2S_{½}$ | | | | | |
| $s^2p^4(^1S)$ | $^2D_{2½}$ | | | | | |
| | $^2D_{1½}$ | | | | | |
| | $^4P_{2½}$ | 24, 872. 32 | | | | $s^2p^5$ $^2P^\circ$; $s^2p^4(^3P)5p^4D^\circ$, $^4P^\circ$, $^4S^\circ$, $^2D^\circ$, $^2P^\circ$, $^2S^\circ$; $s^2p^4(^1D)5p^2D^\circ$. |
| | $^4P_{1½}$ | 24, 541. 98 | −330. 34 | | | |
| $s^2p^4(^3P)$ | $^4P_{0½}$ | 20, 127. 21 | −4, 414. 77 | | | |
| | $^2P_{1½}$ | 20, 225. 12 | | | | $s^2p^4(^3P)5p^4S^\circ$, $^2D^\circ$, $^2P^\circ$, $^2S^\circ$; $s^2p^4(^1D)5p^2$ $D^\circ$, $^2P^\circ$. |
| | $^2P_{0½}$ | 19, 674. 55 | −550. 57 | | | |

TABLE 2.—*Krypton II term table*—Continued

EVEN TERMS—Continued

| Configuration and limit | Symbol | Term value | Differences | g-values: Landé | g-values: Observed | Term combinations |
|---|---|---|---|---|---|---|
| $s^2p^4(^1D)$ | $7s\ {}^3D_{2\frac{1}{2}}$ | | | | | |
| | $7s\ {}^1D_{1\frac{1}{2}}$ | | | | | |
| $s^2p^4(^1S)$ | $7s\ {}^2S_{0\frac{1}{2}}$ | | | | | |
| $s^2p^4(^3P)$ | $5g\ {}^4G_{3\frac{1}{2}}$ | 19,339.61 | | | | $s^2p^4(^3P)\ 5f\,{}^4F°,\ {}^2F°.$ |
| | $5g\ {}^4G_{4\frac{1}{2}}$ | 19,370.70 | 31.09 | | | |
| | $5g\ {}^4G_{3\frac{1}{2}}$ | 19,366.49 | −4.21 | | | |
| | $5g\ {}^4G_{2\frac{1}{2}}$ | 19,321.12 | −45.37 | | | |
| | $j$ | | | | | $s^2p^5.{}^2P°;\ s^2p^4(^1D)5p\,{}^2F°_2, D°, {}^2P°;\ s^2p^4(^1S)$ $5p\,{}^2P°;\ s^2p^4(^3P)5f\,{}^4F°, {}^2F°, {}^2D°;\ s^2p^4(^1D)$ $5f\,{}^2F°, {}^2D°, {}^2P°.$ 26,622.00. |
| | $2\frac{1}{2}$ | 65,209.50 | | | | |
| | $1\frac{1}{2}$ | 59,686.98 | | | | $s^2p^5.{}^2P°;\ s^2p^4(^1D)5p\,{}^2F°, {}^2D°, {}^2P°;\ s^2p^4(^1D$ $5f\,{}^2F°.$ |
| | $3\frac{1}{2}$ | 31,180.55 | | | | $s^2p^4(^3P)5p\,{}^4D°, {}^4P°, {}^4S°, {}^2D°, {}^2P°.$ |

TABLE 3.—*Classified lines of the Kr II spectrum in the extreme ultraviolet*

| Intensity | $\lambda_{vac}$ I.A | $\nu_{vac}\,cm^{-1}$ | Term combination |
|---|---|---|---|
| 0 | 575.92 | 173,635 | $s^2p^5.{}^2P°_{1\frac{1}{2}}$—$s^2p^4(^3P)\,7s\,{}^4P_{1\frac{1}{2}}$ |
| 2 | 581.51 | 171,966 | $s^2p^5.{}^2P°_{1\frac{1}{2}}$—$s^2p^4(^1S)\,4d\,{}^2D_{2\frac{1}{2}}$ |
| 1 | 589.25 | 169,707 | $s^2p^5.{}^2P°_{1\frac{1}{2}}$—$s^2p^4(^3P)\,5d\,{}^2D_{2\frac{1}{2}}$ |
| 2 | 595.56 | 167,909 | $s^2p^5.{}^2P°_{1\frac{1}{2}}$—$s^2p^4(^3P)\,5d\,{}^2D_{1\frac{1}{2}}$ |
| 1 | 599.99 | 166,669 | $s^2p^5.{}^2P°_{0\frac{1}{2}}$—$s^2p^4(^1S)\,4d\,{}^2D_{1\frac{1}{2}}$ |
| 2 | 605.74 | 165,087 | $s^2p^5.{}^2P°_{1\frac{1}{2}}$—$s^2p^4(^3P)\,5d\,{}^4F_{2\frac{1}{2}}$ |
| 2 | 608.14 | 164,436 | $s^2p^5.{}^2P°_{1\frac{1}{2}}$—$s^2p^4(^1S)\,6s\,{}^2S_{0\frac{1}{2}}$ |
| 1 | 621.10 | 161,005 | $s^2p^5.{}^2P°_{1\frac{1}{2}}$—$s^2p^4(^3P)\,5d\,{}^4P_{2\frac{1}{2}}$ |
| 3 | 621.90 | 160,798 | $s^2p^5.{}^2P°_{1\frac{1}{2}}$—$s^2p^4(^3P)\,5d\,{}^4P_{0\frac{1}{2}}$ |
| 1 | 633.36 | 157,888 | $s^2p^5.{}^2P°_{1\frac{1}{2}}$—$s^2p^4(^3P)\,6s\,{}^4P_{1\frac{1}{2}}$ |
| 0 | 634.33 | 157,647 | $s^2p^5.{}^2P°_{0\frac{1}{2}}$—$s^2p^4(^3P)\,5d\,{}^4D_{0\frac{1}{2}}$? |
| 0 | 638.94 | 156,509 | $s^2p^5.{}^2P°_{0\frac{1}{2}}$—$s^2p^4(^3P)\,6s\,{}^4P_{0\frac{1}{2}}$ |
| 0 | 639.33 | 156,414 | $s^2p^5.{}^2P°_{0\frac{1}{2}}$—$s^2p^4(^3P)\,5d\,{}^4D_{1\frac{1}{2}}$? |
| 0 | 640.86 | 156,040 | $s^2p^5.{}^2P°_{0\frac{1}{2}}$—$s^2p^4(^3P)\,5d\,{}^4P_{1\frac{1}{2}}$ |
| 2 | 643.40 | 155,424 | $s^2p^5.{}^2P°_{0\frac{1}{2}}$—$s^2p^4(^3P)\,5d\,{}^4P_{0\frac{1}{2}}$ |
| 1 | 657.11 | 152,182 | $s^2p^5.{}^2P°_{1\frac{1}{2}}$—$s^2p^4(^1D)\,4d\,{}^2P_{0\frac{1}{2}}$ |
| 0 | 633.06 | 150,816 | $s^2p^5.{}^2P°_{1\frac{1}{2}}$—$s^2p^4(^1D)\,4d\,{}^2F_{2\frac{1}{2}}$ |
| 4 | 665.88 | 150,177 | $s^2p^5.{}^2P°_{1\frac{1}{2}}$—$s^2p^4(^1D)\,4d\,{}^2D_{1\frac{1}{2}}$ |
| 4 | 668.80 | 149,552 | $s^2p^5.{}^2P°_{1\frac{1}{2}}$—$s^2p^4(^1D)\,4d\,{}^2D_{2\frac{1}{2}}$ |
| 2 | 681.16 | 146,808 | $s^2p^5.{}^2P°_{0\frac{1}{2}}$—$s^2p^4(^1D)\,4d\,{}^2P_{0\frac{1}{2}}$ |
| 5 | 682.82 | 146,452 | $s^2p^5.{}^2P°_{0\frac{1}{2}}$—$s^2p^4(^1D)\,4d\,{}^2P_{1\frac{1}{2}}$ |
| 2 | 685.71 | 145,834 | $s^2p^5.{}^2P°_{1\frac{1}{2}}$—$s^2p^4(^1S)\,5s\,{}^2S_{0\frac{1}{2}}$ |
| 2 | 690.61 | 144,800 | $s^2p^5.{}^2P°_{0\frac{1}{2}}$—$s^2p^4(^1D)\,4d\,{}^2D_{1\frac{1}{2}}$ |
| 1 | 712.02 | 140,446 | $s^2p^5.{}^2P°_{0\frac{1}{2}}$—$s^2p^4(^1S)\,5s\,{}^2S_{0\frac{1}{2}}$ |
| 0 | 722.04 | 138,496 | $s^2p^5.{}^2P°_{1\frac{1}{2}}$——59,687 |
| 4 | 729.41 | 137,097 | $s^2p^5.{}^2P°_{1\frac{1}{2}}$—$s^2p^4(^3P)\,4d\,{}^2F_{2\frac{1}{2}}$ |
| 2 | 743.15 | 134,562 | $s^2p^5.{}^2P°_{1\frac{1}{2}}$—$s^2p^4(^3P)\,4d\,{}^2D_{2\frac{1}{2}}$ |
| 4 | 752.03 | 132,973 | $s^2p^5.{}^2P°_{1\frac{1}{2}}$—$s^2p^4(^3P)\,4d\,{}^2P_{0\frac{1}{2}}$<br>$s^2p^5.{}^2P°_{1\frac{1}{2}}$—$s^2p^4(^3P)\,4d\,{}^2D_{1\frac{1}{2}}$ |
| 2 | 761.16 | 131,378 | $s^2p^5.{}^2P°_{1\frac{1}{2}}$—$s^2p^4(^3P)\,4d\,{}^4P_{2\frac{1}{2}}$ |
| 1 | 763.97 | 130,895 | $s^2p^5.{}^2P°_{1\frac{1}{2}}$—$s^2p^4(^3P)\,4d\,{}^4P_{1\frac{1}{2}}$ |

TABLE 3.—*Classified lines of the Kr II spectrum in the extreme ultraviolet*—Con.

| Intensity | $\lambda_{air}$ I.A | $\nu_{vac}$ cm$^{-1}$ | Term combination |
|---|---|---|---|
| 0 | 766. 19 | 130, 516 | $s^2p^5.{}^2P^\circ_{1½}$—$s^2p^4(^3P)4d^4P_{0½}$ |
| 3 | 770. 98 | 129, 705 | $s^2p^5.{}^2P^\circ_{1½}$—$s^2p^4(^3P)4d^4F_{2½}$ |
| 3 | 773. 66 | 129, 256 | $s^2p^5.{}^2P^\circ_{0½}$—$s^2p^4(^3P)4d^2P_{1½}$ |
| 5 | 782. 06 | 127, 867 | $s^2p^5.{}^2P^\circ_{1½}$—$s^2p^4(^1D)5s^2D_{2½}$ |
| 3 | 783. 72 | 127, 597 | $s^2p^5.{}^2P^\circ_{0½}$—$s^2p^4(^3P)4d^2P_{0½}$<br>$s^2p^5.{}^2P^\circ_{2½}$—$s^2p^4(^3P)4d^2D_{1½}$<br>$s^2p^5.{}^2P^\circ_{1½}$—$s^2p^4(^1D)5s^2D_{1½}$ |
| 1 | 799. 10 | 125, 139 | $s^2p^5.{}^2P^\circ_{0½}$—$s^2p^4(^3P)4d.{}^4P_{0½}$ |
| 5 | 818. 11 | 122, 233 | $s^2p^5.{}^2P^\circ_{2½}$—$s^2p^4(^1D)5s.{}^2D_{1½}$ |
| 2 | 821. 11 | 121, 786 | $s^2p^5.{}^2P^\circ_{1½}$—$s^2p^4(^3P)4d^4D_{0½}$ |
| 3 | 826. 40 | 121, 007 | $s^2p^5.{}^2P^\circ_{1½}$—$s^2p^4(^3P)5s^2P_{0½}$<br>$s^2p^5.{}^2P^\circ_{1½}$—$s^2p^4(^3P)4d^4D_{1½}$ |
| 4 | 830. 36 | 120, 430 | $s^2p^5.{}^2P^\circ_{1½}$—$s^2p^4(^3P)4d^4D_{2½}$ |
| 6 | 844. 06 | 118, 475 | $s^2p^5.{}^2P^\circ_{1½}$—$s^2p^4(^3P)5s^2P_{1½}$ |
| 2 | 850. 31 | 117, 604 | $s^2p^5.{}^2P^\circ_{1½}$—$s^2p^4(^3P)5s^4P_{0½}$ |
| 4 | 859. 04 | 116, 409 | $s^2p^5.{}^2P^\circ_{2½}$—$s^2p^4(^3P)4d^4D_{0½}$ |
| 5 | 864. 78 | 115, 636 | $s^2p^5.{}^2P^\circ_{0½}$—$s^2p^4(^3P)5s^2P_{0½}$<br>$s^2p^5.{}^2P^\circ_{0½}$—$s^2p^4(^3P)4d^4D_{1½}$ |
| 4 | 868. 85 | 115, 095 | $s^2p^5.{}^2P^\circ_{1½}$—$s^2p^4(^3P)5s^4P_{1½}$ |
| 2 | 884. 13 | 113, 106 | $s^2p^5.{}^2P^\circ_{0½}$—$s^2p^4(^3P)5s^2P_{1½}$ |
| 8 | 886. 29 | 112, 830 | $s^2p^5.{}^2P^\circ_{1½}$—$s^2p^4(^3P)5s^4P_{2½}$ |
| 6 | 890. 99 | 112, 235 | $s^2p^5.{}^2P^\circ_{2½}$—$s^2p^4(^3P)5s^4P_{0½}$ |
| 3 | 911. 39 | 109, 722 | $s^2p^5.{}^2P^\circ_{0½}$—$s^2p^4(^3P)5s^4P_{1½}$ |
| 7 | 917. 40 | 109, 004 | $s^2p^5.{}^2P^\circ_{1½}$—$sp^6.{}^2S_{0½}$ |
| 12 | 964. 93 | 103, 634 | $s^2p^5.{}^2P^\circ_{0½}$—$sp^6.{}^2S_{0½}$ |

TABLE 4.—*The first spark spectrum of krypton (Kr II)*

| Intensity and character | $\lambda_{air}$ I.A. | $\nu_{vac}$ cm$^{-1}$ | Term combination | Zeeman effect | |
|---|---|---|---|---|---|
| | | | | Observed | Computed |
| 1 | 2, 080. 53 | 48, 049. 30 | $s^2p^4(^3P)4d^4D_{3½}$–$s^2p^4(^3P)5f^2F^\circ_{3½}$ | | |
| 2 | 2, 082. 60 | 48, 001. 55 | | | |
| 1– | 2, 083. 87 | 47, 972. 30 | $s^2p^4(^3P)4d^4D_{2½}$–$s^2p^4(^3P)5f^4F^\circ_{3½}$ | | |
| 1 | 2, 084. 54 | 956. 88 | $s^2p^4(^3P)4d^4D_{2½}$–$s^2p^4(^3P)5f^4F^\circ_{2½}$ | | |
| 5 | 2, 086. 73 | 906. 56 | $s^2p^4(^3P)4d^4D_{3½}$–$s^2p^4(^3P)5f^4F^\circ_{3½}$ | | |
| 20 | 2, 088. 16 | 873. 75 | $s^2p^4(^3P)4d^4D_{3½}$–$s^2p^4(^3P)5f^4F^\circ_{4½}$ | | |
| 3 | 2, 093. 37 | 754. 62 | $s^2p^4(^3P)4d^4D_{2½}$–$s^2p^4(^3P)5f^4F^\circ_{3½}$ | | |
| 1 | 2, 095. 02 | 717. 02 | $s^2p^4(^3P)4d^4D_{1½}$–$s^2p^4(^3P)5f^4D^\circ_{2½}$ | | |
| 15 | 2, 096. 24 | 689. 25 | $s^2p^4(^3P)4d^4D_{2½}$–$s^2p^4(^3P)5f^4F^\circ_{4½}$ | | |
| 1h– | 2, 098. 97 | 627. 23 | $s^2p^4(^3P)4d^4D_{1½}$–$s^2p^4(^3P)5f^2D^\circ_{1½}$ | | |
| 5 | 2, 109. 81 | 382. 56 | $s^2p^4(^3P)4d^4D_{1½}$—$s^2p^4(^3P)5f^4F^\circ_{2½}$ | | |
| 1 | 2, 116. 00 | 243. 96 | | | |
| 12 | 2, 118. 83 | 180. 87 | $s^2p^4(^3P)4d^4D_{1½}$—$s^2p^4(^3P)5f^4F^\circ_{3½}$ | | |
| 1 | 2, 123. 22 | 083. 33 | | | |
| 3 | 2, 123. 48 | 077. 57 | | | |
| 2 | 2, 125. 56 | 47, 031. 51 | | | |
| 1 | 2, 129. 75 | 46, 938. 98 | | | |
| 1 | 2, 129. 80 | 937. 88 | $s^2p^4(^3P)4d^4D_{0½}$—$s^2p^4(^3P)5f^4D^\circ_{0½}$ | | |
| 1 | 2, 130. 26 | 927. 75 | | | |
| {2 | 2, 130. 43 | 924. 01 | | | |
| {2 | 2, 130. 55 | 921. 35 | | | |
| 1 | 2, 131. 16 | 907. 94 | | | |
| 1 | 2, 132. 86 | 870. 55 | | | |
| 2 | 2, 133. 85 | 848. 81 | $s^2p^4(^3P)4d^4D_{0½}$—$s^2p^4(^3P)5f^2D^\circ_{1½}$ | | |
| 1 | 2, 135. 80 | 806. 04 | | | |
| 1 | 2, 138. 70 | 742. 58 | | | |

TABLE 4.—*The first spark spectrum of krypton (Kr II)*—Continued

| Intensity and character | $\lambda_{air}$ I.A. | $\nu_{vac}$ cm$^{-1}$ | Term combination | Zeeman effect | |
|---|---|---|---|---|---|
| | | | | Observed | Computed |
| 1h− | 2, 140. 27 | 708. 30 | $s^2p^4(^3P)4d\,^4D_{0½}$—29691.33 | | |
| 1 | 2, 142. 49 | 659. 91 | | | |
| 1 | 2, 142. 97 | 649. 46 | | | |
| 10 | 2, 145. 08 | 603. 57 | $s^2p^4(^3P)4d\,^4D_{0½}$—$s^2p^4(^3P)5f\,^4F_{1½}$ | | |
| 1 | 2, 148. 03 | 539. 58 | | | |
| 2 | 2, 148. 58 | 527. 67 | | | |
| 1 | 2, 149. 70 | 503. 43 | | | |
| 1− | 2, 149. 86 | 499. 97 | | | |
| 1− | 2, 150. 68 | 482. 24 | | | |
| 1 | 2, 155. 38 | 380. 89 | | | |
| 1 | 2, 158. 43 | 315. 36 | | | |
| 2h | 2, 159. 02 | 302. 71 | | | |
| 3 | 2, 162. 50 | 228. 20 | | | |
| 1− | 2, 163. 41 | 208. 76 | | | |
| 4h | 2, 164. 38 | 188. 05 | | | |
| 1 | 2, 165. 63 | 161. 40 | | | |
| 1 | 2, 169. 02 | 089. 26 | | | |
| 2 | 2, 170. 83 | 050. 84 | | | |
| 1 | 2, 172. 25 | 46, 020. 73 | | | |
| 1h− | 2, 173. 78 | 45, 988. 35 | | | |
| 1 | 2, 175. 35 | 955. 16 | | | |
| 1 | 2, 175. 99 | 941. 64 | | | |
| 3h | 2, 177. 79 | 903. 68 | | | |
| 1h | 2, 179. 56 | 866. 41 | | | |
| 1 | 2, 180. 91 | 838. 02 | | | |
| 1− | 2, 182. 13 | 812. 39 | | | |
| 1 | 2, 183. 71 | 779. 25 | | | |
| 4 | 2, 185. 52 | 741. 34 | | | |
| 1 | 2, 186. 70 | 716. 66 | | | |
| 2 | 2, 191. 91 | 608. 01 | | | |
| 1H+ | 2, 192. 20 | 601. 97 | | | |
| 2 | 2, 197. 25 | 497. 18 | | | |
| 1H+ | 2, 197. 53 | 491. 38 | | | |
| 2 | 2, 199. 17 | 457. 46 | | | |
| 1h− | 2, 202. 43 | 390. 18 | | | |
| 1− | 2, 202. 92 | 380. 09 | | | |
| 1 | 2, 205. 34 | 330. 30 | | | |
| 1 | 2, 208. 41 | 267. 28 | $s^2p^4(^1D)5s^2D_{2½}$—$s^2p^4(^1D)5f\,^2F^1_{3½}$ | | |
| 5 | 2, 211. 71 | 199. 75 | $s^2p^4(^3P)4d\,^2F_{2½}$—$s^2p^4(^1D)5f\,^2F^2_{3½}$ | | |
| 6 | 2, 212. 29 | 187. 90 | | | |
| 5 | 2, 212. 96 | 174. 22 | $s^2p^4(^1D)5s^2D_{1½}$—$s^2p^4(^1D)5f\,^2D^2_{2½}$ | | |
| 2 | 2, 215. 60 | 120. 40 | | | |
| 1 | 2, 215. 88 | 114. 70 | | | |
| 1 | 2, 218. 40 | 063. 46 | | | |
| 1− | 2, 219. 14 | 45, 048. 45 | | | |
| 1− | 2, 221. 86 | 44, 993. 29 | | | |
| 1 | 2, 223. 50 | 960. 11 | | | |
| 1 | 2, 224. 06 | 948. 79 | | | |
| 1− | 2, 224. 71 | 935. 66 | | | |
| 2 | 2, 225. 18 | 926. 17 | | | |
| 30 | 2, 227. 92 | 870. 92 | $s^2p^4(^1D)5s^2D_{2½}$—25447. 85 | | |
| 1 | 2, 230. 69 | 815. 21 | | | |
| 1 | 2, 232. 01 | 788. 71 | | | |
| 1 | 2, 232. 32 | 782. 49 | | | |
| 1 | 2, 232. 98 | 769. 25 | | | |
| 1 | 2, 233. 77 | 753. 42 | | | |
| 2 | 2, 234. 34 | 742. 01 | | | |
| 2 | 2, 236. 43 | 700. 20 | | | |
| 4 | 2, 237. 15 | 685. 81 | | | |
| 2 | 2, 240. 89 | 611. 24 | | | |
| 1 | 2, 244. 24 | 544. 65 | | | |
| 10 | 2, 245. 39 | 521. 85 | | | |
| 8 | 2, 250. 32 | 44, 424. 32 | | | |
| 1 | 72. 55 | 43, 989. 80 | $s^2p^4(^3P)4d\,^4F_{3½}$—$s^2p^4(^1D)5f\,^2F^1_{3½}$ | | |
| 8 | 73. 24 | 976. 46 | | | |

TABLE 4.—*The first spark spectrum of krypton (Kr II)*—Continued

| Intensity and character | $\lambda_{air}$ I.A. | $\nu_{vac}$ cm$^{-1}$ | Term combination | Zeeman effect | |
|---|---|---|---|---|---|
| | | | | Observed | Computed |
| 30 | 83.07 | 787.13 | | | |
| 30 | 22, 87.79 | 696.80 | $s^2p^4(^1D)5s^3D_{2\frac{1}{2}}$–26622.00 | | |
| 6 | 23, 00.38 | 457.67 | $s^2p^4(^3P)4d^4F_{3\frac{1}{2}}$–$s^2p^4(^1D)5f^2F^0_{3\frac{1}{2}}$ | | |
| 6 | 01.73 | 432.18 | $s^2p^4(^3P)4d^4F_{2\frac{1}{2}}$–$s^2p^4(^1D)5f^2F^0_{2\frac{1}{2}}$ | | |
| 3 | 02.67 | 414.46 | $s^2p^4(^3P)4d^4F_{1\frac{1}{2}}$–$s^2p^4(^1D)5f^2F^0_{2\frac{1}{2}}$ | | |
| 6 | 12.00 | 239.27 | $sp^{6\,2}S_{0\frac{1}{2}}$–$s^2p^4(^1D)5p^2P^0_{1\frac{1}{2}}$ | | |
| 6 | 14.24 | 197.42 | | | |
| 8 | 15.52 | 173.55 | $s^2p^4(^3P)4d^4P_{0\frac{1}{2}}$–$s^2p^4(^1D)5f^2P^0_{1\frac{1}{2}}$ | | |
| 10 | 16.32 | 43, 158.64 | | | |
| 10 | 44.38 | 42, 642.12 | $s^2p^4(^3P)4d^4P_{0\frac{1}{2}}$–$s^2p^4(^1D)5f^2F^0_{1\frac{1}{2}}$ | | |
| 2 | 52.86 | 488.44 | $s^2p^4(^3P)4d^4F_{4\frac{1}{2}}$—29,691.33 | | |
| 50 | 53.68 | 473.64 | | | |
| 6 | 62.74 | 310.79 | $s^2p^4(^3P)4d^4P_{2\frac{1}{2}}$—$s^2p^4(^1D)5f^2P^0_{1\frac{1}{2}}$ | | |
| 3 | 65.52 | 261.07 | $s^2p^4(^3P)4d^4P_{1\frac{1}{2}}$—$s^2p^4(^1D)5f^2F^0_{2\frac{1}{2}}$ | | |
| 3 | 68.94 | 200.07 | $s^2p^4(^3P)4d^4P_{0\frac{1}{2}}$—$s^2p^4(^1D)5f^2D^0_{1\frac{1}{2}}$ | | |
| 4 | 73.68 | 115.80 | $s^2p^4(^3P)4d^4F_{4\frac{1}{2}}$—$s^2p^4(^3P)5f^4F^0_{3\frac{1}{2}}$ | | |
| 20 | 75.52 | 42, 083.19 | $s^2p^4(^3P)4d^4F_{4\frac{1}{2}}$—$s^2p^4(^3P)5f^4F^0_{4\frac{1}{2}}$ | | |
| 4 | 90.50 | 41, 819.50 | $s^2p^4(^1P)5s^3P_{1\frac{1}{2}}$—$s^2p^4(^1D)5f^2D^0_{1\frac{1}{2}}$ | | |
| 10 | 2, 392.78 | 779.65 | $s^2p^4(^1P)4d^4P_{2\frac{1}{2}}$—$s^2p^4(^1D)5f^2F^0_{2\frac{1}{2}}$ | | |
| 5h | 2, 408.52 | 506.64 | | | |
| 5 | 9.06 | 497.33 | $s^2p^4(^3P)4d^2F_{2\frac{1}{2}}$—$s^2p^4(^1D)5f^2F^0_{2\frac{1}{2}}$ | | |
| 10h | 13.81 | 415.68 | | | |
| 10 | 14.89 | 397.16 | | | |
| 2 | 2, 414.94 | 41, 396.31 | $s^2p^4(^3P)4d^4P_{2\frac{1}{2}}$—$s^2p^4(^1D)5f^2D^0_{2\frac{1}{2}}$ | | |
| 4 | 18.41 | 336.91 | | | |
| 10 | 26.36 | 201.48 | $sp^{5\,2}S^0_{0\frac{1}{2}}$—$s^2p^4(^1D)5p^2P^0_{1\frac{1}{2}}$ | | |
| 20 | 28.35 | 167.72 | | | |
| 8 | 32.74 | 41, 093.44 | | | |
| 8 | 46.44 | 40, 863.34 | $s^2p^4(^1D)5s^2D_{1\frac{1}{2}}$—$s^2p^4(^2P)5f^2F^0_{2\frac{1}{2}}$ | | |
| 2 | 55.04 | 720.20 | $s^2p^4(^2P)4d^2D_{1\frac{1}{2}}$—$s^2p^4(^1D)5f^2P^0_{1\frac{1}{2}}$ | | |
| 2 | 55.31 | 715.72 | 65,209.50—$s^2p^4(^1D)5f^2P^0_{1\frac{1}{2}}$ | | |
| 6 | 56.07 | 703.13 | | | |
| 2 | 62.33 | 599.65 | $s^2p^4(^1D)5s^2D_{2\frac{1}{2}}$—$s^2p^4(^3P)5f^2F^0_{3\frac{1}{2}}$ | | |
| 2 | 63.27 | 584.16 | $s^2p^4(^1D)5s^2D_{1\frac{1}{2}}$—$s^2p^4(^3P)5f^4F^0_{2\frac{1}{2}}$ | | |
| 100h | 64.77 | 559.47 | $s^2p^4(^3P)4d^4F_{3\frac{1}{2}}$—29,691.33 | | |
| 10h | 70.45 | 466.22 | | | |
| 2h | 74.69 | 396.89 | $s^2p^4(^1D)5s^2D_{2\frac{1}{2}}$—$s^2p^4(^3P)5f^2F^0_{3\frac{1}{2}}$ | | |
| 3 | 78.85 | 329.10 | $s^2p^4(^3P)4d^4F_{3\frac{1}{2}}$—$s^2p^4(^3P)5f^2F^0_{3\frac{1}{2}}$ | | |
| 2 | 83.57 | 252.47 | | | |
| 1 | 83.62 | 251.66 | $s^2p^4(^3P)4d^4F_{3\frac{1}{2}}$—$s^2p^4(^3P)5f^4F^0_{3\frac{1}{2}}$ | | |
| 3 | 87.50 | 188.88 | $s^2p^4(^3P)4d^2D_{1\frac{1}{2}}$—$s^2p^4(^1D)5f^2F^0_{2\frac{1}{2}}$ | | |
| 4 | 87.62 | 186.94 | $s^2p^4(^3P)4d^4F_{1\frac{1}{2}}$—$s^2p^4(^3P)5f^4F^0_{2\frac{1}{2}}$ | | |
| 8h | 89.39 | 158.37 | 65,209.50—$s^2p^4(^1D)5f^2F^0_{2\frac{1}{2}}$ | | |
| 1 | 2, 494.66 | 40, 040.16 | $s^2p^4(^2P)5p^2D^0_{2\frac{1}{2}}$—$s^2p^4(^1D)5d^2D_{1\frac{1}{2}}$ | | |
| 2hl | 2497.42 | 40029.25 | | | |
| 7Hl | 2503.87 | 39926.15 | $s^2p^4(^3P)4d^2F_{3\frac{1}{2}}$—26622.00 | | |
| 5Hl | 06.56 | 883.30 | | | |
| 5 | 10.56 | 819.76 | $s^2p^4(^3P)5p^4D^0_{2\frac{1}{2}}$—$s^2p^4(^1D)5d^2G_{3\frac{1}{2}}$ | | |
| 3 | 11.74 | 801.05 | 65209.50—$s^2p^4(^1D)5f^2D^0_{2\frac{1}{2}}$ | | |
| 1Hl | 13.40 | 774.77 | | | |
| 8 | 17.95 | 702.90 | | | |
| 1h | 25.28 | 587.67 | | | |
| 3hl | 27.16 | 558.22 | | | |
| 1 | 31.73 | 486.82 | $s^2p^4(^3P)5s^4P_{2\frac{1}{2}}$—$s^2p^4(^1D)5p^2D^0_{2\frac{1}{2}}$ | | |
| 5Hl | 38.34 | 384.00 | $s^2p^4(^3P)5p^4P^0_{2\frac{1}{2}}$—$s^2p^4(^3P)7s^4P_{2\frac{1}{2}}$ | | |
| 2 | 50.13 | 201.03 | | | |
| 6 | 55.91 | 113.28 | | | |
| 6 | 56.36 | 106.40 | | | |
| 8h | 59.10 | 064.53 | $s^2p^4(^3P)4d^2P_{1\frac{1}{2}}$—$s^2p^4(^1D)5f^2P^0_{1\frac{1}{2}}$ | | |
| 3hl | 61.94 | 021.23 | $s^2p^4(^3P)5p^4P^0_{1\frac{1}{2}}$—$s^2p^4(^3P)7s^4P_{2\frac{1}{2}}$ | | |
| 1H | 62.04 | 39, 019.71 | $s^2p^4(^3P)4d^4F_{2\frac{1}{2}}$—$s^2p^4(^3P)5f^4D^0_{1\frac{1}{2}}$ | | |
| 1h | 66.61 | 38, 950.23 | $s^2p^4(^2P)5p^2P^0_{1\frac{1}{2}}$—$s^2p^4(^3P)7s^4P^0_{1\frac{1}{2}}$ | | |
| 10h | 72.03 | 868.16 | | | |
| 2H | 74.25 | 834.64 | | | |
| 2 | 78.98 | 763.42 | $s^2p^4(^3P)4d^4F_{3\frac{1}{2}}$—$s^2p^4(^3P)5f^2F^0_{3\frac{1}{2}}$ | | |

TABLE 4.—*The first spark spectrum of krypton (Kr II)*—Continued

| Intensity and character | $\lambda_{air}$ I.A. | $\nu_{vac}$ cm$^{-1}$ | Term combination | Zeeman effect | |
|---|---|---|---|---|---|
| | | | | Observed | Computed |
| 2 | 80.12 | 746.30 | | | |
| 5H*l* | 81.74 | 721.99 | | | |
| 3*h* | 84.15 | 685.87 | $s^2p^4(^3P)4d^4F_{3\frac{1}{2}}$—$s^2p^4(^3P)5f^4F^0_{1\frac{1}{2}}$ | | |
| 30 | 89.08 | 612.22 | | | |
| 2h | 90.74 | 587.48 | $s^2p^4(^3P)4d^2D_{2\frac{1}{2}}$—$s^2p^4(^1D)5f^2F^0_{2\frac{1}{2}}$ | | |
| 1*h* | 91.25 | 579.88 | $s^2p^4(^3P)5p^2P^0_{0\frac{1}{2}}$—$s^2p^4(^1D)5d^2P_{1\frac{1}{2}}$ | | |
| 60 | 92.48 | 561.58 | $s^2p^4(^3P)4d^4F_{3\frac{1}{2}}$—$s^2p^4(^3P)5f^2F^0_{3\frac{1}{2}}$ | | |
| 4 | 94.40 | 533.04 | $s^2p^4(^3P)4d^2F_{1\frac{1}{2}}$—$s^2p^4(^1D)5f^2F^0_{1\frac{1}{2}}$ | | |
| 4H | 95.36 | 518.79 | $s^2p^4(^3P)4d^4F_{1\frac{1}{2}}$—$s^2p^4(^1S)5p^2P^0_{0\frac{1}{2}}$ | | |
| 5H | 96.73 | 498.47 | | | |
| 7 | 2,597.73 | 483.95 | $s^2p^4(^3P)4d^4F_{3\frac{1}{2}}$—$s^2p^4(^3P)5f^4F^0_{3\frac{1}{2}}$ | | |
| 7 | 02.11 | 418.88 | $s^2p^4(^3P)4d^4F_{3\frac{1}{2}}$—$s^2p^4(^3P)5f^4F^0_{4\frac{1}{2}}$ | | |
| 1H*l* | 05.41 | 370.22 | $s^2p^4(^3P)5p^2P^0_{1\frac{1}{2}}$—$s^2p^4(^3P)7s^2P^0_{1\frac{1}{2}}$ | | |
| 1*h* | 2,610.76 | 38,291.60 | $s^2p^4(^1D)5s^2D_{2\frac{1}{2}}$—32,026.50 | | |
| 10*h* | 2,610.98 | 38,288.37 | | | |
| 10*h* | 2,616.71 | 38,204.54 | $s^2p^4(^3P)4d^2D_{2\frac{1}{2}}$—$s^2p^4(^1D)5f^2D^0_{3\frac{1}{2}}$<br>$s^2p^4(^3P)4d^4P_{0\frac{1}{2}}$—$s^2p^4(^3P)5f^4D^0_{1\frac{1}{2}}$ | | |
| 40*h* | 20.44 | 150.16 | $s^2p^4(^3P)4d^2D_{1\frac{1}{2}}$—$s^2p^4(^1D)5f^2D^0_{2\frac{1}{2}}$ | | |
| 6*h* | 20.65 | 147.10 | | | |
| 2 | 22.82 | 115.54 | $s^2p^4(^3P)4d^4P_{0\frac{1}{2}}$—$s^2p^4(^3P)5f^2D^0_{1\frac{1}{2}}$ | | |
| 1 | 23.11 | 111.33 | | | |
| 6H*l* | 24.78 | 087.08 | | | |
| 3H | 27.22 | 051.71 | | | |
| 7 | 27.75 | 38,044.04 | $s^2p^4(^3P)5p^4P^0_{2\frac{1}{2}}$—$s^2p^4(^1S)4d^2D_{2\frac{1}{2}}$<br>$s^2p^4(^3P)4d^4P_{1\frac{1}{2}}$—$s^2p^4(^1S)5p^2P^0_{1\frac{1}{2}}$ | | |
| 6*h* | 34.41 | 37,947.86 | $s^2p^4(^3P)4d^4P_{0\frac{1}{2}}$—$s^2p^4(^3P)5f^4F^0_{1\frac{1}{2}}$ | | |
| 3*hl* | 36.51 | 917.64 | $s^2p^4(^3P)5p^2P^0_{1\frac{1}{2}}$—$s^2p^4(^3P)7s^4P_{0\frac{1}{2}}$ | | |
| 2*h* | 38.32 | 891.63 | $s^2p^4(^3P)5p^4D^0_{0\frac{1}{2}}$—$s^2p^4(^3P)7s^4P_{0\frac{1}{2}}$ | | |
| 2*hl* | 40.74 | 856.91 | $s^2p^4(^3P)5p^4P^0_{2\frac{1}{2}}$—$s^2p^4(^3P)7s^4P_{1\frac{1}{2}}$ | | |
| 4*hl* | 42.08 | 837.71 | $s^2p^4(^3P)5p^2D^0_{2\frac{1}{2}}$—$s^2p^4(^3P)7s^2P_{1\frac{1}{2}}$ | | |
| 20*h* | 43.06 | 823.68 | $s^2p^4(^3P)4d^4P_{1\frac{1}{2}}$—$s^2p^4(^3P)5f^4D^0_{1\frac{1}{2}}$ | | |
| 20*h* | 48.15 | 750.99 | | | |
| 20 | 49.27 | 735.02 | $s^2p^4(^3P)4d^4P_{1\frac{1}{2}}$—$s^2p^4(^3P)5f^2D^0_{1\frac{1}{2}}$ | | |
| 4H*l* | 49.67 | 729.33 | $s^2p^4(^3P)5p^2D^0_{1\frac{1}{2}}$—$s^2p^4(^1D)5d^2D_{1\frac{1}{2}}$ | | |
| 6 | 53.95 | 668.49 | $s^2p^4(^3P)4d^4P_{0\frac{1}{2}}$—$s^2p^4(^3P)5f^4F^0_{1\frac{1}{2}}$ | | |
| 15*h* | 56.38 | 634.03 | | | |
| 2H*l* | 59.60 | 588.47 | $s^2p^4(^3P)5p^2D^0_{2\frac{1}{2}}$—$s^2p^4(^1D)5d^2F_{2\frac{1}{2}}$ | | |
| 8*hl* | 60.97 | 569.12 | $s^2p^4(^3P)5p^4D^0_{1\frac{1}{2}}$—$s^2p^4(^3P)7s^4P_{1\frac{1}{2}}$ | | |
| 1 | 61.22 | 565.45 | $s^2p^4(^3P)4d^4P_{1\frac{1}{2}}$—$s^2p^4(^3P)5f^2F^0_{2\frac{1}{2}}$<br>$s^2p^4(^3P)5p^2D^0_{2\frac{1}{2}}$—$s^2p^4(^1D)5d^2P_{1\frac{1}{2}}$ | | |
| 5 | 61.47 | 562.06 | $s^2p^4(^3P)4d^4P_{2\frac{1}{2}}$—$s^2p^4(^1S)5p^2P^0_{1\frac{1}{2}}$ | | |
| 2*hl* | 62.57 | 546.54 | $s^2p^4(^3P)5p^2P^0_{1\frac{1}{2}}$—$s^2p^4(^1D)5d^2P_{1\frac{1}{2}}$ | | |
| 8 | 64.00 | 526.39 | $s^2p^4(^3P)5p^4P^0_{1\frac{1}{2}}$—$s^2p^4(^3P)7s^4P_{2\frac{1}{2}}$ | | |
| 4 | 64.37 | 521.18 | $s^2p^4(^3P)5p^4D^0_{0\frac{1}{2}}$—$s^2p^4(^1D)5d^2P_{1\frac{1}{2}}$ | | |
| 6*h* | 66.61 | 489.66 | $s^2p^4(^3P)4d^4P_{1\frac{1}{2}}$—$s^2p^4(^3P)5f^4F^0_{1\frac{1}{2}}$ | | |
| 3 | 72.79 | 402.99 | $s^2p^4(^3P)4d^2F_{2\frac{1}{2}}$—$s^2p^4(^1D)5f^2D^0_{2\frac{1}{2}}$ | | |
| 4*h* | 75.31 | 367.76 | $s^2p^4(^3P)4d^4P_{1\frac{1}{2}}$—$s^2p^4(^1S)5p^2P^0_{1\frac{1}{2}}$ | | |
| 6 | 77.20 | 341.38 | $s^2p^4(^3P)4d^4P_{2\frac{1}{2}}$—$s^2p^4(^3P)5f^4D^0_{1\frac{1}{2}}$ | | |
| 15 | 83.55 | 253.02 | $s^2p^4(^3P)4d^4P_{2\frac{1}{2}}$—$s^2p^4(^3P)5f^2D^0_{1\frac{1}{2}}$ | | |
| 1 | 85.79 | 221.96 | | | |
| 4*h* | 88.37 | 186.24 | | | |
| 2 | 91.20 | 147.14 | $s^2p^4(^3P)5s^4P_{1\frac{1}{2}}$—$s^2p^4(^1D)5p^2P^0_{0\frac{1}{2}}$ | | |
| 30*h* | 2,695.70 | 085.13 | $s^2p^4(^3P)4d^4P_{2\frac{1}{2}}$—$s^2p^4(^3P)5f^2F^0_{2\frac{1}{2}}$ | | |
| 3*h* | 2,700.60 | 017.84 | | | |
| 15*h* | 2,701.34 | 37,007.70 | $s^2p^4(^3P)5p^2P^0_{0\frac{1}{2}}$—$s^2p^4(^1D)5d^2D_{1\frac{1}{2}}$<br>$s^2p^4(^3P)4d^4P_{2\frac{1}{2}}$—$s^2p^4(^3P)5f^4F^0_{1\frac{1}{2}}$ | | |
| 3 | 10.27 | 36,885.78 | $s^2p^4(^3P)4d^4P_{2\frac{1}{2}}$—$s^2p^4(^1S)5p^2P^0_{0\frac{1}{2}}$ | | |
| 2 | 11.11 | 874.35 | $s^2p^4(^3P)5s^4P_{2\frac{1}{2}}$—$s^2p^4(^1D)5p^4F^0_{3\frac{1}{2}}$ | | |
| 80*h* | 12.40 | 856.81 | $s^2p^4(^3P)4d^2F_{2\frac{1}{2}}$—29,691.33 | | |
| 3*h* | 14.49 | 828.44 | $s^2p^4(^3P)4d^2F_{2\frac{1}{2}}$—$s^2p^4(^3P)5f^2F^0_{2\frac{1}{2}}$ | | |
| 10*h* | 16.16 | 805.79 | $s^2p^4(^3P)4d^4P_{2\frac{1}{2}}$—$s^2p^4(^3P)5f^4F^0_{2\frac{1}{2}}$ | | |
| 1H | 17.18 | 791.98 | $s^2p^4(^3P)5p^2D^0_{1\frac{1}{2}}$—$s^2p^4(^1D)5d^2P_{0\frac{1}{2}}$ | | |
| 1*h* | 17.70 | 784.94 | $s^2p^4(^3P)5p^4S^0_{1\frac{1}{2}}$—$s^2p^4(^3P)7s^2P_{0\frac{1}{2}}$ | | |
| 5H*l* | 19.90 | 755.19 | | | |

TABLE 4.—*The first spark spectrum of krypton (Kr II)*—Continued

| Intensity and character | $\lambda_{air}$ I.A. | $\nu_{vac}$ cm$^{-1}$ | Term combination | Zeeman effect | |
|---|---|---|---|---|---|
| | | | | Observed | Computed |
| 30h | 29.46 | 626.46 | $s^2p^4(^3P)4d^2F_{3½}-s^2p^4(^3P)5f^2F^0_{3½}$ | | |
| 4h | 32.33 | 587.99 | $s^2p^4(^3P)4d^2F_{3½}-s^2p^4(^1D)5f^2F^0_{3½}$ | | |
| 50 | 33.26 | 575.54 | | | |
| 1Hr | 38.13 | 510.49 | $s^2p^4(^3P)5p^2D^0_{1½}-s^2p^4(^3P)7s^2P_{0½}$ | | |
| 1 | 40.11 | 484.11 | $s^2p^4(^3P)4d^2F_{3½}-s^2p^4(^3P)5f^4F^0_{3½}$ | | |
| 40 | 42.56 | 451.52 | $s^2p^4(^3P)4d^2F_{3½}-s^2p^4(^3P)5f^4F^0_{3½}$ | | |
| 1H | 44.64 | 423.90 | $s^2p^4(^3P)5p^2S^0_{½}-s^2p^4(^1D)5d^2P_{0½}$ | | |
| 15 | 46.31 | 401.75 | $s^2p^4(^3P)4d^4P_{0½}-s^2p^4(^3P)5f^4F^0_{½}$ | | |
| 2Hl | 47.41 | 387.18 | | | |
| 5Hl | 51.59 | 331.90 | $s^2p^4(^3P)5p^4S^0_{1½}-s^2p^4(^3P)7s^4P_{0½}$ | | |
| 4Hl | 59.02 | 234.07 | $s^2p^4(^3P)5p^4S^0_{1½}-s^2p^4(^3P)7s^2P_{1½}$ | | |
| 1h | 67.59 | 121.87 | | | |
| 10h | 72.60 | 056.60 | $s^2p^4(^3P)4d^2F_{3½}-s^2p^4(^1D)5f^2F^0_{3½}$ | | |
| 3 | 74.59 | 36,030.75 | $s^2p^4(^3P)4d^2F_{3½}-s^2p^4(^1D)5f^2F^0_{3½}$ | | |
| 1— | 77.96 | 35,987.04 | $s^2p^4(^3P)5p^4S^0_{1½}-s^2p^4(^1D)5d^2F_{3½}$ | | |
| 2 | 78.99 | 973.70 | $s^2p^4(^3P)5p^2P^0_{1½}-s^2p^4(^1D)5d^2D_{1½}$ | | |
| 20 | 79.11 | 972.15 | $s^2p^4(^3P)4d^2D_{1½}-s^2p^4(^1S)5p^2P^0_{1½}$ | | |
| 4 | 79.51 | 966.97 | $65,209.50-s^2p^4(^1S)5p^2P^0_{1½}$ | | |
| 1Hl | 79.97 | 961.02 | $\begin{cases} s^2p^4(^3P)5p^4S^0_{1½}-s^2p^4(^1D)5d^2P_{1½} \\ s^2p^4(^3P)5p^2D^0_{1½}-s^2p^4(^3P)7s^2P_{1½} \end{cases}$ | | |
| 3Hl | 89.83 | 833.93 | | | |
| 80h | 95.81 | 757.29 | | | |
| 2 | 2,796.26 | 751.53 | $s^2p^4(^3P)4d^2D_{1½}-s^2p^4(^3P)5f^4D^0_{1½}$ | | |
| 2Hl | 2,800.98 | 691.31 | $s^2p^4(^3P)5p^2S^0_{½}-s^2p^4(^3P)7s^4P_{0½}$ | | |
| 2Hl | 2,801.23 | 688.11 | $s^2p^4(^3P)5p^2D^0_{1½}-s^2p^4(^1D)5d^2P_{1½}$ | | |
| 20h | 03.20 | 663.03 | $s^2p^4(^3P)4d^2D_{1½}-s^2p^4(^3P)5f^2D^0_{1½}$ | | |
| 4h | 03.60 | 657.94 | $65,209.50-s^2p^4(^3P)5f^2D^0_{1½}$ | | |
| 1h | 07.07 | 613.87 | | | |
| 1h | 08.72 | 592.94 | $s^2p^4(^3P)5p^2S^0_{½}-s^2p^4(^3P)7s^2P_{1½}$ | | |
| 60 | 16.46 | 495.14 | $s^2p^4(^3P)4d^2D_{1½}-s^2p^4(^3P)5f^2F^0_{2½}$ | | |
| 30 | 16.87 | 489.97 | $65,209.50-s^2p^4(^3P)5f^2F^0_{2½}$ | | |
| 5 | 22.63 | 417.55 | $\begin{cases} s^2p^4(^3P)4d^2D_{1½}-s^2p^4(^3P)5f^4F^0_{1½} \\ s^2p^4(^3P)5p^4P^0_{1½}-s^2p^4(^3P)5d^2D_{1½} \end{cases}$ | | |
| 2h | 23.03 | 412.53 | $65,209.50-s^2p^4(^3P)5f^4F^0_{1½}$ | | |
| 3hl | 30.43 | 319.95 | $s^2p^4(^3P)5p^2S^0_{½}-s^2p^4(^1D)5d^2P_{1½}$ | | |
| 2 | 32.39 | 295.51 | $s^2p^4(^3P)4d^2D_{1½}-s^2p^4(^1S)5p^2P^0_{½}$ | | |
| 100 | 2,833.00 | 35,287.91 | $65,209.50-s^2p^4(^3P)5f^2F^0_{1½}$ | | |
| 8hl | 2,835.35 | 35,258.66 | $s^2p^4(^3P)5p^4D^0_{1½}-s^2p^4(^3P)7s^4P_{1½}$ | | |
| 20 | 38.79 | 215.94 | $s^2p^4(^3P)4d^2D_{1½}-s^2p^4(^3P)5f^4F^0_{½}$ | | |
| 2 | 39.20 | 210.86 | $65,209.50-s^2p^4(^3P)5f^4F^0_{1½}$ | | |
| 20 | 44.46 | 145.75 | $65,209.50-s^2p^4(^3P)5f^4F^0_{1½}$ | | |
| 25h | 47.36 | 109.96 | $s^2p^4(^3P)5s^4P_{1½}-s^2p^4(^1D)5p^2P^0_{1½}$ | | |
| 1H | 49.38 | 35,085.07 | | | |
| 2Hl | 62.17 | 34,928.29 | $s^2p^4(^3P)5p^4D^0_{1½}-s^2p^4(^3P)7s^4P_{2½}$ | | |
| 4Hl | 73.72 | 787.92 | $s^2p^4(^3P)5p^4P^0_{½}-s^2p^4(^1D)6s^2D_{1½}$ | | |
| 2h | 75.71 | 763.84 | | | |
| 1Hl | 77.16 | 746.33 | | | |
| 2 | 84.21 | 661.40 | $59,686.98-s^2p^4(^1D)5f^2F^0_{2½}$ | | |
| 2Hl | 94.63 | 536.63 | $s^2p^4(^3P)5p^2P^0_{½}-s^2p^4(^3P)7s^4P_{1½}$ | | |
| 1h | 2,895.92 | 521.25 | $s^2p^4(^3P)4d^2F_{3½}-32,026.50$ | | |
| 1h | 2,907.15 | 387.90 | $s^2p^4(^3P)5p^2S^0_{½}-s^2p^4(^1D)5d^2D_{1½}$ | | |
| 5 | 08.62 | 370.52 | $s^2p^4(^3P)4d^2D_{1½}-s^2p^4(^1S)5p^2P^0_{1½}$ | | |
| 4 | 13.23 | 316.14 | $s^2p^4(^3P)4d^2P_{1½}-s^2p^4(^1S)5p^2P^0_{1½}$ | | |
| 2Hl | 19.07 | 247.48 | | | |
| 4Hl | 21.92 | 214.08 | | | |
| 2Hl | 30.40 | 115.08 | $s^2p^4(^3P)5p^2D^0_{1½}-s^2p^4(^1D)5d^2D_{1½}$ | | |
| 1 | 32.06 | 095.76 | $s^2p^4(^3P)4d^2P_{1½}-s^2p^4(^3P)5f^4D^0_{1½}$ | | |
| 2 | 39.70 | 34,007.16 | $s^2p^4(^3P)4d^2P_{1½}-s^2p^4(^2P)5f^2D^0_{1½}$ | | |
| 15h | 49.54 | 33,893.71 | $s^2p^4(^3P)4d^2D_{2½}-s^2p^4(^3P)5f^2F^0_{2½}$ | | |
| 30h | 50.21 | 886.02 | | | |
| 1Hl | 51.25 | 874.08 | | | |
| 12h | 54.28 | 839.33 | $\begin{cases} s^2p^4(^3P)4d^2P_{1½}-s^2p^4(^3P)5f^2F^0_{2½} \\ s^2p^4(^3P)5s^2P_{1½}-s^2p^4(^1D)5p^2D^0_{2½} \end{cases}$ | | |
| 3h | 56.30 | 816.21 | $s^2p^4(^3P)4d^2D_{2½}-s^2p^4(^3P)5f^4F^0_{½}$ | | |
| 20H | 58.35 | 792.78 | $s^2p^4(^1D)4d^2D_{2½}-14,873.45$ | | |

TABLE 4.—*The first spark spectrum of krypton (Kr II)*—Continued

| Intensity and character | $\lambda_{air}$ I.A. | $\nu_{vac}$ cm$^{-1}$ | Term combination | Zeeman effect | |
|---|---|---|---|---|---|
| | | | | Observed | Computed |
| 40H | 60. 14 | 772. 33 | | | |
| 5 | 60. 78 | 765. 05 | $s^2p^4(^3P)5s^2P_{1½}$–$s^2p^4(^1D)5p^2P^0_{0½}$ | | |
| 4 | 61. 05 | 761. 97 | $s^2p^4(^3P)4d^2P_{1½}$–$s^2p^4(^3P)5f^4F^0_{1½}$ | | |
| 2 | 63. 11 | 738. 50 | | | |
| 2 | 65. 11 | 715. 74 | $s^2p^4(^3P)5s^2P_{1½}$–$s^2p^4(^1D)5p^2D^0_{1½}$ | | |
| 1H | 65. 59 | 710. 29 | | | |
| 3H*p* | 66. 13 | 704. 15 | | | |
| 80H | 67. 25 | 691. 43 | $s^2p^4(^3P)4d^2D_{2½}$–$s^2p^4(^3P)5f^4F^0_{3½}$ | | |
| 2 | 68. 11 | 681. 67 | | | |
| 1H | 68. 74 | 674. 52 | | | |
| 4*h* | 71. 80 | 639. 85 | $s^2p^4(^3P)4d^2P_{1½}$–$s^2p^4(^1S)5p^2P^0_{0½}$ | | |
| 2*h* | 72. 34 | 633. 73 | $s^2p^4(^3P)5p^4D^0_{1½}$–$s^2p^4(^3P)5d^2D_{2½}$ | | |
| 25*h* | 74. 04 | 614. 51 | $s^2p^4(^3P)4d^2D_{2½}$–$s^2p^4(^3P)5f^4F^0_{3½}$ | | |
| 1*h* | 75. 24 | 600. 95 | | | |
| 3*h* | 75. 92 | 593. 28 | $s^2p^4(^3P)5p^4P^0_{1½}$–$s^2p^4(^3P)5d^2F_{2½}$ | | |
| 3*h* | 76. 28 | 589. 21 | $s^2p^4(^3P)5p^4D^0_{½}$–$s^2p^4(^1S)4d^2D_{2½}$ | | |
| 1*h* | 76. 48 | 586. 95 | | | |
| 25 | 78. 87 | 560. 01 | $s^2p^4(^3P)4d^2P_{1½}$–$s^2p^4(^3P)5f^4F^0_{2½}$ | | |
| 20 | 79. 81 | 549. 42 | $s^2p^4(^3P)4d^2D_{2½}$–$s^2p^4(^3P)5f^4F^0_{3½}$ | | |
| 1*h* | 82. 34 | 520. 97 | $s^2p^4(^3P)5p^2D^0_{2½}$–$s^2p^4(^3P)7s^4P_{1½}$ | | |
| 2H*l* | 83. 94 | 502. 99 | $s^2p^4(^3P)5p^2P^0_{½}$–$s^2p^4(^3P)7s^4P_{1½}$ | | |
| 4H*l* | 85. 33 | 487. 39 | | | |
| 3H*l* | 88. 69 | 449. 75 | $s^2p^4(^1D)4d^2D_{2½}$–15216.41 | | |
| 1H | 89. 80 | 437. 33 | | | |
| 1*h* | 90. 90 | 425. 03 | | | |
| 20 | 96. 60 | 361. 45 | $sp^6.{}^2S_{0½}$–$s^2p^4(^3P)5p^2S^0_{½}$ | | |
| 40*h* | 2999. 84 | 325. 42 | $s^2p^4(^1D)4d^2D_{2½}$–15340.81 | | |
| 2*hl* | 3002. 48 | 296. 12 | $s^2p^4(^1D)4d^2D_{2½}$–15370.10 | | |
| 8*h* | 08. 42 | 230. 38 | $s^2p^4(^3P)5p^4P^0_{½}$–$s^2p^4(^3P)5d^2F_{2½}$ | | |
| 1*h* | 12. 00 | 190. 89 | $s^2p^4(^3P)5p^2D^0_{2½}$–$s^2p^4(^3P)7s^4P_{2½}$ | | |
| 20Hv | 17. 65 | 128. 75 | $s^2p^4(^1D)4d^2D_{1½}$–14873.45 | | |
| 1 | 18. 30 | 121. 61 | $s^2p^4(^3P)5p^4P^0_{2½}$–$s^2p^4(^3P)5d^4F_{1½}$ | | |
| 5h | 22. 49 | 33, 075. 70 | $s^2p^4(^3P)5p^4P^0_{½}$–31180.55 | | |
| 4 | 30. 01 | 32, 993. 61 | $sp^6.{}^2S_{½}$–$s^2p^4(^3P)5p^2D^0_{1½}$ | | |
| 5Hv | 31. 59 | 976. 42 | | | |
| 5H | 32. 77 | 963. 59 | | | |
| 2h | 34. 16 | 948. 43 | $s^2p^4(^3P)5p^2P^0_{½}$–$s^2p^4(^1S)4d^2D_{1½}$<br>$s^2p^4(^1D)4d^2D_{2½}$–15717.15 | | |
| 3Hl | 38. 38 | 902. 73 | | | |
| 8Hv | 49. 23 | 785. 66 | $s^2p^4(^1D)4d^2D_{1½}$–15216.41 | | |
| 1h | 51. 75 | 758. 59 | $s^2p^4(^3P)5p^4P^0_{1½}$–$s^2p^4(^3P)5d^4F_{1½}$ | | |
| 3 | 55. 31 | 720. 42 | $sp^6.{}^2S_{½}$–$s^2p^4(^3P)5p^4P^0_{1½}$ | | |
| 30H | 56. 01 | 712. 92 | $s^2p^4(^3P)5p^4P^0_{1½}$–31180.55 | | |
| 30Hv | 60. 84 | 661. 30 | $s^2p^4(^1D)4d^2D_{1½}$–15340.81 | | |
| 6h | 61. 51 | 654. 16 | | | |
| 3hl | 63. 57 | 632. 20 | $s^2p^4(^1D)4d^2D_{1½}$–15370.10 | | |
| 2 | 66. 72 | 598. 68 | $s^2p^4(^3P)5s^4P_{0½}$–$s^2p^4(^1D)5p^2P^0_{1½}$ | | |
| 2h | 80. 20 | 456. 03 | | | |
| 1 | 88. 73 | 366. 40 | | | |
| 30hv | 95. 14 | 299. 37 | $s^2p^4(^1D)4d^2D_{1½}$–15702.73 | | |
| 20hv | 3, 096. 52 | 284. 98 | $s^2p^4(^1D)4d^2D_{1½}$–15717.15 | | |
| 1hl | 3, 105. 68 | 189. 76 | $s^2p^4(^3P)5p^4D^0_{½}$–$s^2p^4(^1D)6s^2D_{1½}$ | | |
| 2h | 11. 45 | 130. 06 | $s^2p^4(^3P)5p^4P^0_{½}$–$s^2p^4(^3P)5d^2D_{1½}$ | | |
| 2 | 13. 92 | 104. 58 | $s^2p^4(^3P)4d^4D_{2½}$–$s^2p^4(^1D)5p^2D^0_{2½}$ | | |
| 1h | 3, 115. 67 | 32, 086. 55 | | | |
| 6*h* | 3, 126. 02 | 31, 980. 32 | | | |
| 4H | 32. 84 | 910. 70 | | | |
| 8 | 35. 10 | 887. 70 | $s^2p^4(^3P)4d^4D_{2½}$–$s^2p^4(^1D)5p^2D^0_{2½}$<br>$s^2p^4(^3P)5p^4D^0_{½}$–$s^2p^4(^1S)4d^2D_{1½}$ | | |
| 2 | 38. 24 | 855. 79 | | | |
| 20 | 39. 58 | 842. 20 | $s^2p^4(^3P)5p^4D^0_{½}$–$s^2p^4(^3P)5d^2D_{1½}$ | | |
| 4 | 39. 86 | 839. 36 | $s^2p^4(^3P)4d^2F_{2½}$–$s^2p^4(^1S)5p^2P^0_{1½}$ | | |
| 3*hl* | 40. 44 | 833. 48 | $s^2p^4(^3P)5p^2P^0_{1½}$–$s^2p^4(^1S)4d^2D_{2½}$ | | |
| 1 | 47. 39 | 763. 19 | $s^2p^4(^3P)4d^4D_{2½}$–$s^2p^4(^1D)5p^2D^0_{1½}$ | | |
| 80h | 50. 93 | 727. 50 | $s^2p^4(^3P)5s^2P_{1½}$–$s^2p^4(^1D)5p^2P^0_{1½}$ | (0.20) 1.42 | (0.00, 0.28) 1.23, 1.42, 1.61 |

TABLE 4.—*The first spark spectrum of krypton (Kr II)*—Continued

| Intensity and character | $\lambda_{air}$ I.A. | $\nu_{vac}$ cm$^{-1}$ | Term combination | Zeeman effect | |
|---|---|---|---|---|---|
| | | | | Observed | Computed |
| 2H | 53.34 | 703.26 | | | |
| 1 | 56.07 | 675.84 | | | |
| 1 | 60.40 | 632.44 | | | |
| 3Hl | 64.94 | 587.06 | $s^2p^4(^2P)5p^4S_{1½}$—$s^2p^4(^3P)7s^4P_{2½}$<br>$s^2p^4(^3P)4d^2D_{2½}$—32026.50 | | |
| 2 | 70.63 | 530.38 | $s^2p^4(^3P)4d^2F_{2½}$—$s^2p^4(^3P)5f^2D_{1½}$ | | |
| 40H | 75.67 | 480.34 | $s^2p^4(^1D)4d^2P_{1½}$—14,873.45 | | |
| 15Hl | 76.94 | 467.76 | $s^2p^4(^3P)5p^2P^0_{1½}$—$s^2p^4(^1D)6s^2D_{2½}$ | | |
| 1 | 78.92 | 448.16 | $s^2p^4(^3P)5p^4D^0_{½}$—$s^2p^4(^3P)5d^2F_{2½}$ | | |
| 5H | 81.25 | 425.13 | | | |
| 1h | 83.03 | 407.55 | | | |
| 1 | 83.63 | 401.63 | | | |
| 1 | 85.84 | 379.85 | | | |
| 4 | 87.61 | 362.43 | $s^2p^4(^3P)4d^2F_{2½}$—$s^2p^4(^3P)5f^2F^0_{3½}$ | | |
| 2 | 92.54 | 314.00 | $s^2p^4(^3P)4d^4D_{1½}$—$s^2p^4(^1D)5p^2D^0_{2½}$<br>$s^2p^4(^3P)5p^2D^0_{1½}$—$s^2p^4(^3P)7s^4P_{2½}$ | | |
| 2 | 95.50 | 284.99 | $s^2p^4(^3P)4d^2F_{2½}$—$s^2p^4(^3P)5f^2F^0_{3½}$ | | |
| 4hl | 3, 197.65 | 263.96 | $s^2p^4(^3P)5p^4P^0_{2½}$—$s^2p^4(^3P)5d^4F_{1½}$ | | |
| 50h | 3, 200.40 | 237.10 | $s^2p^4(^3P)5s^2P^0_{1½}$—$s^2p^4(^1D)5p^2P^0_{2½}$ | (0.00) 0.70 | (0.00) 0.70 |
| 15hl | 3, 202.54 | 216.23 | $s^2p^4(^3P)5p^4P^0_{½}$—$s^2p^4(^3P)5d^2P_{1½}$ | | |
| 4 | 05.26 | 189.73 | $s^2p^4(^3P)4d^4D_{1½}$—$s^2p^4(^1D)5p^2D^0_{1½}$ | | |
| 2 | 05.44 | 187.98 | $s^2p^4(^3P)5s^2P_{0½}$—$s^2p^4(^1D)5p^2D^0_{1½}$ | | |
| 1 | 07.29 | 170.00 | $s^2p^4(^3P)5p^4P^0_{½}$—$s^2p^4(^3P)5d^2P_{0½}$ | | |
| 40h | 08.28 | 160.38 | $s^2p^4(^3P)4d^2F_{2½}$—$s^2p^4(^3P)5f^2F^0_{3½}$<br>$sp^{6.2}S_{½}$—$s^2p^4(^3P)5p^4D^0_{½}$ | | |
| 7hl | 09.17 | 151.74 | $s^2p^4(^3P)5p^4P^0_{½}$—$s^2p^4(^3P)5d^4F_{2½}$ | | |
| 2h | 10.64 | 137.47 | $s^2p^4(^1D)4d^2P_{1½}$—15,216.41 | | |
| 7 | 10.89 | 135.05 | $sp^{6.2}S_{½}$—$s^2p^4(^3P)5p^2P^0_{1½}$ | | |
| 1 | 14.11 | 103.86 | | | |
| 7h | 16.25 | 083.16 | $s^2p^4(^3P)4d^2F_{2½}$—$s^2p^4(^3P)5f^4F^0_{3½}$ | | |
| 6h | 20.25 | 044.55 | | | |
| 6 | 23.00 | 018.07 | $s^2p^4(^3P)4d^2F_{2½}$—$s^2p^4(^3P)5f^4F^0_{3½}$ | | |
| 12h | 23.52 | 31, 013.06 | $s^2p^4(^1D)4d^2P_{1½}$—15,340.81 | | |
| 5Hl | 26.57 | 30, 983.75 | $s^2p^4(^1D)4d^2P_{1½}$—15,370.10 | | |
| 2h | 32.15 | 930.26 | $s^2p^4(^3P)5p^4D^0_{2½}$—31,180.55 | | |
| 2 | 40.20 | 853.42 | $s^2p^4(^3P)5p^4P^0_{1½}$—$s^2p^4(^3P)5d^2P_{1½}$ | | |
| 2 | 46.18 | 796.59 | | | |
| 12H | 47.00 | 788.81 | $s^2p^4(^3P)5p^4P^0_{1½}$—$s^2p^4(^3P)5d^4P_{2½}$ | | |
| 6H | 48.03 | 779.04 | $s^2p^4(^3P)4d^2P_{0½}$—15,216.41 | | |
| 4 | 56.67 | 697.39 | $s^2p^4(^3P)5s^2P_{1½}$—$s^2p^4(^1D)5p^2F^0_{2½}$ | | |
| 8h | 61.58 | 651.18 | $s^2p^4(^1D)4d^2P_{1½}$—15,702.73 | | |
| 1h | 63.12 | 636.71 | $s^2p^4(^1D)4d^2P_{1½}$—15,717.15 | | |
| 5H | 64.33 | 625.36 | $s^2p^4(^1D)4d^2P_{0½}$—15,370.10 | | |
| 1h | 76.81 | 508.72 | | | |
| 15h | 82.08 | 459.74 | $s^2p^4(^3P)4d^4D_{0½}$—$s^2p^4(^1D)5p^2P^0_{1½}$ | | |
| 2h | 87.38 | 410.63 | $s^2p^4(^3P)4d^4D_{0½}$—$s^2p^4(^1D)5p^2D^0_{1½}$ | | |
| 2H | 87.69 | 407.76 | $s^2p^4(^3P)5p^4D^0_{½}$—$s^2p^4(^1D)6s^2D_{2½}$ | | |
| 1h | 90.31 | 383.55 | | | |
| 2h | 94.43 | 345.56 | | | |
| 3h | 3, 295.29 | 337.64 | | | |
| 4H | 3, 300.18 | 292.69 | $s^2p^4(^1D)4d^2P_{0½}$—15,702.73 | | |
| 5h | 3, 301.75 | 278.28 | $s^2p^4(^1D)4d^2P_{0½}$—15,717.15 | | |
| 4hl | 02.28 | 273.42 | | | |
| 15h | 15.72 | 150.72 | $s^2p^4(^3P)5p^4P^0_{½}$—$s^2p^4(^1S)6s^2S_{0½}$ | | |
| 8 | 21.16 | 101.33 | $sp^{6.2}S_{½}$—$s^2p^4(^3P)5p^2P^0_{½}$ | | |
| 1 | 26.13 | 30, 056.35 | $s^2p^4(^3P)5p^2D^0_{1½}$—$s^2p^4(^1S)4d^2D_{1½}$ | | |
| 4hl | 35.16 | 29, 974.98 | $s^2p^4(^3P)5p^2D^0_{1½}$—$s^2p^4(^1S)4d^2D_{2½}$ | | |
| 2 | 57.58 | 774.83 | $s^2p^4(^3P)4d^4D_{2½}$—$s^2p^4(^1D)5p^2F^0_{1½}$ | | |
| 1h | 72.13 | 646.36 | | | |
| 3h | 75.78 | 614.31 | $s^2p^4(^3P)5p^4D^0_{½}$—$s^2p^4(^3P)5d^2F_{2½}$ | | |
| 15H | 79.03 | 585.83 | $s^2p^4(^3P)5p^2D^0_{1½}$—$s^2p^4(^3P)5d^2D_{2½}$ | | |
| 20H | 81.11 | 567.63 | $s^2p^4(^3P)5p^2P^0_{1½}$—$s^2p^4(^3P)5d^2D_{2½}$ | | |
| 15Hl | 85.23 | 531.64 | $s^2p^4(^3P)5p^4D^0_{½}$—$s^2p^4(^3P)5d^2D_{1½}$ | | |
| 7h | 87.11 | 515.25 | | | |
| 5 | 3, 389.67 | 492.96 | $s^2p^4(^3P)4d^4D_{3½}$—$s^2p^4(^1D)5p^2F^0_{3½}$ | | |
| 2 | 3, 402.79 | 379.25 | $sp^{6.2}S_{½}$—$s^2p^4(^3P)5p^4D^0_{½}$ | | |

TABLE 4.—*The first spark spectrum of krypton (Kr II)*—Continued

| Intensity and character | $\lambda_{air}$ I.A. | $\nu_{vac}$ cm$^{-1}$ | Term combination | Zeeman effect | |
|---|---|---|---|---|---|
| | | | | Observed | Computed |
| 80Hl | 05.16 | 358.80 | $s^2p^4(^3P)5p^4P^1_{1/2}$—$s^2p^4(^3P)5d^3P_{1/2}$ | (0.28) 1.12, 1.69 | (0.29) 1.11, 1.69 |
| 1 | 12.67 | 294.20 | $s^2p^4(^3P)5p^4D^1_{1/2}$—$s^2p^4(^3P)5d^4F_{3/2}$ | | |
| 2h | 13.78 | 284.67 | | | |
| 10 | 14.80 | 275.92 | $s^2p^4(^3P)4d^4D_{3/2}$—$s^2p^4(^1D)5p^3F^1_{1/2}$ | | |
| 1h | 21.26 | 220.65 | | | |
| 20hv | 23.73 | 199.57 | $s^2p^4(^3P)5s^2P^1_{1/2}$—$s^2p^4(^1D)5p^2P^1_{1/2}$ | (0.32) 1.02, 1.66 | (0.31) 1.01, 1.65 |
| 30 | 3,427.71 | 29,165.66 | $s^2p^4(^3P)5s^4P_{3/2}$—$s^2p^4(^3P)5p^2D^1_{1/2}$ | (0.00) 1.90 | (0.13, 0.40) 1.19, 1.46, 1.73, 2.00 |
| 3h | 34.29.91 | 29,146.96 | $s^2p^4(^1D)5p^3F^1_{1/2}$—$s^2p^4(^1D)4d^2D_{3/2}$ | | |
| 8hl | 31.03 | 137.44 | | | |
| 2 | 34.28 | 109.87 | | | |
| 3h | 38.88 | 070.93 | $s^2p^4(^3P)^1p^4D^1_{1/2}$—$s^2p^4(^3P)5d^3P_{1/2}$ | | |
| 5h | 43.29 | 033.70 | | | |
| 50H | 46.51 | 29,006.58 | $s^2p^4(^3P)5p^4D^1_{1/2}$—$s^2p^4(^3P)5d^4F_{3/2}$ | | |
| 1 | 49.98 | 28,977.40 | | | |
| 3h | 53.46 | 948.20 | | | |
| 50 | 60.09 | 892.74 | $s^2p^4(^3P)5s^4P_{3/2}$—$s^2p^4(^3P)5p^4S^1_{3/2}$ | (0.00) 1.67 | (0.03, 0.09) 1.51, 1.57, 1.63, 1.69 |
| 2 | 60.90 | 885.97 | | | |
| 6Hl | 65.41 | 848.38 | $s^2p^4(^3P)5p^4S^1_{3/2}$—$s^2p^4(^1D)6s^2D_{3/2}$ | | |
| 30H | 70.05 | 809.81 | $s^2p^4(^3P)5p^2P^1_{3/2}$—$s^2p^4(^3P)5d^2D_{1/2}$ | (0.29) 0.88, 1.47 | (0,30) 0.88, 1.48 |
| 3hl | 75.31 | 766.20 | | | |
| 5 | 77.89 | 744.87 | $\left.\begin{matrix}s^2p^4(^3P)4d^4D_{3/2}\text{—}s^2p^4(^1D)5p^2F^1_{3/2}\\ s^2p^4(^3P)5p^4P^1_{1/2}\text{—}s^2p^4(^3P)5d^4D_{3/2}\end{matrix}\right\}$ | | |
| 3h | 79.00 | 735.70 | $s^2p^4(^1D)5p^2F^1_{3/2}$—$s^2p^4(^1O)5d^2F_{3/2}$ | | |
| 7h | 87.49 | 665.74 | $s^2p^4(^3P)5p^4D^1_{1/2}$—$s^2p^4(^3P)5d^4F_{1/2}$ | | |
| 30h | 88.65 | 656.21 | $s^2p^4(^3P)5p^4P^1_{3/2}$—$s^2p^4(^1S)6s^2S_{3/2}$ | (0.00) 1.95 | (0.02) 1.96 |
| 8H | 93.04 | 620.20 | $s^2p^4(^3P)5p^4D^1_{1/2}$—31,180.55 | | |
| 2h | 93.57 | 615.86 | $s^2p^4(^1D)5p^2F^1_{1/2}$—$s^2p^4(^1D)5d^2D_{3/2}$ | | |
| 3h | 97.45 | 584.11 | $s^2p^4(^1D)5p^2P^1_{1/2}$—$s^2p^4(^1D)5d^2P_{3/2}$ | | |
| 4Hl | 98.50 | 575.53 | $s^2p^4(^3P)5p^2D^1_{1/2}$—$s^2p^4(^1D)6s^2D_{3/2}$ | | |
| 2H | 3,498.92 | 572.10 | $s^2p^4(^3P)5p^4D^1_{1/2}$—$s^2p^4(^3P)5d^2P_{3/2}$ | | |
| 50Hl | 3,503.25 | 536.79 | $s^2p^4(^1D)5p^2F^1_{1/2}$—$s^2p^4(^1D)5d^2F_{3/2}$ | (0.00) 0.89 | (0.01, 0.04, 0.07) 0.81, 0.84, 0.87, 0.90, 0.93 |
| 5hv | 17.37 | 422.24 | $s^2p^4(^3P)4d^4D_{3/2}$—$s^2p^4(^1D)5p^2P^1_{1/2}$ | | |
| 3hl | 27.42 | 341.26 | | | |
| 1h | 30.95 | 312.93 | | | |
| 1h | 31.82 | 305.95 | | | |
| 1h | 34.43 | 285.05 | | | |
| 50hl | 35.35 | 277.69 | $s^2p(^3P)5p^4P^1_{1/2}$—$s^2p^4(^3P)6s^2P_{3/2}$ | (0.37) 1.31, 2.04 | (0.37) 1.29, 2.04 |
| 30Hl | 44.14 | 207.56 | $s^2p^4(^3P)5p^2S^1_{1/2}$—$s^2p^4(^1D)6s^2D_{3/2}$ | (0.25) 0.75, 1.00 | (0.25) 0.75, 1.00 |
| 30Hl | 44.54 | 204.38 | $s^2p^4(^1D)5p^2F^1_{1/2}$—$s^2p^4(^1D)5d^2F_{3/2}$ | (0.00) 1.14 | (0.00) 1.14 |
| 6 | 48.71 | 171.23 | $s^2p^4(^3P)4d^4D_{1/2}$—$s^2p^4(^1D)5p^2F^1_{3/2}$ | | |
| 20hl | 53.49 | 133.34 | $s^2p^4(^3P)5p^4P^1_{1/2}$—$s^2p^4(^3P)6s^2P_{1/2}$ | (0.00) 1.80 | (0.13, 0.37) 1.20, 1.45, 1.70, 1.98 |
| 8Hl | 55.54 | 117.12 | $s^2p^4(^1D)5p^2P^1_{1/2}$—$s^2p^4(^1D)5d^2D_{3/2}$ | (0.00) 1.00 | (0.07, 0.20) 1.00, 1.13, 1.27, 1.40 |
| 2h | 69.68 | 28,005.75 | $s^2p^4(^1D)5p^2F^1_{1/2}$—$s^2p^4(^1D)5d^2F_{2/2}$ | | |
| 15H | 72.68 | 27,982.23 | $s^2p^4(^3P)5p^4S^1_{1/2}$—$s^2p^4(^3P)5d^2D_{3/2}$ | | |
| 4hl | 77.60 | 943.75 | $s^2p^4(^3P)5p^2P^1_{3/2}$—$s^2p^4(^3P)5d^4F_{1/2}$ | | |
| 12hl | 86.25 | 876.35 | $s^2p^4(^3P)5p^4P_{3/2}$—$s^2p^4(^3P)5d^4D_{1/2}$ | | |
| 70Hl | 89.65 | 849.95 | $s^2p^4(^3P)5p^2P^1_{3/2}$—$s^2p^4(^3P)5d^2P_{3/2}$ | (0.63) 1.14 | (0.63) 1.14 |
| 2hl | 96.86 | 794.13 | $s^2p^4(^3P)5p^2D^1_{3/2}$—$s^2p^4(^3P)5d^2D_{1/2}$ | | |
| 25h | 99.21 | 775.98 | $s^2p^4(^3P)5p^2P^1_{1/2}$—$s^2p^4(^3P)5d^2D_{1/2}$ | (0.11) 1.23 | (0.04, 0.12) 1.14, 1.22, 1.30 |
| 40hl | 3,599.90 | 770.66 | $s^2p^4(^3P)5p^4P^1_{1/2}$—$s^2p^4(^3P)6s^2P_{1/2}$ | (0.45) 1.50 | (0.17, 0.51) 1.16, 1.50, 1.84 |
| 2h | 3,602.12 | 753.54 | $s^2p^4(^1D)5p^2P^1_{1/2}$—$s^2p^4(^3P)7s^2P_{1/2}$ | | |
| 100Hl | 07.88 | 709.23 | $s^2p^4(^3P)5p^2D^1_{3/2}$—$s^2p^4(^3P)5d^2D_{3/2}$ | (0.00) 0.92 | (0.09, 0.27) 0.88, 1.06, 1.24, 1.42 |
| 30hl | 23.61 | 588.95 | $s^2p^4(^3P)5p^4P^1_{1/2}$—$s^2p^4(^3P)6s^4P_{3/2}$ | (0.34) 1.33, 2.00 | (0.34) 1.33, 2.00 |
| 200hl | 31.87 | 526.21 | $s^2p^4(^3P)5p^4P^1_{3/2}$—$s^2p^4(^3P)5d^4D_{1/2}$ | (0.48) 1.48 | (0.10, 0.31, 0.52) 1.05, 1.26, 1.47, 1.68, 1.89 |
| 3h | 33.54 | 513.56 | $s^2p^4(^3P)5p^4P^1_{1/2}$—$s^2p^4(^3P)5d^4D_{1/2}$ | | |
| 3Hl | 34.42 | 506.89 | $s^2p^4(^1D)5p^2P^1_{1/2}$—$s^2p^4(^1D)5d^2F_{2/2}$ | | |
| 20hl | 37.48 | 483.76 | $s^2p^4(^3P)5p^4P^1_{3/2}$—$s^2p^4(^3P)5d^4P_{1/2}$ | | |
| 4Hl | 37.93 | 480.36 | $s^2p^4(^1D)5p^2P^1_{1/2}$—$s^2p^4(^1D)5d^2P_{1/2}$ | | |
| 40hl | 48.61 | 399.92 | $s^2p^4(^3P)5p^2D^1_{3/2}$—$s^2p^4(^3P)5d^2F_{2/2}$ | | |
| 25hl | 3,651.02 | 27,381.83 | $s^2p^4(^3P)5p^2P^1_{1/2}$—$s^2p^4(^3P)5d^2F_{3/2}$ | | |

TABLE 4.—*The first spark spectrum of krypton (Kr II)*—Continued

| Intensity and character | $\lambda_{air}$ I.A. | $\nu_{vac}$ cm$^{-1}$ | Term combination | Zeeman effect | |
|---|---|---|---|---|---|
| | | | | Observed | Computed |
| 250*hl* | 3, 653. 97 | 27, 359. 73 | $s^2p^4(^3P)5p^4P^0_{1/2}$—$s^2p^4(^3P)5d^4D_{3/2}$ | (0.00) **1.02** | (0.09, 0. 27, 0.45) **0.95**, 1.13, 1.31, 1.49, 1.67, 1.85. |
| 15 | 61. 00 | 307. 19 | $s^2p^4(^3P)5s^4P_{3/2}$—$s^2p^4(^3P)5p^2P^0_{1/2}$ | (0.00) **2.07** | (0.17, 0.51) 1.09, 1.43, 1.77, **2.11** |
| 20 | 63. 44 | 289. 00 | $s^2p^4(^3P)5s^4P_{3/2}$—$s^2p^4(^3P)5p^2D^0_{3/2}$ | | |
| 5 | 66. 01 | 269. 88 | $s^2p^4(^3P)5s^4P_{1/2}$—$s^2p^4(^3P)5p^2S^0_{1/2}$ | (0.00) 1.58 | (0.02) 1.52, **1.59** |
| 6 | 68. 59 | 250. 70 | $s^2p^4(^3P)5p^4P^0_{3/2}$—$s^2p^4(^3P)5d^4D^0_{3/2}$ | | |
| 150*hl* | 69. 01 | 247. 58 | | 1.01 (0.00) 1.06 | |
| 7*hl* | 78. 66 | 176. 10 | | | |
| 100H*l* | 80. 37 | 163. 47 | $s^2p^4(^3P)5p^4P^0_{1/2}$—$s^2p^4(^3P)5d^4D_{3/2}$ | (0.15, 0.45) **0.97** | (0.15, 0.45) **0.92**, 1.22, 1.52, 2.02 |
| 80H*l* | 86. 15 | 120. 89 | $s^2p^4(^3P)5p^4P^0_{1/2}$—$s^2p^4(^3P)5d^4P_{1/2}$ | (—, 0.69) 0.96, 1.43, 1.90 | (0.23, **0.69**) 0.98, **1.44**, 1.90 |
| 30 | 3, 690. 65 | 27, 087. 82 | $s^2p^4(^3P)5p^4P^0_{3/2}$—$s^2p^4(^3P)5d^4P_{3/2}$ | | |
| 1*h* | 3, 711. 27 | 26, 937. 32 | $s^2p^4(^1D)5p^2F^0_{5/2}$—$s^2p^4(^1D)5d^2D_{3/2}$ | | |
| 1*h* | 12. 48 | 928. 54 | $s^2p^4(^3P)5p^2D^0_{3/2}$—$s^2p^4(^3P)5d^4F_{3/2}$ | | |
| 12*h* | 15. 04 | 909. 98 | $s^2p^4(^3P)5p^2P^0_{1/2}$—$s^2p^4(^3P)5d^4F_{1/2}$ | (—) 1.00 | (0.37, **1.11**) 0.15, 0.89, 1.63 |
| 4 | 16. 15 | 901. 94 | $s^2p^4(^3P)5s^4P_{1/2}$—$s^2p^4(^3P)5p^2D^0_{1/2}$ | | |
| 300*hl* | 18. 02 | 888. 42 | $s^2p^4(^1D)5p^2F^0_{5/2}$—$s^2p^4(^1D)5d^2G_{7/2}$ | (0.00) **1.05** | (0.02, 0.05, 0.08, 0.11) **1.00**, 1.03, 1.06, 1.10, 1.13, 1.16, 1.19, 1.22 |
| 200*hl* | 18. 63 | 884. 01 | $s^2p^4(^3P)5p^4D^0_{3/2}$—$s^2p^4(^3P)5d^4F_{1/2}$ | (0.25) 0.78 | (0.26) 0.26, **0.78** |
| 150*hl* | 21. 35 | 864. 36 | $s^2p^4(^3P)5p^2P^0_{3/2}$—31180.55 | (0.00) 1.39 | |
| 7*hl* | 28. 04 | 816. 15 | $s^2p^4(^3P)5p^2P^0_{1/2}$—$s^2p^4$ ($^3P$) $5d^2P_{3/2}$ | (0.39) 1.65 | (0.37) 0.88, **1.63** |
| 2*h* | 31. 67 | 790. 06 | $s^2p^4(^3P)5p^4D^0_{1/2}$—$s^2p^4(^3P)5d^2P_{3/2}$ | | |
| 15*h* | 32. 61 | 783. 32 | $s^2p^4(^3P)5p^4P^0_{3/2}$—$s^2p^4(^3P)6s^2P^0_{1/2}$ | (0.53) 1.45 | (0.53) 1.45 |
| 6 | 32. 92 | 781. 09 | $sp^6\,^2S_{0/2}$—$s^2p^4$ ($^1P$)$5p^4P^0_{1/2}$ | | |
| 40*hl* | 35. 78 | 760. 59 | $s^2p^4(^3P)5p^4D^0_{1/2}$—$s^2p^4$ ($^3P$)$5d^2P_{1/2}$ | (0.21) **1.34** | (0.07, **0.21**) 1.19, **1.33**, 1.47 |
| 6 | 40. 73 | 725. 18 | $s^2p^4(^3P)5p^4P^0_{1/2}$—$s^2p^4(^3P)5d^4P_{3/2}$ | | |
| 200*hl* | 41. 69 | 718. 32 | $s^2p^4(^1D)5p^2F^0_{5/2}$—$s^2p^4(^1D)5d^2G_{7/2}$ | (0.00) **0.93** | (0.02,0.05, 0.08) 0.81, 0.84, 0.87, 0.90, 0.94, **0.97** |
| 150*hp* | 44. 80 | 696. 13 | $s^2p^4(^3P)5p^4D^0_{1/2}$—$s^2p^4(^3P)5d^4F_{1/2}$ | (0.00) **1.01** | (0.07, 0.21) **0.91**, 1.05, 1.19, 1.33 |
| 2H | 47. 50 | 676. 90 | | | |
| 1*h* | 3, 748. 57 | 669. 29 | | | |
| 80 | 54. 24 | 629. 01 | $s^2p^4(^3P)5s^4P_{1/2}$—$s^2p^4(^3P)5p^4S^0_{1/2}$ | (0. 00) 1. 55 | (0. 00) 1. 54 |
| 6H*l* | 58. 93 | 595. 78 | $s^2p^4(^1D)5p^2D^0_{1/2}$—$s^2p^4(^1D)5d^2P_{3/2}$ | | |
| 2H | 65. 88 | 546. 70 | $s^2p^4(^1D)5p^2P^0_{3/2}$—$s^2p^4(^1D)5d^2P_{3/2}$ | | |
| 30*h* | 71. 34 | 508. 27 | $s^2p^4(^3P)5p^4p^0_{1/2}$—$s^2p^4(^3P)5d^4P_{3/2}$ | (0.20) **1.48**, 1.88 | (0.20) **1.47**, 1.87 |
| 500*hl* | 78. 09 | 460. 91 | $s^2p^4(^3P)5p^4D^0_{3/2}$—$s^2p^4(^3P)5d^4F_{3/2}$ | (0.00) **1.10** | (0.03, 0.09, 0.15) **1.02**, 1.08, 1.14, 1.20, 1.26, 1.32. |
| 500*hl* | 3, 783. 13 | 425. 66 | $s^2p^4(^3P)5p^4D^0_{3/2}$—$s^2p^4(^3P)5d^4F_{5/2}$ | (0.00) **1.12** | (0.05, 0.14, 0.24, 0.33) **1.00**, 1.10, 1.19, 1.29, 1.38, 1.48, 1.57, 1.67. |
| 30*hl* | 3, 804. 67 | 276. 06 | $s^2p^4(^3P)5p^4P^0_{3/2}$—$s^2p^4(^3P)6s^2P_{1/2}$ | (0.32) **1.01**, 1.66 | (0.32) **1.01**, 1.65 |
| 8H*l* | 06. 17 | 265. 70 | $s^2p^4(^1D)5p^2P^0_{3/2}$—$s^2p^4(^3P)7s^2P^0_{3/2}$ | | |
| 1*h* | 06. 52 | 263. 29 | $s^2p^4(^1D)4d^2G_{7/2}$—$s^2p^4(^1D)5f^2F^0_{5/2}$ | | |
| 15H*l* | 17. 11 | 190. 42 | $s^2p^4(^3P)5p^4S^0_{1/2}$—$s^2p^4(^3P)5d^2D_{1/2}$ | | |
| 2*h* | 26. 15 | 128. 55 | $s^2p^4(^1D)5p^2D^0_{1/2}$—$s^2p^4(^1D)5d^2D_{3/2}$ | | |
| 2H*l* | 31. 17 | 094. 31 | $s^2p^4(^3P)5p^4P^0_{3/2}$—$s^2p^4(^3P)6s^4P^0_{3/2}$ | | |
| 30H*l* | 36. 54 | 057. 79 | $s^2p^4(^3P)5p^4D^0_{1/2}$—$s^2p^4(^1S)6s^2S^0_{1/2}$ | | |
| 4H*l* | 39. 37 | 038. 58 | $s^2p^4(^3P)5p^2P^0_{3/2}$—$s^2p^4(^3P)5d^2P_{1/2}$ | | |
| 2. 0H*l* | 42. 28 | 018. 86 | $s^2p^4(^3P)5p^4P^0_{3/2}$—$s^2p^4(^3P)5d^4D_{1/2}$ | | |
| 50H*l* | 44. 45 | 26, 004. 18 | $s^2p^4(^1D)5p^2D^0_{3/2}$—$s^2p^4(^1D)5d^2D_{3/2}$ | | |
| 5*h* | 3, 846. 83 | 25, 988. 09 | $s^2p^4(^3P)5p^4D^0_{1/2}$—$s^2p^4(^3P)6s^2P_{1/2}$ | | |
| 20H*l* | 3, 857. 32 | 25, 917. 41 | $s^2p^4(^3P)5p^2D^0_{3/2}$—$s^2p^4(^3P)5d^2D_{1/2}$ | | |
| 5H*l* | 58. 78 | 907. 61 | $s^2p^4(^1D)5p^2P^0_{1/2}$—$s^2p^4(^1D)5d^2D_{3/2}$ | | |
| 150H*l* | 75. 44 | 796. 24 | $s^2p^4(^3P)5p^4S^0_{1/2}$—$s^2p^4(^3P)5d^2F_{3/2}$ | (—) **0.28**, 0.51, 0.74. | (0.25, 0.75) **0.29**, 0.79, 1.29, 1.79. |
| 1H | 79. 82 | 767. 12 | | | |
| 2H*l* | 80. 07 | 765. 45 | $s^2p^4(^1D)5p^2D^0_{1/2}$—$s^2p^4(^3P)7s^2P^0_{1/2}$ | | |
| 1 | 85. 28 | 730. 91 | $s^2p^4(^3P)5p^4D^0_{3/2}$—$s^2p^4(^3P)5d^4D_{1/2}$ | | |

TABLE 4.—*The first spark spectrum of krypton (Kr II)*—Continued

| Intensity and character | $\lambda_{air}$ I.A. | $\nu_{vac}$ cm$^{-1}$ | Term combination | Zeeman effect | |
|---|---|---|---|---|---|
| | | | | Observed | Computed |
| 5H*l* | 87. 54 | 715. 95 | $s^2p^4(^1D)5p^3P^0_{2\frac{1}{2}}$—$s^2p^4(^3P)7s^2P_{1\frac{1}{2}}$ | | |
| 60H*l* | 3, 894. 71 | 668. 61 | $s^2p^4(^3P)5p^4D^0_{3\frac{1}{2}}$—$s^2p^4(^3P)5d^4D_{2\frac{1}{2}}$ | (0.00) **1.53** | (**0.03**,0. 09, 0. 14) 1. 28, 1. 34, 1. 40, 1. 46, 1. 51, 1. 57 |
| 10*hl* | 3, 901. 15 | 626. 23 | $s^2p^4$ $(^3P)5p^4P^0_{2\frac{1}{2}}$—$s^2p^4(^3P)5d^4P_{1\frac{1}{2}}$ | | |
| 150*hl* | 06. 25 | 592. 78 | $s^2p^4(^1D)5p^2D^0_{2\frac{1}{2}}$—$s^2p^4(^1D)5d^2F_{3\frac{1}{2}}$ | (0.00) **1.08** | (**0.03**, 0. 09, 0. 14) **1.00**, 1. 06, 1. 11, 1. 17, 1. 23, 1. 28 |
| 70 | 12. 59 | 551. 31 | $s^2p^4(^3P)5s^4P_{2\frac{1}{2}}$—$s^2p^4(^3P)5p^4D^0_{1\frac{1}{2}}$ | (0.17, 0.52) —, 1.43, 1.77, **2.09** | (**0.17**, 0.51) 1.09, **1.43**, 1.77, **2.11** |
| 5*hl* | 12. 88 | 549. 41 | $s^2p^4(^3P)5p^2S^0_{2\frac{1}{2}}$—$s^2p^4(^3P)5d^2D_{1\frac{1}{2}}$ | | |
| 3*hl* | 16. 90 | 523. 19 | $s^2p^4(^3P)5p^2D^0_{1\frac{1}{2}}$—$s^2p^4(^3P)5d^2F_{2\frac{1}{2}}$ | | |
| 50H*l* | 17. 64 | 518. 37 | $s^2p^4(^1D)5p^2D^0_{2\frac{1}{2}}$—$s^2p^4(^1D)5d^2F_{3\frac{1}{2}}$ | (0.00) **0.96** | (**0.04**, 0.13) 0.75, 0.84, 0.93, **1.02** |
| 200*hl* | 20. 14 | 502, 10 | $s^2p^4(^3P)5p^4D^0_{3\frac{1}{2}}$—$s^2p^4(^3P)5d^4D_{3\frac{1}{2}}$ | (0.10) **1.41** | (0.01, 0.04, 0.07, 0.10) 1.32, 1.35, 1.38, **1.41**, 1.44, 1.47, 1.50 |
| 6*hl* | 21. 68 | 492. 08 | $s^2p^4(^1D)5p^2D^0_{1\frac{1}{2}}$—$s^2p^4(^1D)5d^2P_{1\frac{1}{2}}$ | (0.57) **1.00** | (0.19, **0.57**) 0.61, 0.99, 1.37 |
| 20*hl* | 29. 26 | 442. 91 | $s^2p^4(^1D)5p^2P^0_{1\frac{1}{2}}$—$s^2p^4(^1D)5d^2P_{1\frac{1}{2}}$ | (**0.24**) 0.94 **1.42** | (**0.24**) 0.94, **1.42** |
| 20 H*l* | 38. 88 | 380. 77 | $s^2p^4(^3P)5p^4D^0_{2\frac{1}{2}}$—$s^2p^4(^3P)5d^4D_{2\frac{1}{2}}$ | | |
| 5 H*l* | 40. 92 | 367. 63 | $s^2p^4(^1D)5p^2D^0_{2\frac{1}{2}}$—$s^2p^4(^1D)5d^2P_{1\frac{1}{2}}$ | | |
| 20 H*l* | 42. 93 | 354. 70 | | | |
| 5 *hl* | 45. 48 | 338. 31 | $s^2p^4(^3P)5p^4D^0_{\frac{1}{2}}$—$s^2p^4(^3P)5d^4P_{1\frac{1}{2}}$ | | |
| 1 *hl* | 45. 83 | 336. 06 | $s^2p^4(^3P)5p^2P^0_{1\frac{1}{2}}$—$s^2p^4(^1S)6s^2S_{0\frac{1}{2}}$ | | |
| 5 h*l* | 47. 66 | 324. 32 | $s^2p^4(^3P)5p^4S^0_{1\frac{1}{2}}$—$s^2p^4(^3P)5d^4F_{1\frac{1}{2}}$ | | |
| 20 | 53. 59 | 286. 34 | $sp^6$ $^2S_{0\frac{1}{2}}$—$s^2p^4(^3P)5p^4P^0_{1\frac{1}{2}}$ | | |
| 90 H*l* | 54. 78 | 278. 73 | $s^2p^4(^3P)5p^2D^0_{2\frac{1}{2}}$—$s^2p^4(^3P)5d^2F_{3\frac{1}{2}}$<br>$s^2p^4(^3P)5p^4S^0_{1\frac{1}{2}}$—31,180.55 | (0.00) **1.10** | (**0.05**, 0.15, 0.25) **0.99**, 1.09, 1.19, 1.29, 1.39, 1.49 |
| 10 *hl* | 62. 34 | 230. 50 | $s^2p^4(^3P)5p^4D^0_{1\frac{1}{2}}$—$s^2p^4(^3P)5d^4P_{2\frac{1}{2}}$<br>$s^2p^4(^3P)5p^4S^0_{1\frac{1}{2}}$—$s^2p^4(^3P)5d^2P^0_{0\frac{1}{2}}$ | | |
| 30 *hl* | 64. 89 | 214. 27 | $s^2p^4(^3P)5p^4D^0_{3\frac{1}{2}}$—$s^2p^4(^3P)5d^4D_{3\frac{1}{2}}$ | | |
| 1 | 78. 85 | 125. 81 | | | |
| 5H*p* | 87. 09 | 073. 88 | $s^2p^4(^1S)5s^2S_{0\frac{1}{2}}$—27294.47 | (0.48) 1.51 | (0.50) 1.50 |
| 25 | 87. 78 | 069. 54 | $s^2p^4(^3P)5s^4P_{1\frac{1}{2}}$—$s^2p^4(^3P)5p^4D^0_{0\frac{1}{2}}$ | | |
| 15*hl* | 90. 66 | 051. 45 | $s^2p^4(^3P)5p^2D^0_{2\frac{1}{2}}$—$s^2p^4(^3P)5d^4F_{1\frac{1}{2}}$ | | |
| 15 | 91. 94 | 043. 42 | $s^2p^4(^3P)5s^4P_{1\frac{1}{2}}$—$s^2p^4(^3P)5p^2P^0_{1\frac{1}{2}}$ | | |
| 100 | 94. 83 | 025. 30 | $s^2p^4(^3P)5s^4P_{1\frac{1}{2}}$—$s^2p^4(^3P)5p^2D^0_{2\frac{1}{2}}$ | (0.10, 0.30) **1.06**, 1.24 | (**0.10**, 0.30) **1.04**, 1.24, 144, 164 |
| 3 | 96. 69 | 013. 66 | $s^2p^4(^3P)5p^4P^0_{2\frac{1}{2}}$—$s^2p^4(^3P)5d^4P_{0\frac{1}{2}}$ | | |
| 100H*l* | 97. 95 | 005. 78 | $s^2p^4(^3P)5p^2P^0_{1\frac{1}{2}}$—$s^2p^4(^3P)5d^2P_{1\frac{1}{2}}$<br>$s^2p^4(^3P)5p^2D^0_{1\frac{1}{2}}$—31180.55 | | |
| 2*gn* | 3, 998. 82 | 25, 000. 34 | | | |
| 30h*l* | 4, 005. 57 | 24, 958. 20 | $s^2p^4(^3P)5p^2D^0_{1\frac{1}{2}}$—$s^2p^4(^3P)5d^4F_{2\frac{1}{2}}$ | | |
| 1 | 06. 81 | 950. 48 | | | |
| 25 | 08. 08 | 942. 57 | $s^2p^4(^3P)5p^4D^0_{1\frac{1}{2}}$—$s^2p^4(^3P)5d^4P_{2\frac{1}{2}}$ | (0.60), 1.85 (?) | (0.62, 1.86, **3.10**) —0.62, 0.62, **1.86**, 3.10, 4.34 |
| 10H*l* | 08. 48 | 940. 09 | $s^2p^4(^3P)5p^2P^0_{1\frac{1}{2}}$—$s^2p^4(^3P)5d^4F_{2\frac{1}{2}}$ | | |
| 1 | 10. 82 | 925. 54 | | | |
| 30 | 37. 83 | 758. 81 | $s^2p^4(^3P)5s^4P_{0\frac{1}{2}}$—$s^2p^4(^3P)5p^2S^0_{0\frac{1}{2}}$ | (0.57) 2.09 | (0.57) 2.07 |
| 80 | 44. 67 | 716. 94 | $s^2p^4(^1D)5s^2D_{1\frac{1}{2}}$—$s^2p^4(^1D)5p^2D^0_{1\frac{1}{2}}$ | (**0.20**, 0. 60)— 1.40, **1.80** | (**0.20**, 0. 60) 0.60, 1.00, 1.40, **1.80** |
| 50H*l* | 50. 42 | 681. 85 | $s^2p^4(^3P)5p^2S^0_{2\frac{1}{2}}$—$s^2p^4(^3P)5d^2F_{1\frac{1}{2}}$ | | |
| 300*hp* | 57. 01 | 641. 76 | $s^2p^4(^1D)5s^2D_{1\frac{1}{2}}$—$s^2p^4(^1D)5p^2P^0_{0\frac{1}{2}}$ | (0.00) 0.82 | (**0.05**) 0.75, **0.85** |
| 300 | 65. 11 | 592. 66 | $s^2p^4(^1D)5s^2D_{1\frac{1}{2}}$—$s^2p^4(^1D)5p^2D^0_{1\frac{1}{2}}$ | (0.00) 0.79 | (0.00) 0.80 |
| 6H*l* | 66. 09 | 586. 73 | | | |
| 1*h* | 81. 40 | 494. 51 | $s^2p^4(^1D)4d^2G_{3\frac{1}{2}}$—26,795.68 | | |
| 500 | 88. 33 | 452. 99 | $s^2p^4(^1D)5s^2D_{2\frac{1}{2}}$—$s^2p^4(^1D)5p^2D^0_{2\frac{1}{2}}$ | (0.00) 1.20 | (0.00) 1.20 |
| 250 | 98. 72 | 391. 00 | $s^2p^4(^1P)5s^4P_{0\frac{1}{2}}$—$s^2p^4(^3P)5p^2D^0_{1\frac{1}{2}}$ | **0.66**, 1.97 | (**0.65**) **0.68**, 1.98 |
| 3 | 4, 099. 71 | 24, 385. 11 | $s^2p^4(^3P)4d^4F_{3\frac{1}{2}}$—$s^2p^4(^1D)5p^2D^0_{2\frac{1}{2}}$ | | |
| 100*hp* | 4, 109. 23 | 24, 328. 62 | $s^2p^4(^1D)$ $5s^2D_{2\frac{1}{2}}$—$s^2p^4(^1D)5p^2D^0_{1\frac{1}{2}}$ | (**0.19**, 0. 60)— 1.00, 1.40, **1.80** | (**0.20**, 0.60) 0.60, 1.00, 1.40, **1.80** |
| 5H*l* | 10. 16 | 323. 11 | $s^2p^4(^1D)4d^2D_{1\frac{1}{2}}$—$s^2p^4(^1D)5f^2P^0_{1\frac{1}{2}}$ | | |
| 1 | 11. 03 | 317. 97 | | | |
| 8H*l* | 13. 73 | 302. 01 | $s^2p^4(^3P)5p^2P^0_{1\frac{1}{2}}$—$s^2p^4(^1S)6s^2S_{0\frac{1}{2}}$ | | |
| 1 | 15. 11 | 293. 86 | | | |
| 30H*l* | 18. 14 | 275. 98 | $s^2p^4(^3P)5p^4D^0_{\frac{1}{2}}$—$s^2p^4(^1S)6d^2S_{0\frac{1}{2}}$ | | |
| 2*h* | 28. 58 | 214. 60 | | | |
| 5H*l* | 33. 68 | 184. 72 | $s^2p^4(^3P)5p^4D^0_{1\frac{1}{2}}$—$s^2p^4(^3P)6s^2P_{0\frac{1}{2}}$ | | |
| 3*h* | 35. 86 | 171. 97 | $s^2p^4(^1D)4d^2D_{2\frac{1}{2}}$—$s^2p^4(^1D)5f^2P^0_{1\frac{1}{2}}$ | | |
| 50H | 37. 96 | 159. 71 | | | |

TABLE 4.—*The first spark spectrum of krypton (Kr II)*—Continued

| Intensity and character | $\lambda_{air}$ I.A. | $\nu_{vac}$ cm$^{-1}$ | Term combination | Zeeman effect | |
|---|---|---|---|---|---|
| | | | | Observed | Computed |
| 100H*l* | 39. 11 | 153. 00 | | (0.00) 1.20 | |
| 250 | 45. 12 | 117. 98 | $s^2p^4(^3P)5s^4P_{0\frac{1}{2}}$—$s^2p^4(^3P)5p^4S^1_{1\frac{1}{2}}$ | (0. 55) 0. 99, 2.09 | (0.55) 0.99, 2.09 |
| 4*hr* | 59. 00 | 037. 49 | | | |
| 2 | 63. 82 | 24, 009. 66 | $s^2p^4(^3P)5s^4P_{1\frac{1}{2}}$—$s^2p^4(^3P)5p^2P^1_{2\frac{1}{2}}$ | | |
| 20*hl* | 72. 51 | 23, 959. 06 | $s^2p^4(^3P)5p^4P^1_{2\frac{1}{2}}$—$s^2p^4(^3P)6s^4P_{1\frac{1}{2}}$ | | |
| 3*hr* | 77. 02 | 933. 79 | | | |
| 20H*l* | 79. 58 | 919. 13 | $s^2p^4(^1D)5p^2D^1_{1\frac{1}{2}}$—$s^2p^4(^1D)5d^2D_{1\frac{1}{2}}$ | | |
| 50 | 85. 12 | 887. 47 | $s^2p^4(^3P)5s^2P_{1\frac{1}{2}}$—$s^2p^4(^3P)5p^2S^1_{0\frac{1}{2}}$ | (0.00) 1.51 | (0.01) 1.51, 1.53 |
| 30H*l* | 4, 201. 42 | 794. 80 | $s^2p^4(^1D)5p^2D^1_{2\frac{1}{2}}$—$s^2p^4(^1D)5d^2D_{1\frac{1}{2}}$ | | |
| 3H*l* | 04. 31 | 778. 44 | | | |
| 25H*l* | 10. 67 | 742. 52 | | | |
| 1*h* | 12. 37 | 732. 94 | | | |
| 1H*l* | 12. 92 | 729. 84 | | | |
| 2 | 17. 88 | 701. 94 | $s^2p^4(^3P)4d^4F_{1\frac{1}{2}}$—$s^2p^4(^1D)5p^2F^1_{1\frac{1}{2}}$ | | |
| 20*hl* | 22. 20 | 677. 69 | $s^2p^4(^3P)5p^4D^1_{1\frac{1}{2}}$—$s^2p^4(^3P)6s^2P_{1\frac{1}{2}}$ | | |
| 20*hl* | 28. 79 | 640. 79 | $s^2p^4(^1D)4d^2D_{2\frac{1}{2}}$—$s^2p^4(^1D)5f^2F^1_{3\frac{1}{2}}$ | | |
| 8H*l* | 29. 21 | 638. 44 | | | |
| 2*h* | 33. 43 | 614. 88 | | | |
| 100*hl* | 36. 64 | 596. 99 | $s^2p^4(^3P)5p^4P^1_{1\frac{1}{2}}$—$s^2p^4(^3P)6s^4P_{1\frac{1}{2}}$ | | |
| 150 | 50. 58 | 519. 60 | $s^2p^4(^3P)5s^2P_{1\frac{1}{2}}$—$s^2p^4(^3P)5p^2D^1_{1\frac{1}{2}}$ | (0.20) 1.40 | (0.09, 0.28) 1.24, 1.43, 1.61 |
| 50*hr* | 52. 67 | 508. 04 | $s^2p^4(^1D)4d^2D_{1\frac{1}{2}}$—$s^2p^4(^1D)5f^2F^1_{2\frac{1}{2}}$ | | |
| 100*hl* | 54. 85 | 496. 00 | $s^2p^4(^3P)5p^4D^1_{1\frac{1}{2}}$—$s^2p^4(^3P)6s^4P_{0\frac{1}{2}}$ | (−) 0.62, 1. 80 | (0. 54) 0.72, 1. 80 |
| 80*hr* | 59. 44 | 470. 68 | | | |
| 5*hl* | 60. 85 | 462. 91 | $s^2p^4(^3P)5p^2P^1_{1\frac{1}{2}}$—$s^2p^4(^3P)6s^2P_{0\frac{1}{2}}$ | | |
| 60H*l* | 68. 57 | 420. 48 | $s^2p^4(^3P)5p^4D^1_{1\frac{1}{2}}$—$s^2p^4(^3P)5d^4D_{1\frac{1}{2}}$ | | |
| 100H*l* | 68. 81 | 419. 16 | $s^2p^4(^3P)5p^4S^1_{1\frac{1}{2}}$—$s^2p^4(^3P)5d^2P_{1\frac{1}{2}}$ | (0.15) 1.45 | (0. 07, 0.21) 1. 33, 1.47, 1.61 |
| 1*h* | 71. 46 | 404. 63 | | | |
| 4 | 73. 48 | 393. 57 | | | |
| 2 | 75. 75 | 381. 15 | | | |
| 2*h* | 80. 05 | 357. 66 | | | |
| 5*hl* | 80. 61 | 354. 61 | $s^2p^4(^3P)5p^4S^1_{1\frac{1}{2}}$—$s^2p^4(^3P)5d^4F_{2\frac{1}{2}}$ | | |
| 4*h* | 85. 40 | 328. 50 | | | |
| 4H | 87. 45 | 317. 35 | | | |
| 600 | 92. 92 | 287. 64 | $s^2p^4(^3P)5s^4P_{1\frac{1}{2}}$—$s^2p^4(^3P)5p^4D^1_{1\frac{1}{2}}$ | (0.14, 0.43) 1.12, 1.39, 1.67 | (0.14, 0.42) 1.12, 1.40, 1.68 |
| 8*hl* | 4, 295. 21 | 275. 22 | | | |
| 200 | 4, 300. 49 | 246. 65 | $s^2p^4(^3P)5s^2P_{1\frac{1}{2}}$—$s^2p^4(^3P)5p^4S^1_{1\frac{1}{2}}$ | (0.00) 1.51 | (0.01, 0.03) 1.51, 1.53, 1.55 |
| 40 | 01. 53 | 241. 03 | $s^2p^4(^3P)5s^4P_{2\frac{1}{2}}$—$s^2p^4(^3P)5p^4D^1_{2\frac{1}{2}}$ | | |
| 3*h* | 05. 81 | 217. 93 | | | |
| 2*h* A II? | 09. 41 | 198. 53 | | | |
| 500H*l* | 17. 81 | 153. 40 | $s^2p^4(^3P)5p^4P^1_{1\frac{1}{2}}$—$s^2p^4(^3P)6s^4P_{2\frac{1}{2}}$ | (0.00) 1.57 | (0.01, 0.03, 0.05) 1.55, 1.57, 1.59, 1.61, 1.63 |
| 4 | 19. 12 | 146. 38 | $s^2p^4(^3P)5p^2D^1_{2\frac{1}{2}}$—$s^2p^4(^3P)5d^2P_{1\frac{1}{2}}$ | | |
| 150H*l* | 22. 98 | 125. 71 | $s^2p^4(^1S)5s^2S_{0\frac{1}{2}}$—$s^2p^4(^1S)5p^2P^1_{1\frac{1}{2}}$ | (0.39) 0.84, 1.61 | (0.39) 0.84, 1.62 |
| 80H | 31. 24 | 081. 61 | $s^2p^4(^3P)5p^2D^1_{1\frac{1}{2}}$—$s^2p^4(^3P)5d^4F_{2\frac{1}{2}}$ | | |
| 50H | 33. 34 | 070. 42 | $s^2p^4(^3P)5p^4D^1_{1\frac{1}{2}}$—$s^2p^4(^3P)5d^4D_{2\frac{1}{2}}$ | | |
| 8*hl* | 41. 33 | 23, 027. 96 | $s^2p^4(^3P)5p^4D^1_{2\frac{1}{2}}$—$s^2p^4(^3P)5d^4P_{1\frac{1}{2}}$ | | |
| 40H | 51. 02 | 22, 976. 68 | $s^2p^4(^1D)4d^2D_{1\frac{1}{2}}$—$s^2p^4(^1D)5f^2F^1_{2\frac{1}{2}}$ | | |
| 3000 | 55. 47 | 953. 21 | $s^2p^4(^3P)5s^4P_{2\frac{1}{2}}$—$s^2p^4(^3P)5p^4D^1_{3\frac{1}{2}}$ | (0.00) 1.06 | (0.09, 0.26, 0.43) 1.00, 1.17, 1.34, 1.51, 1.69, 1.86 |
| 4*hl* | 64. 61 | 905. 14 | $s^2p^4(^1S)5s^2S_{0\frac{1}{2}}$—$s^2p^4(^3P)5f^4D^1_{1\frac{1}{2}}$ | | |
| 6*hl* | 66. 26 | 896. 48 | $s^2p^4(^3P)5p^2P^1_{1\frac{1}{2}}$—$s^2p^4(^3P)5d^4D_{0\frac{1}{2}}$ | | |
| 1*h* | 4, 367. 01 | 22, 892. 55 | | | |
| 200 | 4, 369. 69 | 22, 878. 51 | $s^2p^4(^1D)5p^2F^1_{2\frac{1}{2}}$—$s^2p^4(^1S)4d^2D_{1\frac{1}{2}}$ | (0.00) 0.91 | (0.03, 0.09) 0.77, 0.83 0.89, 0.94. |
| 20*hl* | 71. 25 | 870. 34 | $s^2p^4(^3P)5p^4D^1_{2\frac{1}{2}}$—$s^2p^4(^3P)5d^4D_{0\frac{1}{2}}$ | | |
| 40*h* | 77. 71 | 836. 60 | | | |
| 100*h* | 81. 52 | 816. 74 | $s^2p^4(^1S)5s^2S_{0\frac{1}{2}}$—$s^2p^4(^3P)5f^2D^1_{1\frac{1}{2}}$ | (0.52)— | (0.49) 0.53. |
| 50H*l* | 85. 27 | 797. 23 | $s^2p^4(^1D)5p^2F^1_{2\frac{1}{2}}$—$s^2p^4(^1S)4d^2D_{2\frac{1}{2}}$ | | |
| 300*hl* | 86. 54 | 790. 63 | $s^2p^4(^3P)5p^4P^1_{1\frac{1}{2}}$—$s^2p^4(^3P)6s^4P_{2\frac{1}{2}}$ | (0.00) 1.51 | (0.03, 0.10) 1.49, 1.56, 1.63, 1.70. |
| 3*hl* | 88. 90 | 778. 37 | $s^2p^4(^3P)5p^2S^1_{0\frac{1}{2}}$—$s^2p^4(^3P)5d^2P_{1\frac{1}{2}}$ | | |
| 20*hl* | 89. 72 | 774. 12 | $s^2p^4(^3P)5p^2P^1_{0\frac{1}{2}}$—$s^2p^4(^3P)6s^4P_{0\frac{1}{2}}$ | | |
| 15*hr* | 4, 399. 39 | 724. 06 | | | |
| 100*hl* | 4, 400. 87 | 716. 42 | $s^2p^4(^3P)5p^4S^1_{1\frac{1}{2}}$—$s^2p^4(^1S)6s^2S_{0\frac{1}{2}}$ | | |
| 30*h* | 04. 33 | 698. 57 | $s^2p^4(^3P)5p^2P^1_{0\frac{1}{2}}$—$s^2p^4(^3P)5d^4D_{1\frac{1}{2}}$ | | |

TABLE 4.—*The first spark spectrum of krypton (Kr II)*—Continued

| Intensity and character | $\lambda_{air}$ I.A. | $\nu_{vac}$ cm$^{-1}$ | Term combination | Zeeman effect | |
|---|---|---|---|---|---|
| | | | | Observed | Computed |
| 40*hv* | 08. 89 | 675. 10 | $s^2p^4(^1D)4d^2P_{1½}$—$s^2p^4(^1D)5f^2P^0_{2½}$ | | |
| 40 | 17. 24 | 632. 23 | $s^2p^4(^3P)5p^4D^0_{½}$—$s^2p^4(^3P)5d^4P_{2½}$ | | |
| 1 | 20. 16 | 617. 29 | $s^2p^4(^3P)4d^4F_{3½}$—$s^2p^4(^1D)5p^2D^0_{2½}$ | | |
| 100*hv* | 22. 70 | 604. 30 | $s^2p^4(^1D)5s^2D_{1½}$—$s^2p^4(^1D)5p^2P^0_{1½}$ | (0.71) 1.07, 1.58 | (0.27, 0.80) 0.53, 1.07, 1.60 |
| 1 | 28. 9 | 572. 7 | $s^2p^4(^3P)4d^4F_{1½}$—$s^2p^4(^1D)5p^2D^0_{2½}$ | | |
| 500 | 31. 67 | 558. 55 | $s^2p^4(^3P)5s^4P_{2½}$—$s^2p^4(^3P)5p^4D^0_{3½}$ | (1.31) 1.31 | (1.32) 1.32 |
| 600 | 36. 81 | 532. 41 | $s^2p^4(^3P)5s^4P_{2½}$—$s^2p^4(^3P)5p^2P^0_{1½}$ | (—) 0.63, 1.94 | (0.57) 0.69, 1.95 |
| 3 | 43. 72 | 497. 37 | $s^2p^4(^3P)4d^4F_{1½}$—$s^2p^4(^1D)5p^2P^0_{2½}$ | | |
| 4*hv* | 50. 34 | 463. 91 | | | |
| 50H*v* | 53. 21 | 449. 43 | $s^2p^4(^1S)5s^2S_{½}$—$s^2p^4(^1S)5p^2P^0_{½}$ | (0.53) 1.44 | (0.55) 1.45 |
| 10H*l* | 54. 37 | 443. 59 | $s^2p^4(^3P)5p^2D^0_{1½}$—$s^2p^4(^1S)6s^2S_{½}$ | | |
| 40H*l* | 57. 25 | 429. 08 | $s^2p^4(^3P)5p^2P^0_{1½}$—$s^2p^4(^3P)6s^2P_{½}$ | | |
| 8*h* | 59. 99 | 415. 30 | $s^2p^4(^3P)5p^4D^0_{½}$—$s^2p^4(^3P)5d^4P_{½}$ | | |
| 1 | 60. 45 | 412. 99 | $s^2p^4(^3P)5p^2D^0_{2½}$—$s^2p^4(^3P)5d^4F_{3½}$ | | |
| 2*hl* | 61. 61 | 407. 17 | | | |
| 800*hv* | 75. 00 | 340. 12 | $s^2p^4(^1D)5s^2D_{2½}$—$s^2p^4(^1D)5p^2P^0_{1½}$ | (0.00) 1.09 | (0.07, 0.20), 1.00, 1.13, 1.27, 1.40. |
| 5H*l* | 79. 86 | 315. 89 | $s^2p^4(^1D)4d^2P_{2½}$—$s^2p^4(^1D)5f^2P^0_{3½}$ | | |
| 50H*l* | 81. 85 | 305. 98 | $s^2p^4(^3P)5p^2P^0_{½}$—$s^2p^4(^3P)5d^4P_{1½}$ | | |
| 3H | 88. 22 | 274. 32 | | | |
| 400*hl* | 4, 489. 88 | 266. 08 | $s^2p^4(^1D)5p^2F^0_{3½}$—$s^2p^4(^1S)4d^2D_{2½}$ | (0.00) 1.07 | (0.03, 0.09, 0.14) 1.00, 1.06, 1.11, 1.17, 1.23, 1.28 |
| 400*hl* | 4, 523. 14 | 102. 36 | $s^2p^4(^3P)5p^4P^0_{½}$—$s^2p^4(^3P)6s^4P_{1½}$ | (0.30) 1.10 | (0.29) 1.09, 1.68 |
| 3*hl* | 28. 62 | 22, 075. 61 | $s^2p^4(^3P)5p^2S^0_{½}$—$s^2p^4(^1S)6s^2S_{½}$ | | |
| 3 | 52. 77 | 21, 958. 51 | $s^2p^4(^1D)4d^2F_{2½}$—$s^2p^4(^1D)5f^2D^0_{3½}$ | | |
| 200*hl* | 56. 61 | 21, 940. 01 | $s^2p^4(^3P)5p^2D^0_{2½}$—$s^2p^4(^3P)6s^2P_{1½}$ | (0.00) 1.35 | (0.00) 1.34 |
| 3*hl* | 60. 38 | 921. 87 | $s^2p^4(^3P)5p^2P^0_{1½}$—$s^2p^4(^3P)6s^2P_{½}$ | | |
| 1*h* | 64. 9 | 899. 98 | $s^2p^4(^3P)5d^4P_{1½}$—14873.45 | | |
| 1*h* | 65. 82 | 895. 75 | $s^2p^4(^3P)5p^4D^0_{½}$—$s^2p^4(^3P)6s^2P_{1½}$ | | |
| 30*hl* | 73. 33 | 859. 80 | $s^2p^4(^1D)4d^2P_{1½}$—$s^2p^4(^1D)5f^2P^0_{½}$ | | |
| 1*h* | 75. 8 | 848. 0 | $s^2p^4(^1D)5p^2P^0_{1½}$—$s^2p^4(^1S)4d^2D_{1½}$ | | |
| 800 | 77. 20 | 841. 32 | $s^2p^4(^1D)5s^2D_{2½}$—$s^2p^4(^1D)5p^2F^0_{3½}$ | (0.00) 1.07 | (0.03, 0.09, 0.14) 1.00, 1.06, 1.11, 1.17, 1.23, 1.28 |
| 2*h* | 80. 11 | 827. 44 | $s^2p^4(^3P)5d^4P_{2½}$—15340.80 | | |
| 300*hl* | 82. 85 | 814. 39 | $s^2p^4(^3P)5p^4D^0_{½}$—$s^2p^4(^3P)6s^4P_{1½}$ | (0.00) 1.04 | (0.18, 0.54) 0.83, 1.19, 1.55, 1.92 |
| 1 | 91. 50 | 773. 29 | $s^2p^4(^3P)4d^4F_{3½}$—$s^2p^4(^1D)5p^2F^0_{3½}$ | | |
| 150H*l* | 92. 80 | 767. 13 | $s^2p^4(^1D)5p^2P^0_{1½}$—$s^2p^4(^1S)4d^2D_{2½}$ | (0.00) 1.04 | (0.07, 0.20) 1.00, 1.13, 1.27, 1.40 |
| 2 | 96. 81 | 748. 14 | | | |
| 50*hl* | 98. 49 | 740. 20 | $s^2p^4(^3P)5p^2P^0_{1½}$—$s^2p^4(^3P)6s^4P_{2½}$ | (—) 0.62 | (0.54) 0.72, 1.80 |
| 1*h* | 4, 599. 44 | 735. 71 | | | |
| 2 | 4, 600. 69 | 729. 80 | | | |
| 1*h* | 01. 42 | 726. 35 | $s^2p^4(^3P)4d^4P_{2½}$—$s^2p^4(^1D)5p^2P^0_{2½}$ | | |
| 60*hl* | 04. 02 | 714. 09 | $s^2p^4(^3P)5p^4D^0_{3½}$—$s^2p^4(^3P)6s^4P_{2½}$ | (1.17) 1.17 | (1.17) 1.17 |
| 1*h* | 05. 25 | 708. 29 | | | |
| 1*h* | 08. 48 | 693. 07 | $s^2p^4(^3P)5p^2P^0_{½}$—$s^2p^4(^3P)5d^4P_{½}$ | | |
| 20*hv* | 09. 72 | 687. 24 | $s^2p^4(^3P)5s^2P_{1½}$—$s^2p^4(^3P)5p^4D^0_{½}$ | | |
| 60*hl* | 10. 65 | 682. 86 | $s^2p^4(^3P)5p^2D^0_{1½}$—$s^2p^4(^3P)5d^4D_{1½}$; $s^2p^4(^3P)5d^4P_{½}$—15702. 73 | | |
| 2*h* | 13. 79 | 668. 10 | $s^2p^4(^3P)5d^4P_{½}$—15717.15 | | |
| 15*gn* | 14. 50 | 664. 77 | $s^2p^4(^3P)5p^2P^0_{1½}$—$s^2p^4(^3P)5d^4D_{1½}$ | | |
| 500 | 4, 615. 28 | 21, 661. 11 | $s^2p^4(^3P)5s^4P_{1½}$—$s^2p^4(^3P)5p^2P^0_{1½}$ | (0.33) 1.15, 1.37, 1.68 | (0.14, 0.42) 1.12, 1.40, 1.68 |
| 1000 | 4, 619. 15 | 21, 642. 96 | $s^2p^4(^3P)5s^2P_{1½}$—$s^2p^4(^3P)5p^2P^0_{2½}$ | (0.00) 1.21 | (0.09, 0.27) 1.07, 1.25, 1.43, 1.61 |
| 5*h* | 19. 99 | 639. 03 | $s^2p^4(^3P)5p^4D^0_{½}$—$s^2p^4(^3P)5d^4D_{1½}$ | | |
| 800 | 33. 88 | 574. 16 | $s^2p^4(^1D)5s^2D_{1½}$—$s^2p^4(^1D)5p^2F^0_{2½}$ | (0.00) 0.90 | (0.03, 0.09) 0.77, 0.83, 0.89, 0.94 |
| 8 | 35. 42 | 567. 00 | $s^2p^4(^3P)4d^4D_{2½}$—$s^2p^4(^3P)5p^2D^0_{1½}$ | | |
| 1*h* | 37. 66 | 556. 58 | $s^2p^4(^3P)5d^4D_{1½}$—15,340.81 | | |
| 2H | 40. 20 | 544. 78 | | | |
| 30 | 50. 17 | 498. 59 | $s^2p^4(^3P)5s^4P_{½}$—$s^2p^4(^3P)5p^2P^0_{½}$ | | |
| 2000 | 58. 87 | 458. 44 | $s^2p^4(^3P)5s^4P_{2½}$—$s^2p^4(^3P)5p^4P^0_{1½}$ | (0.00) 1.51 | (0.03, 0.09) 1.49, 1.55, 1.61, 1.67 |

TABLE 4.—*The first spark spectrum of krypton (Kr II)*—Continued

| Intensity and character | $\lambda_{air}$ I.A. | $\nu_{vac}$ cm$^{-1}$ | Term combination | Zeeman effect | |
|---|---|---|---|---|---|
| | | | | Observed | Computed |
| 2H*l* | 72.09 | 397.73 | $s^2p^4(^1D)5p^2P^0_{1½}$—$s^2p^4(^1D)6s^2D_{2½}$ | | |
| 3 | 73.80 | 389.90 | $s^2p^4(^3P)5d^4D_{2½}$—15,340.81 | | |
| 500 | 80.41 | 359.69 | $s^2p^4(^3P)5s^2P_{0½}$—$s^2p^4(^3P)5p^2S_{½}$<br>$s^2p^4(^3P)5d^4D_{2½}$—15,370.10 | (0.41) 1.09 | (0.40) 1.10 |
| 5 | 83.68 | 344.78 | $s^2p^4(^3P)4d^4P_{1½}$—$s^2p^4(^1D)5p^2P^0_{½}$ | | |
| 8H*l* | 86.30 | 332.84 | $s^2p^4(^3P)5p^2D^0_{½}$—$s^2p^4(^3P)5d^4D_{2½}$ | | |
| 10h*l* | 87.28 | 328.38 | $s^2p^4(^1D)4d^2P_{1½}$—$s^2p^4(^1D)5f^2F^0_{½}$ | | |
| 3h | 88.3 | 323.7 | $s^2p^4(^1D)5p^2D^0_{2½}$—$s^2p^4(^3P)7s^4P_{1½}$ | | |
| 100 | 91.28 | 310.20 | $s^2p^4(^1D)5s^2D_{2½}$—$s^2p^4(^1D)5p^2F^0_{½}$<br>$s^2p^4(^3P)5p^4S^0_{1½}$—$s^2p^4(^3P)5d^4D_{0½}$ | (0.81) | (0.17, 0.51, 0.86) 0.34, 0.69, 1.03, 1.37, 1.71. |
| 200h*l* | 94.44 | 295.86 | $s^2p^4(^3P)5p^4D^0_{½}$—$s^2p^4(^2P)6s^4P_{½}$<br>$s^2p^4(^3P)4d^4P_{1½}$—$s^2p^4(^1D)5p^2P^0_{½}$ | (0.00) 1.67 | (0.09, 0.26, 0.43) 1.00, 1.17, 1.34, 1.52, 1.68, 1.86 |
| 50h*l* | 95.66 | 290.32 | $s^2p^4(^3P)5p^2D^0_{½}$—$s^2p^4(^2P)5d^4P_{1½}$ | | |
| 30H*l* | 4,699.69 | 272.07 | $s^2p^4(^3P)5p^2P^0_{½}$—$s^2p^4(^3P)5d^4P_{1½}$ | | |
| 2h*l* | 4,705.44 | 246.07 | $s^2p^4(^3P)5p^4D^0_{½}$—$s^2p^4(^2P)5d^4P_{1½}$ | | |
| 3 | 06.31 | 242.14 | $s^2p^4(^3P)4d^4F_{2½}$—$s^2p^4(^1D)5p^2F^0_{½}$ | | |
| 1h | 17.0 | 194.00 | | | |
| 3,000 | 39.00 | 095.62 | $s^2p^4(^3P)5s^4P_{2½}$—$s^2p^4(^3P)5p^4P^0_{½}$ | (0.00) 1.58 | (0.01, 0.03, 0.05) 1.55, 1.57, 1.59, 1.61, 1.63 |
| 100h*l* | 52.02 | 037.82 | $s^2p^4(^3P)5p^2D^0_{½}$—$s^2p^4(^2P)5d^4D_{0½}$ | (0.23) 1.53 | (0.23) 1.11, 1.57 |
| 1h | 58.77 | 21,007.98 | $s^2p^4(^3P)5p^4D^0_{½}$—$s^2p^4(^3P)6s^4P_{½}$ | | |
| 300 | 62.43 | 20,991.83 | $s^2p^4(^3P)5s^2P_{0½}$—$s^2p^4(^3P)5p^2D^0_{½}$ | (0.31) 1.01, 1.65 | (0.32) 1.02, 1.65 |
| 1000 | 65.74 | 977.25 | $s^2p^4(^3P)5s^4P_{1½}$—$s^2p^4(^3P)5p^4D^0_{½}$ | (0.15, 0.46) 0.76, 1.07, 1.38, 1.69 | (0.15, 0.46) 0.76, 1.07, 1.38, 1.70 |
| 40h | 73.01 | 945.30 | $s^2p^4(^1D)4d^2P_{1½}$—$s^2p^4(^1D)5f^2D^0_{½}$ | | |
| 2 | 74.46 | 938.94 | $s^2p^4(^3P)4d^4P_{2½}$—$s^2p^4(^1D)5p^2D^0_{½}$ | | |
| 1 | 84.8 | 893.7 | $s^2p^4(^3P)5p^2D^0_{½}$—$s^2p^4(^3P)5d^4P_{2½}$ | | |
| 1h | 86.56 | 886.01 | | | |
| 5h | 88.76 | 876.41 | $s^2p^4(^3P)5p^2P^0_{½}$—$s^2p^4(^3P)5d^4P_{½}$ | | |
| 60h*l* | 4,796.33 | 843.47 | $s^2p^4(^3P)5p^4S^0_{½}$—$s^2p^4(^3P)6s^2P_{0½}$ | | |
| 4 | 4,802.97 | 814.65 | $s^2p^4(^3P)4d^4P_{2½}$—$s^2p^4(^1D)5p^2D^0_{½}$ | | |
| 300 | 11.76 | 776.63 | $s^2p^4(^3P)5s^4P_{0½}$—$s^2p^4(^3P)5p^4D^0_{½}$ | (—) 0.64 | (0.69) 0.59, 1.95 |
| 300 | 25.18 | 718.84 | $s^2p^4(^3P)5s^2P_{0½}$—$s^2p^4(^3P)5p^4S^0_{½}$ | (0.41) 1.11, 1.95 | (0.42) 1.12, 1.96 |
| 800 | 32.07 | 689.30 | $s^2p^4(^3P)5s^4P_{1½}$—$s^2p^4(^3P)5p^4P^0_{½}$ | (0.21) 1.31, 1.76 | (0.22) 1.32, 1.76 |
| 4h | 33.68 | 682.41 | $s^2p^4(^3P)4d^2F_{2½}$—$s^2p^4(^1D)5p^2D^0_{½}$ | | |
| 20h*l* | 36.56 | 670.09 | $s^2p^4(^3P)5p^2S^0_{½}$—$s^2p^4(^3P)5d^4D_{0½}$ | | |
| 4h | 39.04 | 659.50 | $s^2p^4(^3P)5p^2P^0_{½}$—$s^2p^4(^3P)5d^4P_{0½}$ | | |
| 2h | 45.14 | 633.49 | $s^2p^4(^3P)5p^4D^0_{½}$—$s^2p^4(^3P)5d^4P_{0½}$ | | |
| 700 | 46.60 | 627.28 | $s^2p^4(^3P)5s^2P_{1½}$—$s^2p^4(^3P)5p^2P^0_{½}$ | (0.12) 1.38, 1.65 | (0.13) 1.39, 1.65 |
| 2 | 52.61 | 601.73 | $s^2p^4(^2P)6s^4P_{0½}$—15,702.73 | | |
| 150 | 57.20 | 582.26 | $s^2p^4(^3P)4d^4D_{½}$—$s^2p^4(^3P)5p^2S^0_{½}$ | (0.75) 0.75 | (0.75) 0.75 |
| 2h | 62.1 | 561.5 | | | |
| 20H*p* | 70.14 | 527.57 | $s^2p^4(^1D)4d^2P_{0½}$—$s^2p^4(^1D)5f^2D^0_{½}$ | | |
| 1— | 75.63 | 504.46 | $s^2p^4(^3P)4d^4F_{2½}$—$s^2p^4(^1D)5p^2P^0_{½}$ | | |
| 1h | 89.67 | 445.59 | | | |
| 1 | 91.3 | 438.8 | | | |
| 3 | 4,897.2 | 414.1 | | | |
| 2h*l* | 4,908.34 | 367.82 | $s^2p^4(^1D)5p^2P^0_{½}$—$s^2p^4(^1D)6s^2D_{2½}$ | | |
| 2h | 14.62 | 341.79 | $s^2p^4(^1S)5s^2S_{0½}$—32,026.50 | | |
| 100h*l* | 15.94 | 336.33 | $s^2p^4(^3P)5p^4S^0_{½}$—$s^2p^4(^3P)6s^4P_{1½}$ | | |
| 1H | 32.17 | 269.41 | | | |
| 1H | 37.97 | 245.60 | $s^2p^4(^3P)6s^2P_{0½}$—15,370.10 | | |
| 300 | 45.59 | 214.41 | $s^2p^4(^3P)4d^4D_{0½}$—$s^2p^4(^3P)5p^2D^0_{½}$ | | |
| 50h*l* | 4,948.50 | 20,202.52 | $s^2p^4(^3P)5p^2S^0_{½}$—$s^2p^4(^3P)6s^2P_{0½}$ | | |
| 3 | 4,791.15 | 20,866.00 | $s^2p^4(^1D)5p^2F^0_{½}$—$s^2p^4(^1D)6s^2D_{1½}$ | | |
| 100h*l* | 4,960.25 | 20,154.67 | $s^2p^4(^3P)5p^4S^0_{1½}$—$s^2p^4(^2P)6s^4P_{0½}$ | | |
| 100h*l* | 78.89 | 079.21 | $s^2p^4(^3P)5p^4S^0_{1½}$—$s^2p^4(^2P)5d^4D_{1½}$ | | |
| 50h*l* | 82.83 | 063.33 | $s^2p^4(^3P)5p^2D^0_{½}$—$s^2p^4(^3P)6s^2P_{1½}$ | | |
| 1 | 97.22 | 005.56 | $s^2p^4(^3P)4d^4F_{1½}$—$s^2p^4(^1D)5p^2F^0_{½}$ | | |
| 5H*l* | 4,998.54 | 20,000.28 | $s^2p^4(^1D)5p^2F^0_{½}$—$s^2p^4(^2P)5d^2D_{2½}$ | | |
| 100 | 5,013.29 | 19,941.43 | $s^2p^4(^3P)4d^4D_{0½}$—$s^2p^4(^3p)5p^4S^0_{½}$ | | |
| 1 | 15.71 | 931.85 | $s^2p^4(^3P)5d^4D_{0½}$—15,216.41 | | |
| 4H*p* | 20.43 | 913.08 | $s^2p^4(3P)6s^2P_{0½}$—15,702.73 | | |
| 100 | 21.88 | 907.32 | $s^2p^4(^3P)4d^4D_{½}$—$s^2p^4(^3P)5p^2D^0_{½}$ | | |
| 200 | 22.40 | 905.26 | $s^2p^4(^3P)5s^4P_{1½}$—$s^2p^4(^3P)5p^4D^0_{½}$ | | |

TABLE 4.—*The first spark spectrum of krypton* (*Kr II*)—Continued

| Intensity and character | $\lambda_{air}$ I. A. | $\nu_{vac}$ cm$^{-1}$ | Term combination | Zeeman effect | |
|---|---|---|---|---|---|
| | | | | Observed | Computed |
| 30*hl* | 28. 30 | 881. 67 | $s^2p^4(^3P)5p^3D_{1\frac{1}{2}}$—$s^2p^4(^3P)6s^4P_{0\frac{1}{2}}$ | | |
| 3H*v* | 30. 96 | 871. 40 | | | |
| 100H*l* | 33. 85 | 859. 99 | $s^2p^4(^1D)5p^2D_{1\frac{1}{2}}$—$s^2p^4(^1S)4d^2D_{1\frac{1}{2}}$ | | |
| 1*h* | 37. 47 | 845. 72 | | | |
| 80H*l* | 46. 31 | 810. 95 | $s^2p^4(^1D)5p^2P_{1\frac{1}{2}}$—$s^2p^4(^1S)4d^2D_{1\frac{1}{2}}$ | | |
| 4*hl* | 47. 52 | 806. 20 | $s^2p^4(^3P)5p^2D_{1\frac{1}{2}}$—$s^2p^4(^3P)5d^4D_{1\frac{1}{2}}$ | | |
| 30H*l* | 54. 53 | 778. 74 | $s^2p^4(^1D)5p^2D_{1\frac{1}{2}}$—$s^2p^4(^1S)4d^2D_{2\frac{1}{2}}$<br>$s^2p^4(^3P)5d^4D_{0\frac{1}{2}}$—15, 37010 | | |
| 20H*l* | 65. 58 | 735. 59 | $s^2p^4(^1D)5p^2D_{1\frac{1}{2}}$—$s^2p^4(^1S)4d^2D_{1\frac{1}{2}}$ | | |
| 1H | 67. 22 | 729. 20 | $s^2p^4(^3P)5p^4S_{1\frac{1}{2}}$—$s^2p^4(^3P)5d^4D_{2\frac{1}{2}}$ | | |
| 3*h* | 67. 41 | 728. 46 | | | |
| 40 | 72. 55 | 708. 47 | $s^2p^4(^3P)4d^4D_{2\frac{1}{2}}$—$s^2p^4(^3P)5p^2P_{1\frac{1}{2}}$ | | |
| 4H*l* | 75. 92 | 695. 39 | $s^2p^4(^3P)5p^2S_{0\frac{1}{2}}$—$s^2p^4(^3P)6s^2P_{1\frac{1}{2}}$ | | |
| 40 | 77. 23 | 690. 31 | $s^2p^4(^3P)4d^4D_{2\frac{1}{2}}$—$s^2p^4(^3P)5p^2D_{2\frac{1}{2}}$ | | |
| 2H*l* | 78. 19 | 686. 58 | $s^2p^4(^3P)5p^4S_{1\frac{1}{2}}$—$s^2p^4(^3P)5d^4P_{1\frac{1}{2}}$ | | |
| 250*hl* | 5, 086. 52 | 654. 34 | $s^2p^4(^1D)5p^2D_{1\frac{1}{2}}$—$s^2p^4(^1S)4d^2D_{2\frac{1}{2}}$ | | |
| 15H*l* | 5, 123. 16 | 513. 78 | $s^2p^4(^3P)5p^2S_{0\frac{1}{2}}$—$s^2p^4(^3P)6s^4P_{0\frac{1}{2}}$ | | |
| 400H*l* | 25. 73 | 504. 00 | $s^2p^4(^3P)5p^4D_{1\frac{1}{2}}$—$s^2p^4(^3P)6s^4P_{1\frac{1}{2}}$ | | |
| 1 | 33. 52 | 474. 40 | $s^2p^4(^3P)4d^4F_{2\frac{1}{2}}$—$s^2p^4(^1D)5p^2F_{2\frac{1}{2}}$ | | |
| 1H*v* | 41. 10 | 445. 69 | $s^2p^4(^3P)5d^4D_{0\frac{1}{2}}$—15,702.73 | | |
| 60*hl* | 43. 05 | 438. 31 | $s^2p^4(^3P)5p^4S_{1\frac{1}{2}}$—$s^2p^4(^3P)5d^4D_{1\frac{1}{2}}$ | | |
| 4 | 45. 28 | 429. 89 | $s^2p^4(^3P)4d^4F_{1\frac{1}{2}}$—$s^2p^4(^1D)5p^2F_{1\frac{1}{2}}$ | | |
| 3*hl* | 49. 61 | 413. 55 | $s^2p^4(^3P)5p^2D_{1\frac{1}{2}}$—$s^2p^4(^3P)5d^4P_{1\frac{1}{2}}$ | | |
| 3*hl* | 52. 01 | 404. 51 | | | |
| 80 | 66. 80 | 348. 96 | $s^2p^4(^3P)4d^2D_{1\frac{1}{2}}$—$s^2p^4(^1D)5p^2D_{2\frac{1}{2}}$ | | |
| 6H*v* | 77. 71 | 308. 19 | $s^2p^4(^3P)4d^4P_{1\frac{1}{2}}$—$s^2p^4(^1D)5p^2P_{1\frac{1}{2}}$ | | |
| 1*h* | 82. 30 | 291. 09 | $s^2p^4(^3P)5p^4S_{1\frac{1}{2}}$—$s^2p^4(^3P)5d^4P_{2\frac{1}{2}}$ | | |
| 60H*v* | 5, 186. 99 | 273. 65 | $s^2p^4(^3P)4d^2D_{1\frac{1}{2}}$—$s^2p^4(^1D)5p^2P_{0\frac{1}{2}}$ | | |
| 60H*v* | 5, 200. 22 | 224. 62 | $s^2p^4(^3P)4d^2D_{1\frac{1}{2}}$—$s^2p^4(^1D)5p^2D_{1\frac{1}{2}}$ | | |
| 2*h* | 01. 56 | 219. 66 | $s^2p^4(^3P)4d^2P_{0\frac{1}{2}}$—$s^2p^4(^1D)5p^2D_{1\frac{1}{2}}$ | | |
| 500 | 08. 32 | 194. 72 | $s^2p^4(^3P)5s^4P_{1\frac{1}{2}}$—$s^2p^4(^3P)5p^4P_{1\frac{1}{2}}$ | | |
| 30 | 17. 45 | 161. 13 | $s^2p^4(^3P)4d^4D_{1\frac{1}{2}}$—$s^2p^4(^3P)5p^4D_{0\frac{1}{2}}$ | | |
| 12 | 17. 93 | 159. 37 | $s^2p^4(^3P)5s^2P_{0\frac{1}{2}}$—$s^2p^4(^3P)5p^4D_{0\frac{1}{2}}$ | | |
| 7 | 24. 56 | 135. 05 | $s^2p^4(^3P)4d^4D_{1\frac{1}{2}}$—$s^2p^4(^3P)5p^2P_{1\frac{1}{2}}$ | | |
| 8 | 25. 05 | 133. 26 | $s^2p^4(^3P)5s^2P_{0\frac{1}{2}}$—$s^2p^4(^3P)5p^2P_{1\frac{1}{2}}$ | | |
| 60 | 29. 52 | 116. 91 | $s^2p^4(^3P)4d^4D_{1\frac{1}{2}}$—$s^2p^4(^3P)5p^2D_{2\frac{1}{2}}$ | | |
| 3*h* | 30. 15 | 114. 60 | $s^2p^4(^1D)4d^2D_{2\frac{1}{2}}$—$s^2p^4(^3P)5f^2D_{3\frac{1}{2}}$ | | |
| 2*hl* | 41. 29 | 073. 98 | $s^2p^4(^3P)5p^4S_{1\frac{1}{2}}$—$s^2p^4(^3P)5d^4P_{0\frac{1}{2}}$ | | |
| 4H*v* | 45. 25 | 059. 58 | | | |
| 4*hl* | 49. 06 | 045. 74 | $s^2p^4(^3P)5p^2S_{0\frac{1}{2}}$—$s^2p^4(^3P)5d^4P_{1\frac{1}{2}}$ | | |
| 30 | 56. 75 | 19, 017. 88 | $s^2p^4(^3P)5p^2D_{1\frac{1}{2}}$—$s^2p^4(^3P)5d^4P_{2\frac{1}{2}}$ | | |
| 100*h* | 76. 50 | 18, 946. 70 | $s^2p^4(^1D)4d^2D_{2\frac{1}{2}}$—$s^2p^4(^3P)5f^2F_{3\frac{1}{2}}$ | | |
| 2*h* | 86. 86 | 909. 57 | | | |
| 1H | 5, 297. 8 | 18, 870. 5 | $s^2p^4(^1S)6s^2S_{0\frac{1}{2}}$—14,873.45<br>$s^2p^4(^1D)4d^2D_{2\frac{1}{2}}$—$s^2p^4(^3P)5f^2F_{3\frac{1}{2}}$ | | |
| 200 | 5, 308. 66 | 831. 92 | $s^2p^4(^3P)5s^4P_{1\frac{1}{2}}$—$s^2p^4(^3P)5p^4F_{2\frac{1}{2}}$ | | |
| 4*h* | 10. 26 | 826. 25 | $s^2p^4(^3P)4d^4P_{2\frac{1}{2}}$—$s^2p^4(^1D)5p^2P_{1\frac{1}{2}}$ | | |
| 30*hl* | 17. 41 | 800. 93 | $s^2p^4(^3P)5p^2D_{1\frac{1}{2}}$—$s^2p^4(^3P)5d^4P_{0\frac{1}{2}}$ | | |
| 60*hl* | 22. 77 | 782. 00 | $s^2p^4(^3P)5p^2P_{0\frac{1}{2}}$—$s^2p^4(^3P)6s^4P_{1\frac{1}{2}}$ | | |
| 4*h* | 29. 15 | 759. 51 | $s^2p^4(^1D)4d^2D_{1\frac{1}{2}}$—$s^2p^4(^1S)5p^2P_{1\frac{1}{2}}$ | | |
| 500*h* | 33. 41 | 744. 53 | $s^2p^4(^1D)4d^2D_{2\frac{1}{2}}$—$s^2p^4(^3P)5f^2F_{3\frac{1}{2}}$ | | |
| 60*hl* | 46. 76 | 697. 73 | $s^2p^4(^3P)5p^4D_{1\frac{1}{2}}$—$s^2p^4(^3P)6s^4P_{2\frac{1}{2}}$ | | |
| 10*h* | 55. 45 | 667. 39 | $s^2p^4(^1D)4d^2D_{2\frac{1}{2}}$—$s^2p^4(^3P)5f^4F_{3\frac{1}{2}}$ | | |
| 3*h* | 5, 374. 19 | 602. 30 | $s^2p^4(^1D)4d^2F_{3\frac{1}{2}}$—$s^2p^4(^3P)5f^2F_{3\frac{1}{2}}$ | | |
| 30H*v* | 5, 418. 43 | 450. 42 | $s^2p^4(^1D)4d^2D_{1\frac{1}{2}}$—$s^2p^4(^3P)5f^2D_{2\frac{1}{2}}$ | | |
| 1H | 23. 56 | 432. 96 | $s^2p^4(^3P)5p^2S_{0\frac{1}{2}}$—$s^2p^4(^3P)5d^4P_{0\frac{1}{2}}$ | | |
| 2*hv* | 33. 24 | 400. 12 | $s^2p^4(^1D)4d^2F_{3\frac{1}{2}}$—$s^2p^4(^3P)5f^2F_{3\frac{1}{2}}$ | | |
| 40 | 38. 63 | 381. 89 | $s^2p^4(^3P)4d^4D_{0\frac{1}{2}}$—$s^2p^4(^3P)5p^4D_{0\frac{1}{2}}$ | | |
| 1*h* | 39. 38 | 379. 35 | $s^2p^4(^1D)5p^2D_{1\frac{1}{2}}$—$s^2p^4(^1D)6s^2D_{2\frac{1}{2}}$ | | |
| 1*h* | 41. 39 | 372. 56 | | | |
| 1 | 44. 05 | 363. 59 | | | |
| 80 | 46. 34 | 355. 87 | $s^2p^4(^1P)4d^4D_{0\frac{1}{2}}$—$s^2p^4(^3P)5p^2P_{1\frac{1}{2}}$ | | |
| 2H | 49. 61 | 344. 85 | $s^2p^4(^1D)5p^4F_{1\frac{1}{2}}$—$s^2p^4(^3P)5d^2F_{2\frac{1}{2}}$ | | |
| 200*hv* | 68. 17 | 282. 59 | $s^2p^4(^1D)4d^2D_{1\frac{1}{2}}$—$s^2p^4(^3P)5f^2F_{2\frac{1}{2}}$ | | |
| 4H*l* | 76. 46 | 254. 91 | $s^2p^4(^1D)5p^2D_{1\frac{1}{2}}$—$s^2p^4(^1D)6s^2D_{2\frac{1}{2}}$ | | |
| 4*h* | 91. 43 | 205. 15 | $s^2p^4(^1D)4d^2D_{1\frac{1}{2}}$—$s^2p^4(^3P)5f^4F_{1\frac{1}{2}}$ | | |
| 50 | 5, 499. 54 | 178. 30 | $s^2p^4(^3P)5s^4P_{0\frac{1}{2}}$—$s^2p^4(^3P)5p^4P_{0\frac{1}{2}}$ | | |

TABLE 4.—*The first spark spectrum of krypton (Kr II)*—Continued

| Intensity and character | $\lambda_{air}$ I.A. | $\nu_{vac}$ cm$^{-1}$ | Term combination | Zeeman effect | |
|---|---|---|---|---|---|
| | | | | Observed | Computed |
| 60 | 5,522.94 | 101.28 | $s^2p^4(^3P)4d^4D_{1\frac{1}{2}}$—$s^2p^4(^3P)5p^2P^0_{1\frac{1}{2}}$ | | |
| 30 | 23.47 | 099.55 | $s^2p^4(^3P)5s^2P^0_{0\frac{1}{2}}$—$s^2p^4(^3P)5p^2P^0_{1\frac{1}{2}}$ | | |
| 5 | 32.29 | 070.69 | $s^2p^4(^3P)4d^2F_{2\frac{1}{2}}$—$s^2p^4(^1D)5p^2F^0_{2\frac{1}{2}}$ | | |
| 4H$\nu$ | 41.65 | 040.17 | $s^2p^4(^1S)6s^2S_{0\frac{1}{2}}$—15,702.73 | | |
| 5H | 46.11 | 18,025.66 | $s^2p^4(^1S)6s^2S_{0\frac{1}{2}}$—15,717.15 | | |
| 1h | 5,475.49 | 18,258.15 | $s^2p^4(^1D)4d^2F_{2\frac{1}{2}}$—$s^2p^4(^3P)5f^4F^0_{3\frac{1}{2}}$ | | |
| 100H$\nu$ | 5,552.99 | 18,003.33 | $s^2p^4(^1D)4d^2D_{2\frac{1}{2}}$—$s^2p^4(^3P)5f^2F^0_{3\frac{1}{2}}$ | | |
| 100 | 68.65 | 17,952.70 | $s^2p^4(^3P)4d^4D_{2\frac{1}{2}}$—$s^2p^4(^3P)5p^4D^0_{1\frac{1}{2}}$ | | |
| 1h— | 84.4 | 902.1 | $s^2p^4(^3P)5p^4P^0_{2\frac{1}{2}}$—$s^2p^4(^1D)4d^2P_{1\frac{1}{2}}$ | | |
| 1h— | 5,585.4 | 898.9 | $s^2p^4(^3P)5p^4P^0_{1\frac{1}{2}}$—$s^2p^4(^1D)4d^2P_{0\frac{1}{2}}$ | | |
| 2 | 5,617.63 | 796.17 | $s^2p^4(^3P)4d^4P_{2\frac{1}{2}}$—$s^2p^4(^1D)5p^2F^0_{3\frac{1}{2}}$ | | |
| 1 | 27.02 | 766.48 | $s^2p^4(^3P)5p^2D^0_{2\frac{1}{2}}$—$s^2p^4(^3P)6s^4P_{1\frac{1}{2}}$ | | |
| 100h | 33.02 | 747.55 | $s^2p^4(^3P)5p^2P^0_{1\frac{1}{2}}$—$s^2p^4(^3P)6s^4P_{1\frac{1}{2}}$<br>$s^2p^4(^3P)4d^2D_{2\frac{1}{2}}$—$s^2p^4(^1D)5p^2D^0_{2\frac{1}{2}}$ | | |
| 3h$l$ | 41.07 | 722.23 | $s^2p^4(^3P)5p^4D^0_{2\frac{1}{2}}$—$s^2p^4(^3P)6s^4P_{1\frac{1}{2}}$ | | |
| 1H | 45.00 | 709.89 | $s^2p^4(^1D)5p^2P^0_{1\frac{1}{2}}$—$s^2p^4(^3P)5d^2D_{1\frac{1}{2}}$ | | |
| 1H$\nu$ | 48.38 | 699.29 | $s^2p^4(^3P)5d^2P_{1\frac{1}{2}}$—15,340.81 | | |
| 10H | 50.37 | 693.06 | $s^2p^4(^3P)4d^2P_{1\frac{1}{2}}$—$s^2p^4(^1D)5p^2D^0_{2\frac{1}{2}}$ | | |
| 1 | 64.85 | 647.83 | $s^2p^4(^1D)4d^2F_{2\frac{1}{2}}$—$s^2p^4(^3P)5f^2F^0_{3\frac{1}{2}}$ | | |
| 1h | 67.59 | 639.30 | | | |
| 40h$\nu$ | 72.78 | 623.16 | $s^2p^4(^3P)4d^2D_{2\frac{1}{2}}$—$s^2p^4(^1D)5p_{2\frac{1}{2}}D^0_{2\frac{1}{2}}$ | | |
| 30h$\nu$ | 74.52 | 617.76 | $s^2p^4(^3P)4d^2P_{1\frac{1}{2}}$—$s^2p^4(^1D)5p^2P^0_{1\frac{1}{2}}$ | | |
| 400 | 81.89 | 594.91 | $s^2p^4(^3P)5s^2P_{1\frac{1}{2}}$—$s^2p^4(^3P)5p^4D^0_{1\frac{1}{2}}$ | | |
| 200H$\nu$ | 90.35 | 568.75 | $s^2p^4(^3P)4d^2P_{1\frac{1}{2}}$—$s^2p^4(^1D)5p^2D^0_{1\frac{1}{2}}$ | | |
| 5H$l$ | 92.11 | 563.22 | | | |
| 10 | 5,699.84 | 539.50 | $s^2p^4(^3P)4d^2F_{2\frac{1}{2}}$—$s^2p^4(^1D)5p^2F^0_{2\frac{1}{2}}$<br>$s^2p^4(^3P)5p^4P^0_{1\frac{1}{2}}$—$s^2p^4(^1D)4d^2P_{1\frac{1}{2}}$ | | |
| 5H$l$ | 5,749.27 | 388.70 | $s^2p^4(^1D)5p^2D^0_{2\frac{1}{2}}$—$s^2p^4(^3P)5d^2D_{2\frac{1}{2}}$ | | |
| 60 | 52.98 | 377.49 | $s^2p^4(^3P)5s^2P^0_{0\frac{1}{2}}$—$s^2p^4(^3P)5p^4D^0_{1\frac{1}{2}}$ | | |
| 2H | 55.60 | 369.58 | $s^2p^4(^1D)4d^2F_{2\frac{1}{2}}$—$s^2p^4(^3P)5f^4F^0_{3\frac{1}{2}}$ | | |
| 100 | 71.41 | 322.00 | $s^2p^4(^3P)4d^4D_{0\frac{1}{2}}$—$s^2p^4(^3P)5p^2P^0_{0\frac{1}{2}}$ | | |
| 1H$l$ | 5,773.5 | 315.7 | $s^2p^4(^1D)5p^2P^0_{1\frac{1}{2}}$—$s^2p^4(^3P)5d^2F_{2\frac{1}{2}}$ | | |
| 6H$\nu$ | 5,800.16 | 236.14 | $s^2p^4(^3P)4d^2D_{1\frac{1}{2}}$—$s^2p^4(^1D)5p^2P^0_{1\frac{1}{2}}$ | | |
| 1h | 01.81 | 231.23 | $s^2p^4(^3P)4d^2P_{0\frac{1}{2}}$—$s^2p^4(^1D)5p^2P^0_{1\frac{1}{2}}$ | | |
| 1H | 42.49 | 111.26 | $s^2p^4(^1D)4d^2P_{1\frac{1}{2}}$—$s^2p^4(^1S)5p^2P^0_{1\frac{1}{2}}$ | | |
| 1H | 45.28 | 103.09 | | | |
| 4H$l$ | 54.04 | 077.50 | | | |
| 10H$l$ | 60.75 | 17,057.95 | | | |
| 2H$l$ | 82.67 | 16,994.38 | | | |
| 8H$l$ | 94.56 | 960.11 | $s^2p^4(^3P)5p^2D^0_{2\frac{1}{2}}$—$s^2p^4(^3P)6s^4P_{2\frac{1}{2}}$ | | |
| 2H$l$ | 5,897.47 | 951.74 | | | |
| 8H$l$ | 5,900.89 | 941.91 | $s^2p^4(^3P)5p^2P^0_{1\frac{1}{2}}$—$s^2p^4(^3P)6s^4P_{2\frac{1}{2}}$ | | |
| 10H$l$ | 11.72 | 910.87 | | | |
| 1H | 14.79 | 902.10 | | | |
| 2H | 19.4 | 888.9 | | | |
| 1H | 24.24 | 875.14 | | | |
| 8h | 35.03 | 844.46 | $s^2p^4(^1D)5p^2P^0_{1\frac{1}{2}}$—$s^2p^4(^3P)5d^4F_{1\frac{1}{2}}$ | | |
| 4H$\nu$ | 41.82 | 825.21 | | | |
| 3h | 49.93 | 802.28 | $s^2p^4(^1D)4d^2P_{1\frac{1}{2}}$—$s^2p^4(^3P)5f^2D^0_{2\frac{1}{2}}$ | | |
| 15H$\nu$ | 67.54 | 752.69 | $s^2p^4(^1D)4d^2P_{0\frac{1}{2}}$—$s^2p^4(^1S)5p^2P^0_{1\frac{1}{2}}$ | | |
| 2H$l$ | 69.57 | 747.00 | | | |
| 2 | 74.82 | 732.28 | $s^2p^4(^3P)4d^2P_{0\frac{1}{2}}$—$s^2p^4(^1D)5p^2F^0_{1\frac{1}{2}}$ | | |
| 200 | 5,992.22 | 683.70 | $s^2p^4(^3P)5s^4P_{2\frac{1}{2}}$—$s^2p^4(^3P)5p^4P^0_{1\frac{1}{2}}$ | | |
| 3H$\nu$ | 6,008.10 | 639.60 | $s^2p^4(^1D)4d^2D_{2\frac{1}{2}}$—32,026.50 | | |
| 10H | 09.99 | 634.37 | $s^2p^4(^1D)4d^2P_{1\frac{1}{2}}$—$s^2p^4(^3P)5f^2F^0_{2\frac{1}{2}}$ | | |
| 40 | 22.39 | 600.12 | $s^2p^4(^3P)4d^4D_{0\frac{1}{2}}$—$s^2p^4(^3P)5p^4D^0_{1\frac{1}{2}}$ | | |
| 1h | 38.1 | 556.9 | $s^2p^4(^1D)4d^2P_{1\frac{1}{2}}$—$s^2p^4(^3P)5f^4F^0_{2\frac{1}{2}}$ | | |
| 10H$w$ | 40.7 | 549.8 | | | |
| 2H | 44.85 | 538.44 | | | |
| 10H$w$ | 46.06 | 535.13 | | | |
| ?H | 47.13 | 532.20 | $s^2p^4(^1D)4d^2P_{0\frac{1}{2}}$—$s^2p^4(^3P)5f^4D^0_{1\frac{1}{2}}$ | | |
| 20H$\nu$ | 79.71 | 443.61 | $s^2p^4(^1D)4d^2P_{0\frac{1}{2}}$—$s^2p^4(^3P)5f^2D^0_{1\frac{1}{2}}$ | | |
| 30h$l$ | 6,094.50 | 403.71 | $s^2p^4(^3P)5p^4P^0_{1\frac{1}{2}}$—$s^2p^4(^1D)4d^2P_{0\frac{1}{2}}$ | | |
| 5H$lw$ | 6,107.61 | 368.50 | | | |
| 4h | 12.61 | 355.11 | $s^2p^4(^1D)4d^2P_{1\frac{1}{2}}$—$s^2p^4(^3P)5f^4F^0_{1\frac{1}{2}}$<br>$s^2p^4(^3P)5d^2P_{0\frac{1}{2}}$—14,873.45 | | |
| 1h | 16.52 | 344.65 | | | |
| 10H$lw$ | 19.56 | 336.53 | | | |

TABLE 4.—*The first spark spectrum of krypton* (*Kr* II)—Continued

| Intensity and character | $\lambda_{air}$ I.A. | $\nu_{vac}$ cm$^{-1}$ | Term combination | Zeeman effect | |
|---|---|---|---|---|---|
| | | | | Observed | Computed |
| 1H*l* | 25. 52 | 320. 64 | | | |
| 1*h* | 50. 54 | 254. 25 | $s^2p^4(^3P)5p^4P^0_{1\frac{1}{2}}$—$s^2p^4(^1D)4d^2D_{1\frac{1}{2}}$ | | |
| 50 | 68. 80 | 206. 13 | $s^2p^4(^3P)4d^2D_{1\frac{1}{2}}$—$s^2p^4(^1D)5p^2F^0_{2\frac{1}{2}}$ | | |
| 6H*v* | 71. 77 | 198. 33 | $s^2p^4(^1D)4d^2P_{0\frac{1}{2}}$—$s^2p^4(^3P)5f^4F^0_{1\frac{1}{2}}$ | | |
| 7H*l* | 85. 35 | 162. 77 | $s^2p^4(^3P)5p^4S^0_{1\frac{1}{2}}$—$s^2p^4(^3P)6s^4P_{1\frac{1}{2}}$ | | |
| 3H*lw* | 6, 196. 14 | 134. 63 | | | |
| 1H | 6, 228. 14 | 051. 73 | $s^2p^4(^3P)6s^4P_{2\frac{1}{2}}$—$s^2p^4(^1D)5f^2F^0_{2\frac{1}{2}}$ | | |
| 10*hl* | 30. 74 | 045. 03 | $s^2p^4(^3P)5p^4P^0_{0\frac{1}{2}}$—$s^2p^4(^1D)4d^2P_{1\frac{1}{2}}$ | | |
| 2*hlw* | 43. 53 | 012. 16 | | | |
| 1H*l* | 47. 53 | 16, 001. 91 | | | |
| 4*hvw* | 57. 84 | 15, 975. 54 | $s^2p^4(^1D)4d^2D_{1\frac{1}{2}}$—32,026.50 | | |
| 2H*w* | 64. 91 | 957. 52 | | | |
| 1H*w* | 69. 35 | 946. 22 | | | |
| 2*h* | 77. 52 | 925. 46 | | | |
| 3*hl* | 6, 290. 96 | 891. 44 | $s^2p^4(^3P)5p^4P^0_{1\frac{1}{2}}$—$s^2p^4(^1D)4d^2D_{1\frac{1}{2}}$ | | |
| 100 | 6, 303. 66 | 859. 42 | $s^2p^4(^3P)4d^4D_{2\frac{1}{2}}$—$s^2p^4(^3P)5p^4D^0_{2\frac{1}{2}}$ | | |
| 4 | 22. 42 | 812. 36 | $s^2p^4(^3P)5s^2P_{1\frac{1}{2}}$—$s^2p^4(^3P)5p^4P^0_{1\frac{1}{2}}$ | | |
| 4*h* | 44. 61 | 757. 06 | $s^2p^4(^3P)5p^4D^0_{1\frac{1}{2}}$—$s^2p^4(^1D)4d^2P_{1\frac{1}{2}}$ | | |
| 30 | 6, 391. 14 | 15, 642. 34 | $s^2p^4(^3P)4d^4D_{3\frac{1}{2}}$—$s^2p^4(^3P)5p^4D^0_{3\frac{1}{2}}$ | | |
| 2H | 5, 777. 72 | 17, 303. 08 | $s^2p^4(^1D)4d^2F_{2\frac{1}{2}}$—$s^2p^4(^3P)5f^4F^0_{3\frac{1}{2}}$ | | |
| 2H*w* | 5, 918. 81 | 16, 890. 62 | $s^2p^4(^1D)4d^2P_{1\frac{1}{2}}$—$s^2p^4(^3P)5f^4D^0_{1\frac{1}{2}}$ | | |
| 4*hv* | 6, 394. 28 | 15, 634. 66 | $s^2p^4(^3P)4d^2D_{2\frac{1}{2}}$—$s^2p^4(^1D)5p^2P^0_{1\frac{1}{2}}$ | | |
| 3H*w* | 6, 404. 69 | 609. 25 | | | |
| 10H*hv* | 9. 84 | 596. 71 | $s^2p^4(^1D)5p^2D^0_{2\frac{1}{2}}$—$s^2p^4(^3P)5d^2D_{1\frac{1}{2}}$ | | |
| 4*h* | 12. 53 | 590. 17 | $s^2p^4(^3P)5p^4P^0_{2\frac{1}{2}}$—$s^2p^4(^1D)4d^2D_{2\frac{1}{2}}$ | | |
| 60H*v* | 16. 61 | 580. 26 | $s^2p^4(^3P)4d^2P_{1\frac{1}{2}}$—$s^2p^4(^1D)5p^2P^0_{1\frac{1}{2}}$ | | |
| 300 | 20. 18 | 571. 59 | $s^2p^4(^3P)4d^4D_{3\frac{1}{2}}$—$s^2p^4(^3P)5p^4D^0_{3\frac{1}{2}}$ | | |
| 2H | 31. 92 | 543. 17 | | | |
| 5H*l* | 40. 74 | 521. 88 | $s^2p^4(^3P)5p^2S^0_{0\frac{1}{2}}$—$s^2p^4(^3P)6s^4P_{1\frac{1}{2}}$ | | |
| 50 | 70. 89 | 449. 56 | $s^2p^4(^3P)5s^2P_{1\frac{1}{2}}$—$s^2p^4(^3P)5p^4P^0_{2\frac{1}{2}}$ | | |
| 2H | 6, 493. 7 | 395. 3 | $s^2p^4(^3P)5d^2D_{1\frac{1}{2}}$—14,873.45 | | |
| 8*hl* | 6, 510. 14 | 356. 42 | $s^2p^2(^3P)5p^4S^0_{1\frac{1}{2}}$—$s^2p^4(^3P)6s^4P_{2\frac{1}{2}}$ | | |
| 100 | 10. 95 | 354. 51 | $s^2p^4(^3P)4d^4D_{2\frac{1}{2}}$—$s^2p^4(^3P)5p^4D^0_{2\frac{1}{2}}$ | | |
| 6*h* | 65. 32 | 227. 35 | $s^2p^4(^3P)5p^4P^0_{1\frac{1}{2}}$—$s^2p^4(^1D)4d^2D_{2\frac{1}{2}}$ | | |
| 150 | 6, 570. 07 | 216. 34 | $s^2p^4(^3P)4d^2F_{2\frac{1}{2}}$—$s^2p^4(^1D)5p^2D^0_{2\frac{1}{2}}$ | | |
| 10*h* | 6, 602. 90 | 140. 69 | $s^2p^4(^3P)4d^2F_{2\frac{1}{2}}$—$s^2p^4(^1D)5p^2P^0_{1\frac{1}{2}}$ | | |
| 15*h* | 05. 00 | 135. 87 | $s^2p^4(^3P)4d^2D_{2\frac{1}{2}}$—$s^2p^4(^1D)5p^2F^0_{2\frac{1}{2}}$ | | |
| 2H*v* | 24. 22 | 091. 96 | $s^2p^4(^3P)4d^2F_{3\frac{1}{2}}$—$s^2p^4(^1D)5p^2D^0_{2\frac{1}{2}}$ | | |
| 2H*l* | 27. 96 | 083. 44 | $s^2p^4(^3P)5p^2D^0_{1\frac{1}{2}}$—$s^2p^4(^3P)6s^4P_{2\frac{1}{2}}$ | | |
| 15*h* | 6, 634. 36 | 15, 068. 89 | $s^2p^4(^3P)4d^4D_{1\frac{1}{2}}$—$s^2p^4(^3P)5p^4D^0_{2\frac{1}{2}}$ | | |
| 100 | 6, 763. 61 | 14, 780. 93 | $s^2p^4(^3P)4d^4D_{1\frac{1}{2}}$—$s^2p^4(^3P)5p^4P^0_{0\frac{1}{2}}$ | | |
| 80 | 64. 43 | 770. 14 | $s^2p^4(^3P)5s^2P_{2\frac{1}{2}}$—$s^2p^4(^3P)5p^4P^0_{2\frac{1}{2}}$ | | |
| 50 | 6, 771. 22 | 764. 32 | $s^2p^4(^1D)5s^2D_{1\frac{1}{2}}$—$s^2p^4(^3P)5p^2S^0_{0\frac{1}{2}}$ | | |
| 40 | 6, 870. 85 | 550. 23 | $s^2p^4(^3P)4d^2P_{1\frac{1}{2}}$—$s^2p^4(^1D)5p^2F^0_{2\frac{1}{2}}$ | | |
| 10H*l* | 6, 944. 06 | 396. 83 | $s^2p^4(^1D)5s^2D_{1\frac{1}{2}}$—$s^2p^4(^3P)5p^2D^0_{1\frac{1}{2}}$<br>$s^2p^4(^3P)5p^4P^0_{0\frac{1}{2}}$—$s^2p^4(^1D)4d^2D_{1\frac{1}{2}}$ | | |
| 3*h* | 6, 977. 95 | 326. 91 | $s^2p^4(^1D)4d^2P_{1\frac{1}{2}}$—32,026.50 | | |
| 2H | 7, 022. 56 | 235. 89 | $s^2p^4(^1D)5p^2P^0_{1\frac{1}{2}}$—$s^2p^4(^1S)6s^2S_{0\frac{1}{2}}$ | | |
| 60 | 7, 073. 97 | 132. 44 | $s^2p^4(^1D)5s^2D_{2\frac{1}{2}}$—$s^2p^4(^3P)5p^2D^0_{1\frac{1}{2}}$ | | |
| 3 | 7, 078. 44 | 123. 52 | $s^2p^4(^1D)5s^2D_{1\frac{1}{2}}$—$s^2p^4(^3P)5p^4S^0_{1\frac{1}{2}}$ | | |
| 2*hl* | 7, 128. 14 | 025. 04 | | | |
| 60 | 7, 139. 99 | 14, 001. 77 | $s^2p^4(^3P)4d^4D_{0\frac{1}{2}}$—$s^2p^4(^3P)5p^4P^0_{0\frac{1}{2}}$ | | |
| 1— | 7, 156. 81 | 13, 968. 86 | $s^2p^4(^1D)4d^2P_{0\frac{1}{2}}$—32,026.50 | | |
| 250 | 7, 213. 13 | 13, 859. 79 | $s^2p^4(^1D)5s^2D_{2\frac{1}{2}}$—$s^2p^4(^3P)5p^4S^0_{1\frac{1}{2}}$<br>$s^2p^4(^3P)4d^4D_{3\frac{1}{2}}$—$s^2p^4(^3P)5p^4P^0_{2\frac{1}{2}}$ | | |
| 1*h* | 33. 52 | 820. 73 | 59,686.98—$s^2p^4(^1D)5p^2D^0_{2\frac{1}{2}}$ | | |
| 2H*l* | 41. 56 | 805. 38 | $s^2p^4(^3P)5p^4D^0_{1\frac{1}{2}}$—$s^2p^4(^1D)4d^2P_{0\frac{1}{2}}$ | | |
| 4 | 72. 97 | 745. 76 | 59,686.98—$s^2p^4(^1D)5p3P^0_{0\frac{1}{2}}$ | | |
| 400*h* | 7, 289. 78 | 714. 06 | $s^2p^4(^3P)4d\ ^4D_{3\frac{1}{2}}$—$s^2p^4\ (^3P)\ 5p^4P^0_{2\frac{1}{2}}$ | | |
| 4*h* | 7, 301. 29 | 692. 44 | | | |
| 1*h* | 11. 63 | 673. 08 | | | |
| 1*h* | 18. 92 | 659. 46 | | | |
| 3*h* | 59. 97 | 583. 28 | | | |
| 2*h* | 7, 380. 46 | 545. 56 | | | |
| 400*h* | 7, 407. 02 | 496. 99 | $s^2p^4(^3P)4d^4D_{2\frac{1}{2}}$—$s^2p^4(^3P)5p^4P^0_{2\frac{1}{2}}$ | | |
| 1H | 18. 27 | 476. 53 | | | |
| 15*h* | 34. 74 | 446. 67 | $s^2p^4(^3P)5p^4D^0_{1\frac{1}{2}}$—$s^2p^4(^1D)4d^2P_{1\frac{1}{2}}$ | | |

TABLE 4.—*The first spark spectrum of krypton (Kr II)*—Continued

| Intensity and character | $\lambda_{air}$ I. A. | $\nu_{vac}$ cm$^{-1}$ | Term combination | Zeeman effect | |
|---|---|---|---|---|---|
| | | | | Observed | Computed |
| 200*h* | 35.78 | 444.79 | $s^3p^4(^3P)5p^4D_{3\frac{1}{2}}$—$s^3p^4(^1D)4d^3D_{3\frac{1}{2}}$ | | |
| 2H | 44.64 | 428.79 | | | |
| 6H*w* | 7,467.99 | 386.80 | | | |
| 1h | 7,511.42 | 309.40 | | | |
| 2H | 17.52 | 298.60 | | | |
| 300*h* | 24.46 | 286.34 | $s^3p^4(^3P)4d^4D_{1\frac{1}{2}}$—$s^3p^4(^3P)5p^4P_{1\frac{1}{2}}$ | | |
| 20*h* | 7,525.48 | 284.54 | | | |
| 3*h* | 7,615.69 | 127.18 | | | |
| 5*h* | 29.46 | 103.49 | $s^3p^4(^3P)4d^3F_{3\frac{1}{2}}$—$s^3p^4(^1D)5p^3P_{1\frac{1}{2}}$ | | |
| 5 | 35.13 | 093.76 | $s^3p^4(^3P)5d^4P_{1\frac{1}{2}}$—$s^3p^4(^1D)5f^3P_{0\frac{1}{2}}$ | | |
| 150 | 7,641.16 | 13,083.42 | $s^3p^4(^3P)5p^2P_{1\frac{1}{2}}$—$s^3p^4(^1D)4d^3P_{0\frac{1}{2}}$ | | |
| 1 | 7,712.02 | 12,963.21 | | | |
| 250*h* | 35.69 | 923.54 | $s^3p^4(^3P)4d^4D_{1\frac{1}{2}}$—$s^3p^4(^3P)5p^4P_{2\frac{1}{2}}$ | | |
| 1*h* | 49.16 | 901.08 | $s^3p^4(^1D)5p^3P_{1\frac{1}{2}}$—$s^3p^4(^3P)5d^3P_{1\frac{1}{2}}$ | | |
| 100*h* | 81.97 | 846.69 | | | |
| 6H*l* | 7,791.90 | 830.31 | $s^3p^4(^1D)5p^3P_{1\frac{1}{2}}$—$s^3p^4(^3P)5d^4D_{2\frac{1}{2}}$ | | |
| 30H | 56.52 | 724.79 | $s^3p^4(^3P)5p^4P_{1\frac{1}{2}}$—$s^3p^4(^1D)4d^3P_{1\frac{1}{2}}$ | | |
| 1*h* | 7,895.57 | 661.85 | | | |
| 40*h* | 7,931.41 | 604.64 | $s^3p^4(^3P)4d^3F_{2\frac{1}{2}}$—$s^3p^4(^1D)5p^3F_{3\frac{1}{2}}$ | | |
| 3*h* | 57.07 | 563.99 | $s^3p^4(^1S)5s^3D_{1\frac{1}{2}}$—$s^3p^4(^3P)5p^4D_{2\frac{1}{2}}$ | | |
| 120*hw* | 73.62 | 537.91 | $s^3p^4(^1D)5s^3D_{1\frac{1}{2}}$—$s^3p^4(^3P)5p^3P_{1\frac{1}{2}}$ | | |
| 200*h* | 7,993.22 | 507.17 | $s^3p^4(^3P)4d^4D_{0\frac{1}{2}}$—$s^3p^4(^3P)5p^4P_{1\frac{1}{2}}$ | | |
| 3H | 8,095.96 | 348.45 | | | |
| 4 | 8,123.44 | 306.68 | | | |
| 10*h* | 30.03 | 296.70 | $s^3p^4(^3P)4d^4F_{3\frac{1}{2}}$—$s^3p^4(^3P)5p^3D_{1\frac{1}{2}}$ | | |
| 6H | 32.96 | 292.27 | | | |
| 1H | 42.17 | 278.37 | $s^3p^4(^1D)5p^3F_{3\frac{1}{2}}$—$s^3p^4(^3P)5d^4D_{2\frac{1}{2}}$<br>$s^3p^4(^3P)5d^4P_{1\frac{1}{2}}$—$s^3p^4(^1D)5f^3P_{1\frac{1}{2}}$ | | |
| 100H | 45.15 | 273.87 | $s^3p^4(^1D)5s^3D_{2\frac{1}{2}}$—$s^3p^4(^3P)5p^3P_{1\frac{1}{2}}$ | | |
| 1H | 47.70 | 270.03 | $s^3p^4(^1D)6s^3D_{2\frac{1}{2}}$—15,340.81 | | |
| 1H | 49.17 | 267.82 | | | |
| 10*hw* | 57.25 | 255.67 | $s^3p^4(^1D)5s^3D_{2\frac{1}{2}}$—$s^3p^4(^3P)5p^4D_{3\frac{1}{2}}$ | | |
| 2H*w* | 8,178.68 | 223.56 | | | |
| 3h KrI? | 8,192.63 | 202.74 | | | |
| 200*h* | 8,202.72 | 12,187.73 | $s^3p^4(^3P)4d^4F_{3\frac{1}{2}}$—$s^3p^4(^3P)5p^3D_{2\frac{1}{2}}$ | | |
| 2H | 8,333.14 | 11,996.98 | | | |
| 1*h* | 47.24 | 976.72 | | | |
| 2*h* | 8,378.87 | 931.57 | | | |
| 1H | 8,411.14 | 885.73 | $s^3p^4(^3P)5d^4D_{1\frac{1}{2}}$—$s^3p^4(^1D)5f^3P_{1\frac{1}{2}}$ | | |
| 1H | 32.37 | 855.81 | $s^3p^4(^1D)5p^3P_{1\frac{1}{2}}$—$s^3p^4(^3P)6s^3P_{1\frac{1}{2}}$ | | |
| 4*h*/*w* | 64.92 | 810.22 | $s^3p^4(^3P)6s^4P_{0\frac{1}{2}}$—$s^3p^4(^1D)5f^3P_{1\frac{1}{2}}$ | | |
| 100*hl* | 8,473.31 | 798.53 | $s^3p^4(^3P)5p^4D_{1\frac{1}{2}}$—$s^3p^4(^1D)4d^3D_{1\frac{1}{2}}$ | | |
| 3*h* | 8,523.88 | 728.53 | | | |
| 3*h* | 37.98 | 709.16 | $s^3p^4(^3P)5p^2D_{2\frac{1}{2}}$—$s^3p^4(^1D)4d^3P_{1\frac{1}{2}}$ | | |
| 2H | 51.33 | 690.88 | $s^3p^4(^3P)5p^2P_{1\frac{1}{2}}$—$s^3p^4(^1D)4d^3P_{1\frac{1}{2}}$ | | |
| 2H | 63.59 | 674.14 | $s^3p^4(^1D)5p^3P_{1\frac{1}{2}}$—$s^3p^4(^3P)6s^4P_{0\frac{1}{2}}$ | | |
| 4H | 8,595.91 | 630.25 | | | |
| 2*h* | 8,613.58 | 606.39 | | | |
| 1H*w* | 19.34 | 598.63 | $s^3p^4(^1D)5p^3P_{1\frac{1}{2}}$—$s^3p^4(^3P)5d^4D_{1\frac{1}{2}}$ | | |
| 5H*w* | 51.50 | 555.52 | | | |
| 1 | 73.52 | 526.18 | | | |
| 2*h* | 74.26 | 525.20 | $s^3p^4(^3P)5p^4P_{1\frac{1}{2}}$—$s^3p^4(^1S)5s^2S_{0\frac{1}{2}}$ | | |
| 1*h* | 80.94 | 516.33 | | | |
| 100*hw* | 8,690.19 | 504.07 | $s^3p^4(^1D)5s^3D_{1\frac{1}{2}}$—$s^3p^4(^3P)5p^3P_{0\frac{1}{2}}$ | | |
| 8*h* | 8,707.61 | 481.06 | $s^3p^4(^3P)4d^4P_{0\frac{1}{2}}$—$s^3p^4(^3P)5p^3D_{1\frac{1}{2}}$ | | |
| 3H*lw* | 8,798.65 | 362.26 | | | |
| 3H | 8,804.65 | 354.52 | $s^3p^4(^3P)5d^4D_{1\frac{1}{2}}$—$s^3p^4(^1D)5f^3F_{2\frac{1}{2}}$ | | |
| 2H | 10.10 | 347.50 | | | |
| 5H*lw* | 29.38 | 322.72 | $s^3p^4(^3P)5d^4P_{1\frac{1}{2}}$—25447.85<br>$s^3p^4(^3P)5d^4D_{2\frac{1}{2}}$—$s^3p^4(^1D)5f^3D_{3\frac{1}{2}}$ | | |
| 3H | 33.42 | 317.54 | | | |
| 4*h* | 40.09 | 309.01 | $s^3p^4(^1D)5p^3F_{3\frac{1}{2}}$—$s^3p^4(^3P)5d^4F_{3\frac{1}{2}}$ | | |
| 1H | 73.56 | 266.34 | | | |
| 1 | 8,892.99 | 241.73 | | | |
| 1 | 8,901.94 | 230.43 | | | |
| 3H | 8,908.26 | 222.46 | | | |
| 15*h* | 8,978.70 | 134.42 | $s^3p^4(^3P)5p^4D_{1\frac{1}{2}}$—$s^3p^4(^1D)4d^3D_{2\frac{1}{2}}$ | | |

TABLE 4.—*The first spark spectrum of krypton* (*Kr II*)—Continued

| Intensity and character | $\lambda_{air}$ I.A. | $\nu_{vac}$ cm$^{-1}$ | Term combination | Zeeman effect | |
|---|---|---|---|---|---|
| | | | | Observed | Computed |
| 6 | 8, 999. 11 | 109. 16 | $s^2p^4(^3P)5p^4D_{3/2}$—$s^2p^4(^1D)4d^2G_{3/2}$ | | |
| 10 | 9, 006. 15 | 100. 48 | $s^2p^4(^3P)4d^4P_{1/2}$—$s^2p^4(^3P)5p^2D_{1/2}$ | | |
| 10*hl* | 25. 67 | 076. 47 | $s^2p^4(^3P)5p^2P_{1/2}$—$s^2p^4(^1D)4d^2D_{1/2}$ | | |
| 20HL | 39. 95 | 058. 98 | | | |
| 10H | 44. 55 | 053. 35 | $s^2p^4(^3P)6s^4P_{1/2}$—$s^2p^4(^1S)5p^2P_{1/2}$ | | |
| 2H | 87. 18 | 11, 001. 50 | | | |
| 3H | 90. 98 | 10, 996. 90 | | | |
| 2H | 94. 5 | 992. 6 | | | |
| 4H | 96. 49 | 990. 24 | | | |
| 15*h* | 9, 099. 72 | 986. 34 | | | |
| 20HL | 9, 115. 00 | 967. 92 | | | |
| 6H*l* | 31. 21 | 948. 45 | | | |
| 8HL | 33. 4 | 945. 8 | | | |
| 2HL | 57. 82 | 916. 64 | | | |
| 3H*l* | 64. 04 | 909. 23 | | | |
| 40HL | 75. 42 | 895. 70 | | | |
| 10HL | 81. 23 | 888. 80 | | | |
| 1H | 9, 196. 7 | 870. 5 | $s^2p^4(^1S)4d^2D_{3/2}$—15, 340.80 | | |
| 8H*d*? | 9, 207. 27 | 858. 00 | | | |
| 50 | 33. 18 | 827. 54 | $s^2p^4(^3P)4d^4P_{1/2}$—$s^2p^4(^3P)5p^4S_{1/2}$ | | |
| 1 | 35. 30 | 825. 05 | | | |
| 500 | 38. 48 | 821. 32 | $s^2p^4(^3P)5p^4D_{3/2}$—$s^2p^4(^1D)4d^2G_{3/2}$ | | |
| 20HL | 45. 45 | 813. 17 | | | |
| 1H | 50. 0 | 807. 8 | | | |
| 1H | 55. 4 | 801. 5 | | | |
| 2 | 62. 93 | 792. 76 | $s^2p^4(^1D)5p^2P_{3/2}$—$s^2p^4(^3P)5d^4D_{3/2}$ | | |
| 2*h* | 66. 17 | 788. 99 | $s^2p^4(^1S)4d^2D_{1/2}$—15,340.80 | | |
| 2H | 69. 38 | 785. 25 | | | |
| 50 | 71. 99 | 782. 22 | $s^2p^4(^1D)5s^2D_{1/2}$—$s^2p^4(3P)5p^4D_{1/2}$ | | |
| 1H*w* | 76. 2 | 777. 3 | | | |
| 20HL | 89. 95 | 761. 37 | | | |
| 500HL | 93. 82 | 756. 90 | $s^2p^4(^3P)5f^4F_{1/2}$—$s^2p^4(^3P)5g^4G_{3/2}$ | | |
| 60H | 9, 296. 1 | 754. 3 | | | |
| 1H | 9, 305. 76 | 743. 09 | $s^2p^4(^3P)5f^4F_{3/2}$—$s^2p^4(^3P)5g^4G_{3/2}$ | | |
| 30*h* | 17. 84 | 729. 16 | $s^2p^4(^3P)5f^4F_{3/2}$—$s^2p^4(^3P)5g^4G_{3/2}$ | | |
| 200H | 20. 99 | 725. 53 | $s^2p^4(^3P)5f^4F_{3/2}$—$s^2p^4(^3P)5g^4G_{3/2}$ | | |
| 4*h* | 26. 19 | 719. 55 | | | |
| 5*h* | 30. 66 | 714. 42 | $s^2p^4(^3P)6s^2P_{1/2}$—$s^2p^4(^1D)5f.^2D^0_{3/2}$ | | |
| 2H | 37. 73 | 706. 31 | | | |
| 100H | 45. 11 | 697. 85 | $s^2p^4(^3P)5f^4F_{1/2}$—$s^2p^4(^3P)5g^4G_{3/2}$ | | |
| 100H | 49. 08 | 693. 31 | $s^2p^4(^3P)5f^4F_{1/2}$—$s^2p^4(^3P)5g^4G_{3/2}$ | | |
| 300 | 61. 95 | 678. 61 | 59, 686. 98—$s^2p^4(^1D)5p^2F_{3/2}$ | | |
| 1*h* | 63. 6 | 676. 7 | $s^2p^4(^3P)6s^2P_{1/2}$—25,447.85 | | |
| 50H*l* | 88. 08 | 648. 89 | | | |
| 1H | 90. 3 | 646. 4 | | | |
| 1H*v* | 9, 392. 42 | 643. 97 | | | |
| 200H*v* | 9, 402. 82 | 632. 19 | $s^2p^4(^3P)5f^4F_{3/2}$—$s^2p^4(^3P)5g^4G_{3/2}$ | | |
| 3 | 13. 32 | 620. 33 | | | |
| 100 | 9, 414. 94 | 618. 50 | $s^2p^4(^3P)4d^4P_{2/2}$—$s^2p^4(^3P)5p^2D_{1/2}$ | | |
| 2*h* | 8, 717. 31 | 11, 468. 28 | $s^2p^4(^3P)5d^4D_{3/2}$—$s^2p^4(^1D)5f^2F^0_{3/2}$ | | |
| 5H | 9, 430. 25 | 10, 601. 27 | $s^2p^4(^3P)5f^4F_{1/2}$—$s^2p^4(^3P)5g^4G_{3/2}$ | | |
| 20H | 37. 21 | 593. 45 | $s^2p^4(^1D)5p^2F^0_{1/2}$—$s^2p^4(^3P)5d^4F_{3/2}$ | | |
| 100H | 40. 02 | 590. 29 | $s^2p^4(^3P)6s^2P_{3/2}$—$s^2p^4(^1D)5f^2F^0_{1/2}$ | | |
| 1*h* | 41. 6 | 588. 5 | | | |
| 1*h* | 55. 29 | 573. 19 | | | |
| 3*h* | 61. 67 | 566. 06 | | | |
| 200H | 70. 93 | 555. 73 | $s^2p^4(^3P)5f^4F_{1/2}$—$s^2p^4(^3P)5g^4G_{3/2}$ | | |
| 100H | 75. 06 | 551. 13 | $s^2p^4(^3P)5f^4F_{3/2}$—$s^2p^4(^3P)5g^4G_{4/2}$ | | |
| 5H | 76. 4 | 549. 6 | | | |
| 1H | 9, 490. 08 | 534. 43 | | | |
| 100H | 9, 500. 60 | 522. 77 | | | |
| 100 | 04. 70 | 518. 23 | $s^2p^4(^1D)5s^2D_{3/2}$—$s^2p^4(^3P)5p^4D_{1/2}$ | | |
| 4 | 20. 23 | 501. 07 | | | |
| 10H | 43. 64 | 475. 31 | $s^2p^4(^3P)5f^4F_{1/2}$—$s^2p^4(^3P)5g^4G_{3/2}$ | | |
| 2*h* | 49. 4 | 469. 0 | | | |

TABLE 4.—*The first spark spectrum of krypton (Kr II)*—Continued

| Intensity and character | $\lambda_{air}$ I.A. | $\nu_{vac}$ cm$^{-1}$ | Term combination | Zeeman effect | |
|---|---|---|---|---|---|
| | | | | Observed | Computed |
| 10H | 52.85 | 465.21 | | | |
| 2H | 61.26 | 456.01 | | | |
| 5H | 64.32 | 452.66 | | | |
| 500 | 77.52 | 438.26 | $s^2p^4(^3P)4d^4F_{3/2}$—$s^2p^4(^3P)5p^2P^0_{1/2}$ | | |
| 1H | 90.5 | 424.1 | | | |
| 100 | 9,594.24 | 420.06 | $s^2p^4(^3P)4d^4F_{3/2}$—$s^2p^4(^3P)5p^2D^0_{3/2}$<br>$s^2p^4(^3P)4d^4F_{3/2}$—$s^2p^4(^3P)5p^4D^0_{5/2}$ | | |
| 500H | 9,605.80 | 407.52 | | | |
| 100H | 13.80 | 398.87 | $s^2p^4(^3P)5f^2F^0_{5/2}$—$s^2p^4(^3P)5g^4G_{7/2}$ | | |
| 400H | 19.61 | 392.58 | | | |
| 3H*l* | 22.5 | 389.5 | | | |
| 200 | 63.34 | 345.55 | $s^2p^4(^3P)4d^4P_{3/2}$—$s^2p^4(^3P)5p^4S^0_{3/2}$ | | |
| 5H | 72.90 | 335.33 | | | |
| 2H*l* | 9,693.27 | 313.61 | | | |
| 200H | 9,711.60 | 294.14 | | | |
| 10H | 17.16 | 288.25 | | | |
| 3H | 20.6 | 284.6 | | | |
| 2H | 39.4 | 264.8 | | | |
| 1 | 63.79 | 239.12 | | | |
| 2H*l* | 70.1 | 232.5 | | | |
| 2H | 77.6 | 224.7 | | | |
| 1H*w* | 93.3 | 208.3 | | | |
| 2H | 9,795.1 | 206.4 | $s^2p^4(^1D)5p^2P^0_{3/2}$—$s^2p^4(^3P)5d^4P_{1/2}$ | | |
| 5*h* | 9,800.6 | 200.7 | | | |
| 500 | 9,803.14 | 198.02 | | | |
| 100H | 23.39 | 177.00 | | | |
| 100H | 26.58 | 173.68 | | | |
| 5H | 33.8 | 166.2 | | | |
| 3*h* | 51.40 | 148.1 | | | |
| 10*h* | 9,892.97 | 105.42 | $s^2p^4(^3P)5p^4S^0_{3/2}$—$s^2p^4(^1D)4d^2P_{3/2}$ | | |
| 20H | 9,954.75 | 042.70 | $s^2p^4(^3P)5p^2P^0_{3/2}$—$s^2p^4(^1D)4d^2D_{3/2}$ | | |
| 5*h* | 9,966.67 | 10,030.69 | $s^2p^4(^3P)5p^4P^0_{3/2}$—$s^2p^4(^1S)5s^2S_{0/2}$ | | |
| 20H*v* | 10,017.97 | 9,979.33 | | | |
| 20HL | 042.27 | 955.18 | 32,026.50—$s^2p^4(^1D)5d^2D_{3/2}$ | | |
| 4 | 127.74 | 871.17 | $s^2p^4(^3P)5d^4P_{3/2}$—27,294.47? | | |
| 2H | 157.07 | 842.66 | $s^2p^4(^3P)5d^4D_{3/2}$—26,886.30 | | |
| 10H | 167.61 | 832.46 | $s^2p^4(^3P)5p^2D^0_{3/2}$—$s^2p^4(^1D)4d^2P_{3/2}$ | | |
| 3H | 177.41 | 822.99 | $s^2p^4(^3P)5p^2S^0_{1/2}$—$s^2p^4(^1D)4d^2P_{3/2}$ | | |
| 1000 | 221.46 | 780.66 | $s^2p^4(^3P)4d^4F_{3/2}$—$s^2p^4(^3P)5p^4D^0_{3/2}$ | | |
| 100 | 361.15 | 648.79 | $s^2p^4(^3P)4d^4P_{5/2}$—$s^2p^4(^3P)5p^4D^0_{3/2}$<br>$s^2p^4(^3P)5f^2F^0_{5/2}$—$s^2p^4(^1D)5d^2F_{7/2}$ | | |
| 8*h* | 389.28 | 622.68 | $s^2p^4(^3P)4d^4P_{3/2}$—$s^2p^4(^3P)5p^2P^0_{1/2}$ | | |
| 10 | 428.40 | 586.57 | | | |
| 2*h* | 431.84 | 583.41 | | | |
| 4*h* | 562.84 | 464.56 | $s^2p^4(^3P)5p^2S^0_{1/2}$—$s^2p^4(^1D)4d^2D_{3/2}$ | | |
| 6*h* | 639.34 | 396.51 | $s^2p^4(^3P)5p^2D^0_{3/2}$—$s^2p^4(^1D)4d^2D_{3/2}$ | | |
| 1*h*— | 10,659.5 | 9,378.73 | $s^2p^4(^3P)5p^2P^0_{1/2}$—$s^2p^4(^1D)4d^2D_{3/2}$ | | |

WASHINGTON, May 31, 1933.

U.S. DEPARTMENT OF COMMERCE

BUREAU OF STANDARDS

# BUREAU OF STANDARDS JOURNAL OF RESEARCH

October 1933

Vol. VI, No. 4



UNITED STATES

GOVERNMENT PRINTING OFFICE

WASHINGTON, 1933